



**UCL**  
**Université**  
**catholique**  
**de Louvain**

CENTER FOR SYSTEMS ENGINEERING AND  
APPLIED MECHANICS

AND

LABORATORY OF NEUROPHYSIOLOGY

# **The use of extraretinal information to compensate for self-movement**

GUNNAR BLOHM

*Thesis submitted in partial  
fulfillment of the requirements  
for the degree of **Docteur en  
Sciences Appliquées***

Jury:

Prof. Vincent Blondel (FSA, UCL)

Prof. J. Douglas Crawford (Center for Vision Research, York University,  
Toronto)

Prof. Marc Crommelinck (MD, UCL)

Prof. Philippe Lefèvre (FSA, UCL, promoter)

Prof. Guillaume Masson (Centre de Recherche en Sciences Cognitives,  
CNRS, Marseille)

Prof. Marcus Missal (MD, UCL)



## ACKNOWLEDGEMENTS

The work that I accomplished during the last few years and that resulted in the thesis text you hold in your hands right now would not have been possible without the contribution of many people.

I would like to express my gratitude to all the members of the Centre for Systems Engineering and Applied Mechanics as well as the Laboratory of Neurophysiology for the friendly working ambiance. My deepest considerations go to Prof. Philippe Lefèvre. He was for me a mentor, friend and example. I am also very thankful to Prof. Marcus Missal for his fresh ideas, his friendly consideration and all the fun we had together. And the kindness and support of Prof. Marc Crommelinck was always an invaluable motivation for me. I am also indebted to Prof. Vincent Blondel for accepting to preside over the thesis jury.

My special thanks go to the external members of the thesis jury. Prof. Guillaume Masson and Prof. J. Douglas Crawford kindly accepted to critically examine the preliminary version of the manuscript. Their comments, questions and suggestions largely enhanced its quality.

I will not forget all the present and former members of the oculomotor research group. My special thanks go to my former officemate Sophie de Brouwer for her precious help with the experimental set-up. Although constantly in a hurry, Demet Yüksel was always present to provide medical (she is a clinical ophthalmologist) and mental support. Aside all the fun we had together, I also obtained great assistance from Jean-Jacques Orban de Xivry to conduct the experiments that used the Cambridge Visual Stimulus Generator. Thank you and all the others for your friendship.

Finally, I would like to express my deepest gratitude to my family and particularly to my wife Annick, who supported me with courageous patience and loving kindness. And the smile and joy of my son Joachim was a permanent source of decompression and happiness.



*To my lovely wife Annick  
and to my son Joachim, our  
little sunshine.*



# TABLE OF CONTENTS

<b>CHAPTER I.....</b>	<b>1</b>
<b>INTRODUCTION – SCIENTIFIC BACKGROUND .....</b>	<b>1</b>
1. THE SCOPE OF THIS WORK.....	1
2. THE EYE AND ITS MOVEMENTS .....	2
2.1. <i>The eye plant, extra-ocular muscles and brainstem signals</i> .....	2
2.2. <i>Saccades</i> .....	4
2.2.1. General behavior .....	4
2.2.2. Latencies .....	5
2.2.3. Model .....	7
2.2.4. Neurophysiology .....	7
2.3. <i>Smooth pursuit</i> .....	9
2.3.1. General behavior .....	9
2.3.2. Model .....	9
2.3.3. Neurophysiology .....	10
2.4. <i>Other eye movements</i> .....	11
3. INTERACTION BETWEEN SMOOTH PURSUIT AND SACCADES .....	12
3.1. <i>Velocity input to the saccadic system</i> .....	12
3.2. <i>Position input to the smooth pursuit system</i> .....	15
3.3. <i>Common neural pathways</i> .....	16
4. EXTRARETINAL SIGNALS AND THE SENSE OF MOTION .....	18
4.1. <i>The role of proprioception in oculomotor control</i> .....	18
4.2. <i>Efferent feedback loops and eye movements</i> .....	20
4.3. <i>Self-generated motion and space constancy</i> .....	22
4.3.1. Eye position information.....	22

TABLE OF CONTENTS

---

4.3.2.	Tracking self-generated motion .....	23
4.3.3.	Open questions and motivation of this thesis .....	24
5.	CONTENT OF THE THESIS .....	26
6.	LIST OF PUBLICATIONS .....	28
6.1.	<i>Journal articles</i> : .....	28
6.2.	<i>Journal articles submitted</i> :.....	28
6.3.	<i>Conference abstracts</i> :.....	28
<b>CHAPTER II .....</b>		<b>31</b>
<b>PROCESSING OF RETINAL AND EXTRARETINAL SIGNALS FOR MEMORY GUIDED SACCADES DURING SMOOTH PURSUIT .....</b>		<b>31</b>
1.	ABSTRACT .....	31
2.	INTRODUCTION .....	32
3.	EXPERIMENTAL PROCEDURES .....	34
3.1.	<i>Experimental set-up</i> .....	34
3.2.	<i>Paradigm</i> .....	35
3.3.	<i>Data acquisition and analysis</i> .....	37
4.	RESULTS.....	39
4.1.	<i>Programming of 1<sup>st</sup> saccade</i> .....	41
4.2.	<i>Saccadic latency distribution</i> .....	48
4.3.	<i>Time course of orientation</i> .....	58
5.	DISCUSSION.....	60
5.1.	<i>Saccadic reaction times</i> .....	61
5.2.	<i>Saccades compensate for self-motion</i> .....	62
5.3.	<i>Hypothesized underlying neural mechanisms</i> .....	65
<b>CHAPTER III.....</b>		<b>69</b>
<b>INTERACTION BETWEEN SMOOTH ANTICIPATION AND SACCADES DURING OCULAR ORIENTATION IN DARKNESS .....</b>		<b>69</b>
1.	ABSTRACT .....	69
2.	INTRODUCTION .....	70
3.	MATERIALS AND METHODS.....	72
3.1.	<i>Experimental set-up</i> .....	72
3.2.	<i>Paradigm</i> .....	72
3.3.	<i>Data acquisition and analysis</i> .....	74
4.	RESULTS.....	75

TABLE OF CONTENTS

---

4.1. <i>General saccadic properties</i> .....	77
4.2. <i>Programming of the first saccade</i> .....	80
4.3. <i>Time course of orientation</i> .....	84
5. DISCUSSION.....	90
5.1. <i>Saccade properties</i> .....	91
5.2. <i>Programming of the first orienting saccade</i> .....	91
5.3. <i>Time course of the orientation process</i> .....	92
5.4. <i>Proposed model</i> .....	93
6. CONCLUSION .....	96
<b>CHAPTER IV .....</b>	<b>97</b>
<b>SMOOTH ANTICIPATORY EYE MOVEMENTS ALTER THE MEMORIZED POSITION OF FLASHED TARGETS.....</b>	<b>97</b>
1. ABSTRACT .....	97
2. INTRODUCTION.....	98
3. METHODS.....	99
3.1. <i>Experiment 1</i> .....	99
3.1.1. Experimental set-up .....	99
3.1.2. Paradigm .....	100
3.1.3. Data acquisition and analysis.....	101
3.2. <i>Experiment 2</i> .....	102
3.2.1. Experimental set-up .....	102
3.2.2. Paradigm .....	103
3.2.3. Data acquisition and analysis.....	103
4. RESULTS.....	104
4.1. <i>Experiment 1</i> .....	104
4.1.1. General observations.....	104
4.1.2. Localization error.....	107
4.1.3. Temporal evolution of the error .....	109
4.2. <i>Experiment 2</i> .....	110
5. DISCUSSION.....	112
5.1. <i>Gaze orientation and perceptual localization</i> .....	113
5.2. <i>Time course of the flash-lag illusion</i> .....	113
5.3. <i>Origin of the perceptual bias</i> .....	114
6. CONCLUSIONS .....	117
<b>CHAPTER V.....</b>	<b>119</b>

TABLE OF CONTENTS

---

<b>A MODEL THAT INTEGRATES EYE VELOCITY COMMANDS TO KEEP TRACK OF SMOOTH EYE DISPLACEMENTS.....</b>	<b>119</b>
1. ABSTRACT.....	119
2. INTRODUCTION.....	120
3. BACKGROUND.....	123
4. METHODS.....	126
4.1. <i>The saccadic pathway</i> .....	126
4.2. <i>LIP mechanism</i> .....	128
4.3. <i>CB mechanism</i> .....	131
4.4. <i>Behavioral experiments</i> .....	134
5. RESULTS.....	134
5.1. <i>Analysis of LIP mechanism</i> .....	135
5.2. <i>Analysis of CB mechanism</i> .....	140
6. DISCUSSION.....	146
6.1. <i>General model discussion</i> .....	147
6.2. <i>Model comparison with data</i> .....	148
6.3. <i>Hypothesized neural substrates</i> .....	149
<b>CHAPTER VI.....</b>	<b>153</b>
<b>CONCLUSION – IMPLICATIONS OF THIS WORK AND FUTURE INVESTIGATIONS.....</b>	<b>153</b>
1. WHAT WAS THE PURPOSE?.....	153
2. MAJOR FINDINGS.....	153
3. OPEN QUESTIONS.....	155
3.1. <i>Anticipation</i> .....	155
3.2. <i>Perceptual mislocalization of flashed targets</i> .....	156
3.3. <i>Smooth eye displacement compensation</i> .....	157
4. MODEL RESULTS.....	159
<b>APPENDIX I.....</b>	<b>161</b>
<b>THE EXPERIMENTAL SET-UP.....</b>	<b>161</b>
1. GOAL.....	161
2. IMPLEMENTATION.....	162
2.1. <i>Hardware</i> .....	162
2.2. <i>Software</i> .....	164
2.2.1. <i>Basic structure of EyeLab</i> .....	164
2.2.2. <i>Building an experimental protocol</i> .....	166

TABLE OF CONTENTS

---

2.2.3. Controlling the measurement hardware .....	166
3. PERFORMANCE, SUGGESTIONS AND EXTENSIONS .....	168
3.1. <i>Performances of EyeLab</i> .....	168
3.2. <i>Possible extensions</i> .....	168
3.3. <i>Suggestions to improve the set-up</i> .....	169
<b>APPENDIX II .....</b>	<b>171</b>
<b>STATISTICS .....</b>	<b>171</b>
1. NOTATIONS .....	171
2. ONE VARIABLE, TWO SAMPLES STATISTICAL TESTS.....	172
2.1. <i>Difference between means of two samples</i> .....	172
2.1.1. Normally distributed samples (parametric tests) for $s_x' = s_y'$ .....	172
2.1.2. Normally distributed samples (parametric tests) for $s_x' \neq s_y'$ .....	173
2.1.3. Arbitrarily distributed samples (non-parametric tests) .....	174
2.2. <i>Difference between variances of two samples</i> .....	175
2.2.1. Normally distributed samples (parametric tests) .	175
2.2.2. Arbitrarily distributed samples (non-parametric tests) .....	176
2.2.3. Standard error, confidence interval and statistical significance .....	177
3. PROBABILITY DISTRIBUTION TESTS .....	178
3.1. <i>Normality tests</i> .....	178
3.1.1. The Shapiro-Wilks W-test for normality .....	178
3.1.2. The Jarque-Bera test for normality .....	179
3.1.3. Lilliefore's normality test.....	179
3.2. <i>Other distributions test</i> .....	179
3.2.1. The $\chi^2$ goodness of fit test.....	179
3.2.2. The Kolmogorov-Smirnov test .....	180
4. LINEAR REGRESSIONS.....	181
4.1. <i>Simple regression</i> .....	181
4.1.1. The regression line and significance of regression parameters .....	181
4.1.2. The correlation coefficient and its significance ...	181
4.1.3. Confidence limits around a predicted value of Y	182
4.2. <i>2<sup>nd</sup> order and multiple regression</i> .....	182

TABLE OF CONTENTS

---

4.2.1.	2 <sup>nd</sup> order and multiple regression parameters .....	182
4.2.2.	The multiple correlation coefficient.....	183
4.2.3.	Partial correlation coefficients .....	184
4.2.4.	Standard deviation of parameter estimates .....	185
4.3.	<i>Identical regressions</i> .....	185
4.3.1.	Comparison of simple regression parameters .....	185
4.3.2.	Comparison of two regression points .....	186
5.	NON-LINEAR REGRESSIONS AND CURVE FITTING .....	186
<b>APPENDIX III.....</b>		<b>189</b>
<b>DIRECT EVIDENCE OF A POSITION INPUT TO THE SMOOTH PURSUIT SYSTEM.....</b>		<b>189</b>
1.	ABSTRACT.....	189
2.	INTRODUCTION.....	190
3.	EXPERIMENTAL PROCEDURES.....	191
4.	RESULTS.....	193
4.1.	<i>General response properties</i> .....	193
4.2.	<i>Influence of flash position on smooth eye velocity</i> .....	195
4.3.	<i>Characterization of movement onset and offset</i> .....	198
4.4.	<i>Smooth pursuit deviation?</i> .....	203
5.	DISCUSSION.....	203
5.1.	<i>General discussion</i> .....	203
5.2.	<i>Smooth pursuit gain control</i> .....	205
5.3.	<i>Neural substrate of the position error input to the smooth pursuit system</i> .....	206
<b>ABBREVIATIONS .....</b>		<b>207</b>
<b>REFERENCES .....</b>		<b>209</b>

# CHAPTER I

## INTRODUCTION – SCIENTIFIC BACKGROUND

*“Everything should be made as simple as possible, but not simpler.”*  
*Albert Einstein*

### 1. The scope of this work

Mother Nature constantly inspires scientists. One of the most important sources of inspiration for engineers is the human brain. This is the case for a wide range of applications. First of all, the whole field of mathematical neural networks computation emerged from the attempt to understand the brain’s basic mechanisms. Also, many features of medical science and image analysis rely on knowledge about the visual system. Another example is the use of human movement control principles in systems engineering and industrial control mechanisms. Indeed, Johann Bernoulli (1696) and later Isaac Newton (1697) first mentioned that the quest for optimality is a fundamental property of motion in natural systems. Thus, since naturally occurring systems exhibit optimality in their motion, it makes sense to design man-made control systems in such an optimal fashion.

In 1960, R. Kalman formalized the notion of *optimality in control theory* by minimizing a general quadratic energy function, an approach first used by C.F. Gauss (1777-1855) in planetary orbit estimation. However, in biological systems different motor commands need to be coordinated and optimal control needs also to account for different motor strategies that are adapted to the actual environment. The planning and execution of natural behavior thus becomes very complex. In an attempt to gain a better understanding of optimality in natural behavior, this thesis will propose to

study a particular instance of the control of eye movements that occur in everyday life.

Vision is probably our most important sense. It drives, guides or accompanies many aspects of our behavior. Thus, it is not surprising that almost half of our cerebral cortex is involved in vision-related functions. On the other hand, another large part of our brain is dedicated to the generation and control of movement. Indeed, movement is the major behavioral response to an external stimulation. Today, vision and action systems still tend to be separated for analysis. However, one major function of the brain is to transform visual information into accurate motor commands for movement. In addition, these motor commands need to be coordinated and optimized in a behavioral and economical sense in order to ensure the species' survival.

Very particular cases of movements are those of the eye, i.e. the visual sensor itself. Here, different types of orienting and stabilizing eye movements need to be coordinated and the global movement has to be optimized to allow clear detail vision. To challenge these requirements, the brain uses different movement strategies predominantly based on visual information. However when those visual inputs are absent (e.g. in darkness), it is not yet clear, what the role of extraretinal (non visual) signals for movement coordination is.

The goal of this work is to further investigate the role of extraretinal signals in coordinating movements. In other words, how does the brain manage to keep an accurate representation of space in darkness to program and execute accurate movements? This is a major issue for space constancy, i.e. the perceptual experience of a stable world. I will use different eye movement systems as a testing bench to examine the brain's ability to control movement in darkness.

## **2. The eye and its movements**

### ***2.1. The eye plant, extra-ocular muscles and brainstem signals***

The eye provides the main sensory input from the external world to the brain. The particular optical arrangement of the eye allows the visual

world to be projected onto the back of the eye, where light is transformed into neural signals. It is indeed the retina that is responsible for this transformation. Two types of light capturing devices coexist: rods and cones (contrast and colour vision). Primates also possess a particular region on the central retina, where the surface density of cones is very high (rods have higher density in the retinal periphery). This region is called the fovea and represents the zone of maximal visual acuity (visual acuity declines steeply towards the retinal periphery).

Because primates have a fovea, they need to orient it toward the object of interest. Indeed, precise vision of an object requires its image to be held fairly steadily on the foveal region of the retina. Therefore, the eye plant is equipped of three pairs of antagonist muscles (Fig. I-1) that can move the eyes to ensure visual stability. The Medial and Lateral Recti muscles adduct and abduct the eye (rotation around the y-axis), i.e. they move the eyeball towards the nose or away from it. The four other muscles have more complicated actions because their movement is composed of vertical and torsional components (Suzuki et al. 1999).

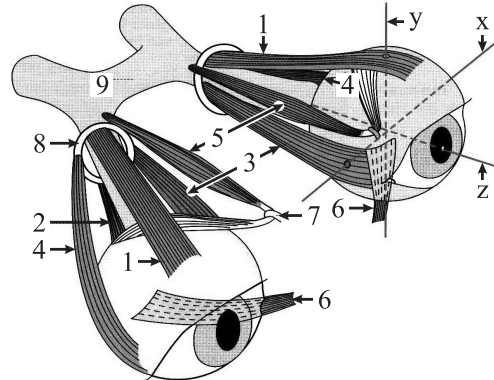


**Figure I-1:** Extra-ocular muscles. (1) Superior rectus, (2) inferior rectus, (3) medial rectus; (4) lateral rectus; (5) superior oblique; (6) inferior oblique; (7) trochlea; (8) annulus; (9) optic chiasm. (x,y,z) stand for the three axes of possible eye rotations.

Extra-ocular muscles are innervated by three groups of motoneurons. The Lateral Rectus is innervated by the Abducens Nerve (cranial nerve VI), the Superior Oblique muscle is innervated by the Trochlear Nerve (cranial nerve IV) and all the other extra-ocular muscles are

innervated by the Oculomotor Nerve (cranial nerve III). To move the eye, the brain has to overcome the mechanical constraints of the eye plant. Therefore, a motor command is sent to the muscles by means of a *pulse* of innervation, i.e. a burst of activity of the motoneurons. Once the eye reached a new position in the orbit, a position command (*step* of innervation) is sent to the muscles. This step of innervation ensures steady contraction of the extra-ocular muscles to overcome the elastic restoring forces that tend to bring the eye back to its primary position. Thus, to move the eyes, the brain applies a combined *pulse-step* command (Robinson 1975). This pulse-step command is generated by the brainstem neural structures (Keller and Missal 2003).

Moving the eye is essential to orient the line of sight and / or to stabilize gaze on a stationary or moving object of interest. During self-movement, several eye movement reflexes perform this stabilization. There are three principal orientation eye movements, two stabilization eye movements and fixation. Hereafter, I will shortly describe these movements with emphasis on two orienting eye movements, i.e. smooth pursuit and saccades. Note that in this thesis only eye movements are analysed and the head is supposed to be fixed.

## 2.2. *Saccades*

### 2.2.1. *General behavior*

Saccades are the fastest eye movements used to bring an object of interest onto the foveal region of the retina. As the word “saccade” (*French*: jerk) indicates, they are rapid step-like eye movements that reorient the eyes in space (see Fig. I-2B). Saccades are very stereotyped with extremely high acceleration and deceleration (up to 30 000 deg/s<sup>2</sup>) and can reach velocities around 500 deg/s in the human (Bahill et al. 1975). Because of their high speed and short duration (typically < 100 ms), saccades are executed in open-loop, i.e. their execution is not controlled by visual feedback (visual delay  $\approx$  100 ms), and were thus initially considered as ballistic movements. Saccades can be made to visual, remembered, tactile, auditory or even imaginary targets at will.

The main input used by the oculomotor system to program the amplitude of a saccade is the distance between the target and the eyes, i.e. position error. The saccadic system uses an undershooting strategy with a

gain around 0.9 for eye movements to visual targets (Becker 1991). Usually, the saccadic reaction time is around 200 ms (Robinson 1965), but this latency can be reduced to less than 100 ms in particular experimental conditions (Findlay 1981; Fischer and Ramsperger 1986).

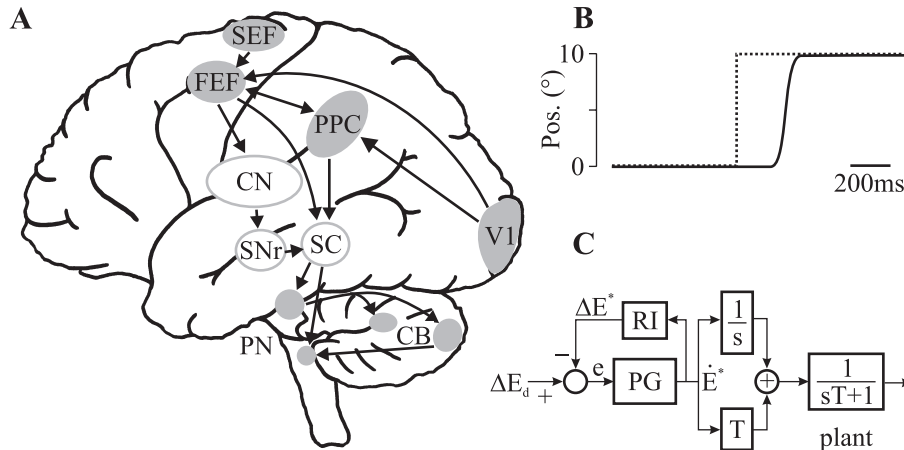


**Figure I-2:** The saccadic system. **A.** Main neural structures involved in the control of saccades. Grey structures are on the surface of the cortex, white structures are hidden by the cortex. **B.** Typical example of a saccadic eye movement. Target (dotted line) and eye (solid line) positions are represented over time. **C.** Schematic representation of a model of the saccadic system. See text for more details.

### 2.2.2. Latencies

Saccadic latency shows some natural variability, even under fixed experimental conditions, where the influence of attention, target selection or other factors is minimized. One can find many attempts in the literature to explain this variability. Statistical considerations about the process of decision-making have led to a variety of hypothetical probability density functions for reaction time analysis. Practically, to describe the observed form of those probability density functions (not normally distributed), they need to meet only two requirements, i.e. the probability for reaction times  $< 0$  must be zero and the shape of the distribution must be skewed out for latencies above the maximum probability. These conditions are met by a large number of statistical functions, like the Lower Bound Extreme Value Distribution, the Fisk (or Log-Logistic) distribution, the Gumbel (or Log-Weibull, Gompertz or Fischer-Tippett) distribution, the Inverse Normal (or

Inverse Gaussian or Wald) distribution, the Log-Normal (or Cobb-Douglas or Anti-Log-Normal) distribution, the Burr distribution, the  $\chi^2$  distribution, the Weibull distribution or the Gamma distribution. However, here I will describe in detail a very successful saccade latency distribution model, called the LATER (Linear Approach to Threshold with Ergodic Rate) model (Carpenter and Williams 1995).

The LATER model (Fig. I-3) provides a simple explanation for the distribution of the saccadic reaction times (Carpenter and Williams 1995). A decision signal  $S$  rises linearly from an initial level  $S_0$  in response to a stimulus, until it reaches a threshold level  $S_T$  at which point a saccade is initiated. The distribution of saccadic latency  $T$  is explained by assuming that the rate of rise  $r$  varies randomly between trials in a Gaussian fashion. Since the reaction time  $T$  is proportional to  $(S_T - S_0)/r = \theta/r$ , this will make the inverse of  $T$  normally distributed and thus  $T$  is recinormal.

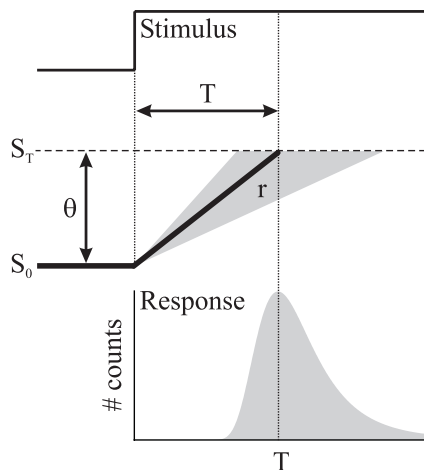


**Figure I-3:** A model for saccade latencies: LATER. Once a stimulus appears, a decision signal (bold line) rises from an initial level  $S_0$  to a threshold  $S_T$ . The rate of rise  $r$  is gaussian. The response is a smeared out latency distribution.

The advantage of the recinormal probability density function is twofold. (1) Empirically, this distribution fits very well the data (Asrress and Carpenter 2001; Carpenter and Williams 1995; Leach and Carpenter 2001; Reddi et al. 2003; Reddi and Carpenter 2000). And (2), the theoretically assumed rise-to-threshold of a decision signal has a neural counterpart, as demonstrated for neurons in the Frontal Eye Fields (FEF) (Hanes and Schall 1996; Schall 2001; Schall and Bichot 1998; Schall and Hanes 1998; Schall and Thompson 1999). Another interesting property of the LATER distribution is the linear relationship between the median latency

$[= (S_T - S_0)/\mu]$ , where  $\mu$  is the mean latency] and the prior log-likelihood  $S_0 = \log(p)$  ( $p$ : prior probability for the decision process). This behaviour has been verified experimentally (Carpenter and Williams 1995). In addition to the description of saccadic latencies, the LATER model has also been extended successfully to saccadic countermanding (Asrress and Carpenter 2001) by assuming a winner-take-all competition between two independent LATER decision processes for the start and stop signals.

### 2.2.3. Model

The very stereotyped dynamics of saccadic eye movements are reflected in the so-called “main sequence relationship” (Bahill et al. 1975; Robinson 1968) between saccade duration, amplitude and maximum speed. Robinson developed one of the first models of the saccadic system (Robinson 1975; Westheimer 1954). Today, the basic architecture of Robinson’s model still holds, although some modifications with respect to the nature of the input signals and the internal feedback loops have been proposed. Here, I shortly describe the basic architecture of an adapted saccade model (Jürgens et al. 1981; Scudder 1988) based on Robinson’s initial ideas (Fig. I-2C). They suggested that a desired eye movement  $\Delta E_d$  is compared to an internal representation of eye displacement  $\Delta E^*$  to produce an error signal  $e$ . The pulse generator (PG) transforms this error signal  $e$  into a desired eye velocity signal  $\dot{E}^*$ . On one hand, because visual delays do not allow control of saccades by continuous visual feedback, this desired motor command  $\dot{E}^*$  is internally monitored by a resettable integrator (RI, reset after each saccade) to obtain an internal representation  $\Delta E^*$  of instantaneous eye displacement. On the other hand, the desired eye velocity command  $\dot{E}^*$  is sent to two parallel premotor pathways, a direct and an integral pathways that compensate for the eye plant dynamics and provide the pulse-step motor command. This command is then sent to the eye plant that is modelled by a low-pass filter.

### 2.2.4. Neurophysiology

At the neural level, visual information is first projected from the retina via LGN to the Primary Visual Cortex (V1) and to the superficial layers of the Superior Colliculus (SC), where the location of a visual stimulus is coded in retinal coordinates (Leigh and Zee 1999). The saccadic

system has to transform this two-dimensional retinotopic representation of the stimulus into a motor command for the three-dimensional arrangement of the extra-ocular muscles, encoded in terms of discharge frequency and duration. Furthermore, a transformation from retinal coordinates into craniotopic coordinates is necessary (Crawford et al. 2003; Crawford and Guitton 1997; Crawford et al. 2000; Henriques and Crawford 2000; Klier and Crawford 1998). This will be accomplished by a large number of areas in the brain. Figure I-2A represents only the most important structures classically involved in the generation of saccades (Leigh and Zee 1999).

Schematically, V1 projects to regions in the Posterior Parietal Cortex (PPC) that encode visual targets in spatial coordinates (Andersen et al. 1990b) and play also a role in visual attention (Morrow 1996). V1 also projects (indirectly) to the Frontal Eye Fields (FEF), involved in visuo-motor planning and target selection (Schall 2001). In addition, FEF receives input from PPC (Andersen et al. 1990a; Blatt et al. 1990) and the Supplementary Eye Fields (SEF) that are involved in eye movements as part of learned complex behaviours (Leigh and Zee 1999), like sequences of memory-guided saccades or anticipatory saccades (Gaymard et al. 1990; Petit et al. 1996). V1, PPC and FEF all project to a central structure for saccade production, i.e. the Superior Colliculus (SC) (Leigh and Zee 1999). Superficial layers of SC are “visual” whereas intermediate layers are “motor”. Despite direct connections between superficial and intermediate layers of SC, intermediate SC receives its primary input from cortical areas and visually induced activity (from V1) in the superficial layers of SC does not necessarily lead to movement activity in intermediate layers and conversely. While PPC has direct projections to intermediate SC, FEF has two distinct pathways, i.e. one direct and one indirect via the Caudate Nucleus (CN) – concerned with complex aspects of oculomotor behaviour like memory, expectation, attention and reward (Hikosaka et al. 1989; Kawagoe et al. 1998) – and the Substantia Nigra (SNr) that appears to facilitate the initiation of more voluntary, self-generated saccades made in the context of learned behaviour (Hikosaka and Wurtz 1983a, b, c, d). The motor command from the intermediate SC is sent to the Pontine Nuclei (PN) and the Cerebellum (CB) (Leigh and Zee 1999). CB appears to be important for the control of saccade accuracy, dynamics and trajectory in both online and long-term aspects. The brainstem circuit then shapes the final output commands (Keller and Missal 2003) and sends them to the extra-ocular

muscles. Of course, this is not a full description of all the brain areas involved in the generation and execution of saccades, but for the sake of clarity, only the most important pathways were presented.

### 2.3. *Smooth pursuit*

#### 2.3.1. *General behavior*

To allow clear vision of a moving target, its image must be stabilized on the retina. The eyes thus need to track the target, a movement called smooth pursuit. The main input to the smooth pursuit system is the relative speed between the eye and a visual stimulus, i.e. retinal slip. However, position error and target acceleration have also been shown to have some influence on smooth pursuit. Because smooth pursuit is a slow eye movement ( $< 100$  deg/s), it is controlled in closed loop with respect to vision.

The smooth pursuit latency is about 100 ms but can drop down to less than 70 ms in particular situations. For low frequencies, the pursuit gain is close to unity but drops rapidly for frequencies above 1 Hz. If a smooth pursuit target suddenly disappears, the smooth pursuit response decays after around 100 ms, usually with a time constant of 90 ms. Beside the feedback control, there is also a predictive component of smooth pursuit, i.e. smooth anticipation. If a target motion is predictable, the smooth pursuit system takes advantage of that knowledge and drives anticipatory smooth eye movements to overcome the pursuit reaction time.

#### 2.3.2. *Model*

Smooth pursuit has classically been described by a negative feedback loop (Robinson et al. 1986) as shown in Fig. I-4C. Eye velocity  $\dot{E}$  is subtracted from target velocity  $\dot{T}$  to produce the retinal slip  $\dot{e}$  (Krauzlis and Lisberger 1994; Lisberger et al. 1987). The desired eye acceleration  $\ddot{E}^*$  is generated by three separate pathways: a motion transient, a velocity and an acceleration pathway. The memory loop (MEM) works as a neural integrator to transform  $\ddot{E}^*$  into the desired eye velocity  $\dot{E}^*$  (Churchland et al. 2003). Beside its neural integrator function, MEM is also used to memorize previous target velocity or sequences in order for the model to mimic smooth anticipatory eye movements and smooth pursuit maintenance during

transient target extinction (Bennett and Barnes 2003). The final pulse-step pathway is in common with the saccadic system (see section 2.2.3).

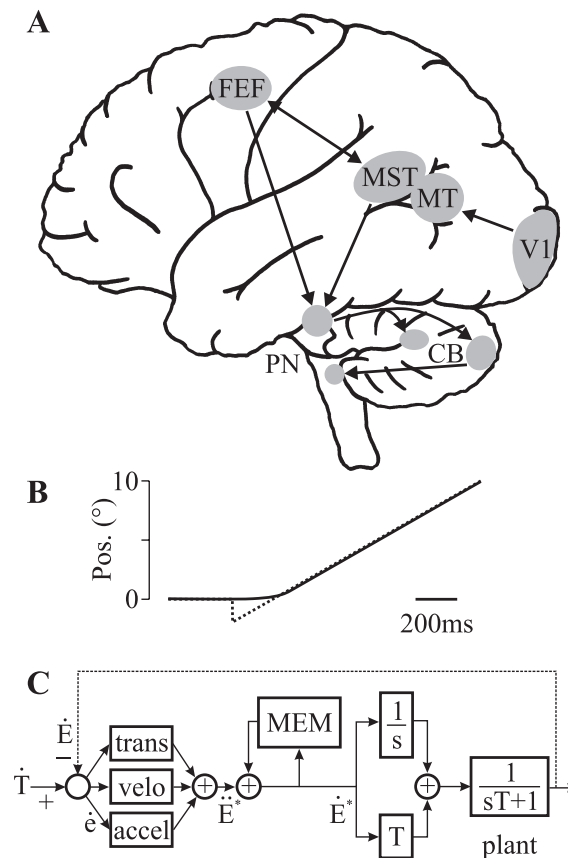


**Figure I-4:** The smooth pursuit system. **A.** Major neural structures involved. **B.** Typical response. **C.** Hypothetical model. See text for more details.

### 2.3.3. Neurophysiology

Figure I-4A represents a hypothetical neural scheme for the generation of smooth pursuit eye movements (Leigh and Zee 1999). The Primary Visual Cortex (V1) projects to the Middle Temporal area (MT) involved in visual processing of direction and speed of moving visual stimuli encoded in retinotopic coordinates (Newsome et al. 1985; Newsome et al. 1988). MT projects to the Middle Superior Temporal visual area (MST) that lies adjacent to MT (Ungerleider and Desimone 1986). MST neurons are also involved in motion processing and smooth pursuit generation, but differ

from MT neurons by taking into account the effect of eye and head movements (Bradley et al. 1996; Komatsu and Wurtz 1988a, b; Newsome et al. 1988; Squatrito and Maioli 1997; Thier and Erickson 1992). This implies that MST receives an efference copy of the eye and head movement commands to estimate the direction of heading during smooth pursuit. Visual areas MT and MST have reciprocal connections with the Frontal Eye Fields (FEF), believed to play a role in predictive aspects of smooth pursuit (Tusa and Ungerleider 1988; Ungerleider and Desimone 1986). Both MT/MST and FEF project to the Pontine Nuclei (PN) (Leigh and Zee 1999), which contain cells encoding a mixture of eye movement signals and visual information (Mustari et al. 1988; Suzuki et al. 1990; Thier et al. 1988). PN projects to several regions in the Cerebellum (CB). CB plays a critical role in synthesizing the pursuit signal from visual and ocular motor inputs (Leigh and Zee 1999). Finally, the pontine pathways shape the muscle innervation commands for the eye movement (Keller and Missal 2003). Once again, this very brief description of smooth pursuit pathways is far from being complete and only gives a rough overview of the most important areas involved in smooth pursuit generation.

#### **2.4. *Other eye movements***

Beside the two above-mentioned eye movements, there is a third gaze-shifting mechanism – vergence – needed for binocular vision. Indeed, convergence ensures that the system keeps both eyes aligned with the visual targets as those targets vary in depth. At the neural level, this is accomplished by adding for each eye an opposite gaze control signal to the shared saccadic and pursuit signal. This concept, that a common saccadic and/or pursuit signal is sent equally to both eyes and that vergence signals are added for each eye separately, is known as Hering’s law of equal innervation.

To these gaze-shifting mechanisms are added two types of gaze stabilizing eye movements. Their purpose is to counteract self-motion or large-field motion thus ensuring a stable image of the visual world on the retina – a good visual acuity. These gaze stabilizing movements counterrotate the eyes during head, body or background movements. Generally, we distinguish two types of gaze stabilization mechanisms, i.e. the vestibulo-ocular and the optokinetic systems. The vestibulo-ocular reflex (VOR) receives information about head rotation from the semicircular

canals. The optokinetic reflex (OKN) relies on the speed and direction at which the visual world shifts across the retina. Both systems then precisely compensate for this rotation by an exact counterrotation of the eyes. However, their dynamics are very different. VOR is an open-loop mechanism with respect to vision with reaction times as short as 16 ms and its performance is best for high frequencies (0.5 to 10 Hz), where the gain reaches between 0.8 and 1.0 (phase lag 180°). Because the VOR frequency domain is close to the natural head movement frequency, these performances ensure low values for the image slip on the retina. In contrast to VOR, OKN is controlled closed-loop with respect to vision. Because of the visual delays, it needs more than 70 ms to move the eyes and hence performs best for low frequencies (0.05 to 0.5 Hz). Therefore VOR and OKN are complementary and work in synergy to ensure the best visual stability during self-motion.

### **3. Interaction between smooth pursuit and saccades**

Primates use a combination of smooth pursuit and saccadic eye movements in order to center and stabilize the retinal images of objects of interest. If the oculomotor system would control both eye movements independently, it would run into trouble because both movement strategies could be potentially conflicting and choose distinct, independent tracking goals, e.g. in the presence of multiple visual objects. Therefore it seems most natural that smooth pursuit and saccades work in synergy. This view will be defended hereafter.

#### ***3.1. Velocity input to the saccadic system***

In natural conditions, visual objects of interest often move in the environment. To orient gaze toward such moving targets, the oculomotor system triggers so-called “catch-up saccades” that are typically preceded and/or followed by smooth pursuit eye movements. In this situation, the question arises if and how the saccadic system adapts its motor command to account for the smooth eye and object motion.

In contrast with the initial believe (Jürgens and Becker 1974), the smooth pursuit and saccadic motor commands add up during catch-up saccades (Keller and Johnsen 1990; Smeets and Bekkering 2000). This has been confirmed for catch-up saccades triggered to a target that initially moved at constant velocity and suddenly changed velocity combined with a

target jump (de Brouwer et al. 2002a). de Brouwer et al. (2002a) used the saccadic main sequence relationship (Bahill et al. 1975) to show unambiguously that there is a linear addition of smooth pursuit and saccades. As a consequence, the smooth pursuit component of the measured saccade amplitude has to be removed in order to study the saccadic motor command in isolation.

As previously mentioned, the classical input to the saccadic system is position error, sampled around 100 ms before the onset of the saccade. However, if this were the only input, saccades to moving targets would miss their goal because of the relative motion between target and eyes during the saccadic latency period. Therefore, it has been proposed very early that catch-up saccades might use information about target speed to adapt their metrics (Newsome et al. 1985; Rashbass 1961; Robinson 1965, 1973). It has been demonstrated since then, that after fixation, catch-up saccades used target velocity information sampled around 100 ms before the onset of the eye movement to extrapolate the future target position (Gellman and Carl 1991; Keller and Johnsen 1990; Ron et al. 1989a, b). This is illustrated in Fig. I-5.

However, only very recently, the exact nature of the predictive component of catch-up saccades has been described (de Brouwer et al. 2002a; de Brouwer et al. 2001). de Brouwer et al. (2002a) showed that beside the position error, the saccadic system uses the relative velocity between target and eyes (retinal slip) to program catch-up saccades. They estimated that retinal slip information needed a minimum of 90 ms to be taken into account in the prediction of the future trajectory of the moving target. As a result, catch-up saccades (the saccadic command without the smooth pursuit contribution) were found to be programmed as follows:

$$S_{Amp} = 0.9 \cdot PE + 0.15 \cdot RS \quad \text{Eq. I-1}$$

Position error (PE) and retinal slip (RS) were sampled 100 ms before the onset of the saccade. PE was thus taken into account by 90% whereas RS was used to predict the future target position 150 ms after the sampling time.

Another important question is how the saccadic system takes the decision to trigger a saccade. About 40 years ago, Rashbass (1961) established a fundamental link between the control of smooth pursuit and

saccades by showing that saccades are not triggered if the system estimates that smooth pursuit alone is sufficient to track the target accurately. However, only recently, de Brouwer et al. (2002b) showed that the system really uses an instantaneous prediction of the time when the eyes will cross the target trajectory (“eye crossing time”) to evaluate whether a saccade needs to be triggered or not. This linear extrapolation uses combined PE and RS information. If the eye crossing time falls between 40 and 180 ms, no saccade is triggered and the target tracking remains purely smooth. If the eyes leave this “smooth zone”, a catch-up saccade is triggered after around 125 ms.

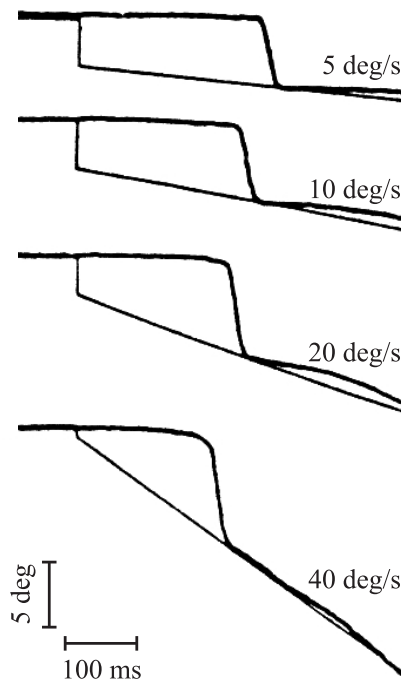


**Figure I-5:** Saccade amplitude modulated by retinal slip. The initial target step size was adapted to keep the saccade amplitude approximately constant. Four different target speeds are represented. Adapted from Keller and Johnsen (1990).

These results nicely illustrate how two very different motor systems interact to optimise performance. However, the above-mentioned results only apply to visually guided eye movements, i.e. where retinal slip information is present. In the following original work, I will investigate how this interaction is implemented when visual information about motion lacks.

### 3.2. Position input to the smooth pursuit system

As described in section 2.3, the classical input to the negative feedback smooth pursuit control system is retinal slip. However, behavioural research has revealed that position error could also drive the smooth pursuit system, at least in certain conditions and to some extent. Pola and Wyatt (1980) first reported experimental situations where target position evoked a smooth pursuit response. They used a square wave stimulus and asked subjects to track the target, which produced large smooth pursuit eye velocities. In an additional experiment, these authors also observed that during smooth pursuit initiation to a step-ramp target (the target made a variable step in position followed by a constant velocity pursuit ramp) the pursuit velocity was modulated by the size of the position step. This study initiated several other investigations.

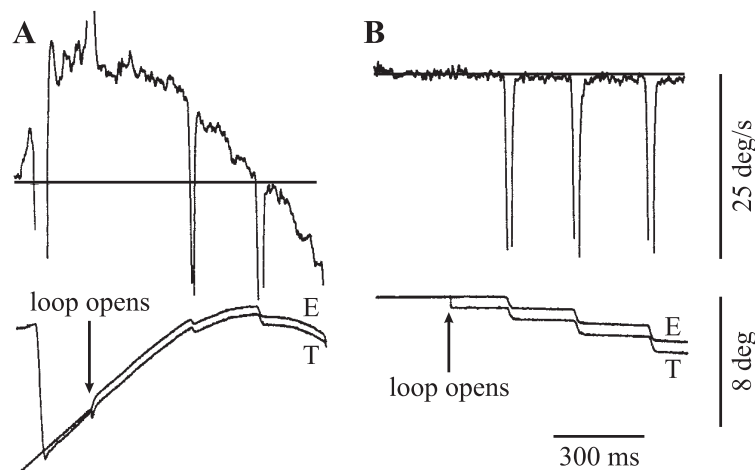


**Figure I-6:** Position input to smooth pursuit system. A. During ongoing smooth pursuit a constant offset between target (T) and eye (E) positions (lower panel) modulates the smooth eye velocity (upper panel). B. In contrast, during fixation a position error artificially held constant does not initiate a smooth pursuit response. Adapted from Morris and Lisberger (1987).

An interesting observation is that small target steps during ongoing smooth pursuit modulate the eye velocity, contrarily to target steps during visual fixation (Carl and Gellman 1987; Morris and Lisberger 1987). This modulation is directed towards the target and presents an asymmetry with

respect to the ongoing movement direction, i.e. the modulation is larger when the target jumps back. In addition to this finding, it has also been reported that a sudden target jump produces large smooth eye movement responses in a situation where the target is stabilized on a retinal position slightly offset from the fovea (Morris and Lisberger 1987; Segraves and Goldberg 1994; Wyatt and Pola 1981). Figure I-6 nicely illustrates these properties.

Although the oculomotor community generally agrees on the presence of a position input to the smooth pursuit system, not much is known about its dynamics and neural origins. One of the reasons for this lack of knowledge is certainly the experimental difficulty to separate position and velocity stimuli in order to investigate their effects in isolation. In one of the following chapters, I will present an original study where I address this problem.

### ***3.3. Common neural pathways***

Historically, saccades and smooth pursuit have been viewed as largely independent motor systems that overlap only in the initial visual pathway [retina – Lateral Geniculate Nucleus (LGN) – Striate Cortex (V1)] and at the final stages of the oculomotor pathway [in the brainstem at the level of the Motor Neurons (MN)]. However, several findings show that the originally proposed segregation of both motor systems does not hold. Contrarily, there seems to be a tight interaction between both motor systems at the neural level, as the above-described behavioural results would have suggested. This interaction takes place at all levels of visual, perceptual, pre-motor and motor processing and includes most of the classical areas initially attributed exclusively to one motor system. Therefore, I will only give a brief overview of where the most important interactions take place, starting from the cortical level down to the brainstem.

- Areas MT and MST are part of the motion processing pathway for the smooth pursuit system. However, lesions in these areas alter the metrics of catch-up saccades (Newsome et al. 1985) and microstimulation of MT/MST delays the onset of saccades to stationary targets (Komatsu and Wurtz 1989).
- Area LIP also appears to be involved in the control of both saccades and pursuit, as stimulation produces both types of eye movements (Kurylo

---

and Skavenski 1991). During pursuit, many LIP neurons exhibit direction-specific activity (Bremmer et al. 1997; Sakata et al. 1983) often modulated by eye position and other extraretinal signals. This is consistent with the role of LIP in transforming visual stimuli into different non-retinotopic reference frames.

- At the level of FEF, smooth pursuit and saccade related neurons are located in two distinct, mostly non-overlapping regions, which suggests that they are parallel but distinct. Furthermore, it has been suggested that area SEF might participate in the planning of both saccade and pursuit eye movements (Heinen 1995; Heinen and Liu 1997; Missal and Heinen 2001; Russo and Bruce 2000; Schall 1991a, b; Schlag and Schlag-Rey 1987; Tian and Lynch 1995).
- Neurons in the rostral SC (rSC), corresponding to the representation of the central visual field, show activity during saccades, smooth pursuit and fixation (Krauzlis et al. 2000, 1997), compatible with the idea that one function of rSC might be to specify the eye movement goal regardless of the adopted motor strategy (Krauzlis 2003, 2004; Krauzlis et al. 2004).
- In addition to its role in modulating the motor command for saccades (Noda and Fujikado 1987), the cerebellar oculomotor Vermis is also involved in pursuit. Current knowledge proposes that the Vermis might shape the trajectories of pursuit and saccades (Krauzlis 2004; Krauzlis and Miles 1998; Robinson et al. 1993; Takagi et al. 2000), i.e. modify the commands for eye acceleration / deceleration.
- Brainstem “burst” neurons in Paramedian Pontine Reticular Formation (PPRF) and the rostral interstitial nucleus of the Medial Longitudinal Fasciculus (riMLF) – classically, the caudal pons (PPRF) is important for horizontal saccades and the rostral mesencephalon (riMLF) for vertical saccades (Buttner-Ennever and Horn 1997) – are active during both saccades and pursuit (Keller and Missal 2003; Missal et al. 2000). In addition, some Omni-directional Pause Neurons (OPNs) – classically gating saccades – modulate their activity by one-third during smooth pursuit (Missal and Keller 2002). These findings suggest that common mechanisms assemble and gate the motor commands for saccades and pursuit, involving shared circuitry at the brainstem level (Keller and Missal 2003).

As mentioned by Krauzlis (2004), an alternative view to the large number of interactions between distinct smooth pursuit and saccadic pathways might be that the control of pursuit and saccades represent two different outcomes from a single cascade of sensory-motor function.

#### **4. Extraretinal signals and the sense of motion**

Now that we described how the two major eye movement systems interact using retinal information, we can investigate what signals are employed to account for self-generated motion in the absence of vision. When our eyes navigate through the visual environment, the perception of space has to be constantly updated. Nevertheless, usually we perceive stationary objects as immobile, a property named “space constancy”. To achieve visual stability, the brain must discriminate between changes in the retinal image arising from self-generated movements (eye movements, head movements, etc) and changes originating from movements in the visual environment. Therefore, the visual system requires retinal motion input and extraretinal internal motor command information. In addition, extraretinal proprioceptive (= sensation of movement, position and muscle tension from the extra-ocular muscles) signals might also be available. The brain thus needs to account for self-movement to remap the internal representation of space. In the next few paragraphs, I will first discuss the controversial issue of proprioception in oculomotor control, known as “inflow” hypothesis (Fig. I-7A). Secondly, the alternative “outflow” hypothesis (Fig. I-7B) that uses “efference” copies of the outgoing motor command (also called corollary discharge) will be described. In a third part, I will shortly lay out how these signals contribute (if they do) to the perception of self-motion to ensure space constancy.

##### ***4.1. The role of proprioception in oculomotor control***

The inflow hypothesis holds that afferent signals from the extra-ocular muscles provide the necessary information about position and movement of the eyes (Sherrington 1918). Indeed, two types of receptors provide muscle proprioceptive signals, i.e. tendon organs and muscle spindles (reviewed by Ruskell 1999). The principal role of Golgi tendon organs (absent in humans contrarily to other primates) is to measure tension (position sensitivity), whereas the function of muscle spindles is to measure

the length of the muscle (position and velocity sensitivity). Proprioceptive afferents from the extra-ocular muscles are found in all of the important structures involved in visual and oculomotor control, including the Cerebellum, the Superior Colliculus, the Thalamus, the Lateral Geniculate Nucleus and the Visual Cortex.

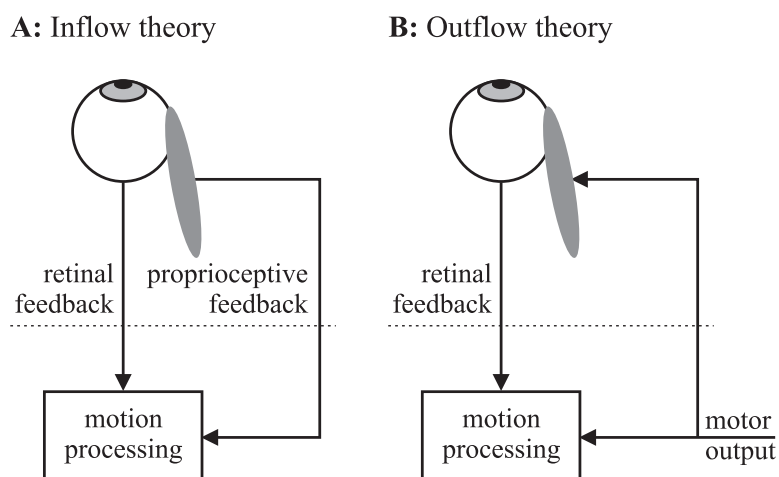


**Figure I-7:** The two hypotheses of eye position sense. **A.** The inflow theory uses proprioceptive input from the extra-ocular muscles. **B.** In the outflow theory motion processing mechanisms have access to a copy of the outgoing motor command.

How does proprioception influence oculomotor control? Today, the role of proprioception remains uncertain and speculative (Weir et al. 2000). Several findings indicate that proprioception may contribute to the immediate online control of eye movements. First, extra-ocular muscle proprioception seems to contribute to fixation stability (Fiorentini and Maffei 1977) and the maintenance of ocular alignment during fixation (Lewis et al. 1994). Second, after a period of passive deviation of one eye, a change in phoria (*def.*: any tendency of the lines of vision to deviate from the normal when binocular fusion of the retinal images is prevented) is observed, which corresponds to the direction of the original deviation (Gauthier et al. 1995; Gauthier et al. 1994). Also, using extra-ocular muscle vibration, the horizontal and vertical position of the non-stimulated eye could be modified depending on the stimulated muscle (Lennerstrand et al. 1997). Third, saccade and smooth pursuit eye movements could be modified by a perturbation in proprioception. Memory guided saccades were

influenced by vibrating the extra-ocular muscles (Allin et al. 1996) and impeding the movement of one eye reduced the amplitude of the other eye (Knox et al. 2000). Proprioception also changed the initiation and early maintenance of smooth pursuit (Weir and Knox 2001) and the smooth pursuit response to a change in target velocity has also been modified using proprioceptive feedback (van Donkelaar et al. 1997). And fourth, extra-ocular muscle vibration produces illusory motion of visual targets (Roll et al. 1991; Skavenski 1972).

However, other studies provide evidence that there is no (or only very limited) direct influence of proprioception in online oculomotor control. First, the oculomotor system in primates lacks a stretch reflex (Keller and Robinson 1971). Second, after deafferentation, monkeys could still make accurate saccades (Guthrie et al. 1983). Third, one has only a very limited (or no) knowledge of where the eyes are pointing (Bock 1986; Bock and Kommerell 1986; Skavenski 1972). Fourth and most importantly, a recent study examined the effect of bilateral proprioceptive deafferentation of the extra-ocular muscles on eye movements in monkeys (Lewis et al. 2001). Lewis et al. (2001) analysed the alignment of the eyes, saccades, smooth pursuit, VOR and did also examine visually mediated adaptation of ocular alignment, saccades and pursuit. They reported no effect of the deafferentation on baseline oculomotor control for both the acute and long-term (after 5 weeks) measures.

Taking it all together, extra-ocular muscle proprioception seems to play a limited role in the online control of eye movements. A detailed examination of muscle spindles questions their capacity to provide useful proprioceptive information (Ruskell 1999). It has been suggested that the proprioceptive mode of action was consistent with a long-term adaptive effect in which afferent feedback together with retinal information calibrates the efferent motor commands (Lewis et al. 2001). Another possible role of proprioception might lie in the development and maintenance of binocular visual function (reviewed by Buisseret 1995).

#### ***4.2. Efferent feedback loops and eye movements***

The outflow hypothesis (von Helmholtz 1866) holds that central monitoring of a copy of the motor command sent to the extra-ocular muscles – called efference copy or corollary discharge – provides the necessary

extraretinal information to determine gaze direction. As a way to monitor eye movements, corollary discharge has two main advantages over proprioception: (1) it provides information even before movement onset and (2) it does not rely on the integrity of sensory receptors. Note that an eye position efference copy signal is always accurate, since in natural conditions the eye is never perturbed (as this might be the case for example for head or arm movements). Therefore a corollary discharge signal is sufficient to provide information about the current eye position in the orbit and a priori there is no need for proprioception.

The presence of corollary discharge signals in the brain is well established and no more a matter of debate (reviewed by Bridgeman 1995; Sommer and Wurtz 2004b). Efference copy accompanies all voluntary and some involuntary eye movements including pursuit, saccades, VOR and OKN. Motor related signals are in fact exchanged between different cortical and subcortical levels. Here are some of the major identified pathways involved in smooth pursuit and saccadic eye movements.

- It seems unlikely that motoneuron activity reached the saccade generating circuit (Bridgeman 1995). However, signals from the saccade generating circuitry related to the saccade dynamics reach SC (Keller and Edelman 1994; Keller et al. 1996a; Soetedjo et al. 2002) and SC seems to be inside the online gaze control feedback loop (Matsuo et al. 2004), although this is still controversial.
- Recently, one of the best known corollary discharge pathways is the one that ascends from SC via MD to FEF (Sommer 2003; Sommer and Wurtz 2002, 2004a, b). But there are other structures related to the saccadic and smooth pursuit systems that also project to FEF via the Thalamus, like SNr and the Dentate Nucleus (DN) in CB (Lynch et al. 1994).
- The parietal cortex – implicated in sensory processing, sensory-motor integration and visuo-motor spatial updating mechanisms (Crawford et al. 2004; Medendorp et al. 2003) – receives multiple corollary discharge signals. These are either direct or indirect (via Thalamus) projections originating from SC, Hippocampus (presumably involved in a spatial memory system useful for navigation) and DN (Clower et al. 2001).

Behaviourally, several important findings have been attributed to efference copy signals. First, it has been stated that efference copy must

provide information on eye position since the absence of extra-ocular muscle proprioception does not acutely affect eye movement control (Bridgeman 1995; Lewis et al. 2001). Second, in darkness subjects perceive an afterimage as moving with the eye (Matin 1986). However, because an afterimage is stationary on the retina, its apparent movement in space must be due to extraretinal information (efference copy) signalling eye movement. This argument does also hold for the proprioception hypothesis. Third, the errors and compression of visual space measured in localization experiments of perisaccadic flashes reflect the anticipation of the consequences of the upcoming saccade (Awater and Lappe 2004; Kaiser and Lappe 2004; Michels and Lappe 2004; Morrone et al. 1997; Ross et al. 1997; Ross et al. 2001). This suggests the use of efference copy signals.

### ***4.3. Self-generated motion and space constancy***

#### *4.3.1. Eye position information*

Everybody has a subjective spatial perception of body position relative to the environment. This egocentric space is determined by vision and by the position of the eyes in the head and the head relative to the body. For instance, an object foveated at an eccentric orbital position is perceived as offset by the same amount from the straight-ahead direction. It is well established that neck muscle proprioception provides information about the head position relative to the body (Biguer et al. 1988; Han and Lennerstrand 1999; Karnath et al. 1994). However, today the mechanism to determine eye position in the head is not established.

Classically, the literature supports the outflow theory as the main source for extraretinal signal that provides eye position information (Bridgeman 1995). However, recent evidence suggests that proprioception also plays a role in spatial localization, although not a predominant one (Weir et al. 2000). E.g. manual pointing shifts induced by passively rotating on eye (Gauthier et al. 1994), induced by eye muscle vibration (Velay et al. 1994) or after anaesthesia of the ophthalmic branch of the trigeminal nerve (proprioception) (Ventre-Dominey et al. 1996) have been reported. Based on several experimental results, Bridgeman (1995) estimated the respective contribution of proprioception and efference copy signals on space perception. He found that in the absence of visual context (like a structured background, etc), the resulting gains for outflow and inflow were 0.612 and

0.256 respectively. This means that if efference copy were absent, there would be a movement induced shift in space perception of 74%, whereas the absence of proprioception would result in a perceptual offset of 39% with respect to movement amplitude. Note that the overall gain for extraretinal signals is less than 1.

#### 4.3.2. *Tracking self-generated motion*

Irrespectively of the relative role of efference copy and proprioception, space constancy during self-generated motion has been extensively studied for the *saccadic* system by means of two experimental paradigms, i.e. the double-step and the colliding saccades paradigms (Aslin and Shea 1987; Becker and Jürgens 1979; Dassonville et al. 1992; Dominey et al. 1997; Goossens and Van Opstal 1997; Hallett and Lightstone 1976a, b; Mays and Sparks 1980; Mushiake et al. 1999; Schlag and Schlag-Rey 1990; Schlag et al. 1989; Tian et al. 2000). In both conditions, a saccadic eye displacement is induced – either visually or by microstimulation – before subjects have to orient gaze towards a memorized target. Thus, to perform a spatially correct second saccade, the brain must take into account the first eye movement. The system's ability to do so has been attributed to the presence of efference copy information that might remap the internal spatial representation of the target in PPC following eye movements (Andersen et al. 1985; Bremmer et al. 1997; Duhamel et al. 1992a; Heide et al. 1995; Tobler et al. 2001). Figure I-8 illustrates this behaviour.

The first saccadic eye displacement in the double-step paradigm might also be replaced by another movement, like a smooth pursuit eye movement or a head / body displacement. Therefore, the saccadic system has to receive information about the initial movement from another motor system to update the amplitude and direction of orientation saccades. In the case of head or body rotations, the saccadic system indeed receives appropriate vestibular and proprioceptive information to remap the spatial location of memorized objects (Baker et al. 2003; Bloomberg et al. 1988; Bloomberg et al. 1991; Israel et al. 1993; Medendorp et al. 2002a; Mergner et al. 1998; Mergner et al. 2001). This is also the case for head translations (Israel and Berthoz 1989; Medendorp et al. 2002b). Furthermore, accurate self-motion information is used by the limb motor system when pointing to remembered visual targets after trunk displacements (Medendorp et al. 1999). However, as mentioned before, in these situations it is well known

that extraretinal signals about body orientation and displacement are available via vestibular and proprioceptive signals.

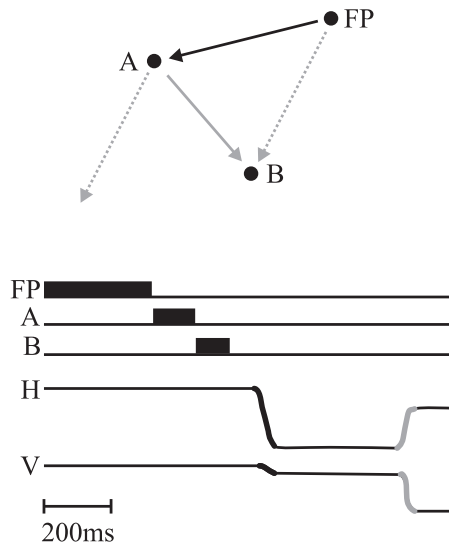


**Figure I-8:** The double-step paradigm. FP: initial fixation point. B: memorized target. The eye is deviated visually (black arrow) to the point A before the saccade to target B is executed (solid bars indicate illumination of targets). Retinal position information (dotted grey arrows) is updated to execute a spatially accurate saccade (solid grey arrow). Adapted from Duhamel et al. (1992a).

#### 4.3.3. *Open questions and motivation of this thesis*

We saw that the saccadic system is able to keep track of saccades, head and body rotations using afferent extraretinal information. However, a much more complicated situation arises when the first step in the double-step paradigm is replaced by a smooth eye movement (“smooth double-step” paradigm, Fig. I-9). In this situation, contradictory results have been described. No compensation for smooth eye movements has been reported in some studies (Gellman and Fletcher 1992; McKenzie and Lisberger 1986). Others claim that saccades to targets memorized before a smooth eye movement are accurate (Baker et al. 2003; Herter and Guitton 1998; Ohtsuka 1994; Schlag et al. 1990; Zivotofsky et al. 1996), whether these were smooth eye movements in isolation or combined eye and head movements.

Today, the question remains how the brain keeps track of smooth pursuit eye movements when no visual information about the smooth eye displacement is available. The above-mentioned contradictory results need to be reunified and the mechanisms that lead to space constancy during smooth eye movements in darkness need to be discovered. Answering this question might shed light on different aspects of oculomotor control, spatial perception and extraretinal signal processing. Here are some open problems:

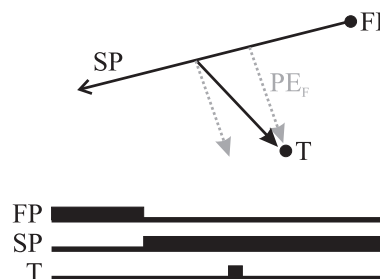


**Figure I-9: The “smooth double-step” paradigm.** FP: initial fixation point. SP: smooth pursuit target movement. T: memorized target. During ongoing smooth pursuit, a target (T) is briefly presented. The question arises whether the system could update the retinal position error ( $PE_F$ ) to perform a spatially accurate eye movement towards the flashed target T.

- First of all, when and how has the system access to extraretinal information about smooth eye movements in darkness? Behaviourally, contradictory reports need further investigation to uncover the timing and availability of such signals.
- What are the perceptual consequences? E.g. do previous results suggest space constancy at long time scales but no space constancy for shorter time scales?
- What are the underlying neural structures and mechanisms? What pathways are responsible for space constancy and movement integration – especially for smooth movements in darkness?
- What would the origin of such extraretinal signals be? For smooth eye movements, there are essentially two candidates, i.e. internal efference copy signals about the smooth motor command or – alternatively or in combination – proprioceptive signals from extra-ocular muscles encoding the actual eye position in the orbit. Although some results exist, additional specific experiments are needed to address this question and to analyse their respective importance in space perception and motor control. Furthermore, the underlying neural substrates need to be better identified and characterized with respect to their role in vision and action.

The main question addressed in this thesis is how the pursuit and saccadic systems interact in the absence of continuous visual feedback to keep track of smooth self-generated eye movements. Since visual feedback is absent, extraretinal signals must come into play. I will concentrate on the first three questions pointed out above. The motor consequences of smooth

movement integration will be revealed and investigated here. The saccadic and smooth pursuit contribution to the orientation towards a memorized target will be analysed separately. Furthermore, the role of smooth eye movement related extraretinal signals on perceived space will also be examined.

## **5. Content of the thesis**

This thesis contains six chapters. These chapters are arranged in a logical order to guide the reader through different aspects of the main subject, i.e. how extraretinal signals are used for the interaction of smooth pursuit and saccades to maintain space constancy. In addition, three annexes provide supplementary information on the experimental procedures for data acquisition (Appendix 1), the statistics used to analyze the data presented here (Appendix 2) and an additional analysis of the smooth response to a target flashed during ongoing smooth pursuit (Appendix 3).

### *Chapter 1*

The present introductory chapter provides an overview of a series of issues addressed in this thesis. It is meant to give a general summary of the oculomotor system to the naive reader. In addition, some more specific topics – like space constancy, smooth pursuit and saccade interactions and the role of extraretinal signals – are briefly described. This should allow the reader to position this work in the context of previous research results. The following chapters will analyse the system's use of extraretinal signals to ensure space constancy during smooth eye movements in darkness.

### *Chapter 2*

How are memory-guided saccades programmed during smooth eye movements? In this chapter I will essentially focus on the initial saccadic response to a target briefly flashed during smooth eye movements in darkness. I will show when and how extraretinal signals about the smooth eye displacement are taken into account to adjust the saccade amplitude. As a result, I will provide evidence for a retinal-to-spatial reference frame transformation that was delayed with respect to the smooth eye movement. The system thus used delayed extraretinal smooth eye displacement information as soon as it became available.

### Chapter 3

The time course of compensation for smooth eye movements in darkness was examined in this chapter. I was particularly interested in the long latency response of the saccadic system to a smooth eye displacement evoked by smooth anticipatory eye movements in darkness. In addition to the analysis of the first orientation saccades in Chapter 2, I will demonstrate that the role of secondary compensatory saccades was to compensate for the yet uncompensated smooth eye displacement. I provide additional evidence for a delayed compensation of smooth eye displacements with respect to the eye movement. In addition, the use of smooth anticipation allowed us to exclude a possible influence of information related to a prior smooth pursuit tracking target on the compensation mechanism.

### Chapter 4

In addition to the saccadic motor response of the system in the “smooth double-step” paradigms, I analysed the perceptual consequences of smooth eye movements in darkness. I will show that a briefly flashed target was mislocalized during smooth anticipatory eye movements. This was despite the fact that subjects had no sense of movement during the task. Thus space perception was altered despite the absence of motion perception. The time course of the perceptual mislocalization will demonstrate that this mislocalization was built up during the retinal-to-spatial transformation of the internal target representation.

### Chapter 5

In Chapter 5, a new model of the saccadic system will be proposed. This model will take into account the novel findings of a retinal-to-spatial reference frame transformation described in Chapters 2 and 3. Therefore, the eye-centred representation of the target was updated to account for smooth and saccadic eye movements. The smooth eye displacement was estimated by two original alternative mechanisms for the integration of a smooth eye velocity signal. I will show that both mechanisms for the retinal-to-spatial transformation in a “smooth double-step” paradigm provided a good fit of the experimental data. Furthermore, our model could reproduce previous findings from the literature and reconcile initially contradictory results.

### Chapter 6

The concluding chapter will summarize the contribution of this thesis to open questions in the field. Furthermore – and more importantly – a series of open questions related to this work will be described. Several proposals for future investigations are also included in this chapter. In addition, I will discuss the potential importance of the model I developed with regard to the two hypotheses of neural mechanisms for smooth eye displacement estimation in the brain using extraretinal eye velocity information. Finally, I propose to use the dynamics of one of our smooth eye displacement estimation mechanisms to implement an alternative version of the classical neural integrator of the saccadic system.

## **6. List of publications**

### **6.1. Journal articles :**

DE BROUWER S, YUKSEL D, BLOHM G, MISSAL M, LEFÈVRE P, What triggers catch-up saccades during visual tracking?, *Journal of Neurophysiology* 87, pp. 1646-50 (2002)

BLOHM G, MISSAL M, LEFÈVRE P, Interaction between smooth anticipation and saccades during ocular orientation in darkness, *Journal of Neurophysiology* 89, pp. 1423-1433 (2003)

BLOHM G, MISSAL M, LEFÈVRE P, Smooth anticipatory eye movements alter the memorized position of flashed targets, *Journal of Vision* 3, pp. 764-773 (2003)

### **6.2. Journal articles submitted:**

BLOHM G, MISSAL M, LEFÈVRE P, Direct evidence for a position input to the smooth pursuit system. *Submitted to Journal of Neurophysiology*

BLOHM G, MISSAL M, LEFÈVRE P, Processing of retinal and extraretinal signals for memory guided saccades during smooth pursuit. *Submitted to Journal of Neurophysiology*

### **6.3. Conference abstracts:**

BLOHM G, LEFÈVRE P, What can we learn from the oculomotor system? 20<sup>th</sup> Benelux Meeting on Systems and Control, Houffalize (Belgium) 2001

---

BLOHM G, MISSAL M, LEFÈVRE P, Target localization during anticipatory smooth eye movements, 31<sup>st</sup> annual meeting of the Society for Neuroscience, San Diego (USA) 2001

BLOHM G, CROMMELINCK M, MISSAL M, LEFÈVRE P, The time course of compensation for anticipatory smooth eye movements in a target localization task, 32<sup>nd</sup> annual meeting of the Society for Neuroscience, Orlando (USA) 2002

SCHREIBER C, BLOHM G, MISSAL M, LEFÈVRE P, Catch-up saccades in two dimensions, 32<sup>nd</sup> annual meeting of the Society for Neuroscience, Orlando (USA) 2002

BLOHM G, MISSAL M, LEFÈVRE P, Smooth and saccadic eye movements interact in the absence of vision, 22<sup>nd</sup> Benelux Meeting on Systems and Control, Lommel (Belgium) 2003

BLOHM G, MISSAL M, LEFÈVRE P, Memory guided saccades during and after smooth pursuit, 33<sup>rd</sup> annual meeting of the Society for Neuroscience, New Orleans (USA) 2003

BLOHM G, MISSAL M, LEFÈVRE P, Direct evidence for a position input to the smooth pursuit system, 14<sup>th</sup> annual meeting of the Neural Control of Movement Society, Sidges (Spain) 2004



## CHAPTER II

# PROCESSING OF RETINAL AND EXTRARETINAL SIGNALS FOR MEMORY GUIDED SACCADES DURING SMOOTH PURSUIT<sup>\*</sup>

*If knowledge can create problems, it is not  
through ignorance that we can solve them.*

Isaac Asimov

### 1. Abstract

It is an essential feature for the visual system to keep track of self-motion in order to maintain space constancy. Therefore, the saccadic system uses extraretinal information about previous saccades to update the internal representation of memorized targets, an ability that has been identified in behavioral and electrophysiological studies. However, a *smooth* eye movement induced in the latency period of a memory guided saccade yielded contradictory results. Indeed some studies described spatially accurate saccades, whereas others reported retinal coding of saccades. Today, it is still unclear how the saccadic system keeps track of *smooth* eye movements in the absence of vision.

Here, we developed an original 2-D behavioral paradigm to further investigate how smooth eye displacements could be compensated to ensure space constancy. Human subjects were required to pursue a moving target and to orient their eyes toward the memorized position of a briefly presented second target (flash) once it appeared.

The analysis of the first orientation saccade revealed a bi-modal latency distribution related to two different saccade programming strategies. Short latency (< 175 ms) saccades were coded using the only available

---

<sup>\*</sup> The contents of this chapter has been submitted for publication in The Journal of Neurophysiology

retinal information, i.e. position error. In addition to position error, longer latency ( $> 175$  ms) saccades used extraretinal information about the smooth eye displacement during the latency period to program spatially more accurate saccades. Sensory parameters at the moment of the flash (retinal position error and eye velocity) influenced the choice between both strategies.

We hypothesize that this tradeoff between speed and accuracy of the saccadic response reveals the presence of two coupled neural pathways for saccadic programming. A fast striatal-collicular pathway might only use retinal information about the flash location to program the first saccade. The slower pathway could involve the Posterior Parietal Cortex to update the internal representation of the flash once extraretinal smooth eye displacement information becomes available to the system. We propose several electrophysiological experiments to test these hypotheses.

## **2. Introduction**

Space constancy is an essential feature of the visual system that allows us to perceive a stationary object as immobile during self-movement even though its image shifts across the retina (Bridgeman 1995; Deubel et al. 1998; Niemann and Hoffmann 1997; Stark and Bridgeman 1983). In the case where visual information is absent, the question arises whether space constancy of memorized targets still holds during eye movements. This issue has been extensively studied for the saccadic system using the so-called double-step and colliding saccade paradigms (Aslin and Shea 1987; Becker and Jürgens 1979; Dassonville et al. 1992; Dominey et al. 1997; Goossens and Van Opstal 1997; Hallett and Lightstone 1976a, b; Mays and Sparks 1980; Mushiaké et al. 1999; Schlag and Schlag-Rey 1990; Schlag et al. 1989; Tian et al. 2000). In both experimental conditions, a saccadic eye movement is evoked either visually or by microstimulation before primates have to direct their line of sight to a previously memorized spatial location. In this situation, the retinal error of the memorized target does not correspond anymore to the required eye movement. Nevertheless, saccades are spatially accurate. The authors conclude that extra-retinal information about the first eye movement is available to the saccadic system to adapt the second saccade amplitude. The saccadic system is thus able to keep track of its own movements.

During *smooth* pursuit movements, the question of space constancy becomes more complicated. In this case, a *smooth* eye movement is induced before the occurrence of the saccade directed towards the memorized target. Again, to align gaze with the correct spatial location of the memorized target, the retinal input has to be updated by extraretinal signals about the smooth eye displacement. Thus, the saccadic system needs additional information from another motor system – the smooth pursuit system – to compensate for smooth eye displacements. Today, it is still not clear how such memory-guided saccades are programmed during smooth eye movements. Recent studies indicate that gaze shifts to targets memorized before visually guided smooth pursuit and executed after the end of pursuit are spatially accurate (Baker et al. 2003; Herter and Guitton 1998). Also, when targets were briefly flashed during smooth pursuit but the localization was performed only after the smooth pursuit target disappeared, memory guided saccades seemed to be better predicted by the spatial error hypothesis (i.e. saccades directed to the actual target position in space, accounting for the retinal error and intervening movements during the latency period) than by the retinal error hypothesis (i.e. saccade directed to the retinal position of the target irrespective of intervening eye movements) (Ohtsuka 1994; Schlag et al. 1990; Zivotofsky et al. 1996). Taken together, these results suggest that the saccadic system has indeed access to information about smooth eye displacement during the memory period. However, when a target is briefly flashed at the moment of the smooth pursuit target extinction and a targeting saccade is immediately triggered, its amplitude is better predicted by the retinal error than by the spatial error (Gellman and Fletcher 1992; McKenzie and Lisberger 1986). These results are clearly contradictory with the above-mentioned hypothesis of space constancy during smooth eye movements and the question arises what can explain this apparent contradiction.

To answer this question, we propose to investigate how memory guided saccades are programmed during smooth pursuit. In particular, because long memory periods seemed to allow space constancy during self generated movement (Baker et al. 2003; Herter and Guitton 1998; Ohtsuka 1994; Schlag et al. 1990; Zivotofsky et al. 1996), whereas this was not the case for short memory periods (Gellman and Fletcher 1992; McKenzie and Lisberger 1986), we will investigate the role of response latency in the saccade programming process. By doing this, we will be able to make the link between the above-mentioned results of short-latency retinal and long-

latency spatial saccade programming. Therefore, we developed a new two-dimensional (2-D) experimental paradigm in which we presented a briefly flashed target during smooth pursuit eye movements. This 2-D arrangement of the paradigm allowed us to separate retinal and extraretinal signals and to obtain saccade programming parameters for horizontal and vertical eye movement components separately. Furthermore, a detailed analysis of saccade latencies made it possible for the first time to link the saccadic execution time to the programming of the memory guided eye movement. As a result, we will show that there is a transition between retinally coded short latency saccades and spatially coded longer latency eye saccades and that this transition is reflected in a bi-modal saccadic latency distribution. We will also analyze which sensory parameters influence the system's decision to trigger short or longer latency saccades. These results shed light on the use of extra-retinal signals when tracking smooth eye movements in the absence of visual input and reconcile previous contradictory results concerning the programming of memory-guided saccades during smooth self-motion. Our paradigm thus allowed us to identify two coupled processes for saccade execution. We suggest several electrophysiological experiments to identify the neural substrates underlying these two saccade programming modes.

### **3. Experimental procedures**

Eight healthy human subjects aged between 23 and 38 years and without any known oculomotor anomalies were recruited after informed consent. Three of them were completely naïve of oculomotor experiments. All procedures were conducted with approval of the Université catholique de Louvain Ethics Committee, in compliance with the Helsinki declaration (1996).

#### ***3.1. Experimental set-up***

Subjects faced a 1-m distant, tangent translucent screen that covered about  $\pm 45^\circ$  horizontally and  $\pm 40^\circ$  vertically of their visual field. They sat in complete darkness and their head was restrained using a chin rest. Two different targets – a green and a red spot – were back-projected onto the screen. The green spot was projected by a Tektronix (Beaverton, OR, USA) 606A oscilloscope using custom optics and measured

approximately  $1.5^\circ$ . This green spot was the smooth pursuit target. A second target was a red LASER spot that measured  $0.2^\circ$  and was projected onto the screen via two M3-Series mirror galvanometers (GSI Lumonics, Billerica, LA, USA). This red spot was only briefly presented during 10 ms and we will thus refer to it as a “flash” (flash durations between 5 and 20 ms have been used successfully (Gellman and Fletcher 1992; Schlag et al. 1990)). A dedicated real-time computer running LabViewRT (National Instruments, Austin, TX, USA) software controlled position, velocity and illumination of both targets. We recorded the movements of one eye using the scleral search coil technique (Skalar Medical BV, Delft, The Netherlands) (Collewijn et al. 1975; Robinson 1963).

### 3.2. *Paradigm*

All recording sessions were composed of blocks of 40 trials each. Data acquisition started with two blocks of fixation control (FIX) trials followed by a varying number of blocks of test trials, such that a total recording duration of 30 minutes was not exceeded. Flashes were presented during fixation (control FIX) or during ongoing smooth pursuit (test).

Fixation control (FIX) trials started with a green central fixation spot. At a random time 500-1000 ms after the trial began, a 10-ms red flash was presented at a random position between  $-10^\circ$  and  $+10^\circ$  horizontally and vertically. One thousand ms after the flash, the green fixation spot was extinguished for 500 ms to indicate the end of the trial. Once the red flash appeared, subjects were asked to fixate its memorized position until the end of the trial.

Test trials started with a 500-ms initial fixation period (green target) at  $20^\circ$  eccentricity (Fig. II-1A, IF) in a random direction around the straight-ahead position. The initial fixation point was thus located at a random position on a  $20^\circ$  circle around the straight-ahead direction (Fig. II-1A, dotted circle). Then, the green spot performed a step away from the center of the screen and a ramp movement (Fig. II-1A, ramp) back toward the center of the screen. The size of the step was calculated in such a way that the target crossed the initial fixation point after 200 ms. This step was introduced to reduce the probability of occurrence of a catch-up saccade during pursuit initiation (Rashbass 1961). The ramp velocity varied randomly between  $10^\circ/\text{s}$  and  $40^\circ/\text{s}$ . A 10-ms red flash (Fig. II-1A, flash) was

presented at a random time between 500 and 1500 ms after the ramp movement onset. The flash position was randomly chosen in a squared  $\pm 10^\circ$  (horizontal and vertical) window around the actual pursuit ramp position. The ramp movement continued until the end of the trial. All trials lasted for 3s. Subjects were instructed to follow the green pursuit target and to look at the memorized position of the flash as soon as they saw the flash.

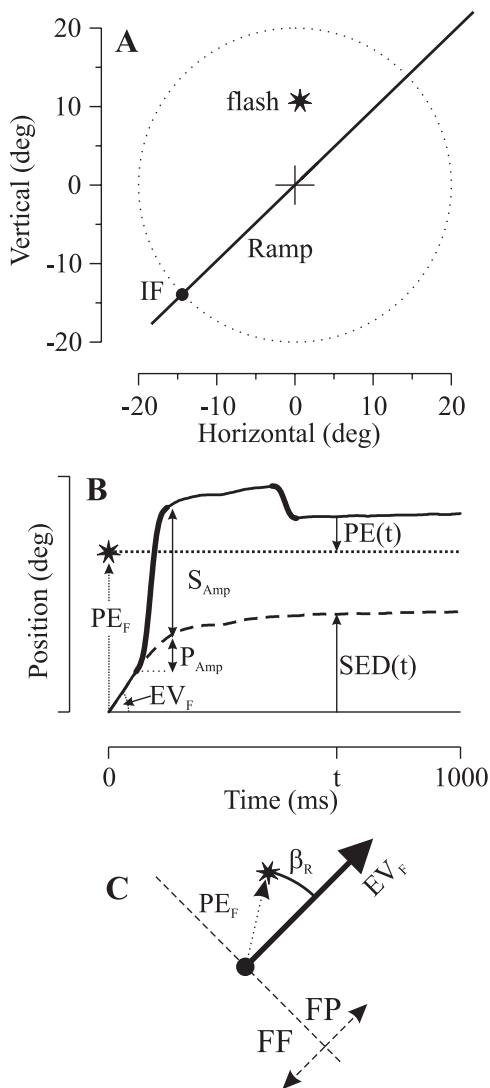


**Figure II-1: Experimental paradigm and data analysis. A.**

Test trials paradigm. The initial fixation point (dot, IF), the pursuit ramp and the flash (star) are represented. The dotted circle stands for the possible positions of the initial fixation point. **B.**

Extracted parameters. At the time of the flash (star, dotted line) represents the memorized flash position, position error ( $PE_F$ ) and eye (solid line, saccades in bold) velocity ( $EV_F$ ) were sampled. The first saccade amplitude was divided into the purely saccadic ( $S_{Amp}$ ) and the smooth ( $P_{Amp}$ ) component. Position error ( $PE(t)$ ) and smooth eye displacement ( $SED(t)$ ) are also represented. **C.**

Direction of smooth pursuit with respect to the location of the flash.  $\beta_R$  is the angle between position error ( $PE_F$ ) and eye velocity ( $EV_F$ ) at the moment of the flash. The visual field was divided into foveofugal (FF) and foveopetal (FP) hemifields. See text for more details.

In addition to the test trials, all subjects performed “flash after ramp” control (FAR) trials. FAR controls were similar to test trials, but the green pursuit ramp target was extinguished at a random time between 500 and 1000 ms after the ramp movement onset and remained extinguished until the end of the trial. At a random time 0-500 ms after the pursuit ramp extinction, a red flash was presented in a  $\pm 10^\circ$  window (horizontally and vertically) around the extrapolated ramp position. Beside this, all stimulus parameters and subject’s instructions remained the same as for test trials.

### 3.3. Data acquisition and analysis

Two NI-PXI-6025E data acquisition boards (National Instruments, Austin, TX, USA) sampled the position of one eye and both targets (horizontally and vertically) at 500 Hz. Collected data were stored on a hard disk for off-line analysis with Matlab scripts (Mathworks Inc., Natick, MA, USA). Position signals were low-pass filtered using a zero-phase digital filter (autoregressive forward-backward filter; cutoff frequency: 50 Hz). Velocity and acceleration were derived from position signals using a weighted central difference algorithm on a  $\pm 10$ -ms interval.

All trials were aligned on flash onset. Figure II-1B illustrates an example in one dimension, starting from the moment of the flash onset (time 0 ms) until 1,000 ms after the flash. The smooth eye displacement was defined as the integral of the smooth eye velocity  $EV_S(t)$  over time, starting

at the moment of the flash [ $SED(t) = \int_0^t EV_S(t') dt'$ ]. The smooth eye

velocity  $EV_S(t)$  was obtained by removing saccades from the velocity trace. Saccades were detected using a  $500^\circ/s^2$  acceleration threshold. We then measured the eye velocity before and after the saccades and interpolated linearly between these values to obtain an estimation of the smooth eye velocity during saccades (see Methods section of de Brouwer et al. (2002a) for more details).

To analyze the 1<sup>st</sup> saccade programming, the saccadic amplitude had to be corrected for the contribution of the smooth pursuit system. It has indeed been shown for horizontal eye movements that the smooth pursuit system does not pause during saccades and thus has a significant contribution to the measured saccade amplitude (de Brouwer et al. 2002a; de

Brouwer et al. 2001; Keller and Johnsen 1990; Smeets and Bekkering 2000). Therefore, to examine the output of the saccadic system in isolation, the measured value of the saccade amplitude (AMP) has to be corrected by an estimate of the smooth pursuit contribution  $P_{\text{Amp}}$  (see Fig. II-1B). The corrected saccade amplitude is then  $S_{\text{Amp}} = \text{AMP} - P_{\text{Amp}}$ . The smooth pursuit contribution  $P_{\text{Amp}}$  is calculated by multiplying the saccade duration  $S_{\text{Dur}}$  with the mean value of the eye velocity before and after the saccade (de Brouwer et al. 2002a; de Brouwer et al. 2001; Keller and Johnsen 1990; Smeets and Bekkering 2000). Here, we performed the same correction of the saccade amplitude for 2-D saccades. We tested the validity of the correction for each subject individually on the main sequence relationship between saccade duration  $S_{\text{Dur}}$  and vectorial amplitude AMP. For all subjects, the corrected vectorial saccade amplitude  $S_{\text{Amp}}$  was significantly better correlated to  $S_{\text{Dur}}$  than the uncorrected amplitude AMP (t-test,  $p < 0.01$ ). We thus validated the previously proposed method of the saccade amplitude correction for 2-D data. All analyses in this paper will thus use the corrected saccade amplitude  $S_{\text{Amp}}$ .

For our analysis, we measured different parameters as illustrated in Fig. II-1B. The range of these parameters is provided in Table II-1. At the moment of the flash, we measured the horizontal and vertical component of the position error  $PE_F$  (= retinal error) and eye velocity  $EV_F$  and also the smooth pursuit gain ( $\text{gain}_{\text{SP},F}$ ). Following the above described procedure, the total saccade amplitude AMP was divided into a purely saccadic component  $S_{\text{Amp}}$  and a smooth pursuit contribution  $P_{\text{Amp}}$ . Position error  $PE(t)$  and smooth eye displacement  $SED(t)$  were measured continuously until 1,000 ms after the flash. For the analysis of the saccade latency, we partitioned our data into two distinct subsets, i.e. foveofugal (FF) and foveopetal (FP) flashes (see Fig. II-1C). In FP (FF) trials, the flash was presented ahead (behind) the actual eye position with respect to the direction of the eye velocity  $EV_F$ . We also calculated the angle  $\beta_R$  between  $EV_F$  and the position error  $PE_F$  at the moment of the flash.

We performed our statistical analyses either using Statistica (StatSoft Inc., Tulsa, OK, USA) or Matlab (Mathworks Inc., Natick, MA, USA) programs. For the presentation and description of our results, we used the classical expression of the regression coefficient R (and corresponding p-

values for significance) to provide an indication of the goodness-of-fit. This was the case for linear regressions as well as for non-linear fitting.

## 4. Results

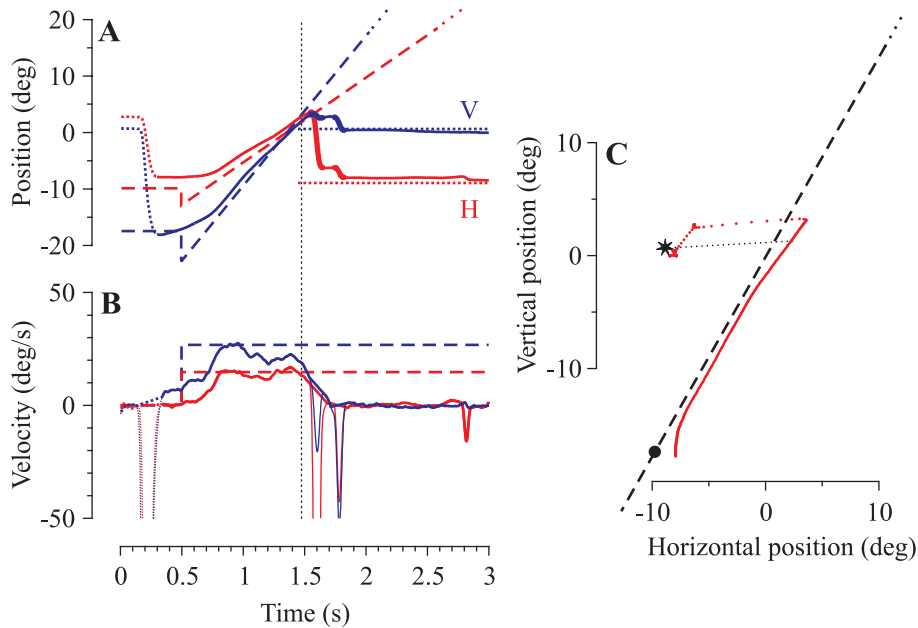
We recorded a total of 5,855 test trials. All trials were visually inspected. We discarded trials with saccades occurring around the moment of the flash up to 65 ms after the flash onset ( $N = 956$ ) and trials where subjects could not localize correctly the flashed target (final error  $> 10^\circ$ ) or did not trigger any saccade ( $N = 435$ ). The total number of valid trials we used in our analyses was thus  $N = 4,464$  (~76%). We also recorded a total of 1,957 control FIX trials and 5,919 control FAR trials, out of which 1,542 (~79%) and 4,402 (~74%) respectively were valid. Subjects reported that they did not have any difficulties in performing the experimental tasks.

Figures II-2, 3 and 4 show three trials with a typical short latency, long latency and very long latency first saccade respectively. We were only interested in saccades that occurred after the onset of the flash (dotted vertical line in panels A and B of Fig. II-2, 3 and 4). The first orientation saccade in Fig. II-2 had a latency of 104 ms with respect to the flash and was almost parallel to the position error vector at the moment of the flash  $PE_F$  (= retinal error; dotted line in Fig. II-2C). It seems that this saccade did not take into account the smooth eye movement during the latency period. However, a second saccade was triggered and compensated for the remaining error.

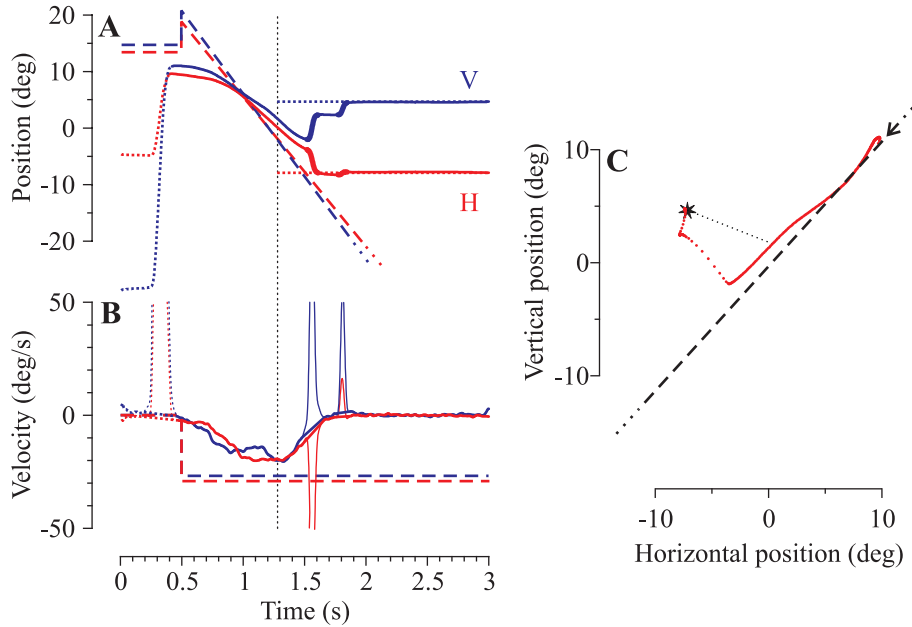
A different behavior is shown in the second typical trial, in Fig. II-3, where the first saccade towards the flash had a latency of 238 ms and was not parallel to  $PE_F$  vector. Indeed, this saccade seemed to take into account the fact that the eye was moving during the latency period. However, a second saccade was still needed to correct for the remaining error.

Figure II-4 shows an extreme case where the first saccade was triggered very late (latency: 674 ms). This example shows an almost perfect compensation for the smooth eye displacement that took place during the latency period. Remarkably, although the horizontal retinal position error at the moment of the flash was negative, the horizontal saccade amplitude was positive. These three trials in Fig. II-2, 3 and 4 illustrate the influence of latency on the characteristics of the 1<sup>st</sup> saccade. The programming of short

latency saccades appears to be directed to the retinal position of the flash whereas there is a bias towards the spatial location of the flash when saccade latency increases.



**Figure II-2: Typical short-latency trial.** **A.** Position vs. time representation of the pursuit target (dashed lines), the flash (horizontal dotted lines stand for the memorized flash position) and the movement of one eye (solid lines) separately for horizontal (red, H) and vertical (blue, V) components. Relevant saccades are represented with bold lines. The vertical dotted line indicates when the flash was presented. **B.** Velocity vs. time representation of the trial. Saccades are represented with thin lines; other conventions are the same as in panel A. **C.** Vertical vs. horizontal representation of the trial. The black dot indicated the initial fixation point and the dashed line the pursuit ramp target. The eye position is represented with a red dot every 6 ms. When the dots are separated, this indicates a fast (saccadic) eye movement; otherwise the movement is smooth. The flash (star) is connected to the eye trace by a thin dotted line that indicates where the eye was at the moment of the flash (= PE<sub>F</sub>). The first saccade had a latency of 104 ms.



**Figure II-3: Typical long-latency trial.** The same conventions as in Fig. II-2 apply for all panels. Here, the first saccade had a latency of 238 ms.

#### 4.1. Programming of 1<sup>st</sup> saccade

Trials in Fig. II-2, 3 and 4 seemed to indicate that short and long latency saccades were not programmed in the same way. Short latency saccades (see Fig. II-2) appeared to be parallel to the vector of retinal position error at the moment of the flash, whereas long latency saccades (see Fig. II-3 and 4) indicate that extra-retinal signals about the ongoing eye movement during the latency period of the saccade could also influence its programming. Long latency saccades would thus be spatially more accurate than the retinal short latency saccades.

We compared the two hypotheses of saccade programming, i.e. the retinal and the spatial hypothesis (see Introduction section), using the following regression formulas for the saccade amplitude (equivalent expressions were used for the saccade direction):

$$\text{Retinal progr.: } S_{Amp} = \alpha + \beta \cdot \left\| \begin{pmatrix} PE_{F,X} \\ PE_{F,Y} \end{pmatrix} \right\| \quad \text{Eq. II-1}$$

$$\text{Spatial progr.: } S_{\text{Amp}} = \alpha + \beta \cdot \left\| \begin{pmatrix} PE_{F,X} \\ PE_{F,Y} \end{pmatrix} - \begin{pmatrix} SED_{S,\text{end},X} \\ SED_{S,\text{end},Y} \end{pmatrix} \right\| \quad \text{Eq. II-2}$$

, where  $PE_F$  was the position error at the moment of the flash (X/Y: in horizontal/vertical direction) and  $SED_{S,\text{end}}$  was the smooth eye displacement at the end of the saccade (see Methods for more details).  $\alpha$  and  $\beta$  were regression parameters. Table II-1 summarizes the values and ranges of the variables used for this analysis and for the following computations.

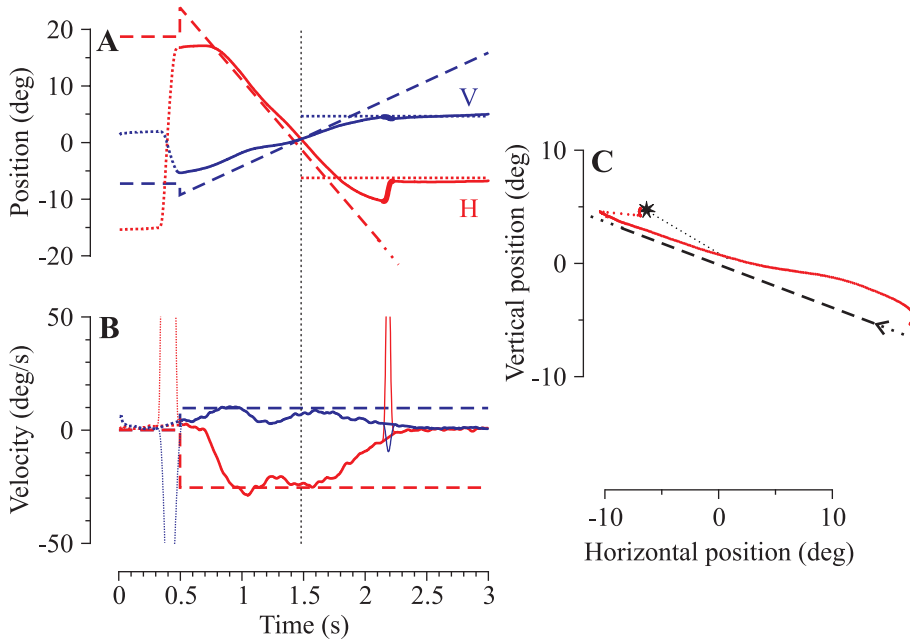


**Figure II-4: Very long latency trial.** The same conventions as in Fig. II-2 and 3 apply for all panels. Here, the saccade latency was 674 ms.

Figure II-5 shows a comparison of the retinal versus the spatial saccadic programming hypothesis as a function of saccade latency (50-ms bins). Panels A-D show scatter plots of the first saccade direction for the retinal and spatial error hypothesis, for short ( $< 150$  ms) and long ( $> 300$  ms) latency trials separately. We used the correlation coefficient  $R$  as an indicator for the goodness-of-fit in panels E and F. Figure II-5E represents the latency dependence of the correlation coefficients  $R_{\text{Amp}}$  between the saccade amplitude and the retinal ( $R$ , dashed line, Eq. II-1) or the spatial ( $S$ , solid line, Eq. II-2) hypothesis separately. Figure II-5F illustrates the latency

dependence of the correlation coefficients  $R_{Dir}$  for the saccade direction and thus summarizes Fig. II-5A-D.

Figure II-5 thus confirmed the tendency shown in our example trials (Fig. II-2, 3 and 4), i.e. short latency saccades were better described by the retinal error hypothesis whereas long latency saccades were spatially more accurate. A qualitatively and quantitatively very similar behavior was observed for FAR control trials (data not shown). The crossing-over of both correlation coefficients in Fig. II-5E and F nicely illustrates this behavior. Note however, that the moment of time where the crossing-over occurred did not correspond to the time when extraretinal motion information was taken into account. That is, the crossing time indicated only when the retinal and spatial hypotheses were equally accurate, i.e. when the saccade programming was midway between retinal and spatial. As a consequence, extra-retinal information was already taken into account for earlier saccades.

**Table II-1:** Measured parameters (N = 4,464)

Parameter	component	mean $\pm$ SD	median [25..75]%
<b>Parameters at the moment of the flash</b>			
PE <sub>F</sub>   (°)	X	5.447 $\pm$ 3.478	5.258 [2.644..7.878]
	Y	5.531 $\pm$ 3.619	5.253 [2.584..7.997]
EV <sub>F</sub>   (°/s)	X	10.819 $\pm$ 7.718	9.395 [4.687..15.231]
	Y	9.201 $\pm$ 6.459	8.077 [4.220..12.853]
gain <sub>SP,F</sub> (.)		0.678 $\pm$ 0.256	0.708 [0.500..0.865]
<b>Saccade-related parameters</b>			
S <sub>Amp</sub> *  (°)	X	5.057 $\pm$ 3.524	4.506 [2.187..7.348]
	Y	4.573 $\pm$ 3.602	3.770 [1.670..6.716]
gain <sub>S</sub> (.)	X	0.908 $\pm$ 0.371	0.898 [0.683..1.117]
	Y	0.805 $\pm$ 0.388	0.791 [0.546..1.024]
SED <sub>S,beg</sub>   (°)	X	1.992 $\pm$ 1.848	1.440 [0.661..2.771]
	Y	1.669 $\pm$ 1.472	1.239 [0.617..2.268]
SED <sub>S,end</sub>   (°)	X	2.568 $\pm$ 2.166	2.010 [0.974..3.632]
	Y	2.168 $\pm$ 1.724	1.742 [0.926..2.989]
<b>Final orientation parameters</b>			
PE <sub>end</sub>   (°)	X	2.319 $\pm$ 2.030	1.778 [0.816..3.311]
	Y	2.156 $\pm$ 1.889	1.684 [0.817..2.912]
SED <sub>end</sub>   (°)	X	3.217 $\pm$ 2.640	2.595 [1.219..4.503]
	Y	2.851 $\pm$ 2.256	2.329 [1.165..4.012]

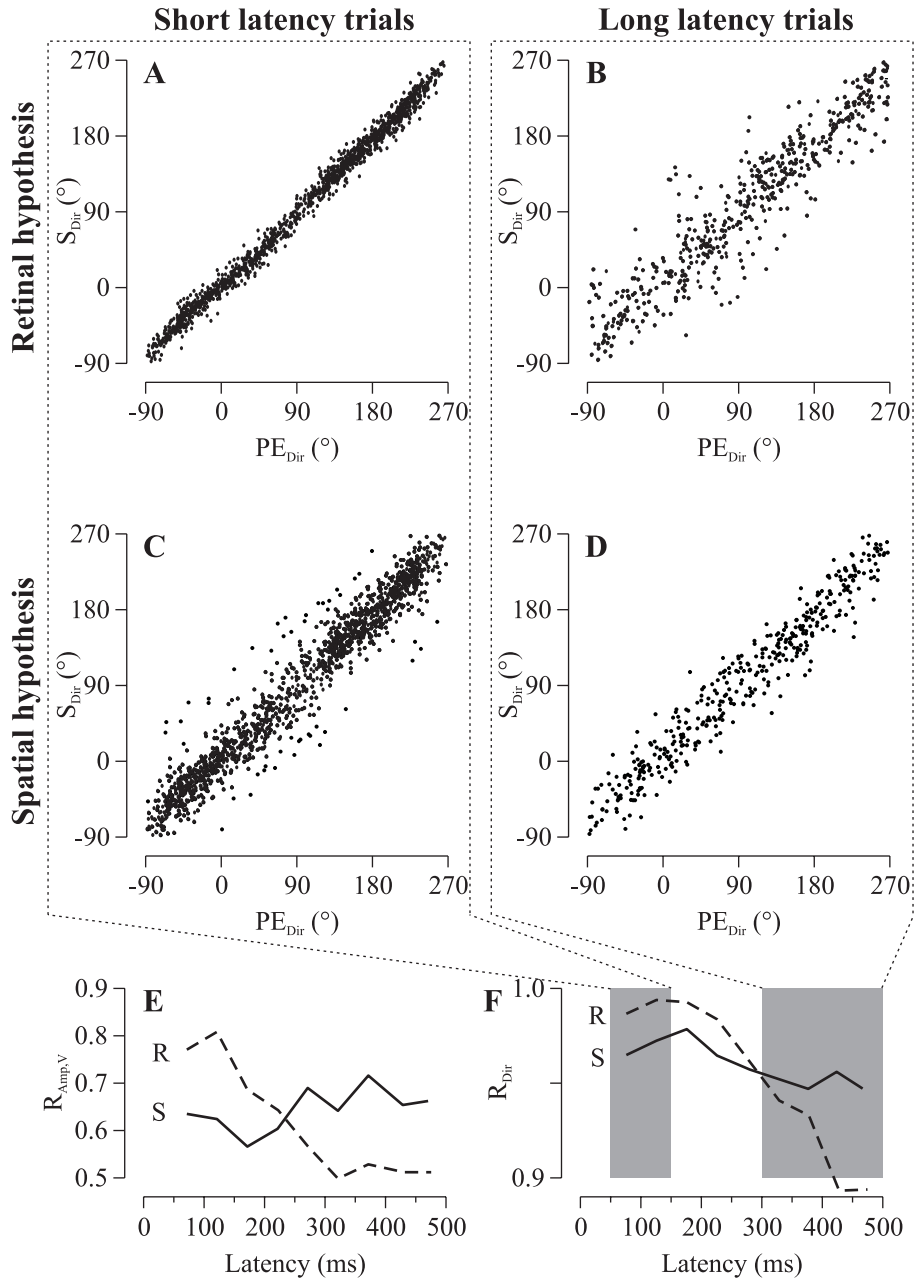


**Figure II-5: Retinal vs. spatial saccade programming.** A-D. Scatter plots of raw data for the first saccade direction ( $S_{Dir}$ ) as a function of the direction of the position error ( $PE_{Dir}$ ). The retinal error hypothesis (panels A and B) is compared to the spatial error hypothesis (panels C and D) separately for short latency trials (latency  $<$   $\rightarrow$

To further illustrate the transition between the retinal and spatial programming of the first orientation saccade, we developed a smooth eye displacement compensation index (CI). This index varies from zero (retinal error hypothesis) to one (spatial saccade programming) and is calculated as follows:

$$CI = 1 + \frac{PE_{\parallel}}{SED} \quad \text{Eq. II-3}$$

Position error ( $PE_{\parallel}$ ) and smooth eye displacement (SED) were measured in the direction of (and thus parallel to) smooth pursuit. Following Eq. II-3, if  $PE_{\parallel} = -SED$ , then the system did not compensate for SED and thus  $CI = 0$  (retinal programming). If the system does compensate for SED, then  $PE_{\parallel} = 0$  and thus  $CI = 1$  (spatial programming). Values for CI between 0 and 1 indicate the percentage of SED compensation of a saccade. Figure II-6 shows the results of this analysis.

Figure II-6A shows the distribution of the compensation index CI for short (< 150 ms, gray histogram) and long (> 300 ms, white histogram) latency first saccades. In panel B, we represented the evolution of CI with saccade latency. This confirms results from our previous analysis indicating that short latency saccades are programmed retinally whereas there is a transition towards the spatial error hypothesis for longer saccade latencies.

To gain better insight into the programming of the 1<sup>st</sup> orientation saccade as a function of its latency, we performed a multiple regression analysis for the saccade amplitude  $S_{Amp}$ . As independent variables for this analysis, we took extraretinal information about the smooth eye displacement  $SED_{S,beg}$  that took place during the latency period in addition to retinal information  $PE_F$  about the location of the flash. Therefore, we used the following regression formula:

---

150 ms, panels A and C) and long latency trials (latency > 300 ms, panels B and D). **E.** Correlation coefficients  $R_{Amp}$  for the correlation of the 1<sup>st</sup> saccade amplitude with the amplitude of retinal (dashed line, R; see Eq. II-1) and spatial (solid line, S; see Eq. II-2) position error, respectively, as a function of saccade latency. **F.** The same representation of the correlation coefficients  $R_{Dir}$  for the correlation of 1<sup>st</sup> saccade direction with the direction of retinal and spatial position error, respectively. Shaded areas correspond to short and long latency data presented in more detail in panels A-D.

$$S_{Amp}(t) = \alpha(t) + \beta(t) \cdot PE_F + \gamma(t) \cdot SED_{S,beg}(t) \quad \text{Eq. II-4}$$

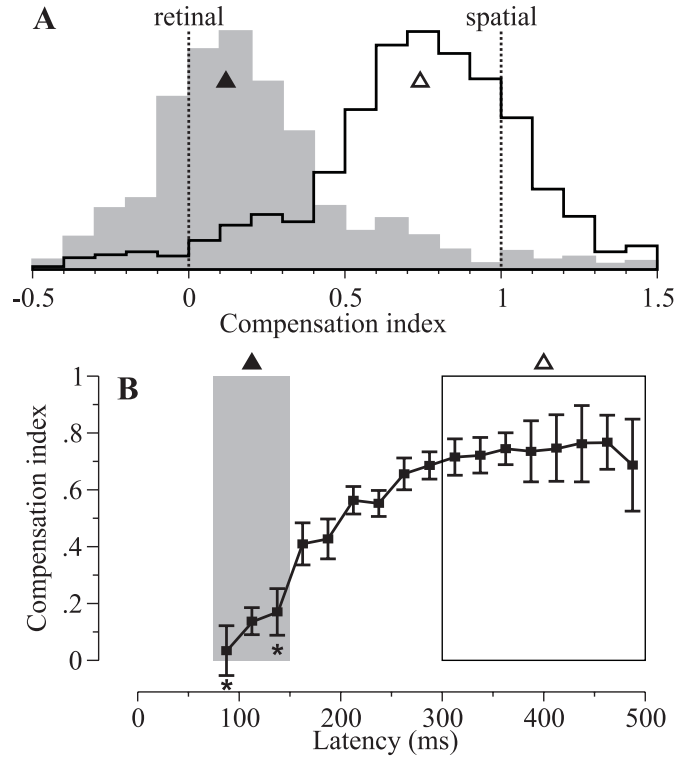


**Figure II-6: First saccade compensation index for smooth eye movements. A.** Histograms for the distribution of the compensation index as calculated in Eq. II-3 for short latency trials (latency < 150 ms, gray histogram) and long latency trials (latency > 300 ms, white histogram). A zero compensation index corresponds to retinal saccade programming whereas a unitary compensation index corresponds to spatially accurate saccades. Open and solid triangles refer to panel B. Histograms are normalized in amplitude. **B.** Evolution of the compensation index for different saccade latencies. Squares and whiskers indicate mean and standard error (25-ms bins). Asterisks indicate when the means are not significantly different from zero (t-test,  $p > 0.05$ ). The gray shaded area with the solid triangle corresponds to the data represented in the gray histogram of panel A. The white box with the open triangle indicates the data range of the white histogram in panel A.

We performed this analysis for different 25-ms bins of saccade latency. Therefore, Eq. II-4 was time dependent – time corresponded to the center of the 25-ms latency bins. Parameter  $\alpha$  is an offset,  $\beta$  and  $\gamma$  were  $PE_F$  gain and  $SED_{S,beg}$  gain respectively. Figure II-7 shows the results of this multiple regression analysis for the programming of the horizontal

component of saccades. Similar results were obtained for the vertical component of saccades (data not shown).

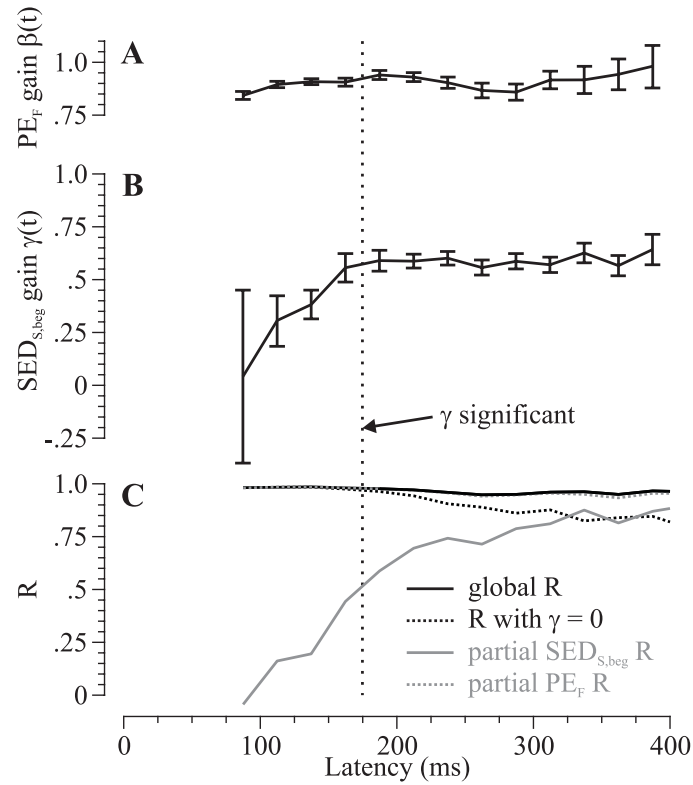


**Figure II-7: 2-parameter regression results for saccade programming.**

Parameters refer to Eq. II-4 and only the horizontal results are represented as a function of the 1<sup>st</sup> saccade latency (25-ms bins used). **A.**  $PE_F$  gain parameter  $\beta(t)$ . **B.**

$SED_{S,beg}$  gain parameter  $\gamma(t)$ . Solid lines and whiskers indicate mean and 95% confidence interval in both panels. **C.** Correlation coefficients  $R$  for the overall regression (solid black) and the regression with  $\gamma = 0$  (dotted black) are represented. We also show the partial correlation coefficients for  $\beta$  (dotted gray line) and for  $\gamma$  (solid gray line). The vertical dotted line indicated when the contribution of the parameter  $SED$  significantly increased the regression coefficient (t-test,  $p < 0.05$ ).

The offset parameter  $\alpha(t)$  was not significantly different from zero and is not shown. Figure II-7A represents the  $PE_F$  gain parameter and Fig. II-7B illustrates the  $SED_{S,beg}$  gain as a function of latency. The  $PE_F$  gain parameter  $\beta$  had a mean value of 0.911 for the horizontal and 0.824 for the vertical component of saccades (compared to 0.933 and 0.878 for control

trials). Interestingly,  $\gamma(t)$  changed during the first 150 ms from approximately zero to a mean steady state value of 0.682 (0.881 for the vertical component).

The correlation coefficients in Fig. II-7C provided better insight into the mechanism of the latency dependent  $SED_{s,beg}$  contribution to the saccade amplitude. When comparing the multiple regression results of Eq. II-4 (Fig. II-7C, solid black line) with a regression where  $\gamma(t) = 0$  (Fig. II-7C, dotted black line), we found that both regressions were significantly different after 175 ms (for both horizontal and vertical components of saccades separately) – the regression with  $\gamma(t) \neq 0$  being the best. Furthermore, the partial correlation coefficient of  $SED_{s,beg}$  was very low for short latency saccades and reached high values for longer latency saccades.

Altogether, the multiple regression results of Fig. II-7 showed that the saccadic system needed some time to be able to take the smooth eye displacement during the latency period into account. We observed an almost identical behavior for the programming of the first saccade in FAR control trials (data not shown).

To be sure that the retinal to spatial transition we observed was not due to some side-effect of saccade programming, we measured the saccadic gain orthogonal to the pursuit ramp movement direction. Since there was no SED in this orthogonal direction, the saccadic gain was a good measure of the movement's accuracy. As a result, there was neither a significant modulation of this saccadic gain for different latencies, nor a difference between test trials and FIX control trials.

#### 4.2. Saccadic latency distribution

We plotted the 1<sup>st</sup> saccade latency histogram in Fig. II-8A. One can easily identify two modes in the latency distribution. To further characterize the two modes of this histogram, we fitted a double-recinormal distribution to our data. The double-recinormal distribution for the latencies has the following expression:

$$\frac{1}{T_{lat}} = A_1 \cdot gauss(\mu_1, \sigma_1) + A_2 \cdot gauss(\mu_2, \sigma_2) \quad \text{Eq. II-5}$$

The inverse of the saccade latency  $T_{\text{lat}}$  was thus fitted by two independent gaussians. This is equivalent to the hypothesis of two separate and non-interacting decision processes of the LATER type (Carpenter and Williams 1995). Indeed, the LATER model states that the inverse of saccade latency is proportional to the rate of rise of a decision signal divided by the decision threshold.

The particularity of the LATER model is that the decision signal is assumed to rise linearly with a normally distributed rate of rise. We essentially chose this double-recinormal fit function because it described well our data and allowed us to quantify with very few parameters the entire latency distribution. However, in order to justify the use of this particular probability density function, we performed a k-fold cross-validation applying the Kolmogorov-Smirnov statistical 1-sample distribution test. Therefore, we used a random subset of 75% of our data to estimate the fit parameters of Eq. II-5 by means of standard least-square data fitting using the Gauss-Newton method. Afterwards, we performed a Kolmogorov-Smirnov analysis to test if the remaining 25% of our data were distributed identically to the previously identified distribution. This procedure was performed  $k=1,000$  times. As a result, we found an average 98.3% acceptance of the double-recinormal probability density function hypothesis (5% significance level).

**Table II-2:** Double-recinormal fit parameters for Fig. II-8

<b>Fit</b>	$m_1 \pm s_1$	$m_2 \pm s_2$	<b>mean <math>\pm</math> SD</b>	<b>N</b>	<b>R (p-level)</b>
Fig. II-8A	115 ms $\pm$ 40 ms	225 ms $\pm$ 41 ms	201 ms $\pm$ 83 ms	4,464	0.9915 ( $< 0.0001$ )
Fig. II-8B: FP	110 ms $\pm$ 36 ms	229 ms $\pm$ 42 ms	191 ms $\pm$ 85 ms	2,580	0.9911 ( $< 0.0001$ )
Fig. II-8B: FF	129 ms $\pm$ 43 ms	223 ms $\pm$ 42 ms	214 ms $\pm$ 79 ms	1,884	0.9865 ( $< 0.0001$ )
Controls	134 ms $\pm$ 36 ms	220 ms $\pm$ 21 ms	175 ms $\pm$ 58 ms	1,542	0.9894 ( $< 0.0001$ )

To estimate the fit parameters, we applied the same least-square data fitting as used above. As a result, Table II-2 provides the means and standard deviations (inverse time scale) for the best fit of Eq. II-5 on the

histogram in Fig. II-8A. Table II-2 also shows values for  $m_i = 1/\mu_i$  (location of the maximum) and  $s_i = \frac{1}{2} \cdot \left( \frac{1}{\mu_i - \sigma_i} + \frac{1}{\mu_i + \sigma_i} \right)$  (estimated scatter), which are in the real time domain and thus intuitively easier to interpret. Maxima  $\pm$  scatter were  $115 \pm 40$  ms and  $225 \pm 41$  ms respectively for both modes of the double-recinormal fit (dotted line) on the latency histogram of Fig. II-8A. Table II-2 also provides the fit values for the control data for comparison. Note, that there were also two distinct latency modes for control trials. Interestingly, the minimum between the two modes in Fig. II-8A was located around 175 ms, which was the time needed for the extraretinal smooth eye movement signal to be taken into account for the saccade programming in Fig. II-7.

Previous studies showed that there is an inhibition of saccade initiation to previously attended positions (Klein 2000) and that there is a directional asymmetry of saccade latency during smooth pursuit eye movements (Kanai et al. 2003; Tanaka et al. 1998), i.e. saccades executed in the same direction as pursuit have shorter latencies than saccades in the opposite direction. All these experiments describe saccade latencies to visible stationary or moving targets. Here we investigated whether a similar behavior could also be observed for memory-guided saccades to briefly flashed targets. Furthermore, previous studies that analyzed smooth pursuit related directional differences in saccade latency used only horizontal stimuli and eye movements. Here, our 2-D paradigm will allow us to test saccadic latencies for different positions of the flash with respect to the smooth pursuit direction.

To address the question of a possible directional asymmetry of saccade latencies, we separated our data into foveofugal (FF) and foveopetal (FP) trials (see Methods section, Fig. II-1C). Figure II-6B shows the latency distributions of FF (gray histogram, dashed fit) and FP (white histogram, dotted fit) data separately. Fit parameters of Eq. II-5 were summarized in Table II-2. Interestingly, the relative importance of the short and long latency modes changed between FP and FF trials, while their location was approximately constant. FP trials contain more short latency than long latency saccades, whereas the opposite is the case for FF trials. Thus, the mean latencies for saccades to the FF and FP hemifield were 214 ms and

191 ms respectively. The difference between both means was highly significant (t-test,  $p < 0.0001$ ).

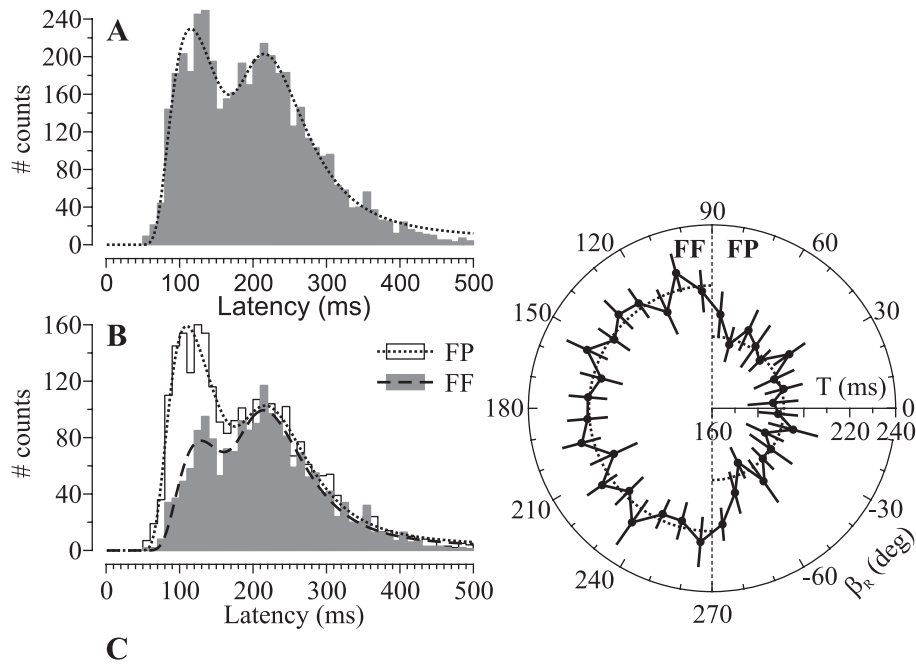


**Figure II-8: Saccade latency dependence on direction.** **A.** Histogram of latencies for all 1<sup>st</sup> saccades ( $N = 4,464$ ). The dotted line represents a double-recinormal fit function with maxima at 115 ms and 225 ms (see text for details). **B.** The same histogram divided into two populations, i.e. foveofugal (FF, gray histogram,  $N = 1,884$ ) and foveopetal (FP, white histogram,  $N = 2,580$ ) flash presentations. Maxima for the latency fit on the data were 129 ms and 223 ms for FF (dashed line) and 110 ms and 228 ms for FP (dotted line) flashes. **C.** Polar plot of saccade latencies as a function of the angle of flash appearance  $\beta_R$  relative to the smooth pursuit direction.  $\beta_R = 0^\circ$  corresponds to a flash presented straight ahead in direction of the eye movement. Black disks and whiskers indicate mean and SE for the 10°-angle bins. Dotted lines stand for mean values of the FF (214 ms) and FP (191 ms) hemifield separately. The difference between both means was highly significant (t-test,  $p < 0.0001$ ). See Table II-2 for detailed parameters.

Note that the FP and FF data sets were slightly different in their total number of trials, which was due to an asymmetry in the paradigm. Therefore, we also tested the FP/FF hemifield difference for a subset of our data with identical properties (we used the same range and distribution of  $PE_F$ ) for FP and FF and found no difference with the above reported results.

On average, the latency of FF saccades was larger but they were spatially more accurate when compared with FP saccades.

Our 2-D paradigm allowed us to go one step further, and to ask for the first time whether the asymmetry in saccade latencies reported in Fig. II-8B was due to a pursuit related focus of attention or whether it might be the result of an inhibitory hemifield effect. Therefore, we present in Fig. II-8C a polar plot of mean saccade latencies depending on the angle  $\beta_R$  between the flash position and the pursuit eye movement direction at the moment of the flash (see Methods section, Fig. II-1C). It can be easily observed that almost all mean latencies within the same hemifield had the same values and that there was a relatively sharp transition between the FP and FF hemifields.

How did the system decide whether to rapidly trigger a short latency but inaccurate saccade or to wait longer and trigger a spatially more accurate saccade? We investigated a possible dependence of the 1<sup>st</sup> saccade latency on the main sensory parameters measured at the moment of the flash appearance, i.e. the position error  $PE_F$  and eye velocity  $EV_F$  at the moment of the flash. In addition, we tested other parameters, like the smooth pursuit gain ( $gain_{SP,F}$ ) at the moment of the flash, the target velocity or the duration of ongoing smooth pursuit eye movement, but the overall regression results were best using the above-mentioned sensory variables. This analysis was also motivated by previous findings that showed a dependence of the mean saccade latency on the distance between the eye and the target (Bell et al. 2000; Clark 1999; Hodgson 2002; Kalesnykas and Hallett 1994).

The position error  $PE_F$  at the moment of the flash was the first sensory parameter that influenced the distribution of saccade latency. Figure II-9A shows the dependence of the 1<sup>st</sup> saccade latency on the distance  $PE_F$  between the flash and the eye. Mean values and standard errors in Fig. II-9A essentially indicated that for small position errors ( $PE_F < 5^\circ$ ) the latency was larger than for larger  $PE_F$ .

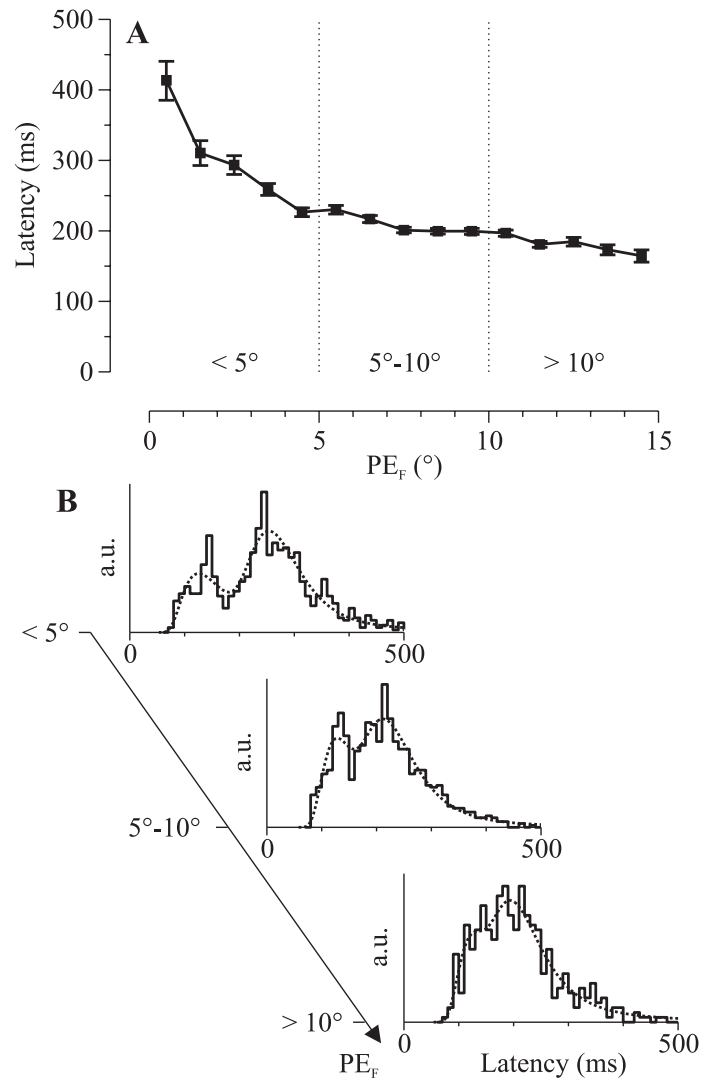


**Figure II-9: Target eccentricity influences saccade latency.** **A.** 1<sup>st</sup> saccade latency as a function of the distance  $PE_F$  between the flash and the eyes. Squares and whiskers indicate mean and SE ( $N = 29$  to  $493$ ). Separations (vertical dotted lines) of data for values of  $PE_F$  refer to histograms in panel B. **B.** Latency histograms (solid lines) and double-recinormal fits (dotted lines) for 3 subsets of data with respect to the range of  $PE_F$  values. See text and Table II-3 for more details.

We separated our data into three categories depending on  $PE_F$ , i.e. small ( $PE_F < 5^\circ$ ), medium ( $5^\circ < PE_F < 10^\circ$ ) and large ( $10^\circ < PE_F$ ) values, and

computed the latency histograms and double-recinormal fits in Fig. II-9B. The corresponding values for the fit parameters of Eq. II-5 to these histograms are summarized in Table II-3. For small  $PE_F$  values, the long latency mode of the histogram was more important than for larger  $PE_F$  values. While the value of the location of the short-latency mode's maximum remained roughly constant, the longer latency mode of the distribution moved towards shorter latencies with increasing  $PE_F$ .

**Table II-3:** Double-recinormal fit parameters for Fig. II-9

<b>Fit</b>	$m_1 \pm s_1$	$m_2 \pm s_2$	<b>mean <math>\pm</math> SD</b>	<b>N</b>	<b>R (p-level)</b>
Fig. II-9B: $PE_F < 5^\circ$	126 ms $\pm 43$ ms	257 ms $\pm$ 45 ms	258 ms $\pm$ 121 ms	817	0.9591 ( $< 0.0001$ )
Fig. II-9B: $5 < PE_F < 10^\circ$	119 ms $\pm 36$ ms	228 ms $\pm$ 40 ms	207 ms $\pm$ 93 ms	2232	0.9883 ( $< 0.0001$ )
Fig. II-9B: $PE_F > 10^\circ$	117 ms $\pm 36$ ms	200 ms $\pm$ 37 ms	182 ms $\pm$ 83 ms	1415	0.9864 ( $< 0.0001$ )

The second sensory parameter we found to influence the 1<sup>st</sup> saccade latency was the smooth eye velocity  $EV_F$  at the moment of the flash. Figure II-10A shows that the saccade latency depended approximately linearly on  $EV_F$ . The regression equation on raw data of the linear fit (solid line) was  $y = 168 \text{ ms} + 2.48 \text{ ms} * x$  ( $R = 0.183$ ,  $p < 0.0001$ ). Similar to Fig. II-9, we subdivided our dataset into different ranges of the sensory parameter  $EV_F$  (vertical dotted lines in Fig. II-10A) and plotted the corresponding latency histograms and double-recinormal fits in Fig. II-10B. Values of the fit parameters were summarized in Table II-4. Figure II-10B clearly demonstrates that the shift in mean saccade latency with higher  $EV_F$  values was due to the increased relative importance of the long-latency mode. This effect was underlined by the fact that the location of the long-latency mode's maximum was slightly shifted towards larger values with increasing  $EV_F$ .

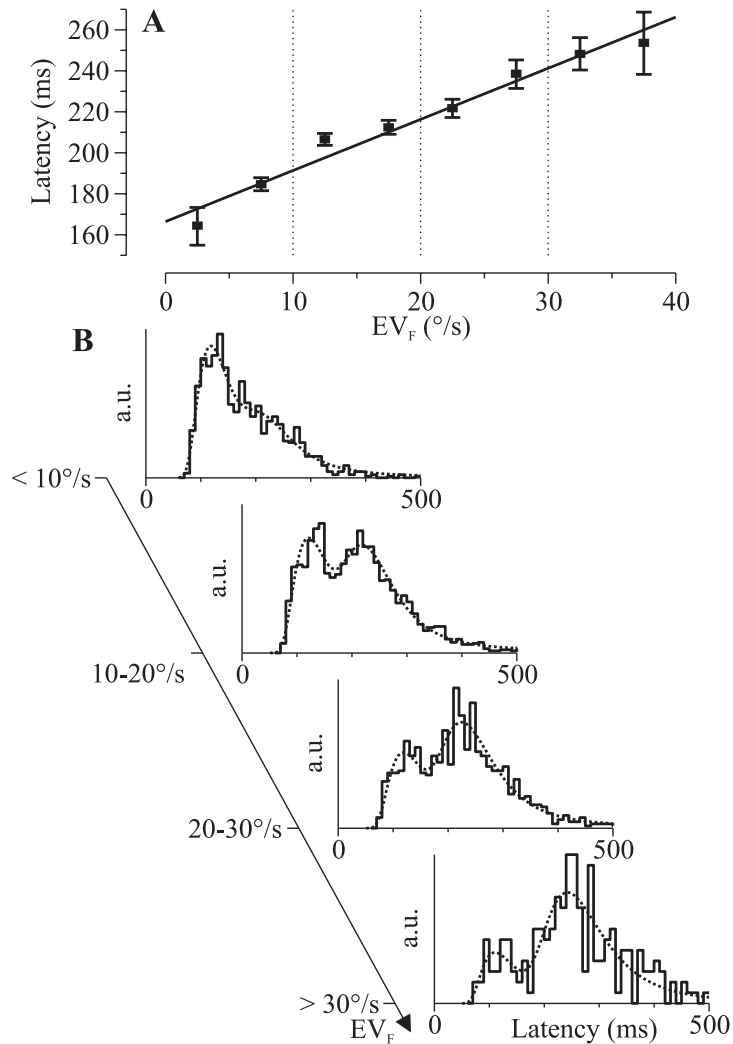


**Figure II-10: Eye velocity modulation of saccade latency.** **A.** 1<sup>st</sup> saccade latency dependence on the eye velocity  $EV_F$  at the moment of the flash. Squares and whiskers indicate mean and SE ( $N = 49$  to 1225). The solid line represents the linear fit on raw data (see text). Vertical separations (dotted lines) refer to panel B. **B.** Latency histograms (solid lines) and double-recinormal fits (dotted lines) for different subsets of the data with respect to different ranges of  $EV_F$  values. See text and Table II-4 for more details.

**Table II-4:** Double-recinormal fit parameters for Fig. II-10

<b>Fit</b>	$m_1 \pm s_1$	$m_2 \pm s_2$	<b>mean <math>\pm</math> SD</b>	<b>N</b>	<b>R (p-level)</b>
Fig. II-10B: $EV_F < 10^\circ/s$	118 ms $\pm 33$ ms	224 ms $\pm 43$ ms	181 ms $\pm$ 90 ms	1124	0.9850 ( $<0.0001$ )
Fig. II-10B: $10 < EV_F < 20^\circ/s$	121 ms $\pm 39$ ms	228 ms $\pm 43$ ms	210 ms $\pm$ 97 ms	2166	0.9878 ( $<0.0001$ )
Fig. II-10B: $20 < EV_F < 30^\circ/s$	119 ms $\pm 39$ ms	230 ms $\pm 46$ ms	228 ms $\pm$ 107 ms	969	0.9720 ( $<0.0001$ )
Fig. II-10B: $EV_F > 30^\circ/s$	110 ms $\pm 35$ ms	245 ms $\pm 52$ ms	251 ms $\pm$ 96 ms	205	0.9126 ( $<0.0001$ )

As a conclusion, our results concerning the influence of the sensory parameters on the 1<sup>st</sup> saccade latency revealed two distinct effects. First, large eye velocity ( $EV_F$ ) and small position error ( $PE_F$ ) increased the relative importance of the long-latency mode with respect to the shorter latency mode. Second, we observed a shift of the long-latency mode towards larger values when eye velocity ( $EV_F$ ) was high and position error ( $PE_F$ ) was small. Performing the same analysis using both sensory parameters in combination increased this effect yielding to an absence of the first latency mode for combined small  $PE_F$  and large  $EV_F$ , whereas long latency saccades disappeared for a combination of large  $PE_F$  and small  $EV_F$  (data not shown).

We would like to emphasize that the hemifield difference between FP and FF flashes (see Fig. II-8C) was still present in all analyses concerning the sensory parameters in Fig. II-9 and 10 (data not shown) and significant (t-test,  $p < 0.01$ ). We explicitly tested that our results were not an artifact of some combined parameter effect or even due to slight asymmetries of our dataset. As a result, we report here that both the FP/FF latency difference and the latency dependence on the sensory parameters at the time of the flash were consistent and unbiased effects. Furthermore, even though there were differences in the individual latency histograms when computed for each subject separately, all the above-described latency effects were present for all subjects.

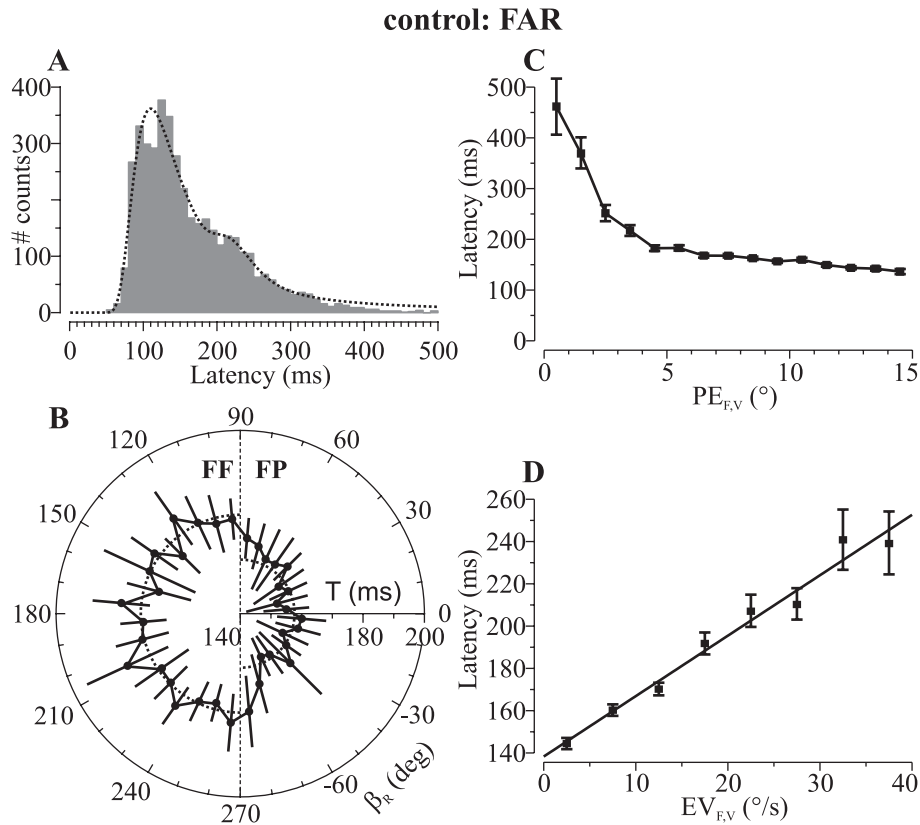


**Figure II-11: Saccadic latency for the flash after ramp (FAR) control. A.**

Histogram of latencies for all 1<sup>st</sup> saccades (N = 4,464) as in Fig. II-8A. The maxima of the double-recinormal fit were at 110 and 222 ms. **B.** Polar plot of saccade latencies as a function of the flash direction relative to the smooth pursuit direction. The same conventions as in Fig. II-8C apply. The mean values of FF and FP hemifield saccade latencies were 172 and 158 ms respectively. The difference between both means was highly significant (t-test,  $p < 0.0001$ ). **C.** Dependence of saccade latency on target eccentricity at the moment of the flash. The same conventions as in Fig. II-9A apply. **D.** 1<sup>st</sup> saccade latency dependence on the eye velocity  $EV_F$  at the moment of the flash. The same conventions as in Fig. II-10A apply.

For the saccade programming analyses, we indicated that results from the FAR control data were very similar. However, because in the FAR control situation the flashed stimulus did not compete any more with the pursuit ramp target, one might expect a different latency behavior. This was indeed the case for the histogram of first saccade latencies shown in Fig. II-11A. Nevertheless, all characteristics of the test trials latency

histogram (see Fig. II-8A) were present. We did still observe two separate modes of latency with approximately the same locations of the maxima (110 and 222 ms compared to 115 and 225 ms for test trials), although the second mode was less frequent. The previously described difference between FF and FP latencies was still present, including the hemifield asymmetry as shown in Fig. II-11B. Furthermore, a very similar modulation of the latency with the sensory parameters at the moment of the flash was observed for FAR control (see Fig. II-11C for  $PE_{F,V}$  and Fig. II-11D for  $EV_{F,V}$ ) compared to test trials (see Fig. II-9A and Fig. II-10A). Altogether, the comparison between FAR control trials and test trials showed that all mechanisms were consistently present in both paradigms and that only their frequency of appearance was different. The reason why we analyzed the test trials in more detail than the FAR control trials was the larger proportion of longer latency saccades. This allowed us to perform a statistically more robust analysis of the transition period from retinal to spatial saccade programming.

### ***4.3. Time course of orientation***

After the 1<sup>st</sup> orientation saccade towards the memorized position of the flash, we usually observed one or more corrective saccades that brought the eye closer to the spatial position of the flash. This was the case irrespectively of whether the first saccade was triggered with short or longer latency (see typical trials in Fig. II-2 and 3). The way in which the system reaches the memorized goal determined by a flash during smooth eye movements has previously been investigated for horizontal eye movements by Blohm et al. (2003b) who showed that the saccadic system was able to compensate for smooth anticipatory eye movements with a certain delay. Here, we observed qualitatively the same behavior, i.e. some time was needed for the smooth eye displacement to be taken into account (see 1<sup>st</sup> saccade programming results).

As already mentioned, the purpose of secondary “catch-up” saccades was to compensate for the remaining uncorrected smooth eye displacement. Thus, to analyze in more details the consequences of the secondary saccades, we computed the compensation index (CI) of Eq. II-3 for up to four saccades after the flash presentation and for different saccade latencies (measured with respect to the flash onset). In addition, we computed the same index, but after removal of the effect of the catch-up saccades. The results of this analysis are shown in Fig. II-12. One can easily

see the difference between the compensation indices when a saccade took place (black solid lines) compared to the same indices when we removed the compensatory effect of the saccade (gray dashed lines). Note that there is an initial increase of the compensation index only for the first saccade (shown in more details on Fig. II-6). For all successive saccades, this index is approximately constant. It should also be noted that the three secondary “catch-up” saccades significantly increase the compensation index (t-test on population mean:  $p < 0.001$  for all saccades but the fourth, where  $p = 0.03$ ).

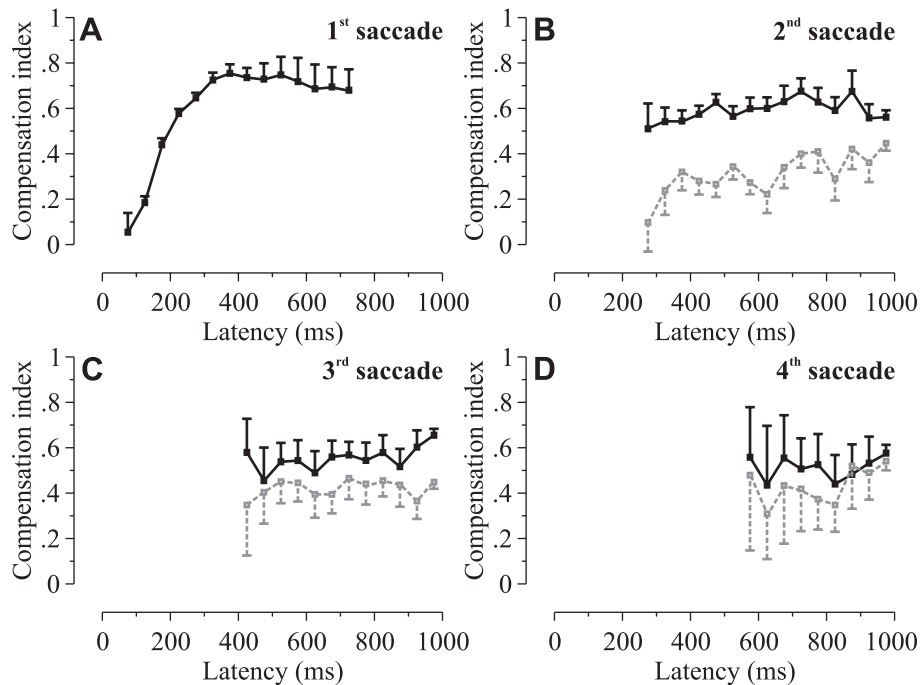


**Figure II-12: Consequences of the secondary “catch-up” saccades.** Compensation indices as a function of saccade latency with respect to the onset of the flash. Squares and whiskers indicate mean and SE. Black solid lines represent data after the occurrence of the saccade. Gray dotted lines indicate the same compensation index after removing the effect of the saccade. **A.** Compensation index for the first saccade (the same data as in Fig. II-6B but with larger bin sizes). **B.** Compensation index with or without the second saccade. The difference between both population means is highly significant (t-test,  $p < 0.001$ ,  $N = 3378$ ). **C.** Effect of the third saccade on the compensation index. The difference between the populations with and without corrective saccades is highly significant (t-test,  $p < 0.001$ ,  $N = 1743$ ). **D.** The presence of the fourth saccade only slightly increases the compensation index as indicated by the low significance of the populations’ difference (t-test,  $p = 0.03$ ,  $N = 707$ ).

Finally, we analyzed the contribution of the total extraretinal smooth eye displacement  $SED_{end}$  to the final position error  $PE_{end}$ , taking into account that there might also be a residual contribution of the retinal position error  $PE_F$  (measured at the moment of the flash) to  $PE_{end}$ . Table II-1 indicates the ranges of these parameters. The 2<sup>nd</sup> order regression for  $PE_{end}$  with the variables  $PE_F$  and  $SED_{end}$  provided the following results for the horizontal and vertical components:

$$PE_{end,X} = (-.121 \pm .037) + (.013 \pm .006) \cdot PE_{F,X} - (.465 \pm .009) \cdot SED_{end,X}$$

(R = 0.622, p < 0.001) Eq. II-6

$$PE_{end,Y} = (-.703 \pm .035) + (.091 \pm .005) \cdot PE_{F,Y} - (.429 \pm .010) \cdot SED_{end,Y}$$

(R = 0.559, p < 0.001) Eq. II-7

As a consequence, the saccadic system compensated for 98.7% (subject variability: 80.1% to 121.1%) of the horizontal (Eq. II-6) and 90.9% (subject variability: 71.3% to 106.5%) of the vertical (Eq. II-7)  $PE_F$  at the end of the orientation process. Note that this was a better performance than after the first orientation saccade (see Fig. II-7 and Table II-1). Furthermore, the final compensation for the smooth eye displacement was 53.4% (subject variability: 36.5% to 87.2%) horizontally (Eq. II-6) and 57.1% (subject variability: 45.0% to 73.3%) vertically (Eq. II-7). Our values were lower than the previously reported 70% overall SED compensation in the case of target localization during smooth anticipatory eye movements (Blohm et al. 2003b).

## 5. Discussion

The programming of memory-guided saccades during smooth eye movements reflects the performance of the system in maintaining space constancy. To investigate this mechanism, we presented a briefly flashed target during smooth pursuit eye movements and analyzed the characteristics of the 1<sup>st</sup> saccade. As a result, we found that short latency saccades were better correlated with retinal error than with spatial error, whereas the opposite was the case for longer latency saccades. The saccadic system approximately needed 175 ms before extraretinal information about the smooth eye displacement could be used in saccade programming. This behavior was also reflected in the latency distribution, where we found two

distinct modes – a short-latency and a longer latency mode – separated at around 175 ms. We interpret our results as evidence for the existence of two different neural processes for saccade programming: one fast but inaccurate and the other slower but spatially more accurate.

### ***5.1. Saccadic reaction times***

We observed a bi-modal distribution of saccade latencies in our test trials and in both control data sets. Similar distributions have been observed previously during saccadic “gap” and “overlap” paradigms (Fischer et al. 1997; Fischer et al. 1993; Reulen 1984a, b; Saslow 1967). One hypothesis for the presence of two separate modes could be related to the disengagement (or not) of attention in the expectance (or not) of a new target to appear. Another possibility will be discussed in the next sections, i.e. the saccadic bi-modality might reflect different mechanisms for saccade programming. However, since we also observed bi-modality in our FIX control trials, we suggest that it might reflect the signature of a more general saccadic mechanism. Further investigation will be needed to shed light on this particular aspect of our findings.

To quantify our bi-modal 1<sup>st</sup> saccade latency distribution, we fitted a double-recinormal distribution to our data. We used this particular distribution because it described very well our data with only very few parameters. However, as already mentioned in the Results section, this procedure is theoretically equivalent to the hypothesis of two distinct saccade trigger mechanisms of the LATER type (Carpenter and Williams 1995; Reddi et al. 2003; Reddi and Carpenter 2000), that work in parallel and do not interact. Although we cannot prove that such a mechanism exists, it is supported by our data since all latency distributions agree with the hypothesis of two parallel decision processes. Thus the system had to choose either one or the other process right away when the flash appeared, i.e. a short or longer latency trigger. Practically, both rise-to-threshold processes of the LATER type could be initiated in parallel, waiting for the system to choose between both during the first 50-75 ms after the flash onset. As we demonstrated in Fig. II-9 and 10, the system’s decision for either of the processes depended on the set of sensory parameters (distance of the target from the fovea and eye velocity) at the moment of the flash. Indeed, the effect of position error on saccade latency has previously been described (Bell et al. 2000; Clark 1999; Hodgson 2002; Kalesnykas and Hallett 1994)

and it makes sense that the system needs more time for small position errors to decide whether it is necessary to trigger a saccade. We did also observe this effect for our fixation control trials (data not shown) and our “flash after ramp” (FAR) controls (Fig. II-11C), i.e. the longer latency mode essentially resulted from flashes presented at small position errors. The influence of eye velocity on saccade latency however was – to our knowledge – a novel finding. Because for large smooth pursuit velocities the error after a short latency saccade (retinally programmed) would be big, the system might prefer to wait longer for extraretinal smooth eye displacement information to become available (see Fig. II-7). This “waiting strategy” allowed the system to perform spatially more accurate initial saccades. Thus the relationship between saccade latency and eye velocity described the system’s tradeoff between speed and accuracy.

We showed in Fig. II-8 and Fig. II-11B that the mean saccadic latency is shorter for flashes presented in the direction of the movement (foveopetal) than for flashed targets presented in the opposite direction (foveofugal). This is compatible with previous findings for horizontal catch-up saccades during smooth pursuit of continuously visible targets (Kanai et al. 2003; Tanaka et al. 1998). In these studies saccades in the same direction as smooth pursuit had shorter latencies than saccades in the opposite direction. In addition, this latency asymmetry was also present in our FAR control trials where no visible target was present. Kanai et al. (2003) hypothesized that this difference in latencies is due to the inhibition of saccades to previously attended positions during smooth pursuit, a particular instantiation of the “inhibition of return” (IOR) effect (see Klein 2000 for a review). At first sight, our data seemed to be compatible with such a hypothesis. However, our 2-D paradigm allowed us for the first time to show that this latency asymmetry is a hemifield effect and not related to a “focus of attention”, as IOR would predict (Maylor and Hockey 1985; Posner et al. 1985). Nevertheless, our results would be compatible with an attentional facilitation in the direction of the movement, if this facilitation is extended to the whole foveopetal hemifield. The purpose of such a hemifield bias could simply be to facilitate movement in the direction of heading.

### ***5.2. Saccades compensate for self-motion***

The analysis of the saccade latencies revealed a bi-modal distribution. The presence of these two different saccade trigger processes

was also reflected in the way saccades were programmed. We showed indeed that saccades with short latencies ( $< 175$  ms) were programmed using the only available retinal information, i.e. position error at the moment of the flash. This is in accordance with previous studies (Gellman and Fletcher 1992; McKenzie and Lisberger 1986) and contrasts with the situation where continuous visual feedback is present. In the latter, orientation saccades to the object's spatial location are programmed using two types of retinal information, i.e. position error and the relative velocity of the eyes with respect to the target (retinal slip) (de Brouwer et al. 2002a; de Brouwer et al. 2001; Gellman and Carl 1991; Keller and Johnsen 1990; Ron et al. 1989a). However, although retinal information about smooth self-motion was absent in our experiment, longer latency ( $> 175$  ms) saccades used a different programming mechanism that included extraretinal information about the smooth eye displacement in addition to the retinal position error.

Our results reconcile previous controversies. McKenzie and Lisberger (1986) reported that short latency memory guided saccades during pursuit eye movements were retinally coded. However, one monkey showed a bias of the suggested retinally saccade coding towards a more accurate spatial amplitude programming, that the authors attributed to the monkey's participation in previous smooth tracking experiments. However, this monkey also had particularly long mean saccade reaction times compared to the two other monkeys. We believe, that our results explain the third monkey's bias toward the spatial coding hypothesis simply as a consequence of longer latencies. Some variability in the saccade amplitudes to targets flashed at the moment of disappearance of a pursuit ramp reported by Gellmann and Fletcher (1992) might also be explained by our findings of a latency dependent saccade amplitude programming. Other studies showed that when memory guided saccades were executed after a delay period, smooth self-motion was compensated and saccades were spatially accurate (Baker et al. 2003; Herter and Guitton 1998; Ohtsuka 1994; Schlag et al. 1990; Zivotofsky et al. 1996), which is fully compatible with our results. Thus, we described here the missing piece in the puzzle of self-motion integration, i.e. the temporal transition between the retinal and spatial representation of the visual world in the oculomotor system.

As a result, we showed that space constancy during smooth pursuit eye movements seems to hold if the memory period is long enough but is

absent for shorter time scales. This view is supported by a recent study demonstrating that short-latency saccades to targets briefly presented during smooth anticipatory eye movements in darkness are programmed using only the retinal position error of the flash (Blohm et al. 2003b). Yet, additional saccades executed later on during the orientation process have also been reported (Blohm et al. 2003b; Mitrani et al. 1979). These saccades bring the eyes closer to the memorized spatial location of the target and compensate on average for 50-100% of the smooth eye displacement in darkness, depending on subjects. We do also report a large variability in the overall smooth eye displacement compensation, but our mean values were typically lower than in these previous studies. We hypothesize that this difference might be related to the different mean smooth eye displacement ranges in the different studies, which was lower in the paradigm we used here. Indeed, the system might trigger a smaller number of saccades when the error is small. However, the variability between subjects might also account at least partially for the difference between studies in the overall smooth self-motion compensation.

Initially, McKenzie and Lisberger (1986) used a paradigm similar to our FAR controls in an attempt to differentiate between two different types of saccade models, i.e. position and displacement models. Position models (Robinson 1975; Van Gisbergen et al. 1981) assume that the signal of desired eye position is compared with a signal of the current position of the eye in the orbit to generate a motor command. In contrast, displacement models (Jürgens et al. 1981; Scudder 1988) assume that a desired displacement – rather than a desired position – signal is used to drive the saccadic eye movement. During a saccade, this desired displacement is compared to an internal representation of the movement already executed to produce the movement command. McKenzie and Lisberger (1986) trained monkeys to saccade to flashes memorized during smooth eye movements to test the position versus the displacement model. The monkeys made saccades to the retinal position of the flash (Gellman and Fletcher 1992; McKenzie and Lisberger 1986), which validated the displacement model, since the position model would have predicted a spatially accurate eye movement. However, our data reported here as well as previous findings (Baker et al. 2003; Herter and Guitton 1998; Ohtsuka 1994; Schlag et al. 1990; Zivotofsky et al. 1996) support the idea that if more time is available to the system before the onset of the orienting eye movement, saccades can

be spatially accurate. This implies that there must be an additional mechanism available to perform this retinal to spatial transformation, but apparently, such a mechanism would take some time and is thus not implemented at the level of the saccadic displacement integrator. Hereafter, we will propose a neural mechanism that could account for all the data.

### ***5.3. Hypothesized underlying neural mechanisms***

As discussed above, the first orientation saccade was executed by one of two different separate mechanisms, i.e. either by a fast retinal coding or by a slower but spatially more accurate process. We believe that this reflects the presence of two different neural mechanisms for retinal and extraretinal information processes characterized by different processing times. In this section, we will shortly lay out one hypothesis of the underlying neural pathways that might be involved in the integration of smooth pursuit eye movements and the orientation to memorized targets.

The major forebrain and midbrain structures involved in the programming and/or control of saccades are the Posterior Parietal Cortex (PPC), the Frontal Eye Fields (FEF), the Dorsolateral Prefrontal Cortex (DLPC), the Basal Ganglia, the Cerebellum (CB) and the Superior Colliculus (SC) (see for a review Krauzlis and Stone 1999; Leigh and Zee 1999). It is generally accepted that SC is essential to generate short latency saccades (Fischer and Ramsperger 1986; Munoz and Wurtz 1992; Schiller et al. 1987). Indeed, Schiller et al. (1987) showed a lateralized absence of short latency saccades in monkeys after unilateral SC ablation, whereas longer latency saccades were still present. This was not the case for FEF ablation, which had no long-term effect on saccade latencies (Schiller et al. 1987). Therefore, we propose that the short latency saccades we reported here were essentially mediated by a fast “striatal-collicular pathway” (Leigh and Zee 1999). This contrasts with longer latency saccades that are known to involve most of the above-cited structures including PPC.

It has previously been suggested (Duhamel et al. 1992a; Heide et al. 1995), that PPC plays a key role to account for extraretinal signals (Tobler et al. 2001) when keeping track of self-motion to ensure space constancy. Indeed, the Lateral Intraparietal area (LIP) and area 7a in PPC receive information about upcoming saccades to update the spatial representation of visual stimuli (Andersen et al. 1985; Bremmer et al. 1997;

Medendorp et al. 2003). Therefore, we propose that the memorized flash position in our experiment is stored in PPC (Barash et al. 1991; Paré and Wurtz 1997; Pierrot-Deseilligny et al. 1991) and updated by smooth eye displacement information when it becomes available. The smooth eye displacement signal could result from an integration process of the smooth motor command (Blohm et al. 2003b), which might take some time. Such a process could involve parts of the Cerebellum – highly involved in generating smooth pursuit (Lisberger et al. 1987; Pola and Wyatt 1991) – and smooth eye displacement information could be projected either directly or via the Thalamus (Clower et al. 2001) to PPC to update the spatial representation of the flash. This would explain why in our data smooth eye displacement information took around 175 ms to become available to the saccadic system. According to this view, the classical saccade pathway would be responsible for retinally coded saccades. An additional feedback pathway for the integration of smooth pursuit eye movements could then be added to these classical structures to ensure space constancy during smooth eye movements. Our observation that smooth eye movement integration was characterized by a delay (~175 ms) implies that the system only compensates for the smooth eye displacement that has already been integrated. This might explain why the compensation mechanism is not an all-or-none process. However, we cannot exclude a possible role of proprioception (Steinbach 2000) for the spatial orientation towards the flash, although proprioception is thought not to be a predominant source for spatial localization (Weir 2000) and the control of eye movements in general (Lewis et al. 2001).

Behaviorally, we identified two different modes for the programming of memory-guided saccades during smooth pursuit eye movements. At a neural level, we proposed that retinally coded short latency saccades were mediated by the classical saccade pathway, i.e. via SC. However, for the spatial coding of longer latency saccades, the system needs to keep track of smooth pursuit commands. Here, we proposed CB as a candidate to monitor smooth eye displacements. Electrophysiological experiments are needed to identify the exact neural correlates of this process and we therefore propose to record in pursuit-related areas of CB to uncover the hypothesized eye velocity integration structures. We also propose electrophysiological recordings in different areas of the Thalamus to identify a neural substrate for the smooth eye displacement efference copy pathway from CB to PPC. Indeed, the Thalamus is an interesting area because similar

---

corollary discharge signals have been found to send saccadic eye movement information from SC via the Mediodorsal Thalamus (MD) to FEF (Sommer 2003; Sommer and Wurtz 2002, 2004a, b) to monitor saccades. Another important question arises from the neural programming of longer latency saccades, i.e. does SC code the total saccade amplitude (including the smooth eye displacement) or is the smooth eye displacement information added to the saccadic command downstream from SC, as this seems to be the case for retinal slip signals in catch-up saccades (Keller et al. 1996b; May et al. 1988; Thurston et al. 1988). We suggest using our original 2-D paradigm in recording studies to identify the neural correlates underlying the monitoring of smooth pursuit. The presence of two separate control modes for memory guided saccades during smooth eye movements could provide a new testing bench to investigate the neural processes of smooth motion integration. More generally, our results provide a new path to investigate the interaction between smooth pursuit and saccadic systems.



# CHAPTER III

## INTERACTION BETWEEN SMOOTH ANTICIPATION AND SACCADES DURING OCULAR ORIENTATION IN DARKNESS\*

*Good ideas are not adopted automatically. They  
must be driven into practice with courageous  
patience.*

Hyman Rickover

### 1. Abstract

A saccade triggered during sustained smooth pursuit is programmed using retinal information about the relative position and velocity of the target with respect to the eye (de Brouwer et al. 2002a). Thus, the smooth pursuit and saccadic systems are coordinated by using common retinal inputs. Yet, in the absence of retinal information about the relative motion of the eye with respect to the target, the question arises whether the smooth and saccadic systems are still able to be coordinated possibly by using extraretinal information to account for the saccadic and smooth eye movements. To address this question, we flashed a target during smooth anticipatory eye movements in darkness and the subjects were asked to orient their visual axis to the remembered location of the flash. We observed multiple orientation saccades (typically 2-3) towards the memorized location of the flash. The first orienting saccade was programmed using only the position error at the moment of the flash and the smooth eye movement was ignored. However, subsequent saccades executed in darkness compensated gradually for the smooth eye displacement (mean compensation  $\cong 70\%$ ). This behavior revealed a 400 ms delay in the time course of orientation for the compensation of the ongoing smooth eye displacement. We conclude

---

\* This chapter has been published: Blohm G, Missal M, Lefèvre P. J Neurophysiol 89: 1423-1433 (2003)

that extraretinal information about the smooth motor command is available to the saccadic system in the absence of visual input. There is a 400 ms delay for smooth movement integration, saccade programming and execution.

## **2. Introduction**

Saccades and smooth pursuit eye movements are used in combination during orientation of the visual axis towards a moving target. It was previously thought that these different eye movements were controlled by independent neural systems, although they act in synergy in order to reach a moving target. This view has recently been challenged at the neuronal level (Keller and Missal 2003; Krauzlis and Miles 1998; Missal et al. 2000; Missal and Keller 2002, 2001). At the behavioral level, the coordination between saccades and smooth pursuit has so far been studied during orientation towards a moving visual target (de Brouwer et al. 2002a; de Brouwer et al. 2001). In this condition, it has been shown that saccadic and smooth pursuit motor commands sum up. Furthermore, the saccadic and smooth pursuit systems could share a common source of information, i.e. the slip of the target image on the retina. This sharing of visual information allows the saccadic system to compensate for the motion of the target during the latency period and the execution of catch-up saccades. Thus, to accurately orient the eyes towards a visual target, the saccadic and smooth pursuit systems interact and movements are programmed using retinal information. Yet, this is only true if there is continuous visual feedback. In the absence of visual input, the question arises whether different movements could still be coordinated. In such a situation, the oculomotor system has to integrate extraretinal signals to account for self-motion.

The role of extraretinal signals in the saccadic system has been addressed in numerous studies by means of the double-step and the colliding saccades paradigms (Aslin and Shea 1987; Becker and Jürgens 1979; Dassonville et al. 1992; Dominey et al. 1997; Goossens and Van Opstal 1997; Hallett and Lightstone 1976a, b; Mays and Sparks 1980; Mushiaké et al. 1999; Schlag and Schlag-Rey 1990; Schlag et al. 1989; Schlag-Rey et al. 1989; Tian et al. 2000). In these studies, saccades towards the memorized position of flashed targets were investigated. If before a saccade the eyes were deviated by another saccade evoked either visually or by microstimulation, the second saccade accurately reached its goal. The system

had to use some information about the first eye movement to adjust the second saccade because the initial retinotopic vector of the second saccade was not accurate anymore. These authors concluded that the saccadic system has access to extraretinal signals, i.e. the efference copy of the saccadic motor command, that update the internal representation of the target in space. Thus, in the absence of retinal input, the saccadic system makes an extensive use of extraretinal signals.

However, the double-step and colliding saccades paradigms investigate only one aspect of the self-movement integration, i.e. whether the oculomotor system keeps track of consecutive saccades by using extraretinal signals. What would happen if prior to a saccade the eyes were displaced by a smooth eye movement instead of a saccade? Would the system have access to extraretinal information about self-movement in order to accurately orient the eyes? If this was the case, could the system adjust the saccadic goal or would there be an a posteriori mechanism that accounted for the smooth perturbation? Both scenarios would need a source of extraretinal information to compensate for the smooth eye displacement. Here, we address the question whether the saccadic system receives such extraretinal information from the pursuit system to account for smooth eye movements in darkness.

In order to investigate this topic, we used a paradigm that could generate smooth eye movements without bringing into play any retinal slip information. This allowed us to rule out the hypothesis that a memorized retinal slip signal could play a role. Furthermore, our protocol provided a saccadic goal using as little retinal information as possible. We achieved this objective by using anticipatory smooth pursuit and memory-guided saccades. Indeed, orientation of the visual axis in the absence of retinal stimulation is possible in both smooth and saccadic systems. Saccades can be aimed towards the memorized position of a previously flashed target (Goldman-Rakic 1987). Anticipatory smooth eye movements can be evoked in the absence of a moving target if there is a previous 'build-up' of the expectation of future target motion (Barnes and Asselman 1991; Kao and Morrow 1994; Kowler et al. 1984). Thus, we reduced the visual information available to the oculomotor system to a minimum. This disabled the ability of the saccadic system to rely on retinal information about motion to program saccades. In that way, we created an original paradigm that allowed us to investigate the

hypothesis of a mechanism that could compensate for the smooth eye movements by means of corrective saccades based on extraretinal signals.

### **3. Materials and Methods**

#### ***3.1. Experimental set-up***

Human subjects sat in darkness in front of a 1 m distant tangent screen, which spanned about  $\pm 45$  deg of their visual field. Their head was restrained by a chin-rest. A 0.2 deg red LASER target spot was back-projected onto the screen and moved horizontally under the control of a mirror-galvanometer. Movements of one eye were recorded with the scleral coil technique, SKALAR MEDICAL BV (Collewyn et al. 1975; Robinson 1963). Healthy subjects without any known oculomotor abnormalities were recruited after informed consent. Among the seven subjects, three were completely naïve of oculomotor experiments. Mean age was 29, ranging from 22 to 36. All procedures were conducted with approval of the Université catholique de Louvain Ethics committee.

#### ***3.2. Paradigm***

Recording sessions were composed of a series of blocks of 40 trials. Each session was divided into 3 parts: First, each subject had to perform one block of control trials towards stationary targets, then a block of build-up trials was presented to build up a smooth anticipatory response and the last (but longest) part of the sessions was composed of several blocks of test trials mixed with build-up trials.

Control trials were composed of two types of randomly presented stimuli (transient and sustained; Fig. III-1A). All control trials began with a fixation period of 800 ms in the center of the screen. After the target disappeared for a variable duration of 100-500 ms (gap), either a 10 ms flash (transient control condition) or a 1000 ms target (sustained control condition) was presented at random locations in a range  $\pm 15$  deg around the central fixation point. All control trials lasted for 2300 ms. Subjects were instructed to orient their eyes towards the target (sustained control condition) or towards the remembered position of the flash (transient control condition).

In order to build up a smooth anticipatory response, we used build-up trials (Fig. III-1B). After a fixation period of 800 ms in the center of the

screen the target disappeared for 300 ms. The gap duration was chosen to give a maximal smooth anticipatory response (Morrow and Lamb 1996). At reappearance, the target moved for 800 ms from the center of the screen at 40 deg/s always in the same direction. The trial ended with a 500 ms fixation period. Subjects were instructed to follow the target as accurately as possible.

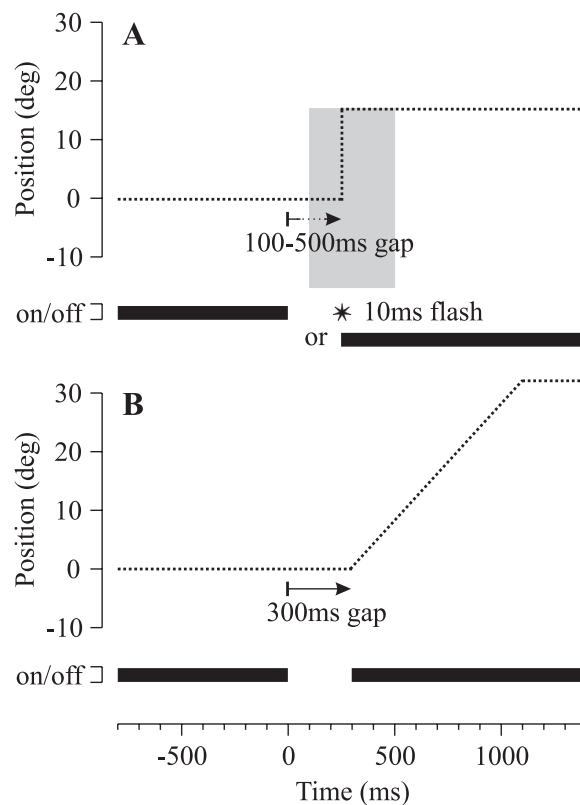


**Figure III-1:** Experimental paradigm. **A:** Test trial condition. The trial starts with a 800 ms fixation period. Afterwards, either a 10 ms flash (transient condition) or a 1000 ms fixation (sustained condition) is presented at random time and position. In grey is indicated the randomisation zone. The gap varies continuously between 100 ms and 500 ms and the target reappears randomly in a range  $\pm 15$  deg around the expected target position. The dotted line represents target position. The horizontal bar in the lower part of the panel represents the presence of the target; the star stands for the 10 ms flash. **B:** Build-up trial condition. After 800 ms fixation, the target disappears for 300 ms (gap) and reappears moving for another 800 ms at 40 deg/s to the right followed by 500 ms of final fixation.

For the third part of the recording session, build-up trials were randomly interleaved with 30% of test trials: transient and sustained test trials (Fig. III-1A). Both test conditions began like the build-up trials with an 800 ms fixation at the center of the screen followed by a gap that varied randomly in duration from 100 ms to 500 ms. After the gap, either a 10 ms flash (transient test condition) or a 1000 ms target (sustained test condition) was presented at a random position in a range  $\pm 15$  deg around the expected target position (= target position of build-up trial). All trials lasted for 2300 ms. Subjects were instructed to follow the target as accurately as possible and to fixate the memorized target position in case of a transient test trial.

### ***3.3. Data acquisition and analysis***

Eye and target position were sampled at 500 Hz and stored on the hard disc of a PC for off-line analysis. MATLAB (Mathworks, Inc.) was used to implement digital filtering, velocity and acceleration estimation algorithms. Position signals were low-pass filtered by a zero-phase digital filter (autoregressive forward-backward filter, cutoff frequency: 50 Hz). Velocity and acceleration were derived from position signals using a central difference algorithm.

In our analysis, only control and test trials were analyzed. We were interested in saccades directed towards the flashed or sustained target. Saccades were detected using an acceleration threshold of  $750 \text{ deg/s}^2$  and their latency was measured with respect to the target onset. We analyzed the first saccade for all stimulus conditions. Up to five orienting saccades were taken into account in the transient condition. Saccades were removed from the eye velocity trace to obtain the smooth velocity. Therefore, we measured the smooth eye velocity before and after the saccade and interpolated linearly between the values to obtain an estimation of the smooth eye velocity during the saccades. This allowed us to quantify the contribution of the smooth pursuit system  $P_{\text{Amp}}$  to the total saccadic amplitude  $S_{\text{Amp}}$ . We also measured different parameters that may play a role in saccadic programming. Position error (PE) and retinal slip (RS) signals were sampled at the moment of the target onset ( $t_0$ ) and 100 ms before the saccade. For more details about the estimation of those parameters, see Methods section of de Brouwer et al. (2002a). Furthermore, the smooth eye velocity signal was integrated to obtain the smooth eye displacement SED. In the transient

test condition, the orientation process continued after the first saccade and the time course of this process was investigated. The final orientation was defined as the eye position after the last saccade before return to the central fixation point.

#### 4. Results

Three examples of the different stimulus conditions are illustrated in Fig. III-2.

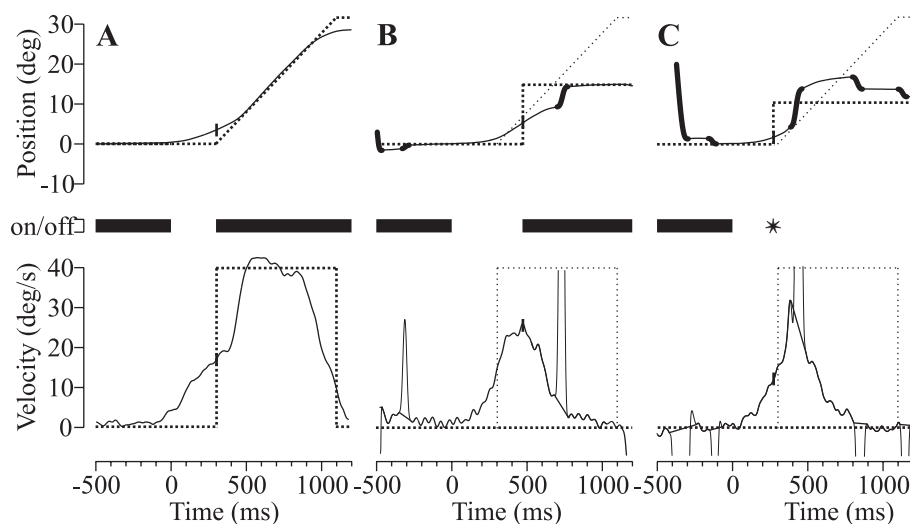


**Figure III-2:** Typical examples. In the upper panels, solid lines represent the eye position (bold lines mark saccades), dotted lines are target position and thin dotted lines stand for the expected build-up target position (in panels B-C). In the lower panels, solid lines represent the smooth eye velocity (without saccades). Saccades are shown as thin solid lines. Dotted lines represent target velocity and thin dotted lines stand for the expected build-up target velocity (in panels B-C). The horizontal bars in the center part of panels A-C represent the presence of the target; the star in the center part of panel C stands for the 10 ms flash. **A:** build-up response. **B:** sustained test trial. **C:** transient test trial.

For build-up trials (Fig. III-2A), the eye movement could be entirely smooth although most of the time anticipatory and/or visually guided saccades were present. In the test trials (Fig. III-2B-C), subjects anticipated as in the build-up trials. Sustained test trials (Fig. III-2B) typically presented one or two saccades towards the target, whereas for transient test trials (Fig. III-2C) subjects typically needed two or three

orienting saccades. Subjects reported that they perceived the 10 ms flash as being stationary. This is in accordance with the findings of Gellman and Fletcher (1992). However, sustained test targets were perceived to be in movement, which is due to the retinal slip caused by the smooth anticipatory eye movement. The last saccade towards the visual or remembered target always occurred when smooth eye velocity was close to 0 deg/s.

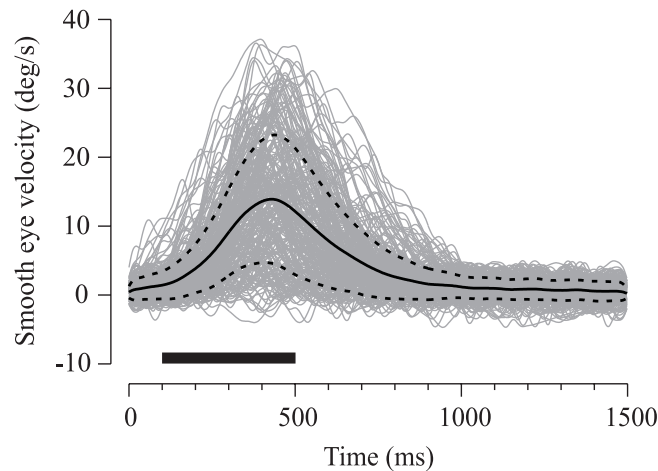


**Figure III-3:** Time course of smooth eye movements for the transient test condition. Gray lines show individual trials. The mean smooth eye movement (solid line) and the associated standard deviation (dashed lines) are also shown. The bar at the bottom of the figure indicates the range of the time of appearance of the flash. All smooth eye movement traces are aligned on the gap onset (time 0).

Figure III-3 shows the pattern of smooth eye movements for transient test trials. The pattern was very similar for sustained test trials. After the gap onset (Fig. III-3, time 0), smooth anticipation built up. The mean smooth anticipatory eye velocity at the moment of the target reappearance (sustained or transient) was  $9.3 \pm 6.3$  deg/s ( $N = 4238$ ) ranging from 0 deg/s to 34 deg/s. The amplitude of the smooth anticipatory movement varied from trial to trial and depended on the trials history across the experimental session (build-up or test trials). This influence of the history of previous trials has first been described by Kowler et al. (1984).

#### 4.1. *General saccadic properties*

In this section, we describe the characteristics of the first saccade towards the test target for both the sustained and the transient test conditions. All results were tested and are valid separately for each condition but will be presented together for the sake of clarity. We first analyzed the main sequence relationship as well as the saccadic latency histogram.

During sustained smooth pursuit the motor commands of the saccadic and smooth pursuit system sum up (de Brouwer et al. 2002a). As the smooth pursuit system is active during the saccadic command execution, the total saccadic amplitude  $S_{Amp} = S_{Amp}^* + P_{Amp}$ , where  $S_{Amp}^*$  is the component from the saccadic system and  $P_{Amp}$  is the contribution of the pursuit system. This is reflected in the saccadic main sequence relationship, where control saccades and those during sustained pursuit (opposite or in the same direction as the saccadic command) fall into three different populations. After correction for the participation of the smooth pursuit system, all three populations merge into one.

Here, we performed this analysis for saccades triggered during smooth anticipatory eye movements. Both main sequence relationships – saccade duration vs. saccade amplitude and saccade peak velocity vs. saccade amplitude – were analyzed. Correlations for both main sequence relationships were significantly better (t-test, p-level < 0.05) after correction for the smooth anticipation component than before correction (total N = 4985). Figure III-4 illustrates this result for the main sequence relationship between saccade duration and amplitude for subject #7. Only for one subject (subject #5) the 2<sup>nd</sup> main sequence relationship did not show a significant improvement after correction for the smooth component.

Taking it all together, we showed here that like smooth pursuit, smooth anticipation adds up to the saccadic motor command. Therefore, when analyzing saccade programming, we first removed the pursuit component ( $P_{Amp}$ ) from the saccade ( $S_{Amp}$ ). All subsequent analyses were thus performed on the corrected saccade amplitude  $S_{Amp}^*$ .

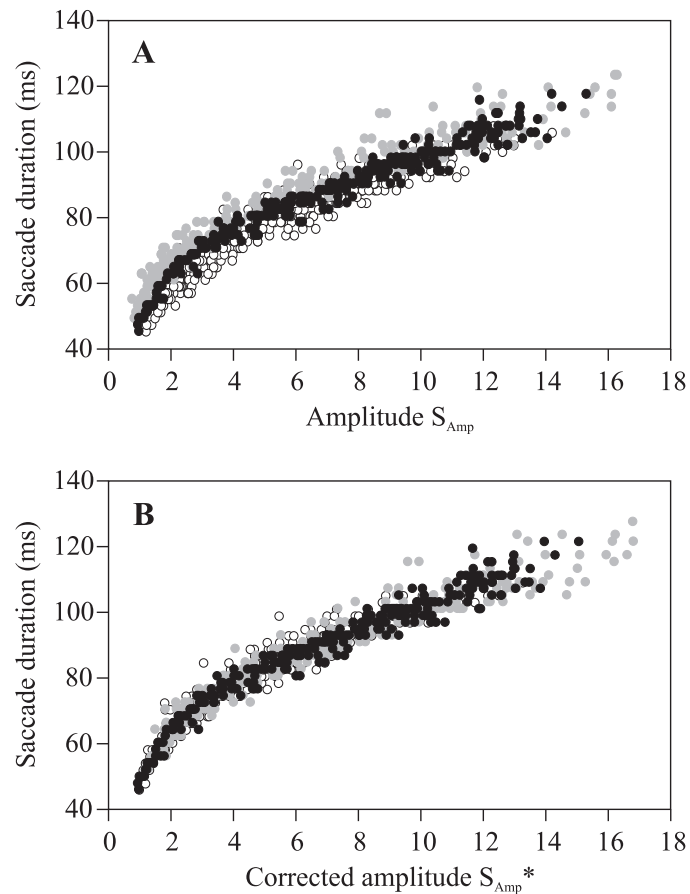


**Figure III-4:** Main sequence relationship between saccade duration and amplitude. Forward saccades (saccades and smooth movements in the same direction, open disks), reverse saccades (saccades and smooth movements in opposite directions, grey disks) and control saccades (black disks) are represented. **A:** The main sequence between duration and amplitude before correction ( $S_{Amp}$ ). Forward, reverse and control saccades fall in three distinct populations. **B:** The same main sequence for the corrected amplitude  $S_{Amp}^*$ , i.e. after correction for the smooth movement ( $P_{Amp}$ ). The three populations merge into one.

For the first orientation saccade after target reappearance, we evaluated whether the information used for its programming was based on the sensory signal of the target or whether it was an anticipatory saccade directed towards the expected moving target. Figure III-5A shows an example of such an anticipatory saccade (latency: 37 ms). This analysis was

done to quantify the minimum saccade latency we could consider for the analysis of saccades during test trials. If the saccade endpoint fell into a  $\pm 5$  deg interval around the target position, the saccade was considered to be visually driven. Otherwise, if the saccade endpoint fell into another  $\pm 5$  deg interval around the expected build-up ramp, the saccade was classified as anticipatory. If the saccade endpoint fell into both intervals, the trial was not classified (6.5 % of trials).

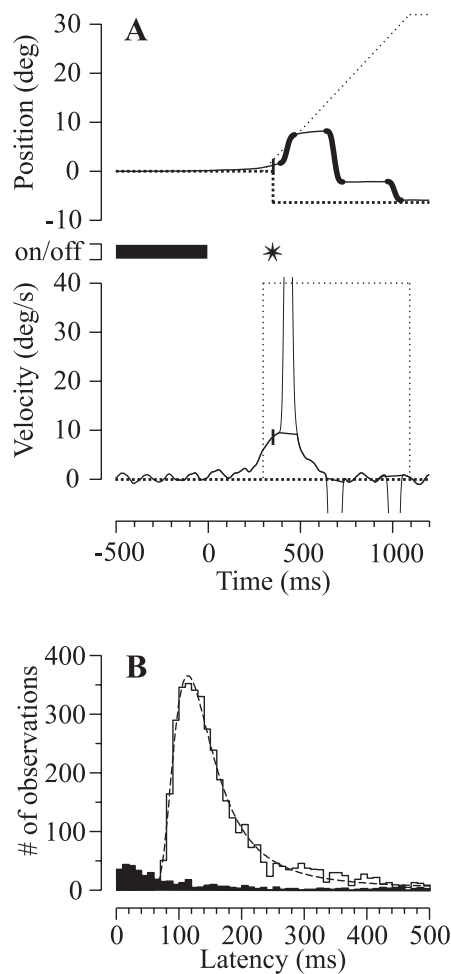


**Figure III-5:** Minimum latency of the first saccade. **A:** Anticipatory saccade directed towards the expected target ramp (latency: 37 ms). The same conventions as in Fig. III-2 are used. **B:** Histogram (10 ms bins) of the trials for which the saccade was programmed towards the actual target (white,  $N = 3832$ ) or to the expected target (black,  $N = 406$ ). Data are pooled for all subjects. The dashed line represents the recinormal distribution fit of the LATER model for saccade latency (Reddi and Carpenter 2000). Fitted parameters of the normal distribution in the reciprocal time domain are mean =  $8.77 \text{ s}^{-1}$  and SD =  $2.38 \text{ s}^{-1}$ .

The histogram of the classified saccadic latencies pooled for all subjects is shown in Fig. III-5B. The dark histogram represents anticipatory saccades ( $N = 406$ ) whereas the white histogram corresponds to visually

guided saccades ( $N = 3832$ ). Saccades that fell into the black histogram for latencies larger than 300 ms came exclusively from the transient test condition. In order to describe the latency histogram with an analytical function, we first tried a normal distribution. However, the Jarque-Bera test for goodness of fit to a normal distribution rejects the hypothesis that the saccadic latencies follow a normal distribution ( $p\text{-level} < 0.001$ ). Thus we described the latency histogram with a recinormal function (Reddi and Carpenter 2000). This function fitted well the data (see dashed line in Fig. III-5B;  $R = 0.972$ ,  $p\text{-level} < 0.001$ ), which means that it is the reciprocal of latency that follows a normal distribution. The maximum of the fitted recinormal distribution lies at 114 ms. The onset of visually guided saccades in the histogram reveals saccadic latencies as short as 80 ms. No significant difference was found between the sustained and the transient test conditions. The maximum of the fitted distribution varied from 88 ms to 132 ms across subjects.

#### 4.2. *Programming of the first saccade*

We were interested in how the saccadic system programs the first orienting saccade after the target reappearance for both the sustained and transient test conditions. In the previous section we showed that the smooth anticipatory command adds linearly to the motor command of the saccadic system. Thus, to analyze the saccade programming, we subtracted the smooth anticipatory eye displacement during the saccade  $P_{\text{Amp}}$  from the measured saccade amplitude  $S_{\text{Amp}}$  to obtain the purely saccadic component  $S_{\text{Amp}}^*$ . In this analysis, we included saccades with latency  $> 125$  ms (de Brouwer et al. 2002a). Table IV-1 summarizes the principal parameters that characterize the sustained and transient test trials. The saccadic gain was defined as the ratio between the measured saccade amplitude  $S_{\text{Amp}}$  and the ideal saccade ( $S_{\text{Amp}} + PE_{\text{after 1st saccade}}$ ). For the transient test trials, Table IV-1 gives also an indication about the final error  $PE_{\text{end}}$  and the total smooth eye displacement  $SED_{\text{total}}$  at the end of the orientation process.

In the case of the sustained test condition, the question is whether the retinal slip is evaluated to program the saccade, as is the case during sustained pursuit (de Brouwer et al. 2002a). Indeed, de Brouwer et al. (2002a) showed that saccades triggered during sustained pursuit are programmed using an estimate of the position error and the retinal slip measured 100 ms before saccade onset. They hypothesized that 100 ms

before saccade onset is the last moment for visual information to be taken into account in saccadic amplitude programming (Becker and Jürgens 1979; Heywood and Churcher 1981).

**Table IV-1:** Mean values and ranges of different parameters that characterize our data set.

<i>Variable</i>	<i>Mean ±SD</i>	<i>[25-75]% Range</i>	<i>N</i>
<b>Sustained</b>			
S <sub>Amp</sub> <sup>*</sup>  , deg	5.633 ± 3.919	[2.298 – 8.544]	984
PE <sub>-100</sub>  , deg	5.870 ± 4.326	[2.107 – 9.292]	984
RS <sub>-100</sub> , deg/s	10.225 ± 8.538	[3.771 – 14.916]	984
PE <sub>after 1st saccade</sub>  , deg	0.806 ± 0.697	[0.289 – 1.102]	984
Saccadic gain	0.929 ± 0.182	[0.834 – 1.043]	984
<b>Transient</b>			
S <sub>Amp</sub> <sup>*</sup>  , deg	6.330 ± 3.478	[3.287 – 8.917]	583
PE <sub>to</sub>  , deg	7.008 ± 3.867	[3.515 – 10.073]	583
EV <sub>to</sub> , deg/s	9.387 ± 6.188	[4.820 – 14.716]	583
SED <sub>after 1st saccade</sub> , deg	2.229 ± 1.682	[0.876 – 3.384]	583
PE <sub>after 1st saccade</sub>  , deg	2.019 ± 1.437	[0.851 – 2.918]	583
Saccadic gain	0.880 ± 0.328	[0.684 – 1.018]	583
PE <sub>end</sub>  , deg	1.069 ± 1.434	[0.114 – 1.556]	1354
SED <sub>total</sub> , deg	2.956 ± 3.393	[1.120 – 4.540]	1354

To test the hypothesis that the system behaves in the same way for anticipatory and visually guided smooth pursuit, we performed a multiple regression analysis for the dependent variable S<sub>Amp</sub><sup>\*</sup> using the independent variables PE<sub>-100</sub> and RS<sub>-100</sub>. The index -100 indicates that we measured these parameters 100 ms before saccade onset. Table IV-2 shows the results of the analysis for the sustained test condition. The best correlation was obtained with PE<sub>-100</sub> and RS<sub>-100</sub> as independent variables (Eq. III-1).

$$S_{Amp}^* = 0.249 + 0.930 \cdot PE_{-100} + 0.059 \cdot RS_{-100} \quad (R = 0.991, N = 984)$$

Eq. III-1

The separate analysis for each subject shows that the multiple regression with PE<sub>-100</sub> and RS<sub>-100</sub> was always significant, except for one subject (subject #5:  $p > 0.05$  for coefficient of RS<sub>-100</sub>). Across subjects, regression coefficients varied for PE<sub>-100</sub> between 0.885 and 0.984 and for RS<sub>-100</sub> between 0.035 and 0.086. As a result, we showed here that the same

strategy is used for saccades to sustained targets during smooth pursuit or during smooth anticipation.

**Table IV-2:** Correlation coefficients for the multiple regression analysis between the dependent variable  $S_{Amp}^*$  and the independent variables for sustained test trials (N = 984).

<i>Indep. variable 1</i>	<i>Indep. variable 2</i>	<i>R</i>	<i>Partial R (variable 1)</i>	<i>Partial R (variable 2)</i>
PE <sub>-100</sub>	-	0.990 (p < 0.01)	-	-
RS <sub>-100</sub>	-	0.185 (p < 0.01)	-	-
PE <sub>-100</sub>	RS <sub>-100</sub>	0.991 (p < 0.01)	0.990 (p < 0.01)	0.340 (p < 0.01)

**Table IV-3:** Correlation coefficients for the multiple regression analysis between the dependent variable  $S_{Amp}^*$  and the independent variables for transient test trials (N = 583).

<i>Indep. variable 1</i>	<i>Indep. variable 2</i>	<i>R</i>	<i>Partial R (variable 1)</i>	<i>Partial R (variable 2)</i>
PE <sub>to</sub>	-	0.989 (p < 0.01)	-	-
EV <sub>to</sub>	-	0.255 (p < 0.01)	-	-
SED	-	0.254 (p < 0.01)	-	-
PE <sub>to</sub>	EV <sub>to</sub>	0.990 (p < 0.01)	0.989 (p < 0.01)	0.034 (p > 0.05)
PE <sub>to</sub>	SED	0.990 (p < 0.01)	0.989 (p < 0.01)	0.074 (p > 0.05)

In the transient test condition, the target was only presented very briefly (for 10 ms) and therefore the system did not have time to evaluate the retinal slip. Furthermore, after the flash, there was no more visual feedback that could be used to program the orienting saccades. The only available sensory information was the memorized position error of the target at the moment of the flash onset PE<sub>to</sub>. Thus, the question here is whether the saccadic system has access to any other internal information such as, for example the smooth eye velocity at the moment of the flash onset EV<sub>to</sub> or the smooth eye displacement SED (= integral of smooth eye velocity) between

the flash and the saccade onset. To test these hypotheses, we performed a multiple regression analysis with the dependent variable  $S_{Amp}^*$  and the independent variables  $PE_{to}$ ,  $EV_{to}$  and  $SED$ . Only saccades with latencies shorter than 250 ms were considered in this analysis. Table IV-3 summarizes the results of this analysis. Single regression results showed that the saccade amplitude was best correlated with  $PE_{to}$ . Partial correlation coefficients in the multiple regression analysis were significant for  $PE_{to}$ , but neither for  $EV_{to}$  nor for  $SED$ . Clearly, our statistical analysis showed that there was no other parameter than  $PE_{to}$  that was used for the first saccade programming in the transient test condition (Eq. III-2).

$$S_{Amp}^* = -0.183 + 0.888 \cdot PE_{to} \quad (R = 0.989, N = 583) \quad \text{Eq. III-2}$$

Regression coefficients for  $PE_{to}$  varied for each subject and ranged from 0.807 to 0.947. In the transient test condition, there was no significant difference in gain of the first saccade between the transient test condition and the transient control trials ( $p > 0.05$ ). This indicates that for flashed targets the smooth eye movement was ignored by the saccadic system. This was compatible with the error measured after the saccade, which was proportional to the smooth eye displacement ( $SED$ ) between the flash and the end of the saccade (Fig. III-6A).

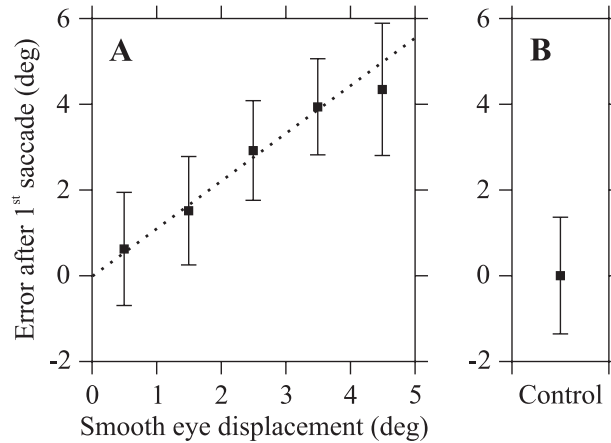


**Figure III-6:** Position error after the first saccade (latency < 250 ms) as a function of the smooth eye displacement  $SED$  (mean and standard deviation). A: Transient test trials. The dotted line is fitted on raw data. The number of points in each 1 deg bin varies between 47 and 233. B: Control trials for comparison ( $SED = 0$  deg,  $N = 1251$ ).

When plotting data for all subjects, the equation of the first order regression was the following:

$$PE = 0.014 + 1.139 \cdot SED \quad (R = 0.665, N = 583) \quad \text{Eq. III-3}$$

The slope of the regression varied between subjects from 0.772 to 1.260 (N = 62 to 123). Figure III-6B provides a comparison with control trials (mean = -0.080, std = 1.444, N = 1251). In the transient test condition, the dependence of the error after the first saccade on SED confirmed that at this time SED was not used by the saccadic system to program the saccade.

### 4.3. Time course of orientation

Until now, we only analyzed the first orienting saccade that occurred after the target reappearance. In the case of the sustained test condition, most of the time the first orienting saccade brought the eye exactly onto the target. If there was a residual error, it was corrected by a second saccade and the orientation process was completed. Thus, no further analysis of the sustained test situation was necessary. But in the case of the transient test condition, our typical example (Fig. III-2C) clearly shows that the orientation process went on after the first saccade and that subsequent saccades contributed significantly to the final gaze orientation. In this case, how did the oculomotor system perform this orientation process without any additional visual feedback? We first quantified the accuracy of the final orientation. For the orientation to be accurate, the subject had to compensate for the total smooth eye displacement after the flash. Figure III-7A shows the error after the last orienting saccade  $PE_{end}$  as a function of the total smooth eye displacement between the flash and the moment of the final orienting saccade  $SED_{total}$ . The first order regression for all subjects pooled together (dashed) follows the equation:

$$PE_{end} = 0.027 + 0.308 \cdot SED_{total} \quad (R = 0.328, N = 1354) \quad \text{Eq. III-4}$$

Across subjects, the slope ranged from 0.075 to 0.572 (N = 168 to 370). In Fig. III-7A, the dotted line corresponds to the regression in Fig. III-6A and allows a direct comparison between compensation for SED after the first saccade versus at the end of the orientation process. This confirmed that the orientation process did not stop after the first saccade and that the final orientation accounted for most of the smooth eye displacement. We can get an idea of the time course of orientation by providing additional

regression lines for two intermediate steps between the first saccade and the final orientation. This is shown in Fig. III-7B.

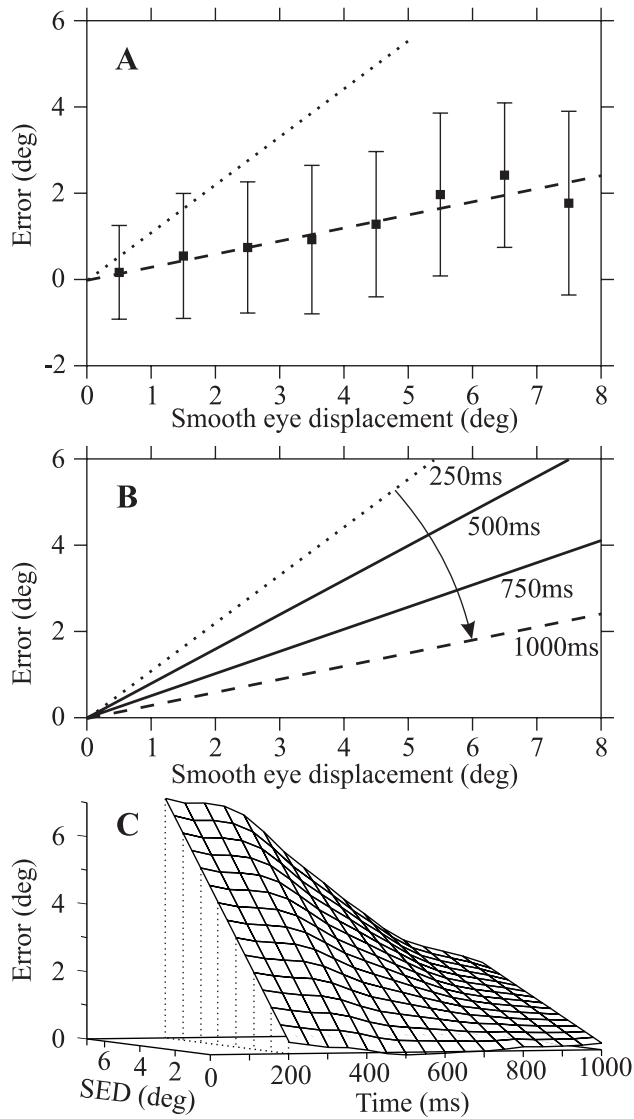


**Figure III-7:** Time course of position error. **A:** Final error as a function of the total smooth eye displacement (mean and standard deviation). The dashed line is fitted on raw data (N = 1354). The dotted line is transposed from Fig. III-6 for comparison. **B:** Time course of error between the first saccade (dotted) and the final orientation (dashed) with two intermediate errors. Labels indicate the moment of sampling. **C:** 3-D representation of the position error as a function of SED and time.

Dotted and dashed lines correspond to regression lines from Fig. III-7A. The slopes of the regression lines at 500 ms and 750 ms after the flash were 0.793 ( $R = 0.598$ ,  $N = 1272$ ) and 0.418 ( $R = 0.469$ ,  $N = 1345$ ) respectively. This indicated that the smooth eye displacement was not accounted for in one step but that there was a gradual orientation process. A more detailed representation of this gradual orientation is provided in Fig. III-7C. The evolution of the time course of orientation error is presented as a function of the smooth eye displacement SED between 200 ms and 1000 ms in 50 ms steps.

In the following section, the time course of the orientation process will be analyzed in more detail. Therefore, position error  $PE(t)$  and smooth eye displacement  $SED(t)$  were sampled at regular 50 ms intervals and a 2<sup>nd</sup> order regression analysis was performed using the sampled position error as dependent variable and the sampled smooth eye displacement  $SED$  and the position error at the moment of the flash  $PE_{t_0}$  as independent variables:

$$PE(t) = \beta(t) + \gamma(t) \cdot PE_{t_0} + \delta(t) \cdot SED(t) \quad \text{Eq. III-5}$$

$PE_{t_0}$  was included in the regression to investigate whether the error due to a saccadic gain  $< 1$  (after the first saccade) was compensated later in the orientation process. The regression coefficients  $\gamma(t)$  and  $\delta(t)$  for  $PE_{t_0}$  and  $SED$  respectively are shown in Fig. III-8A.

From the  $SED$  coefficient  $\delta(t)$ , one can see that the orientation process started around 400 ms after the flash and ended around 800 ms after the flash. Furthermore, this process compensated not only for  $SED$  but also for the saccadic gain error, which is present at the time of the first saccade. At the end of the orientation process, the total saccadic gain was 0.989 compared to 0.888 at 250 ms after the flash. For comparison, we provide in Fig. III-8B the mean and standard deviation of the smooth eye velocity after the flash onset. In Fig. III-8, smooth eye velocity traces are aligned on the flash onset and not on the gap onset, as this was the case in Fig. III-3. Therefore, in Fig. III-8B the variability of the smooth eye movement amplitude is partly due to the variability of the flash onset.

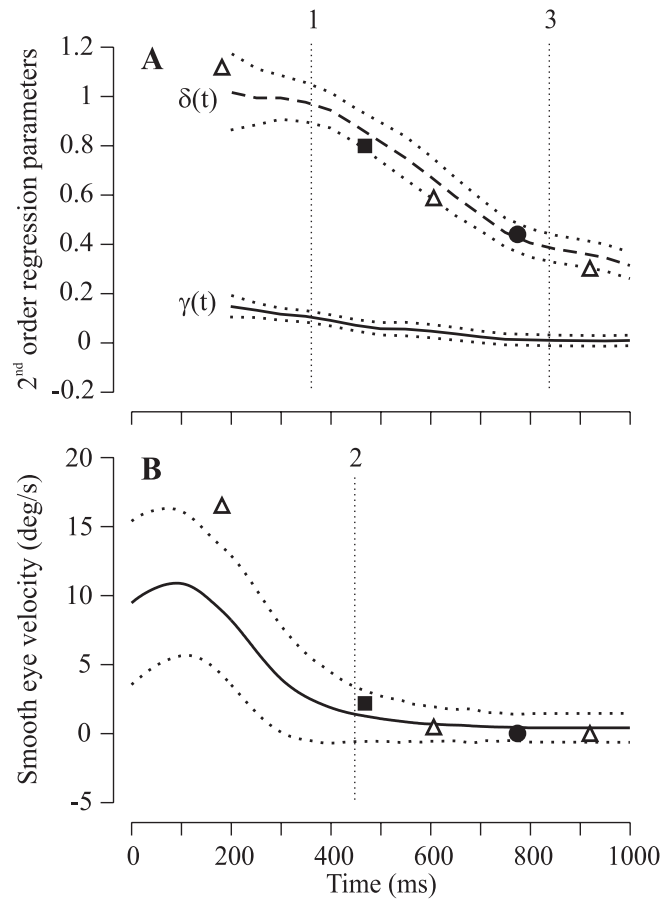


**Figure III-8:** Time course of the orientation process. **A:** 2<sup>nd</sup> order regression coefficients of the error in time are represented (mean and 95% confidence interval). Independent variables are the smooth eye displacement SED (coefficient  $\delta(t)$ , dashed line) and the position error at the moment of the flash  $PE_{t_0}$  (coefficient  $\gamma(t)$ , solid line). **B:** Mean (solid line) and standard deviation (dotted lines) of the smooth eye velocity across all trials. Symbols in both panels refer to examples of Fig. III-9 (see text). Vertical dotted lines represent the onset of the orientation process (1), the end of the smooth eye displacement (2) and the end of the orientation process (3).

The open triangle symbols in Fig. III-8A-B correspond to individual data from the example in Fig. III-9A. The coefficient of SED ( $\delta$ ) and the instantaneous smooth eye velocity were measured after each saccade and follow the average time course of these parameters in Fig. III-8A-B. The solid symbols in Fig. III-8A-B are associated with two other examples

(Fig. III-9B-C) and show that the time course of the coefficient of SED ( $\delta(t)$ ) was not influenced by the sequence of saccades. This can be observed when looking at the first saccade of examples B and C in Fig. III-9. A comparison of example B with example A shows that SED compensation has already started for the first saccade of example B whereas this was not the case for the first saccade of example A. This behavior is even more dramatic if we compare example C with example A. For the first saccade in example C, SED compensation is similar to that of the third saccade in example A. This illustrates that only the time of saccadic execution determines the amount of SED compensation and not whether it is the first, second or third saccade.

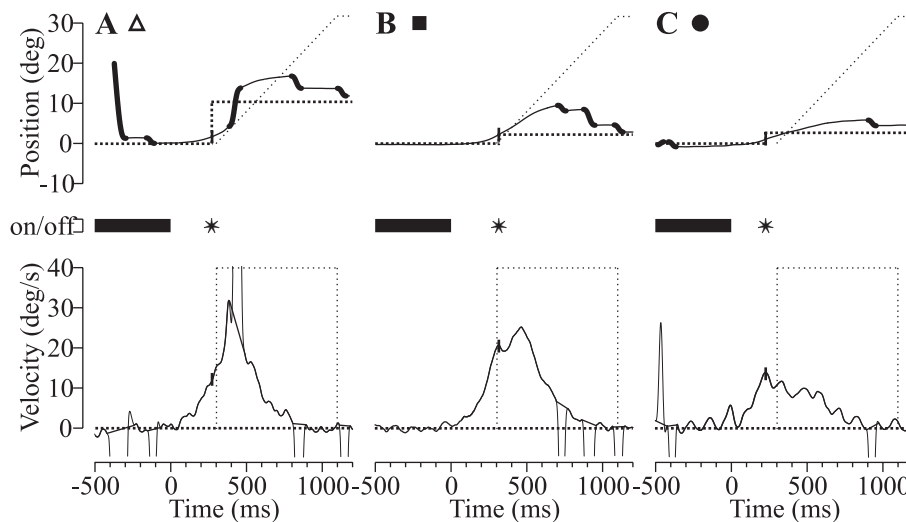


**Figure III-9:** Examples for the transient test condition to illustrate the time course of orientation in Fig. III-8. The same conventions as in Fig. III-2 are used. **A:** Short first saccade latency (106 ms). **B:** Delayed first saccade (latency = 412 ms). **C:** Late first saccade (latency = 716 ms).

Dotted vertical lines in Fig. III-8A-B indicate different landmarks in the orientation process and the eye movement. These were obtained by determining when the measured variable fell below 10% of the maximum or rose above 10% of the minimum with respect to the total scale. We evaluated the beginning (dotted line 1) and the end (dotted line 3) of the orientation process at 363 ms and 835 ms respectively. With the same procedure we measured the end of the smooth eye movement (dotted line 2) at 440 ms after the flash. Thus, there was approximately the same delay of 400 ms between flash onset and the beginning of the compensation process

and between the end of the smooth eye movement and the end of the orientation process.

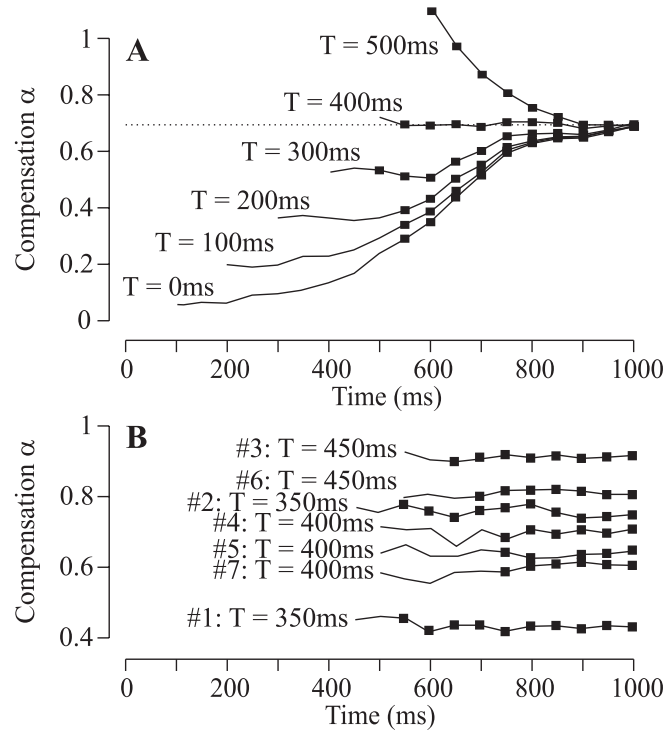


**Figure III-10:** Compensation  $\alpha(t)$  of the smooth eye displacement SED (refer to Eq. III-6 in text). **A:** Solid lines represent the evolution of  $\alpha$  in time for different delays  $T$ . Squares indicate when the compensation  $\alpha(t)$  is significant ( $p$ -level  $< 0.01$ ). For  $T = 400$  ms,  $\alpha$  is approximately constant over time and equal to 0.69. This corresponds exactly to the average contribution of SED to the final error ( $1 - \alpha$ , see Fig. III-7 and 8). This is consistent with the hypothesis that compensation is a delayed process with a constant gain. **B:** Optimal compensation  $\alpha$  of the smooth eye displacement SED for each subject. The optimal delay  $T$  is also given. Numbers refer to the different subjects.

In Fig. III-10A-B we tested the hypothesis that a constant delay model might explain the time course of the orientation process. This means that at a given instant in time  $t$  subjects would compensate for the smooth eye movement accomplished up to time  $t - T$ . Thus, the assumption that the compensation  $\alpha$  is proportional to SED accumulated up to a delay  $T$  before the measure of the position error  $PE(t)$  mathematically translates into the following expression:

$$PE(t) = SED(t) - \alpha(t) \cdot SED(t - T) \quad \text{Eq. III-6}$$

The first term,  $SED(t)$ , describes the proportionality of the error to  $SED$  in the early orientation process. The second term is compensatory and accounts for the smooth eye displacement accumulated up to  $t - T$ . In comparison with Eq. III-5, we removed the term proportional to  $PE_{t_0}$  for this analysis because Eq. III-6 was simpler and the results were qualitatively the same.

Figure III-10A shows the value of  $\alpha(t)$  for different values of the delay  $T$ . The curve for  $T = 0$  ms corresponds to the evolution of  $\delta(t)$  in Fig. III-8A. Interestingly, the value of  $\alpha$  was a constant in time ( $\alpha \cong 0.7$ ) for a delay of 400 ms. This is compatible with the hypothesis that the time course of the compensation process could be explained by a constant compensatory gain combined with a delayed signal of the smooth eye displacement. This hypothesis was confirmed by the analysis performed on each subject individually in Fig. III-10B. For each subject, there was a specific time delay (ranging from 350 ms to 450 ms) that yielded a constant compensatory gain  $\alpha$  (ranging from 0.43 to 0.93).

## 5. Discussion

In the absence of a smooth eye movement, saccades can be aimed towards the spatial location of a memorized or visual target (Becker and Jürgens 1979). In this study, we perturbed this condition by inducing a smooth anticipatory eye movement that participated in the gaze displacement. We found a linear addition of the smooth anticipatory and saccadic motor commands for all test conditions. Furthermore, in the sustained test condition, the saccadic system used a predictive component (based on the retinal slip) in catch-up saccade programming. In the transient test condition, the saccadic system did not take into account the smooth anticipatory eye movements in the early stage of the orientation process towards the target. However, we provided strong evidence for a compensatory mechanism between both oculomotor subsystems later on in the orientation process. Thus, the oculomotor system can rely on extraretinal information to control the coordination between its different components.

### ***5.1. Saccade properties***

The analysis of the main sequence relationship showed evidence that smooth anticipatory and saccadic drives are both operational and are linearly summated during the saccade. The same result was obtained previously for the smooth pursuit system (de Brouwer et al. 2002a). This finding has two implications. Firstly, the smooth anticipatory motor system does not pause during saccades and thus the smooth anticipatory component must be removed for the analysis of saccades executed during anticipation. Secondly, the saccadic system interacts in the same way with the smooth pursuit and smooth anticipatory systems. This finding is compatible with the hypothesis that these two smooth motor systems share common neural structures. This view is supported by several behavioral studies (Boman and Hotson 1988; Braun et al. 1996; Kao and Morrow 1994).

The saccadic latency histogram showed two main properties. Firstly, the minimum latency for saccades aimed at visual targets is very short (around 80 ms). The use of a gap in our paradigm and the fact that the eyes were moving at the appearance of the target might explain this behavior, since both factors release active fixation (Krauzlis and Miles 1996a, b, c). Secondly, saccadic latency histograms in our experiment are well described by the LATER model (Reddi and Carpenter 2000). The recinormal function fitted our data significantly better than a normal distribution. Thus, we showed that this model does not only apply to saccades following fixation but that it also describes the latencies of saccades triggered during smooth anticipatory eye movements in darkness.

### ***5.2. Programming of the first orienting saccade***

In the sustained test condition, the first orienting saccade was programmed using the position error and retinal slip sampled 100 ms before the saccade onset. The behavior was qualitatively the same as during smooth pursuit and thus saccades were accurate (de Brouwer et al. 2002a). However, the coefficient of RS that we found in Eq. III-1 is smaller than in the study by de Brouwer et al. (de Brouwer et al. 2002a), i.e. 0.059 vs. 0.091. It may be due partly to differences between subjects. Nevertheless, we believe that the main effect is due to the difference between the active pursuit paradigm of de Brouwer et al. (de Brouwer et al. 2002a) and the anticipatory pursuit in darkness. In our paradigm, subjects had to reengage active pursuit after the

target appearance, which might result in an underestimation of the retinal slip.

In the case of the transient test condition, the first saccade was programmed only on the basis of the position error at the moment of the flash, which was the only retinal information available to the oculomotor system in this condition. In several previous studies, subjects had to orient gaze towards a target that was briefly flashed after the disappearance of a smooth pursuit target (Gellman and Fletcher 1992; McKenzie and Lisberger 1986; Schlag et al. 1990). These studies are compatible with our finding that first orienting saccades only account for the position error at the moment of the flash. However, these studies only reported data on the first orienting saccade and did not give any indication about the orientation process going on afterwards.

### ***5.3. Time course of the orientation process***

The presence of multiple orientation saccades in our paradigm revealed a compensatory mechanism that accounted for the smooth eye displacement. Compensation started about 400 ms after the flash and lasted until around 400 ms after the end of the smooth eye movement. This process is compatible with the hypothesis of a delayed compensation mechanism. The delay of 400 ms explains the time course of the compensation process and the apparent evolution of the compensatory gain in Fig. III-8. This hypothesis has been confirmed independently in each subject, with a fairly constant delay ( $400 \text{ ms} \pm 50 \text{ ms}$ ) associated with a subject-specific constant compensation gain.

What is the origin of this 400 ms delay? Since the compensation is only apparent after orienting saccades, this delay clearly includes several components. Firstly, it includes the time necessary to make the decision to trigger a saccade and to program this saccade (estimation  $\cong 75 \text{ ms}$ ). Secondly, there is the duration for the execution of the saccade (mean  $\cong 75 \text{ ms}$  in our data). The last component ( $250 \text{ ms} = 400 \text{ ms} - 150 \text{ ms}$ ) reflects some internal delay between the execution of the smooth eye movement and the time when an efferent copy of the smooth motor command can be integrated (to provide SED) and used by the saccadic system.

In our analysis, we found an overall compensation gain of 0.7, which is not perfect. This partial compensation could be related to the fact that targets flashed during a movement may be perceptually mislocalized (see Schlag and Schlag-Rey 2002 for a review). This perceptual mislocalization, which is called the flash-lag effect, may influence the compensation gain we obtained.

#### ***5.4. Proposed model***

During orientation towards visual targets, catch-up saccades use retinal slip information to interact with the smooth pursuit system. Here, we disrupted the ability of the saccadic system to access retinal information about the relative target displacement. Nevertheless, the saccadic system could account for the smooth eye displacement, although with a 400 ms delay. On the one hand, this delayed mechanism suggests that the saccadic system has to rely on an efference copy signal of the smooth motor command. We consider that an efference copy is the only available signal since proprioception is unlikely to play a role in ocular orientation (Lewis et al. 2001). On the other hand, the length of the delay (400 ms) might reflect the implication of several sub-cortical and cortical areas in this pathway.

We propose a model that may account for the observed compensation mechanism (Fig. III-11). This model is composed of three distinct parts: the smooth system (left), an integrator of the smooth motor command (center) and the saccadic system (right). The gap onset acts as a cue for the smooth system to generate an anticipatory motor command that is sent to the smooth movement generator to anticipate the expected ramp target. During the test trials, either a sustained or a flashed target appears. Since the orientation to sustained targets relies on known mechanisms (de Brouwer et al. 2002a), we will only consider the case of the flashed targets in the proposed model.

We hypothesize that the flash influences the smooth and saccadic systems. On the one hand, the flash occurrence is a cue to the smooth motor system to stop the anticipatory eye movement. At the same time this cue resets the integrator of the smooth motor command, which provides SED to the saccadic system. On the other hand, the location of the flash determines a goal  $\Delta E$  for the saccadic system. A first short-latency orienting saccade is executed based on the retinal error information provided by the flash. If the



We will try to propose a hypothesis about the underlying neural correlates that could support our model. Details about the smooth pursuit and saccade generators will not be discussed here (Krauzlis and Stone 1999). Here, we concentrate on the pathway integrating the smooth motor command and programming the compensatory saccades. As we already mentioned, the 400 ms delay suggests that the integration of the smooth motor command takes place in the cerebral cortex. The internal representation of the smooth eye displacement  $\Delta E_{\text{SED}}$  could be used to update the memorized spatial representation of the flashed target.

We propose that the parietal cortex might play a relay role between the smooth pursuit and saccadic systems because areas implied in both types of eye movements project to this brain region. Furthermore, the parietal cortex is strongly implied in processing extraretinal signals (Tobler et al. 2001) and is important for self-movement integration (Duhamel et al. 1992a; Heide et al. 1995). Lateral intraparietal region (LIP) and area 7a receive information about the saccadic commands to encode the location of the visual stimulus in spatial coordinates (Andersen et al. 1985; Bremmer et al. 1997). In addition, LIP neurons discharge prior to saccades and remain active while remembering a desired target location (Barash et al. 1991; Paré and Wurtz 1997) and lesions of the posterior parietal cortex impair the ability to make memory-guided saccades (Pierrot-Deseilligny et al. 1991).

Following our hypothesis not only inputs from the saccadic system could update the internal target representation in the parietal cortex but there might also be a contribution from the smooth pursuit system accounting for the smooth eye displacement. In fact, the smooth pursuit system communicates bilaterally with the posterior parietal cortex (area 7a) via the medial superior temporal (MST) area (Tusa and Ungerleider 1988). Neurons in MST carry information about the smooth eye movements (Newsome et al. 1988) that might come from an efference copy of the smooth motor command (Leigh and Zee 1999). Thus, smooth movement information could update the internal representation of targets in space and saccades could be triggered whenever the parietal cortex communicates information about a smooth eye displacement to the saccadic system.

## **6. Conclusion**

In this paper, we studied the interaction between smooth anticipatory eye movements and saccades. Saccades triggered during smooth anticipation towards a sustained visual target are programmed using the available retinal input, as is the case during sustained smooth pursuit. If flashed targets are presented, no retinal information about the movement is available to program adequate saccades. However, saccades can correct for the smooth eye displacement that took place some time before and this process has been estimated to take around 400 ms. Thus, we believe that the saccadic system has access to an efference copy of the smooth motor command to monitor the smooth eye displacement.

## CHAPTER IV

# SMOOTH ANTICIPATORY EYE MOVEMENTS ALTER THE MEMORIZED POSITION OF FLASHED TARGETS<sup>\*</sup>

*Whilst part of what we perceive comes through  
our senses from the object before us, another  
part (and it may be the larger part) always  
comes out of our own mind.  
William James*

### 1. Abstract

Briefly flashed visual stimuli presented during smooth object- or self-motion are systematically mislocalized. This phenomenon is called the “flash-lag effect” (Nijhawan 1994). Previous studies all had one common characteristic, the subject’s sense of motion. Here, we asked whether motion perception is a necessary condition for the flash-lag effect to occur. In a first experiment, we briefly flashed a target during smooth anticipatory eye movements in darkness and subjects had to orient their gaze toward the perceived flash position. Subjects reported to have no sense of eye motion during anticipatory movements. In a second experiment, subjects had to adjust a cursor on the perceived position of the flash. As a result, we show that gaze orientation reflects the actual perceived flash position. Furthermore, a flash-lag effect is present despite the absence of motion perception. Moreover, the time course of gaze orientation shows that the flash-lag effect appeared immediately after the egocentric to allocentric reference frame transformation.

---

<sup>\*</sup> This chapter has been published: Blohm G, Missal M, Lefèvre P. *J Vis* 3, 764-773 (2003)

## 2. Introduction

It seems natural that in our everyday life we experience the visual environment to be spatially stable. However, when we orient gaze or move through the visual scene, self-motion induces an optic flow. Thus, for a stable space perception during self-motion the central nervous system (CNS) has to use extraretinal signals to compensate for retinal motion. In this condition, the question arises how the brain combines visual signals from the environment with internal signals related to self-motion.

An interesting way to address the issue of a stable percept of the environment is to perform a localization task. To localize a flashed object, the brain has to integrate the object's retinal location with an extra-retinal signal about the direction of gaze (Bridgeman 1995; Festinger and Canon 1965; Mergner et al. 2001; Mon-Williams and Tresilian 1998; van Beers et al. 2001). It is particularly difficult for the CNS to match moving and flashed stimuli because continuously changing variables, i.e. position and velocity signals, have to be matched at key events although they are processed with different delays. A systematic bias of the perceived position shows the limits of this process (see Schlag and Schlag-Rey 2002 for a review).

One condition in which localization errors happen is during smooth object- or self-motion. An impressive demonstration of such a perceptual mislocalization has first been conducted by MacKay (1958) and has later been rediscovered by Nijhawan (1994). In their experiment, two strobed segments that were flashed in alignment with a continuously lit rotating line lagged the moving object and the size of the lag increased with angular velocity. This phenomenon is called the "flash-lag effect" and has been extensively studied using the original, rotational configuration (Brenner and Smeets 2000; Eagleman and Sejnowski 2000; Krekelberg and Lappe 1999; Lappe and Krekelberg 1998; Purushothaman et al. 1998) as well as using constant linear motion (Brenner et al. 2001; Whitney et al. 2000; Whitney and Murakami 1998). However, the flash-lag effect is not restricted to moving objects but also appears during smooth pursuit eye movements (Kerzel 2000; Nijhawan 2001; van Beers et al. 2001). This is also the case for head or whole body movements (Schlag et al. 2000). In both conditions, retinal signals about motion are absent. Even more spectacular is the finding that in certain conditions a flash-lag appears without any motion at all.

Illusory motion perception can induce a perceptual bias of a flashed target (Cai et al. 2000; Nishida and Johnston 1999; Watanabe et al. 2002).

The flash-lag effect shows two characteristic features. Firstly, there is a difference in flash localization error depending on the retinal location of the flash with respect to the motion direction, i.e. a flash presented ahead or behind the gaze direction is mislocalized differently (Kerzel 2000; Nijhawan 2001; van Beers et al. 2001; Whitney et al. 2000; Whitney and Murakami 1998). Secondly, the final gaze orientation error depends linearly on the eye and/or target velocity at the moment of the flash (Brenner et al. 2001; Nijhawan 2001; van Beers et al. 2001).

In all previous studies of the flash-lag effect, it could be hypothesized that it was exclusively due to the perception of motion. In these experiments, a perception of motion was induced either by target motion, self-motion or illusory motion. Is motion perception necessary to evoke a flash-lag? Here, we tested whether a flash-lag could be induced by self-motion but in the absence of motion perception. This was done by testing subjects in a situation where there is no perception of motion despite smooth anticipatory eye movements. In a first experiment, we designed a paradigm inducing smooth anticipatory eye movements that were not perceived by subjects (Kowler and Steinman 1979). During these smooth eye movements, we presented briefly a flashed target and asked subjects to orient gaze towards the remembered target position. In a second experiment, we validated our gaze orientation approach by a perceptual localization task. As a result, we rule out the hypothesis that the bias in spatial perception is due to motion perception. Indeed, we show that spatial perception of human subjects can be altered by self-motion in the absence of the sense of motion.

### **3. Methods**

#### ***3.1. Experiment 1***

##### *3.1.1. Experimental set-up*

Healthy human subjects without any known oculomotor abnormalities participated in the experiment after informed consent. Among the seven subjects, three were completely naïve of oculomotor experiments. Mean age was 29, ranging from 22 to 36. All procedures were conducted

with approval of the Université catholique de Louvain Ethics committee, in compliance with the Helsinki declaration (1996).

Experiments were conducted in a completely dark room. Subjects sat in front of a 1-m distant tangent screen, which spanned about  $\pm 45^\circ$  of their visual field. Their head was restrained by a chin-rest. A horizontally moving  $0.2^\circ$  red LASER target was back-projected onto the screen. The target was controlled via an M3-Series mirror galvanometer (GSI Lumonics) and using a dedicated computer running LabViewRT (National Instruments) software. Movements of one eye were recorded with the scleral coil technique, Skalar Medical BV (Collewijn et al. 1975; Robinson 1963).

### 3.1.2. *Paradigm*

Recording sessions were composed of a series of blocks containing 40 trials each. During the first block of trials, the moving target was always present. These trials were used to build up an anticipatory response and will be referred to as build-up trials. After one block of build-up trials, several blocks of test trials randomly mixed with build-up trials were presented.

Build-up trials (Fig. IV-1A) started with an 800-ms fixation period at the center of the screen. After a 300-ms target extinction period (gap), the target moved from the center of the screen for 800 ms at  $40^\circ/\text{s}$  always in the same direction. The trial ended with another 500-ms fixation period. The gap duration was chosen to provide an optimal smooth anticipatory eye movement (Morrow and Lamb 1996).

In the second part of the recording session, build-up trials were randomly interleaved with 30% of test trials (Fig. IV-1B). Test trials started in the same way as build-up trials with an 800-ms fixation period in the center of the screen. Afterwards, instead of the fixed gap followed by a ramp target motion, the target disappeared for a random duration lasting between 100 and 500 ms. This variable gap was followed by a 10-ms flash presented at a random position  $\pm 15^\circ$  around the expected eye position (= target position of build-up trials). All trials lasted for 2,400 ms. Subjects were instructed to follow the target as accurately as possible during build-up trials, and to orient gaze to the memorized target (flash) position during test trials.

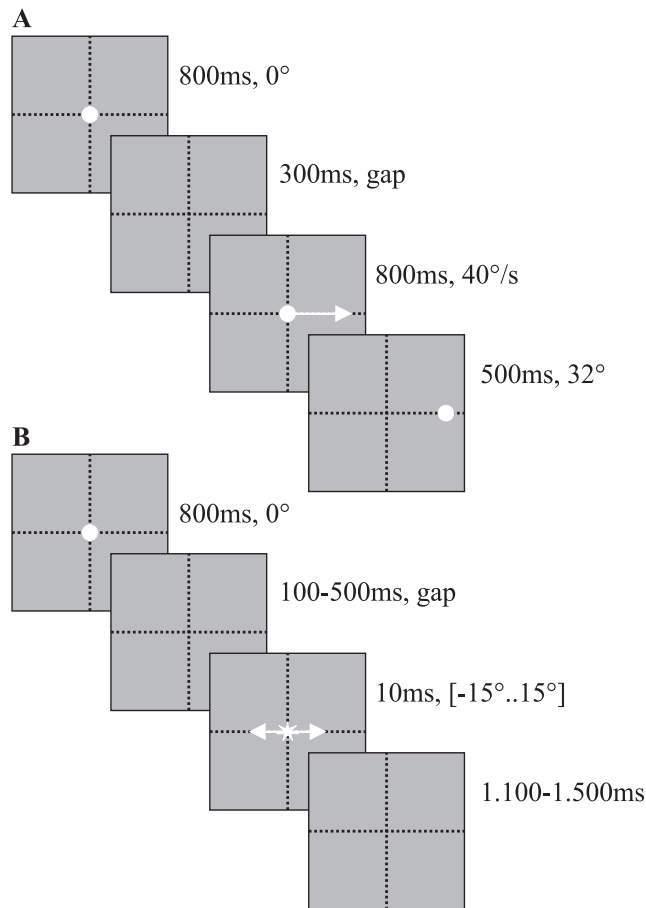


**Figure IV-1:** Experimental paradigm. **A.** Build-up trials. After an 800-ms fixation and a 300-ms gap period, the target moved for 800-ms at 40°/s always in the same direction. **B.** Test trials. Test trials started like build-up trials with an 800-ms fixation. After a variable gap of 100-500 ms, a 10-ms flash appeared at a random position between -15° and 15°.

### 3.1.3. Data acquisition and analysis

Eye and target position were sampled at 500 Hz and stored on the hard disk of a PC for off-line analysis with Matlab (Mathworks) scripts. Position signals were low-pass filtered using a zero-phase digital filter (autoregressive forward-backward filter, cutoff frequency: 50 Hz). Velocity and acceleration were derived from position signals using a central difference algorithm.

In our analysis, only test trials were considered. We were interested in the gaze orientation mechanism toward the flashed target. Position error (PE) and eye velocity (EV) signals were measured at the moment of the flash. The position error is the difference between target (T) and eye (E) position at a given moment in time:  $PE = T - E$ . All trials were aligned on the flash onset. In order to describe the flash localization process, PE was measured every 50 ms starting at the end of the first saccade until 1,000 ms after the flash (see Fig. IV-2).

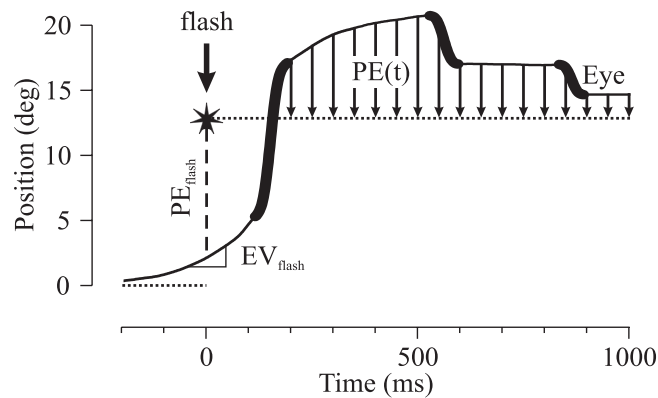


**Figure IV-2:** Data analysis. After the occurrence of the first orientation saccade, eye position error (PE) was sampled every 50 ms. Dotted lines represent the initial fixation point and the flash position. The star stands for the flash. The solid line represents eye position (saccades in bold). At the moment of the flash, position error ( $PE_{flash}$ ) and eye velocity ( $EV_{flash}$ ) were also measured.

### 3.2. Experiment 2

#### 3.2.1. Experimental set-up

Three out of the seven subjects of Experiment 1 participated in this experiment after informed consent. All procedures were conducted with approval of the Université catholique de Louvain Ethics committee, in compliance with the Helsinki declaration (1996).

Experiments were conducted in a completely dark room. Subjects sat in front of a 0.4-m distant, 21 inches Sony GDM-F520 computer screen on which we presented either a  $0.5^\circ$  red circular target or a white, vertical cursor. The screen refresh rate and resolution were 100 Hz and 640\*480 pixels respectively. Subjects were asked to use a computer mouse to move

the cursor. The cursor was composed of two vertical,  $0.1^\circ$  large and  $1.0^\circ$  high bars that were aligned horizontally and separated vertically by  $0.65^\circ$ . Target and cursor presentation were controlled in real time by a VSG2/5 Visual Stimulus Generator (32MB VRAM), Cambridge Research Systems Ltd.

The head of subjects was restrained by a chin-rest. Their eye movements were recorded using a Chronos eye tracker, Skalar Medical BV, which is based on high-frame rate CMOS sensors (Clarke et al. 2002).

### 3.2.2. *Paradigm*

We used a paradigm similar to the one used in Experiment 1, except that we had to reduce the range of the flash position to  $-10^\circ \dots 10^\circ$  because of the limited screen size. Recording sessions were composed of a series of blocks containing 40 trials each. Each block started with three build-up trials (Fig. IV-1A). Afterwards, build-up and test trials (Fig. IV-1B) were mixed with 50% probability. However, in contrast with Experiment 1, after each test trial there was a perceptual localization task (Fig. IV-3) and the next trial was always a build-up trial. Afterwards, there was again a 50% probability for either a build-up or a test trial to appear.

The perceptual localization task consisted in the alignment of the cursor with the memorized perceived position of the flash. Subjects had to press the mouse button to validate their choice of the position of the cursor.

### 3.2.3. *Data acquisition and analysis*

The target position was sampled at 100 Hz and stored on the hard disk of a PC. Images of the eyes were sampled independently of the target at 100 Hz and stored on the hard disk of a second PC. The eye position was extracted off-line from the eye images using the polar correlation algorithm for an ellipse approximation of the iris (Clarke et al. 2002), as implemented in the Iris software (Skalar Medical BV). The cursor position of the perceptual localization task was also recorded. Synchronization between eye and target signals was performed by means of a TTL signal.

In this experiment, four parameters of interest were extracted from the recording files, i.e. position error  $PE_{\text{flash}}$  and eye velocity  $EV_{\text{flash}}$  at the moment of the flash as well as the actual and perceived (= cursor) position of the flash.

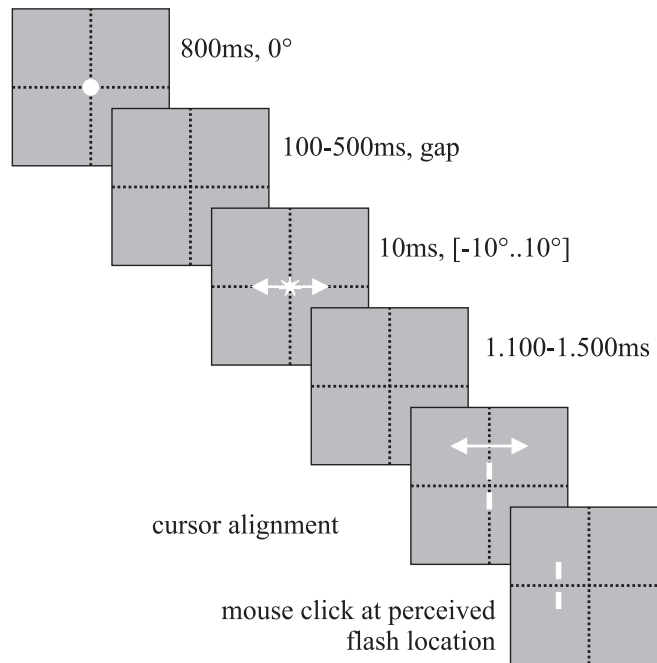


**Figure IV-3:** Perceptual localization task. The trial started with an 800-ms fixation period, a 100-500 ms gap and a 10 ms flash at a random position –  $10^\circ$  to  $10^\circ$ . After each test trial, subjects localized the memorized, perceived position of the flash by means of a cursor. The cursor position could be adjusted by a computer mouse and subjects had to press the mouse button to validate their choice of the perceived flash position.

## 4. Results

### 4.1. Experiment 1

#### 4.1.1. General observations

At the end of each trial, the eyes pointed at the memorized location of the flashed target. Fig. IV-4 shows four typical trials that illustrate the behavior and the gaze orientation performance. If the eyes move toward the flash, the condition is called foveopetal (FP), otherwise we will refer to it as foveofugal (FF).

The smooth eye displacement during the latency period of the first orientation saccade resulted in an overshoot of the first saccade in the FP condition whereas first saccades in FF trials undershot. While in Fig. IV-4B

and D the flash localization is rather precise (FF condition), in Fig. IV-4A and C we observe a remaining error on the final eye position (FP condition). In fact, in the FP condition, subjects generally localized the flash ahead of its actual position. When asked after the experiment, subjects reported that they had no sense of performing smooth anticipatory eye movements during the gap. This is in accordance with previous findings (Kowler et al., 1979).

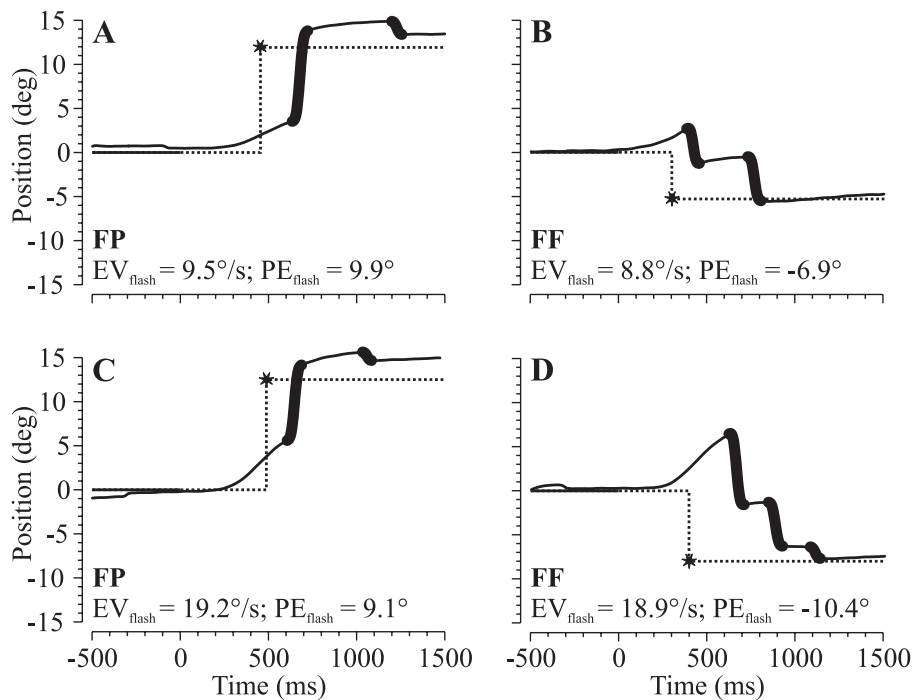


**Figure IV-4:** Typical trials. Thin black solid and dotted lines represent the fixation and the flash position respectively. The star stands for the flash. Eye position (normal solid lines) and saccades (bold lines) are shown for four different conditions: **A, C.** Flash presented at a foveopetal (FP) position during medium (A) and high (C) eye velocity. **B, D.** Flash presented at a foveofugal (FF) position during medium (B) and high (D) eye velocity.

On average, subjects needed 2-3 saccades to orient their eyes to the memorized position of the flash. The general properties and dynamics of this orientation process have been previously described in detail (Blohm et al. 2003b). Here we will concentrate on the directional bias in ocular orientation, which results from the fact that the eyes were moving at the moment of the flash.

To quantify smooth eye velocity after the flash, we provide in Fig. IV-5A the mean behavior and raw data. Panel B shows smooth eye displacement, which is the eye displacement after removing saccades. The smooth eye displacement is thus the integration of the smooth eye velocity. The total smooth eye displacement depended on the eye velocity at the moment of the flash: the higher the eye velocity at the moment of the flash, the larger the total smooth eye displacement.

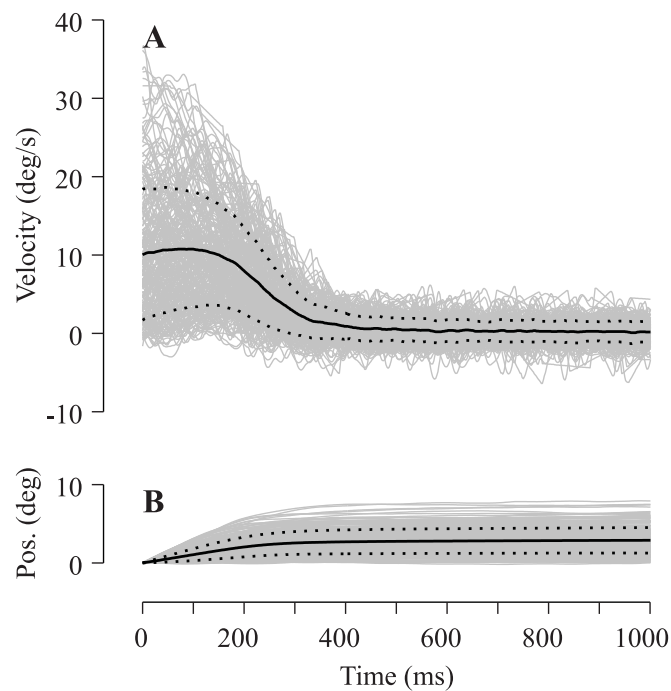


**Figure IV-5:** Smooth eye movement. **A.** Mean and standard deviation of smooth eye velocity (solid and dotted black lines) aligned on the flash onset. All FF and FP conditions are pooled. **B.** Mean and standard deviation of the smooth eye displacement (solid and dotted black lines) accumulated since the flash onset. Gray lines show individual trials. Trials were aligned on flash onset (time zero).

In our analysis, we will only consider the eye position  $PE_{\text{flash}}$  and velocity  $EV_{\text{flash}}$  at the moment of the flash. Indeed,  $PE_{\text{flash}}$  is the only retinal signal that is available to the system to localize the flash. (see Discussion)

#### 4.1.2. Localization error

We examined in this section the two characteristic features of a putative flash-lag effect. Table V-1 summarizes the different parameters that were analyzed in this section. Note that  $-PE_{end}$  ( $PE_{end} = PE(1000ms)$ ) will be the measure of the perceptual offset. If  $-PE_{end} > 0$  (and thus  $PE_{end} < 0$ ), the flash is perceived ahead of its actual position in the direction of the smooth eye movement.

**Table V-1:** Mean values and ranges of parameters that characterize the visual localization data set in Experiment 1.

<i>Variable</i>	<i>Case</i>	<i>Values (mean <math>\pm</math> std)</i>	<i>Range [25...75]%</i>	<i>N</i>
$PE_{flash}$	FF	$6.643 \pm 4.100$	[3.061...9.578]	765
	FP	$6.530 \pm 3.775$	[3.454...9.515]	762
$EV_{flash}$	FF	$10.115 \pm 8.595$	[4.535...14.246]	765
	FP	$9.916 \pm 8.398$	[4.653...13.994]	762
$-PE_{end}$	FF	$0.587 \pm 1.068$	[0.129...1.070]	765
	FP	$1.592 \pm 2.212$	[0.559...2.692]	762

The two signatures of the flash-lag phenomenon are analyzed in Fig. IV-6. Figure IV-6A represents the perceptual offset of the flash for the different flash locations on the retina in the gaze orientation experiment. Figure IV-6A clearly shows that there is an asymmetric perceptual bias in the flash localization. Thus, a flash presented during smooth anticipatory eye movements is mislocalized in the same way as a flash presented during smooth pursuit.

A closer look at this asymmetrical perceptual effect is provided in Fig. IV-6B. Here, we separated the data into two populations, i.e. foveopetal (FP) and foveofugal (FF) flash presentations. We observed a clear effect of the smooth eye velocity at the moment of the flash  $EV_{flash}$  on the perceptual offset for the FP condition (see Eq. IV-2), while the effect was much more attenuated for the FF condition (see Equation 1).

$$\mathbf{FF:} \quad -PE_{end} = 0.163 + 0.029 \cdot EV_{flash} \quad (N = 765, \quad R = 0.139, \quad p = 0.023)$$

Eq. IV-1

$$\text{FP: } -PE_{\text{end}} = -0.073 + 0.129 \cdot EV_{\text{flash}} \quad (N = 762, R = 0.378, p < 0.001)$$

Eq. IV-2

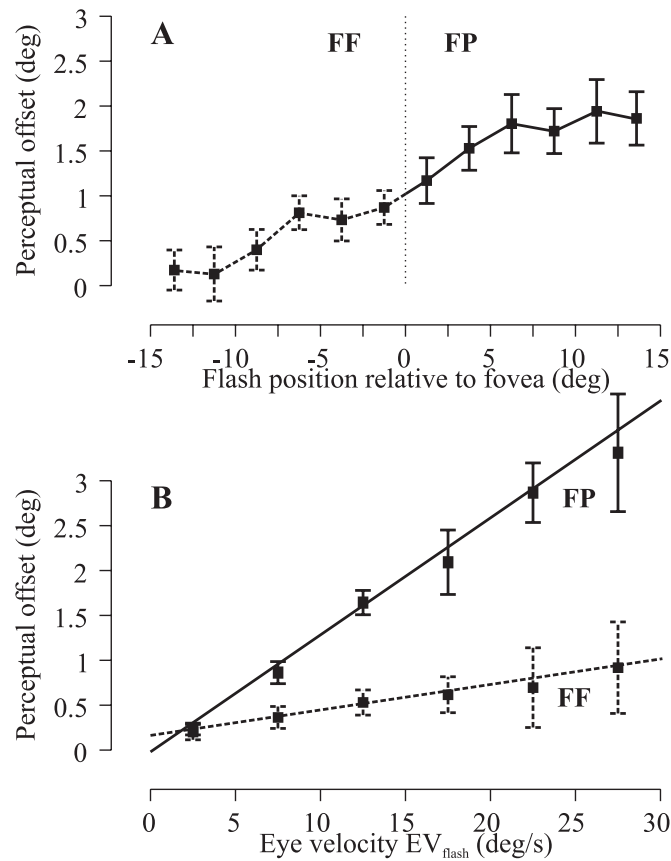


**Figure IV-6:** Final gaze orientation toward flashed targets during smooth anticipation. **A.** Dependency of the perceptual offset ( $-PE_{\text{end}}$ ) on the retinal target position relative to the fovea. **B.** The perceptual offset depends strongly on the eye velocity at the moment of the flash  $EV_{\text{flash}}$  in FP condition. In FF condition, only a weak influence of the smooth eye velocity is observed. Whiskers indicate the standard error of the mean (see text for details). Bins of  $2.5^\circ$  (panel A) and  $5^\circ/\text{s}$  (panel B) are centered on the binning interval.

Figure IV-6B shows separately the dependence of the final gaze orientation error on the smooth eye velocity  $EV_{\text{flash}}$  at the moment of the flash for both FF and FP conditions. Individual analyses of the data for all subjects resulted in regression coefficients that varied between –

0.021...0.064 (N = 78...190, p = 0.001...0.914) for the FF condition in Eq. IV-1 and between 0.070...0.234 (N = 83...194, p < 0.001...0.017) in the FP condition in Eq. IV-2.

Taken all together, we showed that targets flashed during smooth anticipatory eye movements are affected by a flash-lag illusion. This was the case although subjects had no perception of any eye movements when the flash occurred.

#### 4.1.3. *Temporal evolution of the error*

After having shown in the previous section that an anticipatory smooth eye movement distorts the perceived space when tested with a short flash, we wondered whether we could reveal the temporal evolution of the flash-lag effect. Therefore, we performed the following regression analysis independently for both FF and FP conditions and for each time step during gaze orientation:

$$PE(t) = \alpha(t) - \beta(t) \cdot EV_{flash} \quad \text{Eq. IV-3}$$

The results of the regression in Eq. IV-3 are represented in Fig. IV-7. Individual regression coefficients for each time step and FF or FP condition ranged from R = 0.1393...0.7597 (p < 0.001...0.023). The non-zero offset  $\alpha$  in the early orientation (Fig. IV-7A) was essentially due to the saccadic undershoot strategy (Gellman & Fletcher, 1992) and the system compensated for this error later on in the orientation process.

Figure IV-7B shows the evolution of the error dependence on  $EV_{flash}$  over time. Interestingly, in the earlier orientation process, there was no difference between FP and FF relationships (p > 0.05). Indeed, Blohm et al., 2003 showed that the first orientation saccade did not take into account the smooth eye displacement. Therefore, at this time, the gain element  $\beta(t)$  is the same in the FP and FF condition (t-test, p > 0.05). However, afterwards, the p-level that quantifies the difference of the regression parameter  $\beta(t)$  between FP and FF conditions decreased. After 450 ms, the regression parameters  $\beta(t)$  became significantly different (p < 0.05) and even highly significantly different (p < 0.001). Furthermore, in Fig. IV-7, the 95% confidence intervals of the regressions for FP and FF conditions separately also decrease, which indicates that individual regressions improve over time. Hence, although Eq. IV-3 is not a signature of the flash-lag effect, the

resulting separation of both FP and FF populations in Fig. IV-7B shows the relevance of this analysis in characterizing the temporal evolution of the flash-lag effect.

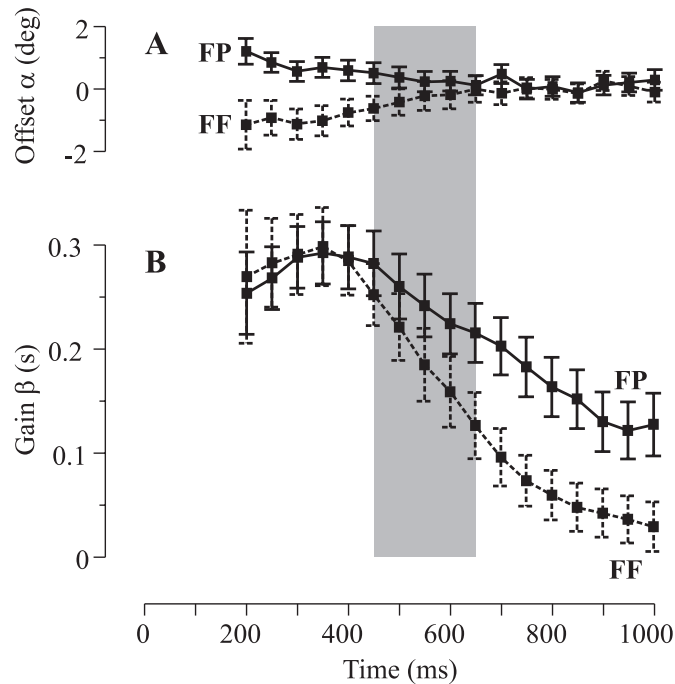


**Figure IV-7:** Temporal evolution of the gaze orientation error. Regression variables of Eq. IV-3 are represented for both FF and FP conditions and for each time step. The gray zone shows the transition between the early and late orientation (see text for details) when the difference between FP and FF conditions became significant. Whiskers indicate the 95% confidence intervals of the means. **A.** Offset  $\alpha(t)$ . **B.** Gain  $\beta(t)$ .

## 4.2. Experiment 2

In order to test if the final gaze orientation reflects the perceived position of the flash, we performed a perceptual localization experiment. As in Experiment 1, subjects reported to have no sense of performing any smooth eye movements during the gap period.

Table V-2 summarizes the results of this experiment. Here, the cursor localization error  $ERR_{loc}$  replaces the eye position error  $PE_{end}$  of Experiment 1. We verified that the overall eye velocity at the moment of the cursor appearance was small ( $EV = -0.043 \pm 0.928^\circ/s$ , mean  $\pm$  std).

**Table V-2:** Mean values and ranges of parameters that characterize the perceptual localization data set in Experiment 2.

<i>Variable</i>	<i>Case</i>	<i>Values (mean ± std)</i>	<i>Range [25...75]%</i>	<i>N</i>
PE <sub>flash</sub>	FF	5.902 ± 3.568	[2.655...8.301]	312
	FP	4.299 ± 3.251	[1.924...6.875]	284
EV <sub>flash</sub>	FF	10.160 ± 9.401	[3.846...16.034]	312
	FP	9.520 ± 9.498	[3.665...16.237]	284
-ERR <sub>loc</sub>	FF	0.602 ± 1.310	[-0.325...1.619]	312
	FP	1.957 ± 2.021	[0.403...3.934]	284

Figure IV-8 illustrates the results of the perceptual localization experiment. Panel A shows the dependence of the localization error on the retinal location of the flash. Compared to the gaze orientation experiment in Fig. IV-6, the flash-lag is qualitatively the same, although the effect is more selective concerning the eye position error at the moment of the flash (see Discussion).

Figure IV-8B recapitulates the effect of the eye velocity ( $EV_{flash}$ ) at the moment of the flash on the perceptual localization of the target. Qualitatively, we obtained the same results as for Experiment 1: FP flashes are mislocalized in the direction of the eye movement whereas this behavior is much reduced for FF flashes. This is expressed in the following regression equations:

$$\mathbf{FF:} \quad -ERR_{loc} = 0.053 + 0.023 \cdot EV_{flash} \quad (N = 312, R = 0.083, p = 0.094)$$

Eq. IV-4

$$\mathbf{FP:} \quad -ERR_{loc} = 0.451 + 0.116 \cdot EV_{flash} \quad (N = 284, R = 0.197, p = 0.002)$$

Eq. IV-5

Individual values of the regression coefficients for all subjects ranged from 0.017...0.029 ( $N = 84...131$ ,  $p = 0.143...0.697$ ) for the FF condition in Eq. IV-4 and 0.083...0.154 ( $N = 81...128$ ,  $p = 0.015...0.072$ ) for the FP condition in Eq. IV-5. However, we would like to point out that this perceptual localization task was conducted to confirm that the final gaze orientation really represents the perceived position of the flash. We claim

that our results show that both localization procedures reveal the same phenomenon.

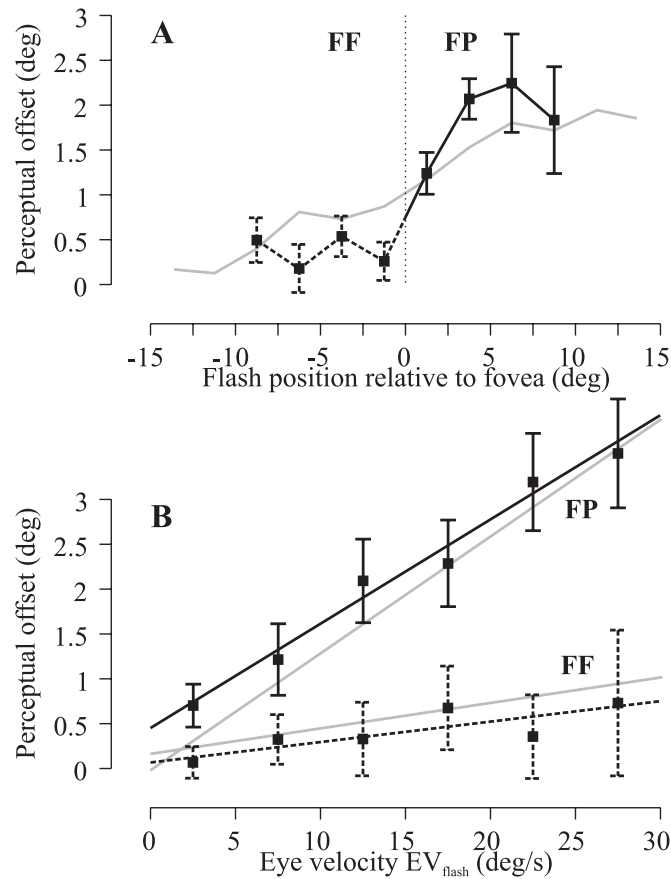


**Figure IV-8:** Perceptual localization of flashed targets during smooth anticipatory eye movements. **A.** The perceptual localization error ( $-ERR_{loc}$ ) was strongly modulated by the retinal location of the flash. **B.** Asymmetrical influence of the eye velocity ( $EV_{flash}$ ) at the moment of the flash on space perception. Whiskers indicate the standard error of the mean. Gaze orientation results (grey lines) are transposed from Fig. IV-6 for comparison.

## 5. Discussion

A flash presented during perceived movement is perceptually mislocalized (Schlag and Schlag-Rey 2002). Such a bias has previously been observed for targets presented briefly during smooth self-, object- or illusory-motion and is called “flash-lag”. Here we asked whether the

observed asymmetrical perceptual offset might be due to motion perception. Therefore, a briefly flashed target was presented during unperceived smooth anticipatory eye movements in darkness and subjects had to localize the flash. This revealed the presence of a self-movement induced flash-lag illusion despite the absence of the sense of self-movement. Thus, space perception is decoupled from movement perception, although a perceived movement might influence the perceived space (Cai et al. 2000; Nishida and Johnston 1999; Watanabe et al. 2002).

### ***5.1. Gaze orientation and perceptual localization***

Our gaze orientation and perceptual localization results show the same trend, i.e. almost the same dependency of the perceptual offset on the eye velocity at the moment of the flash and a very similar behavior for the influence of retinal flash position. However, we observed slightly different shapes and regression parameters in the gaze orientation task and the perceptual localization experiment. There might be a difference between gaze orientation and manual localization motor strategies. Indeed, it has been shown that visually guided manual pointing to remembered targets leads to an overshoot for small target eccentricities whereas larger distances are more likely to be undershot (Berkinblit, Fookson, Smetanin, Adamovich, & Poizner, 1995; Medendorp, Van Asselt, & Gielen, 1999). Furthermore, a comparison of gaze orientation and perceptual localization of briefly presented targets reveals systematic undershoots for gaze orientation compared to an overshoot in perceptual localization (Eggert, Ditterich, & Straube, 2001; Eggert, Sailer, Ditterich, & Straube, 2002). However, despite these possible differences, we observe very similar regression coefficients in Eq. IV-1 and 2 compared to Eq. IV-4 and 5.

The perceptual localization task allowed us to validate our approach and to confirm that the final gaze direction reflects the perceived position of the flashed target. In addition, the position of the cursor when the mouse button was pressed gave us direct information on the perceived flash position.

### ***5.2. Time course of the flash-lag illusion***

Our analysis in Fig. IV-7 answered the question about the timing of the flash-lag effect in more details. Indeed, we showed in our analysis from what time on the visual illusion affects the eye movements. This is in

accordance with previous results showing that the first orientation saccade does not take into account any movement related information but is only based on the position error  $PE_{\text{flash}}$  at the moment of the flash (Blohm et al. 2003b). Furthermore, Blohm et al. (2003b) revealed a 400-ms delay to account for the smooth eye displacement. If the eye moved smoothly in darkness, the system corrected for this smooth eye displacement around 400 ms later by means of a corrective saccade. Thus, the 400-ms delay represents the time needed for the manifestation of the egocentric to allocentric reference frame transformation. This finding can be compared to the transition period for the visual illusion to influence the ocular orientation process we found here. Indeed, we observe a separation of FF and FP data immediately after the 400 ms delay (Fig. IV-7B). We conclude that the early localization of the flash is not affected by the visual illusion, but once the flash position has been transformed in allocentric coordinates, eye movements reflect the actual perceived flash location. Thus, the bias in space perception might be due to an erroneous reference frame transformation.

The relatively long delay for egocentric to allocentric reference frame transformation may also account partly for the observation that target motion can influence the flash-lag effect even some time after the flash occurred. Durations between 60 ms and 600 ms have been previously proposed for this process (Eagleman and Sejnowski 2000; Krekelberg and Lappe 2000).

In the next section, we discuss the egocentric to allocentric reference frame transformation and propose candidates for the possible underlying neural structures of the flash-lag effect.

### ***5.3. Origin of the perceptual bias***

Why do we observe a spatial illusion during movement? Obviously, the CNS has trouble combining retinal and extraretinal signals at key events, especially when there is a loss of continuity in motion (e.g. the presentation of a flash or the disappearance or direction change of a moving target). To our view, the most intriguing observation is the asymmetry of the flash-lag effect under certain experimental circumstances. Here, we propose a neural mechanism that might account for movement related asymmetrical spatial mislocalizations.

Our hypothesis is based on two observations. First, it has recently been shown that areas MT/MST (middle temporal / medial superior temporal area) are strongly involved in the spatial localization of a flashed target and the neural activity in these areas codes the perisaccadic mislocalization of flashes (Krekelberg et al. 2003). Second, areas MT and MST are involved in processing motion stimuli and it has been suggested that MST plays a role “in generating behavioral and perceptual consequences of pursuit” (Pack et al. 2001). MT neurons contain cells that are direction and speed selective (Born and Tootell 1992; Mikami et al. 1986; Newsome et al. 1988; van Wezel and Britten 2002) and MST cells (MSTd and MSTl) carry signals about the eye movement, i.e. an efference copy of the motor command (Bradley et al. 1996; Eifuku and Wurtz 1998; Komatsu and Wurtz 1988a, b; Newsome et al. 1988; Squatrito and Maioli 1997). We suggest that these areas might be responsible for the observed flash-lag effect.

Figure IV-9 shows a basic model hypothesis that could account for an asymmetric movement related visual illusion. A flash presented during eye movements in either the FF or FP hemifield would be represented in contralateral brain structures. Here, we represented essentially two pathways for the processing of a flashed target's position. One direct pathway to the saccade generator programs the initial gaze orientation (see Krauzlis & Stone, (1999) for a review). A second pathway involves areas MT/MST and the posterior parietal cortex (PPC) and is responsible for the egocentric to allocentric reference frame transformation (Andersen et al. 1985; Pack et al. 2001). PPC receives afferents from MT/MST (Tusa and Ungerleider 1988) and is involved in reference frame transformations and the spatial coding of stimuli (Heide et al. 1995). Furthermore, if the flash occurs during smooth eye movements, contralateral MST neurons encode the eye speed (Newsome et al. 1988). This means that if the eyes move to the right, the left hemisphere encodes the eye velocity.

Furthermore, an FP flash position is represented in the same structures (see Fig. IV-9). Thus, during the egocentric to spatial reference frame transformation, there might be an interaction between position and velocity signals in MST, which would result in a localization error. This is what happens for the perisaccadic presentation of flashes (Krekelberg et al. 2003). However, such an error would not be present in the case of an FF

flash for which the flash position and eye velocity signals are processed by different hemispheres.

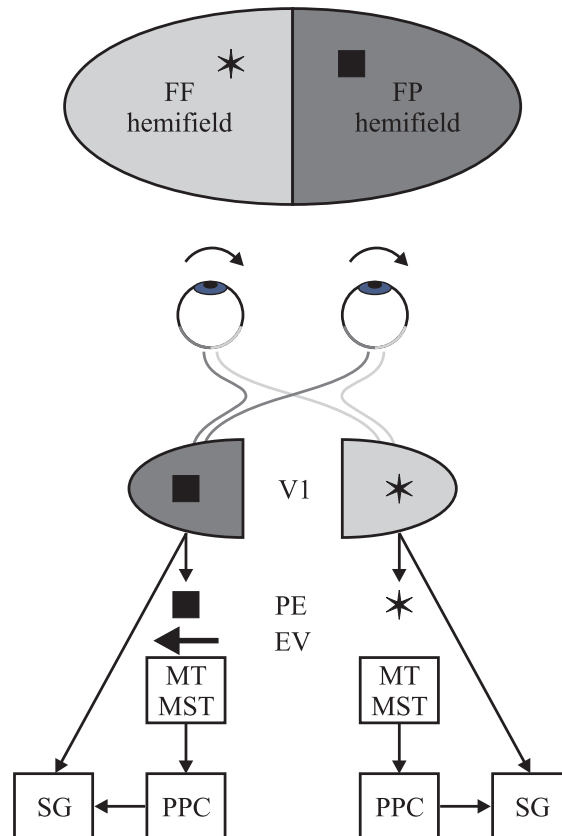


**Figure IV-9:** Flash-lag model hypothesis. A rightward eye movement (arrows) is coded by contralateral MT/MST neurons. Different greyscales code the separate hemifields. Two pathways process a flashed target (square or star). A fast pathway sends the retinal flash position directly via V1 (primary visual cortex) to the saccade generator (SG). A slower process through MT/MST and PPC performs the egocentric to allocentric reference frame transformation. Retinal position signals of an FP flash (star) are thus processed in structures where eye velocity (EV: black arrow represents EV coding) signals are present. An interaction between the two signals might result in a movement related visual illusion.

Our result that motion perception is not a necessary condition for the flash-lag effect supports this hypothesis. Furthermore, this simple model can explain several previous findings. The original rotational motion flash-lag effect (Nijhawan 1994) should thus not present an asymmetry, because

large field target motion is not coded in a particular hemisphere (Newsome et al. 1988). Indeed, no asymmetry has been reported in these experiments (Brenner and Smeets 2000; Eagleman and Sejnowski 2000; Krekelberg and Lappe 1999; Lappe and Krekelberg 1998; Purushothaman et al. 1998). In addition, MST neurons carry information about the head movement (Kawano and Sasaki 1984; Thier and Erickson 1992). Thus, a head in space – but not eye in head – movement should result in a flash-lag similar effect. This has been observed by Schlag et al. (2000). The same reasoning may apply for a perceptual mislocalization during illusory movement (Cai et al. 2000; Nishida and Johnston 1999; Watanabe et al. 2002) or during background motion (Zivotofsky et al. 1996; Zivotofsky et al. 1998).

Unfortunately, the question about the origin of the “cross-talk” between positional and velocity related signals in areas MT/MST as proposed by Krekelberg and colleagues (2003) remains. However, it has been suggested that other visual illusions like the Filehne illusion might also be mediated by area MST (Erickson and Thier 1991). It would be interesting to test this “cross-talk” hypothesis on MT/MST neurons like it has been done for perisaccadic flashes (Krekelberg et al. 2003). The underlying neurophysiological question is whether position and velocity signals are multiplexed in MT/MST neurons, as suggested by McClurkin and coworkers for other object properties in the inferior temporal cortex (McClurkin and Optican 1996; McClurkin et al. 1994).

## **6. Conclusions**

The sense of motion was a common factor in all previous experiments on motion related visual illusions. Here we showed that motion perception is not a necessary condition for such a bias in space perception. Indeed, a flash-lag illusion was observed during unperceived smooth anticipatory eye movements. Furthermore, we showed that gaze orientation to briefly presented targets follows the perceptual localization of the flash. In addition, the gaze orientation analysis reveals the time course of the flash-lag effect. We suggest that this reflects the time needed by the CNS to perform the egocentric to allocentric reference frame transformation.



## CHAPTER V

# A MODEL THAT INTEGRATES EYE VELOCITY COMMANDS TO KEEP TRACK OF SMOOTH EYE DISPLACEMENTS

*“Whenever a theory appears to you as the only  
possible one, take it as a sign that you have  
neither understood the theory nor the problem  
which is was intended to solve”*

*Karl Popper*

### 1. Abstract

Contradictory results have been reported in the literature concerning the oculomotor system’s ability to keep track of smooth eye movements in darkness. Whereas some results indicated that saccades could not compensate for smooth eye displacements, others reported spatially correct memory guided saccades during smooth pursuit. Recently it has been proposed that those findings could be explained by the presence of a delayed mechanism that keeps track of smooth eye displacements (Blohm et al. 2003b, 2004, submitted).

Current saccadic models are unable to account for those findings. Therefore, we proposed here a model of the saccadic system that could explain the available experimental data. The original part of this model consisted of the proposal of two alternative physiologically realistic neural mechanisms for a delayed integration of smooth eye velocity commands. The first hypothesized mechanism was based on an accumulation of the time during which the eyes moved at a certain velocity and was proposed to be compatible with the known physiology of the Lateral Intraparietal Cortex. The alternative hypothesis used an eye velocity modulated neural activity displacement map and could be implemented in the Cerebellum. The read-out of both mechanisms provided an estimation of the smooth eye

displacement. This signal was then used to update the spatial representation of a memorized target in retinotopic coordinates.

We showed that both eye velocity integration mechanisms could estimate equally well the smooth eye displacement during a memory period of a previously presented target. Therefore, we fitted our model on two previously analyzed behavioral data sets (Blohm et al. 2003b, 2004, submitted). In addition, we tested the model simulations on prior results from the literature and accurately predicted those previous findings. This reconciled the initially contradictory reports from the literature.

Two alternative mechanisms for the integration of smooth eye velocity were discussed in the light of recent neurophysiological data. We did also propose alternative structures for the implementation of the smooth eye displacement estimation mechanisms. In addition, we suggest a series of experiments to identify the neural correlates for the here-proposed velocity integration mechanisms and to test the model's predictions.

## **2. Introduction**

Almost two decades ago, McKenzie and Lisberger (1986) performed an experiment that was designed to test whether saccades were directed to an absolute eye position in space or whether the saccade amplitude instead reflected a desired eye displacement. They argued that if actual eye position was compared to a desired spatial position, saccades to memorized targets should always be accurate, even when the eyes move smoothly between the target presentation and the resulting saccade. Using such a "smooth double-step" paradigm, they reported that this prediction was incorrect (McKenzie and Lisberger 1986). Indeed, their monkeys systematically made inaccurate eye movements that were appropriate for the target's retinal error (see Fig. V-1A and B). Their saccades were thus coded as desired displacements (retinal error hypothesis) and were not directed to an absolute position in space (spatial error hypothesis). These results were confirmed by Gellman and Fletcher (1992) for smooth pursuit and by Blohm et al. (2003b; 2004, submitted) for short latency saccades during smooth anticipatory eye movements and during smooth pursuit respectively.

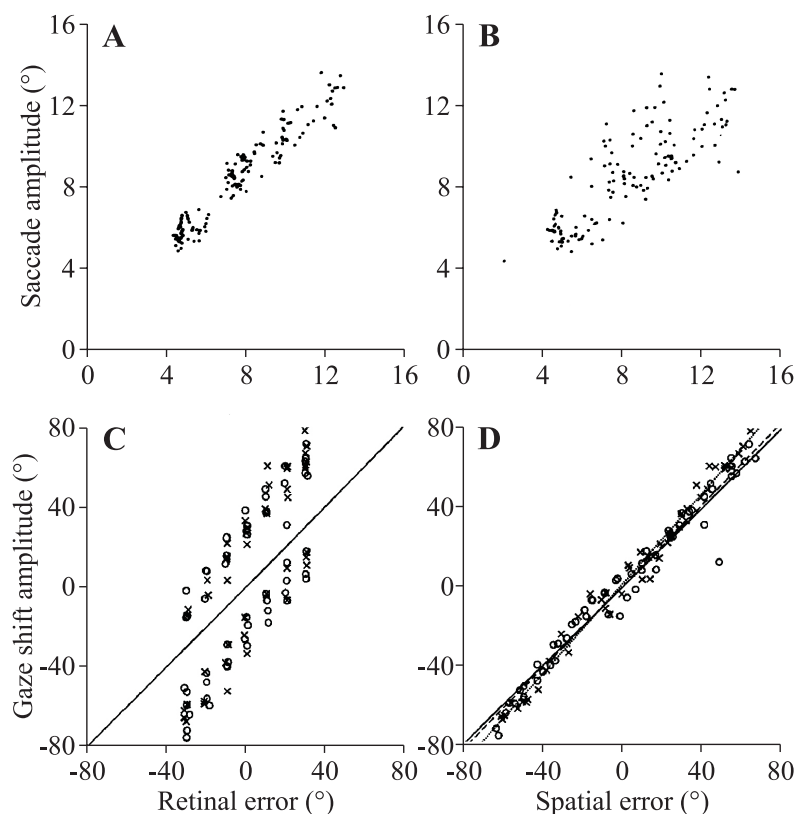


**Figure V-1: Contradictory data from literature.** **A, B.** Results adapted from McKenzie and Lisberger (1986) for the programming of saccades to targets flashed at the moment of extinction of a pursuit target. The saccades were initiated with latencies around 180 ms after the flash presentation. The amplitude of these saccades was predicted by the retinal error (panel A) and were thus spatially inaccurate (panel B). **C, D.** Results adapted from Herter and Guitton (1998) concerning the accuracy of saccades to targets flashed before smooth pursuit. Panel D shows that the amplitude of head-free (open circle) as well as head-fixed (cross) gaze saccades triggered after the pursuit eye movement followed the spatial error. The retinal error hypothesis did not predict their amplitude (panel C).

In contrast to these retinotopically programmed saccades (Gellman and Fletcher 1992; McKenzie and Lisberger 1986), several studies reported that saccades aimed to the location of targets memorized before or during smooth pursuit (Fig. V-1C and D) were spatially accurate (Baker et al. 2003; Herter and Guitton 1998; Ohtsuka 1994; Schlag et al. 1990; Zivotofsky et al. 1996). The major difference between these studies and those reporting retinotopically programmed saccades was the moment of saccade execution.

Whereas retinotopically programmed saccades were naturally triggered by the presentation of the target (mean latencies < 300 ms), spatially accurate saccades intervened after an additional delay period between the presentation of the memorized target and the orienting saccade (mean latencies > 600 ms). This seems to indicate that a retinal-to-spatial transformation for the internal coding of memorized targets could explain the difference between short and long latency orienting eye movements.

The hypothesis of a latency dependent retinal-to-spatial transformation has been addressed in two recent studies for smooth pursuit (Blohm et al. 2004, submitted) and smooth anticipatory eye movements (Blohm et al. 2003b). In these studies, the “smooth double-step” paradigm was used. However, in addition to previous investigations, not only the first orienting eye movement was analyzed but also secondary “catch-up” saccades. As a result, Blohm et al. (2003b; 2004, submitted) demonstrated that extraretinal information about smooth eye displacements was delayed (~175 ms) with respect to the smooth eye movement. However, both primary orientation saccades and secondary “catch-up” saccades used the *available* smooth eye displacement information to compensate for smooth ego-motion (motion in a visual field due to movement of the body or part of the body). These results reconcile previous contradictory findings of retinotopic position coding (Gellman and Fletcher 1992; McKenzie and Lisberger 1986) and spatially accurate saccades (Baker et al. 2003; Herter and Guitton 1998; Ohtsuka 1994; Schlag et al. 1990; Zivotofsky et al. 1996).

It is worth mentioning that this delayed retinal-to-spatial transformation of smooth eye displacements is specific to smooth movements but has not been observed for the saccadic system, i.e. there is no delay between a saccadic eye movement towards a target and the internal spatial update of the target’s position. Indeed, the use of extraretinal signals to maintain space constancy has been extensively studied by means of the so-called “double-step” or “colliding saccades” paradigms (Aslin and Shea 1987; Becker and Jürgens 1979; Dassonville et al. 1992; Dominey et al. 1997; Goossens and Van Opstal 1997; Hallett and Lightstone 1976a, b; Mays and Sparks 1980; Mushiake et al. 1999; Schlag and Schlag-Rey 1990; Schlag et al. 1989; Tian et al. 2000). In these experimental conditions, a saccadic eye movement is evoked either visually (double-step) or by microstimulation (colliding saccades) during the latency period of a second

saccadic eye movement to a previously memorized target. Despite this initial deviation from the goal, orienting saccades are spatially accurate. This is also the case for very short intervals between both saccades. The authors conclude that the saccadic system has access to extraretinal signals about previous saccadic eye movements to update the internal target representation in space. This allows the visual system to ensure space constancy, i.e. an accurate spatial perception of the world.

Current saccadic models cannot explain the delayed retinal-to-spatial transformation reported for saccades to targets memorized before a smooth eye displacement. Here, we will propose a model of the saccadic system that can account for the “smooth double-step” data available today. We developed two different hypothetical physiologically realistic neural mechanisms for a delayed internal estimation of the smooth eye displacement. Both mechanisms provided a good estimation of our data and previous observations in the literature. Since behavioral experiments cannot distinguish between those two mechanisms, we will suggest a series of electrophysiological experiments to discriminate one model with respect to the other.

### **3. Background**

It is generally accepted that the Posterior Parietal Cortex (PPC) is implicated in visual short-term memory and coordinate transformations for saccadic eye movements. Lateral Intraparietal (LIP, an area of PPC) neurons remain active while remembering a desired target location, i.e. a memory of motor error (Barash et al. 1991; Curtis et al. 2004; Gnadt and Andersen 1988; Paré and Wurtz 1997). Furthermore, electrical stimulation of some neurons in LIP produces fixed vector saccades independently of eye position whereas another neural population encodes saccades to specified targets in spatial coordinates (Thier and Andersen 1998, 1996). LIP neurons are influenced by eye position (Andersen et al. 1990b; Bremmer et al. 1997) and these cells also show a shift in their response fields that anticipates an upcoming gaze saccade (Duhamel et al. 1992a; Mushiaké et al. 1999). In addition, LIP neurons discharge prior to saccades (Barash et al. 1991). Lesions of the human analog of LIP in PPC impair the ability to perform the double-step task, i.e. disrupt the monitoring of previous saccades by efference copy (Duhamel et al. 1992b; Heide et al. 1995). This shows the

importance of PPC in the internal representation of targets in spatial coordinates (Tobler et al. 2001). Furthermore, humans with chronic PPC lesion make inaccurate memory guided saccades (Pierrot-Deseilligny et al. 1991). Moreover, area 7a (an area adjacent to LIP in the monkey's PPC) also contains neurons with eye and head position dependent activity that encode a visual target in spatial or craniotopic coordinates (Andersen et al. 1990b; Andersen et al. 1992; Bremmer et al. 1997; Brotschie et al. 1995). Altogether, this evidence suggests that saccadic goals are memorized with respect to different reference frames (e.g. retinal and spatial) in PPC. When a gaze shift occurs, the oculocentric mapping of saccade targets (Henriques et al. 1998) is updated (Andersen et al. 1997; Colby and Goldberg 1999; Medendorp et al. 2003) using extraretinal information about the gaze shift amplitude (Quaia et al. 1998). Therefore, we believe that – as for the classical “double-step” paradigm – in the “smooth double-step” paradigm PPC receives an internal estimation of the (smooth) eye displacement to update the spatial representation of the memorized goal.

The studies about the target representation in spatial coordinates in PPC report that updates were performed on the basis of *position* signals representing the gaze shift amplitude. However, this implies that in the case of the “smooth double-step” paradigm, where eye *velocity* is monitored, there must be an additional computational step of velocity-to-position transformation. Thus, integration of eye velocity needs to take place before the updating of the spatial target representation in PPC. We believe that this integration step could be performed either within LIP (at a previous stage of computation with respect to the spatial updating mechanism) or in the Cerebellum (CB), where neurons coding eye velocity can be found. Hereafter, we will discuss the electrophysiological evidence that supports these alternatives.

The first smooth eye velocity integration mechanism was based on an integration of ocular motion signals in LIP. An area projecting to LIP that contains neurons encoding eye velocity is the Medial Superior Temporal cortex (MST). Cells in MST are tuned selectively for different eye velocities (Bradley et al. 1996; Komatsu and Wurtz 1988a, b; Newsome et al. 1988; Squatrito and Maioli 1997) and project largely to LIP (Andersen et al. 1990a; Cavada and Goldman-Rakic 1989; Neal et al. 1990). We hypothesized that LIP neurons may read out the activity of eye velocity

sensitive MST cells by integrating their output. Indeed, neurons in LIP integrate time-varying signals that originate in the extrastriate visual cortex, accumulating evidence for a specific behavioral response (Mazurek et al. 2003; Roitman and Shadlen 2002; Shadlen and Newsome 1996). The approximately linearly rising neural activity of these LIP cells has also been related to a representation of elapsed time (Leon and Shadlen 2003; Rao et al. 2001). In our LIP integration hypothesis, an LIP neuron received input from one eye velocity coding MST neuron. The discharge of this integrative LIP cell was thus proportional to the duration at which the eye moved with the preferred velocity of the MST neuron. The readout of this system to provide an estimation of the performed smooth displacement was calculated by synaptically weighting the LIP activity with the MST neuron's preferred velocity (position = time\*velocity). This LIP readout signal was thus an estimation of the smooth eye displacement.

The second smooth eye displacement estimation mechanism was based on the idea that the Cerebellum (CB) monitors eye movements. We believe that the CB was a good candidate for the integration of eye velocity, since eye/gaze velocity signals are present in different areas. Indeed, Parafloccular (PF), Floccular (Floc) and Vermal Purkinje cells encode gaze velocity during smooth pursuit or combined eye-head tracking (Lisberger and Fuchs 1978a, b; Miles and Fuller 1975; Nagao et al. 1997; Suzuki and Keller 1988a, b). Also, CB is thought to be a crucial structure for the generation of smooth pursuit (for a review, see Krauzlis 2004). On the other hand, recent models of the saccadic system interpret the function of CB as a supervisory controller that encodes the sensory consequences of an eye movement (Lefèvre et al. 1998; Optican and Quiaia 2002; Quiaia et al. 1999). In these models, eye velocity signals could evoke a spread of activity in a topologically arranged neural map. This spatial integration of velocity signals thus replaced temporal integration, i.e. the classically used "displacement integrator" (Jürgens et al. 1981). This motivated our hypothesis that CB could contain an eye displacement map. Such a map would enable the saccadic system to monitor smooth eye movements and would allow the oculomotor system to ensure space constancy during smooth eye movements in darkness. The readout of this displacement map must then be sent from CB to LIP to update the spatial representation of the memorized target. Different direct and indirect projections from CB to LIP have been reported (Clower et al. 2001) and support this idea.

## 4. Methods

First, we will provide a general overview of the model of the saccadic system we developed to account for the “smooth double-step” results. The crucial original contribution to this model was a smooth eye velocity integration stage that was necessary to estimate the smooth eye displacement (SED). In the second and third part of this section, we will propose two physiologically realistic neural mechanisms that could perform this velocity-to-position transformation step and provide an SED estimation to the spatial memory structure of the brain. Finally, we will shortly introduce two experimental data sets that were used to fit the simulation parameters.

### 4.1. *The saccadic pathway*

Figure V-2 shows the basic structure of the saccadic model we developed. We used retinal position error ( $PE_R = \text{constant}$ ) and time varying eye velocity (EV) as the inputs to the model. The position memory structure was supposed to be located in LIP and thus had two internal target representations in retinal and in spatial coordinates. The input  $PE_R$  was memorized to represent the target position in retinal coordinates. The spatial representation of the same target was updated dynamically by the amplitude ( $S_{AMP}$ ) of all intervening saccades.

In addition to the spatial update by saccades, the eye velocity (EV) integration mechanism also provided an instantaneous estimation of the smooth eye displacement ( $SED_{est}$ ) to update the spatial stimulus representation in the position memory structure. Therefore, once a saccade was triggered, the saccade generator used the remaining error  $\Delta E$  of the spatial target representation (oculocentric coordinates) to build the saccadic drive. Here, we did not model the saccade trigger mechanism but used instead the times of saccade occurrence from experimental data. To complete the model, the smooth and saccadic eye movement commands were added together before sending the final motor command to the motor neurons and the eye plant.

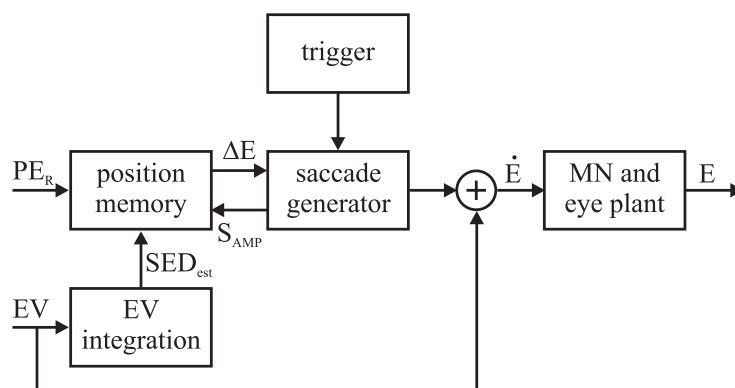


**Figure V-2: General model structure.** The inputs were retinal position error ( $PE_R$ ) and eye velocity ( $EV$ ) over time. An eye velocity integration mechanism provided an instantaneous estimation of the smooth eye displacement ( $SED_{est}$ ) to a target position memory structure. There was thus a velocity-to-position transformation of  $EV$ . The internal representation of target position was updated by  $SED_{est}$  and the actual saccade amplitude ( $S_{AMP}$ ) each time a saccade occurred. Once a saccade was triggered, the saccade generator produced a velocity command that was added up with the smooth eye velocity. The final motor neuron (MN) and eye plant pathway integrated the total velocity command ( $\dot{E}$ ) to provide eye position ( $E$ ).

For the saccade generator we used a classical structure (modified from Jürgens et al. 1981). The position error  $\Delta E$  was sent through a gain element (gain = 0.9) to account for the typically observed saccadic undershoot strategy. This provided the desired eye movement that was compared to the executed eye movement to produce the motor error. This motor error was put through a pulse generator whose output was the saccadic eye velocity command sent to the motor neurons and eye plant. For the pulse generator, we used the following “bi-lateral” version of the burst neurons discharge rate proposed by van Gisbergen et al. (1981):

$$y = \begin{cases} -b_m \cdot \left( 1 - \exp^{\frac{x-e_0}{b_k}} \right) & \text{if } x < -e_0 \\ b_m \cdot \left( \exp^{\frac{x-e_0}{b_k}} - \exp^{\frac{-x-e_0}{b_k}} \right) & \text{if } -e_0 \leq x \leq e_0 \\ b_m \cdot \left( 1 - \exp^{\frac{-x-e_0}{b_k}} \right) & \text{if } x > e_0 \end{cases} \quad \text{Eq. V-1}$$

The input  $x$  was the motor error and the output  $y$  was the saccadic velocity command. We used parameters  $e_0 = 1 \text{ deg}$ ,  $b_m = 600 \text{ deg/s}$  and  $b_k = 3 \text{ deg}$ . The final pulse-step generation pathway of the motor neurons (MN) consisted of the sum of the velocity command (multiplied by  $T_1 = 175 \text{ ms}$ ) and of its integral (Robinson 1970). The eye plant was modeled by a second order system with time constants  $T_1 = 175 \text{ ms}$  and  $T_2 = 13 \text{ ms}$  (Robinson 1973). It should be mentioned that the purpose of this saccadic model implementation was not to reproduce exactly the saccade dynamics but only to embed the smooth eye velocity integration mechanisms in a global framework. Hereafter, we will discuss the two hypotheses for the smooth eye displacement estimation in LIP or CB.

#### 4.2. LIP mechanism

The LIP smooth eye displacement estimation mechanism needed two computational stages. The first stage was composed of a series of neural cells with different tuning curves (TC) for the eye velocity ( $EV$ ) input (Fig. V-3A), in analogy of MST cells. Therefore, the discharge (= output  $a_{VSC}$ ) of these velocity sensor cells (VSC) was modulated by  $EV$  following a normalized log-normal function.

$$a_{VSC}(EV) = \left\langle \frac{1}{EV \cdot \sigma \sqrt{2\pi}} \cdot \exp\left(\frac{-(\ln(EV) - \mu)}{2\sigma^2}\right) \right\rangle \quad \text{Eq. V-2}$$

where  $\mu = \ln(m) + \sigma^2$ ,  $m$  was the maximum of the log-normal function (= preferred velocity of the cell) and  $\sigma = m_i^{-4}$  was its standard deviation. The triangular brackets indicate the normalization of the function

with respect to the maximum, i.e.  $a_{VSC}(m) = 1$ . The shape of this function was represented in Fig. V-3B.

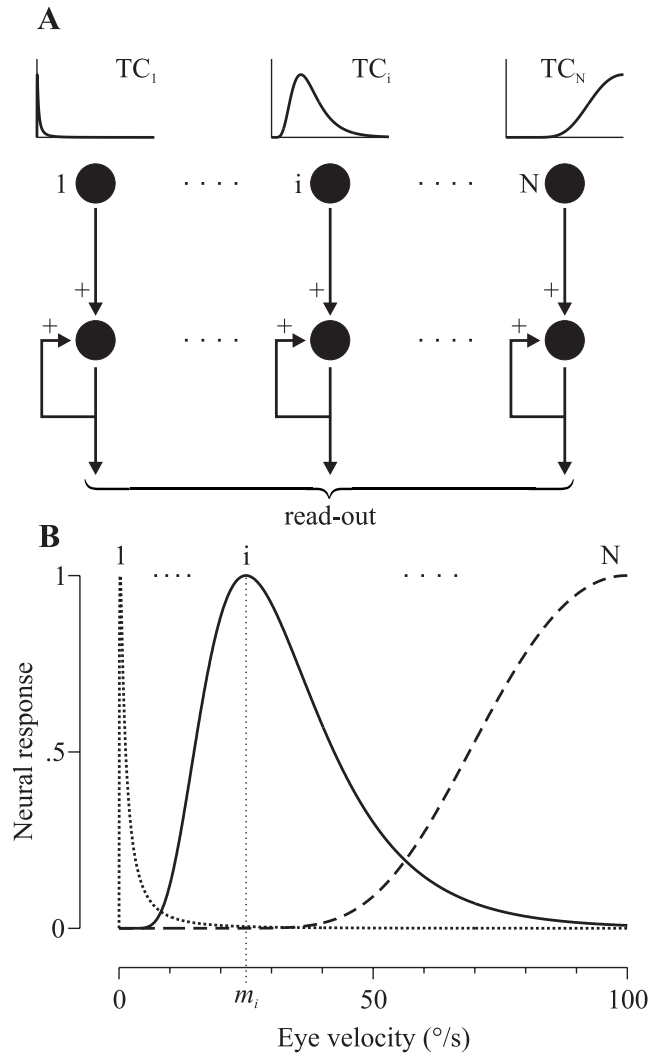


**Figure V-3: LIP mechanism. A.** Model structure. Two layers of neurons were used. The first layer consisted of eye velocity sensitive cells with log-normal tuning curves (TC). The output of these velocity sensor cells was normalized with respect to the distribution's maximum. The second layer integrated the output of the first layer. The read-out of this group of cells was performed by a weighted sum (Eq. V-4 and 5). **B.** Shape of tuning curves (Eq. V-2). Three examples of tuning curves for cells with different preferred velocities  $m_i$  are shown (dotted: 0.25°/s; solid: 25°/s; dashed: 100°/s).

We chose this log-normal expression of the TC characteristics because this appeared to be a physiologically realistic form (DeAngelis and Uka 2003). However, the exact shape of the velocity sensor cell's input-output relationship was not important and did not provide fundamentally different results. For the simulations presented here, we used  $N = 20$  velocity sensitive cells characterized by preferred velocities with squared distances  $m_i = [0.5^2, 1, 1.5^2, 2^2, \dots, 10^2]$ . This particular choice accounted for the increasing width of TC with increasing  $m_i$  to ensure approximately constant TC overlap.

The second, main stage of the LIP mechanism consisted in the integration of the velocity sensor cell's output (see Fig. V-3A), as this might be the case for LIP cells. Each velocity sensor neuron projected to one and only one integration neuron (INT). This integration stage was implemented as follows:

$$T_N \frac{da_{INT}}{dt} = k \cdot a_{VSC} \quad \text{Eq. V-3}$$

$T_N$  was a gain constant representing the natural time constant of the cells (we used  $T_N = 3$  ms) and  $k$  was an accumulation gain that took into account the simulation time step, i.e.  $k = 1/dT$ , where  $dT = 1$  ms was the simulation time step. The level of activity of an LIP integration cell  $a_{INT,i}$  was therefore an approximation of the time during which the eye velocity was close to  $m_i$ . The readout of these integration cells was calculated as a dynamical accumulation of the weighted sum  $WS(t)$  of the integration cell's activities. This read-out provided an estimate of the smooth eye displacement  $SED_{est}(t)$  in the following way:

$$T_{RO} \cdot \frac{dSED_{est}(t)}{dt} = -SED_{est}(t) + c \cdot WS(t) \quad \text{Eq. V-4}$$

$$WS(t) = \sum_{i=1}^N m_i \cdot a_{INT,i}(t) \quad \text{Eq. V-5}$$

$T_{RO}$  was the time constant of the read-out neuron's activity and was adjusted to produce the delay between the smooth eye movement and the compensation for it, as this has been observed experimentally (Blohm et al.

2003b, 2004, submitted). This is equivalent to a low-pass filter of the neural activity read-out. The constant  $c$  was adapted to match  $SED_{est}(t)$  with the real smooth eye displacement and provided the possibility to take into account the different subject's individual overall compensation gain. Note, that this model did not suppose any topologically arranged neurons, since they did not interact with their neighbors. Furthermore, there were only two adjustable parameters, i.e. the read-out time constant  $T_{RO}$  and the gain constant  $c$ .

### 4.3. CB mechanism

The CB model mechanism was based on a topographical representation of the smooth eye displacement in a position map in CB. Again, the only input to this displacement map was eye velocity (EV). The mechanism assumed that the flash appearance initialized the system by resetting the smooth eye displacement map to a gaussian activity corresponding to the zero position on the map (we used a gaussian normalized in amplitude and with  $\mu = 0^\circ$  and  $\sigma = 1^\circ$ ). Afterwards, a neural mechanism made the activity spread as a function of the eye velocity. The read-out of the map provided the instantaneous estimation of the smooth eye displacement. Figure V-4A shows the basic structure of the model.

We used a map of  $N = 51$  neurons, where the neuron #26 corresponded to the zero position in the map. The basic dynamics of the CB map's neural activity  $a_{CB}$  was described by the following rate equation:

$$T_N \cdot \frac{da_{CB}}{dt} = -a_{CB} + I + E \quad \text{Eq. V-6}$$

$T_N = 3$  ms was the neural time constant.  $I$  described the input from the neighboring neurons and  $E$  was the self-excitation input. The input  $I$  of the neighboring neurons (Fig. V-4A) was calculated by taking the positive results of the convolution of the present map activity  $a_{CB}$  with an eye velocity weighted connectivity kernel ( $CK$ ) as follows:

$$I = [CK \otimes a_{CB}]^+ \quad \text{Eq. V-7}$$

$$\text{with } CK = c \cdot EV(t) \cdot M \quad \text{Eq. V-8}$$

and  $M = \begin{pmatrix} 1 & 0 & -1 \end{pmatrix}$

Eq. V-9

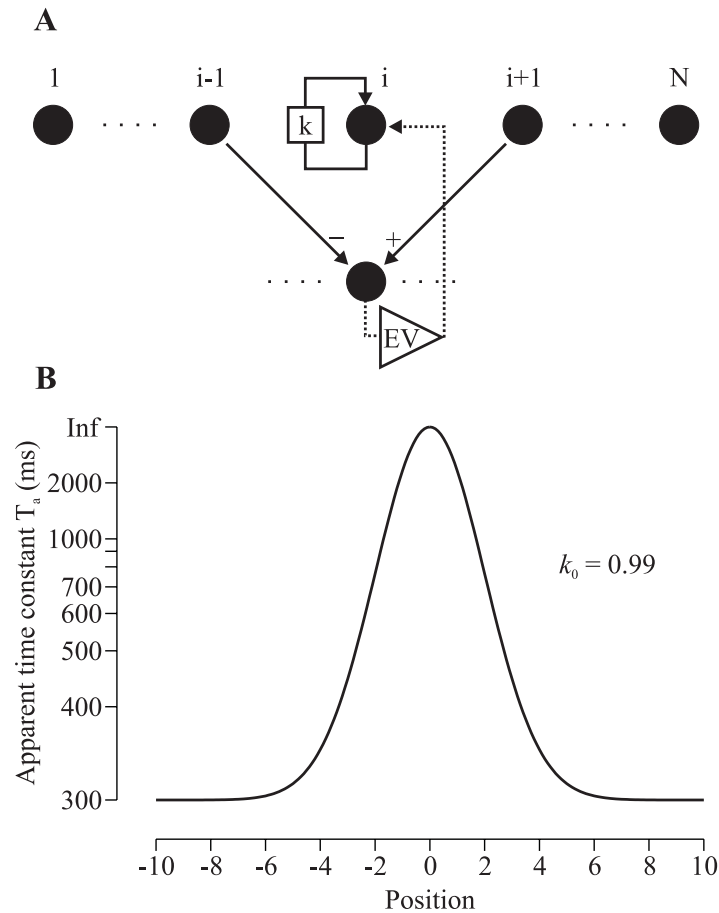


**Figure V-4: CB mechanism.** **A.** Structure of the displacement map. Neuron  $i$  got input from itself (reverberation constant  $k$ ) and from the neighboring neurons. The reverberation gain depended on the location of the activity maximum in the map (Eq. V-10). The input from the neighbors was an eye velocity weighted signal representing the strictly positive part of the map's activity gradient (Eq. V-7, 8 and 9). **B.** The apparent time constant  $T_a$  of the map's activity was presented on a reciprocal scale for  $k_0 = 0.99$ .

$M$  had the form of an edge detection filter, which was equivalent to computing the gradient. Neural activity gradients have been previously used to update retinotopical memory maps (Droulez and Berthoz 1991, 1988). Furthermore, eye/head position or velocity modulation of synaptic gains is believed to be a fundamental neural process in the brain (Chance et al. 2002;

Salinas 2003; Salinas and Sejnowski 2001; Salinas and Thier 2000). Here, the velocity weighted connectivity kernel implements such a gain modulation mechanism. Note that the exact shape of  $M$  was not important. Other filters provided similar results (data not shown). The constant  $c$  was adjusted to match the distance between neurons to 1 deg and also provided the possibility to account for the variability of the subject's overall compensation gain.

The self-excitation input  $E$  allowed the neural map to maintain its activity (Wang 2001). Furthermore, we implemented a particular instance of a center-surround inhibitory mechanism (Salinas 2003). Its goal was to allow the system to increase activity contrast in the neural map. Therefore, we used a reverberation gain that depended on the maximum of the map activity:

$$k = k_0 + (1 - k_0) \cdot \text{gauss}(\mu, \sigma) \quad \text{Eq. V-10}$$

where  $k_0$  was a constant reverberation gain parameter,  $\mu$  was the position of the maximum map activity and  $\sigma=2$  and thus  $E = k \cdot a_{CB}$  (Fig. V-4A). This choice of the self-excitation gain resulted in an activity dependent apparent time constant for the map's activity decay. That is, if eye velocity was zero, the relaxed form of Eq. V-6 (with  $I=0$ ) yielded an apparent time constant  $T_a = \frac{T_N}{1-k}$ . Figure V-4B shows the behavior of the apparent map dynamics as a function of the distance from the location of the map maximum activity for the case  $k_0 = 0.99$ .

Finally, the read-out of the map assumed similar dynamics as for the LIP mechanism, i.e. accumulating evidence for the smooth eye displacement estimation. Again, this form of read-out was chosen to fit the delay between the smooth eye movement and the compensation for it observed in the data (Blohm et al. 2003b, 2004, submitted). The estimate of the instantaneous smooth eye displacement was computed using the center of activity (COA) of the displacement map.

$$T_{RO} \cdot \frac{dSED_{est}(t)}{dt} = -SED_{est}(t) + COA(t) \quad \text{Eq. V-11}$$

where  $COA(t)$  was the activity weighted average of the neural map position  $x_i$ .

$$COA(t) = \frac{\sum_{i=1}^N a_{CB,i} \cdot x_i}{\sum_{i=1}^N a_{CB,i}} \quad \text{Eq. V-12}$$

There were three adjustable parameters for the CB mechanism, i.e. the read-out time constant  $T_{RO}$ , the constant reverberation parameter  $k_0$  and the gain constant  $c$ .

#### 4.4. Behavioral experiments

We used two experimental behavioral data sets from human subjects to fit the model's parameters. Both experiments used the "smooth double-step" paradigm. In a first experiment, smooth anticipatory eye movements provided the initial smooth "step". The second experiment used ongoing smooth anticipatory eye movements for the first "step" displacement. Both paradigms were described in details elsewhere. Please refer to Blohm et al. (2003b) for the anticipatory smooth "step" experiment and to Blohm et al. (2004, submitted) for the "step" induced by ongoing smooth pursuit. We will refer to these experimental data sets as ANTI (smooth anticipatory eye movement data) and SPUR (smooth pursuit data).

Hereafter, we will only present data from the region of interest, i.e. starting at the moment of target presentation (10 ms flash) until 1000 ms after the flash presentation. This memory period included between 1 and 5 orientation saccades. The two-dimensional data from the SPUR paradigm was reduced to one dimension in the direction of pursuit. This allowed us to easily present and compare ANTI and SPUR data in the same format.

## 5. Results

LIP and CB mechanisms were analyzed separately and tested on the same data. We will first describe the basic dynamics for each mechanism. Afterwards, we will fit the model parameters on the experimental data and provide some examples to illustrate the power of each smooth eye displacement estimation mechanism. Finally, we reproduced the major findings of the available experimental data sets and reconciled previous contradictory data from the literature. This validated our approach.

### 5.1. Analysis of LIP mechanism

In a first time, we analyzed the behavior of the LIP mechanism using arbitrary parameters. Figure V-5 shows the LIP behavior (2<sup>nd</sup> layer LIP neurons) with parameters  $T_{RO} = 100$  ms and  $c = 0.5$  for a 500-ms test eye velocity input of  $25^\circ/\text{s}$ . For the presentation, we arranged the neurons in increasing order of their tuning curve's preferred velocity  $m$  in panel A.

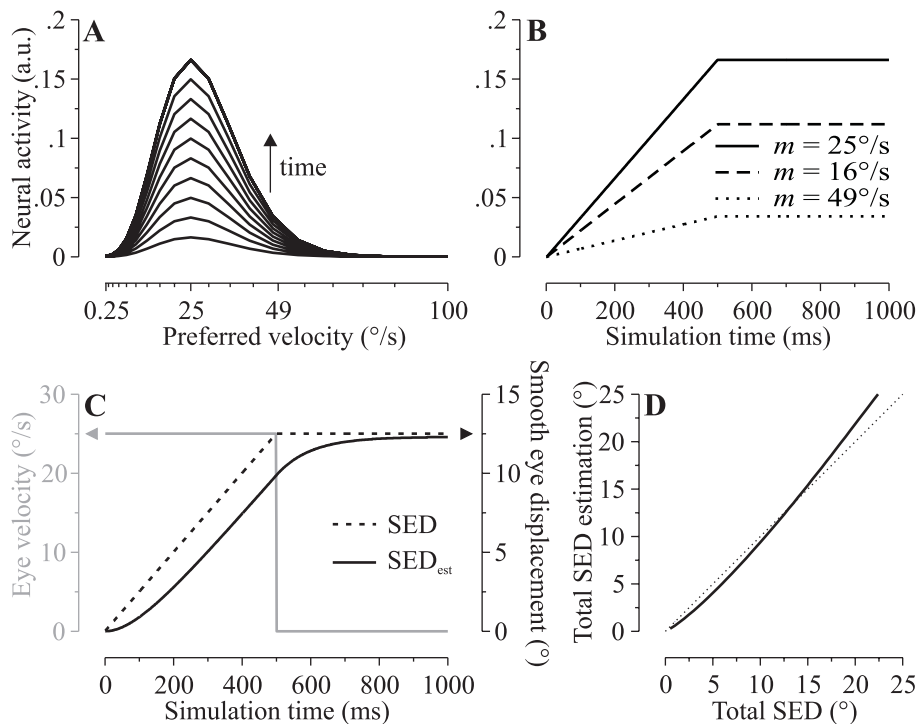


**Figure V-5: Simulation results for the LIP mechanism.** For this simulation, we used a read-out time constant  $T_{RO} = 100$  ms and an accumulation gain  $c = 0.5$ . **A.** Integration cell activity for different simulation times (50 ms step) between 0 and 1000 ms. Neurons were arranged in increasing order of preferred velocity. Simulations were performed with a  $25^\circ/\text{s}$  step eye velocity lasting for 500 ms. **B.** Three examples of integration cell activity over time for different preferred velocity projections (16, 25 and  $49^\circ/\text{s}$ ). **C.** Eye movement and estimation of the smooth eye displacement. The solid gray line was the eye velocity input used (left scale). The dotted black line corresponds to the effective smooth eye displacement and the solid black line was the model estimation of SED (right scale). **D.** Estimation of the final SED as a function of the true SED. The dotted line indicates the desired relationship. The solid line corresponds to the measured (slightly non-linear) model behavior. Simulations were performed with various step-shaped eye velocities lasting for 500 ms.

It can easily be seen, that the activity of individual LIP neurons rose linearly over time (Fig. V-5B). Furthermore, the instantaneous read-out of the smooth eye displacement estimation was delayed with respect to the effective SED (Fig. V-5C). This was due to the accumulation of evidence dynamics for the read-out of neural activity governed by  $T_{RO}$ . Finally, Fig. V-5D shows that the model provided a good estimation of the smooth eye displacement over a large range of effective displacements. Furthermore, the model estimation was almost linearly related to the actual displacement.

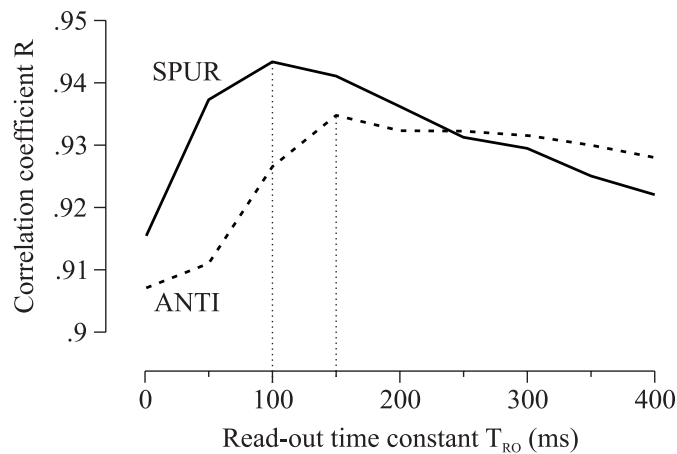


**Figure V-6: LIP simulation best fit on data.** The correlation coefficient  $R$  was used as an indicator for the goodness-of-fit between model simulations using the LIP mechanism and experimental observations from ANTI (dotted line) and SPUR (solid line) data sets.  $R$  was computed for different values of the read-out time constant  $T_{RO}$ . Vertical dotted lines indicate the best-fit values for each data set.

In order to fit the model on the observed behavior, we identified the optimal parameters for the LIP mechanism from experimental data. Therefore, we varied the read-out time constant  $T_{RO} = [1; 50; 100; 150; 200; 250; 300; 350; 400]$  ms and computed the model prediction of the experimental data for all saccades in each trial. The model's gain constant  $c$  was evaluated for each value of  $T_{RO}$  using a step eye velocity profile similar to the one used in Fig. V-5 but varying the magnitude of eye velocity. The gain constant  $c$  was then adapted to provide a regression slope of 1 for the comparison between the estimation of SED and the actual SED generated by the test eye velocity trace. Afterwards, we simulated the

system's response to the flash stimulus using eye velocity, flash stimulus location and timing information concerning the compensatory saccades from data.

There were  $N = 1,354$  ANTI trials and  $N = 4,464$  SPUR trials and a total of  $N = 4,870$  ANTI saccades and  $N = 9,150$  SPUR saccades respectively. As an indicator for the goodness of the model's prediction, we used the correlation coefficient  $R$  between the predicted and observed saccade amplitudes. Figure V-6 shows the evolution of  $R$  for the different values of  $T_{RO}$ . We decided that the maximum of  $R$  indicated the optimal value of  $T_{RO}$ , i.e. 150 ms ( $c = 0.497$ ) for ANTI trials and 100 ms ( $c = 0.493$ ) for SPUR trials. These values were used hereafter for all simulations of the LIP model.

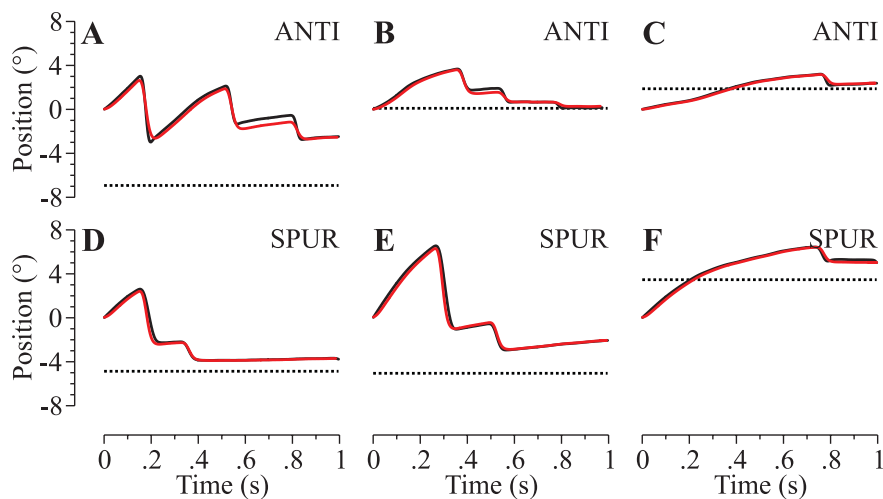


**Figure V-7. Typical examples of comparison between LIP simulations and experimental data.** Panel A-C show three ANTI trials, panels D-F show three SPUR trials for different first saccade latencies (short, long and very long). Black lines were data and red lines correspond to simulations. Time 0 ms was the moment of target presentation (brief flash) in both paradigms. **A.** 1<sup>st</sup> saccade latency = 161 ms. **B.** 1<sup>st</sup> saccade latency = 371 ms. **C.** 1<sup>st</sup> saccade latency = 773 ms. **D.** 1<sup>st</sup> saccade latency = 165 ms. **E.** 1<sup>st</sup> saccade latency = 277 ms. **F.** 1<sup>st</sup> saccade latency = 759 ms.

Figure V-7 shows six typical examples of comparison between simulation and behavior for short latency first saccades, long latency first saccades and very long latency first saccades of both ANTI and SPUR experiments. As one can observe, the simulation generally fitted the data

very well. The remaining error was a combination of SED underestimation (due to the LIP mechanism) and remaining  $PE_R$  due to the saccadic undershoot strategy. The  $PE_R$  compensation was always  $0.9^n$ , where  $n$  was the total number of saccades.

To provide a quantitative comparison between the simulation results of the LIP mechanism and the behavioral findings of previous experimental studies (see Blohm et al. 2003b), we analyzed the main effects of the compensatory saccades using two different indicators. Similarly to the procedures used for ANTI trials in Blohm et al. (2003b), we computed the delayed SED compensation gain  $\alpha$  as follows:

$$\alpha_T(t) = \frac{SED(t) - PE(t)}{SED(t - T)} \quad \text{Eq. V-13}$$

The delayed SED compensation gain  $\alpha$  was calculated at each moment  $t$  for all trials, but only after the occurrence of the first saccade. We performed this computation for varying SED compensation delays  $T$ . The results are shown in Fig. V-8A. As a second indicator for the quantification of the saccade's SED compensation, we used the SED compensation index  $CI$ , previously defined for SPUR data as (see Blohm et al. 2004, submitted):

$$CI = 1 + \frac{PE}{SED} \quad \text{Eq. V-14}$$

$CI$  was calculated after each saccade and indicates to what proportion the actual SED was compensated for. Figure V-8B shows the results of this analysis. The simulation results fitted very well the data. Figure V-8A shows that our model could reproduce the main behavior of the ANTI data, i.e. the delayed compensation gain reached an approximately constant level for a delay  $T = 400$  ms. According to the interpretation of the experimental findings (Blohm et al. 2003b) this constancy of  $\alpha$  is important because it is difficult to conceive a neural mechanism for SED compensation with a time-varying gain. In the case of SPUR data, Fig. V-8B shows a good fit between the simulation  $CI$  and experimental results.

We did also test the LIP mechanism on previous findings reported in the literature and summarized in Fig. V-1. Therefore, we reproduced artificially the experimental stimulus configurations as described in McKenzie and Lisberger (1986) and in Herter and Guitton (1998) and

performed simulations of these experiments with our LIP mechanism using the model parameters identified in Fig. V-6. The results are shown in Fig. V-9 where we overlaid simulation data (red) on Fig. V-1. As it can be observed, our model provided an accurate prediction of the data.

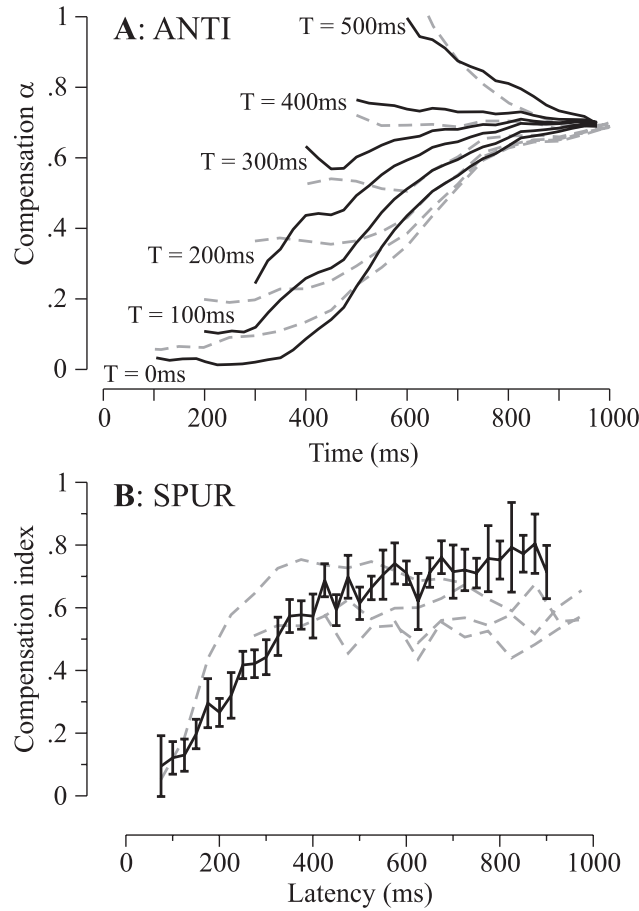


**Figure V-8: Comparison between LIP simulation data and experimental results.** **A.** The delayed compensation index (Eq. V-13) was computed for delays  $T$  between 0 and 500 ms (100 ms step). Dashed gray lines were experimental ANTI data from Blohm et al. (2003b), solid black lines were simulations. **B.** Comparison between the SED compensation index ( $CI$ , Eq. V-14) for experimental SPUR data (dashed gray lines stand for results from saccades 1 to 4) and simulation (black solid line). Lines and whiskers stand for mean and 95% confidence intervals.

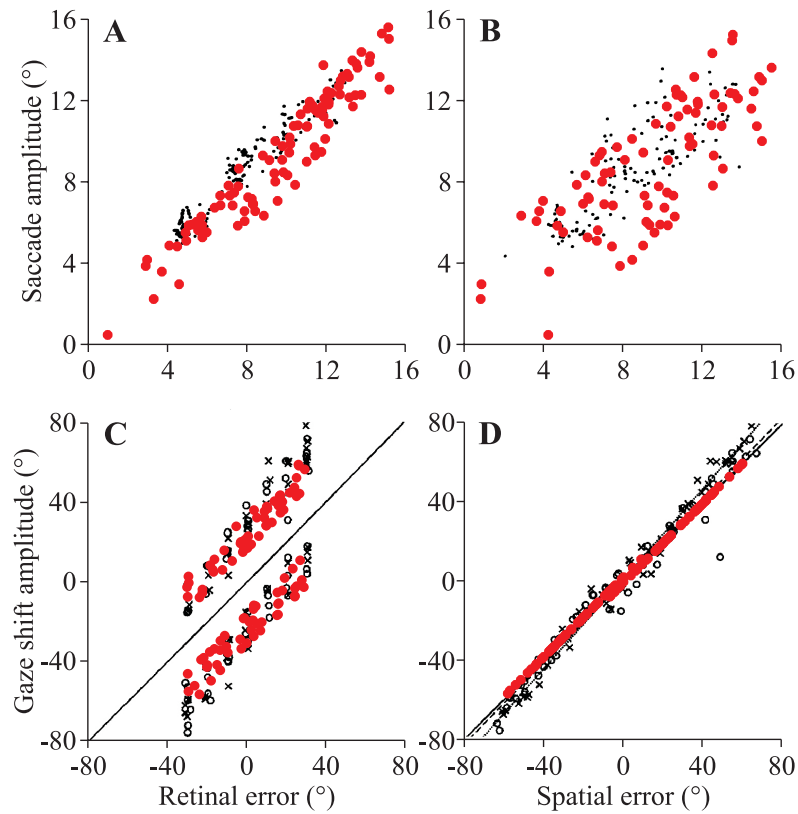


**Figure V-9: LIP simulations of data from literature.** All panels correspond to the examples shown in Fig. V-1. **A, B.** Adapted from McKenzie and Lisberger (1986). **C, D.** Adapted from Herter and Guitton (1998). Simulation data (red dots) were laid over the data from literature.

## 5.2. Analysis of CB mechanism

As for the LIP mechanism, we first analyzed the theoretical behavior of the CB mechanism. Figure V-10 shows the results of this investigation for  $T_{RO} = 100$  ms,  $c = 2.3$  and  $k_0 = 0.99$ . Figure V-10A and B show the evolution of the map's neural activity over time as a response to the 500 ms duration step eye velocity profile of  $25^\circ/\text{s}$ . It can easily be observed that eye velocity “pushed” the map's activity to cells that code higher positions. Furthermore, the center-surround mechanism sharpened the locus of activity. Indeed, the neural activity surrounding the activity maximum decreased over time. This lead to a smooth eye displacement estimation that was delayed and wiped out with respect to the actual SED

(Fig. V-10C). In addition, the estimated SED was almost linear with respect to the actual SED and the estimation gain was close to unity (Fig. V-10D). Thus, as this was the case for the LIP mechanism, the CB mechanism provided a good estimation of the actual smooth eye displacement and introduced the delay necessary to explain the experimental data.

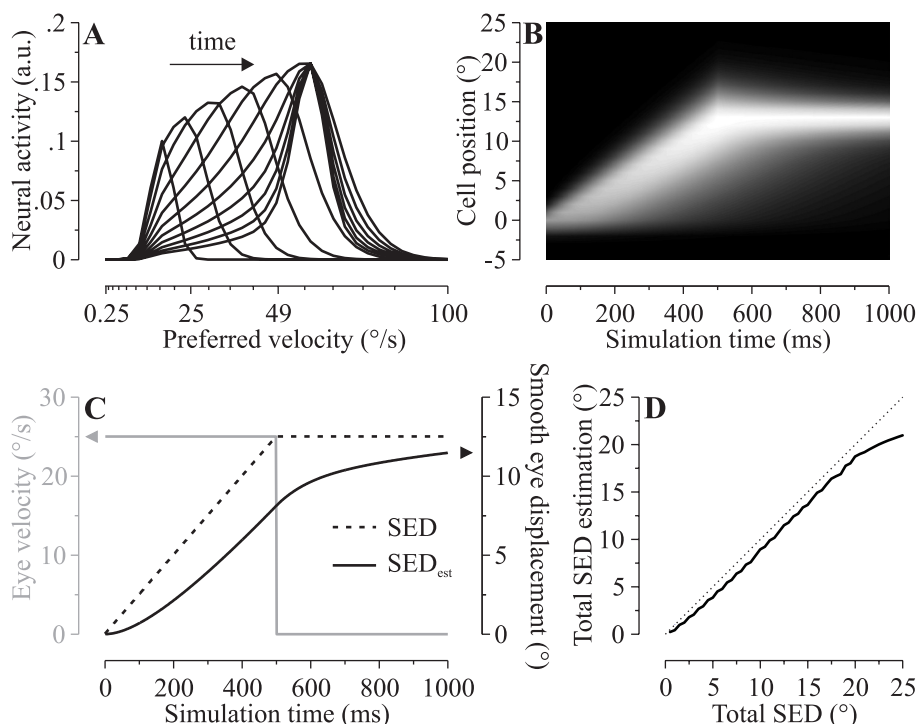


**Figure V-10: Simulation results for the CB mechanism.** For this simulation, we used a read-out time constant  $T_{RO} = 100$  ms, a reverberation gain constant  $k_0 = 0.99$  and an accumulation gain  $c = 2.3$ . **A.** Activity of the neural map at different simulation times (50 ms step) ranging from 0 to 1000 ms. Each cell corresponded to  $1^\circ$  on the position map. Simulations were performed with a  $25^\circ/s$  step eye velocity lasting for 500 ms. **B.** Normalized map activity evolution over time (black = no activity; white = maximum activity). **C.** Eye movement and estimation of the smooth eye displacement. **D.** Estimation of the final SED as a function of the true SED. For panels C and D, the same conventions as for Fig. V-4 apply.

In a second step, we needed to identify the optimal parameters for the CB velocity integration mechanism to fit both ANTI and SPUR data. Therefore, we proceeded similarly to the methods used for the LIP mechanism.

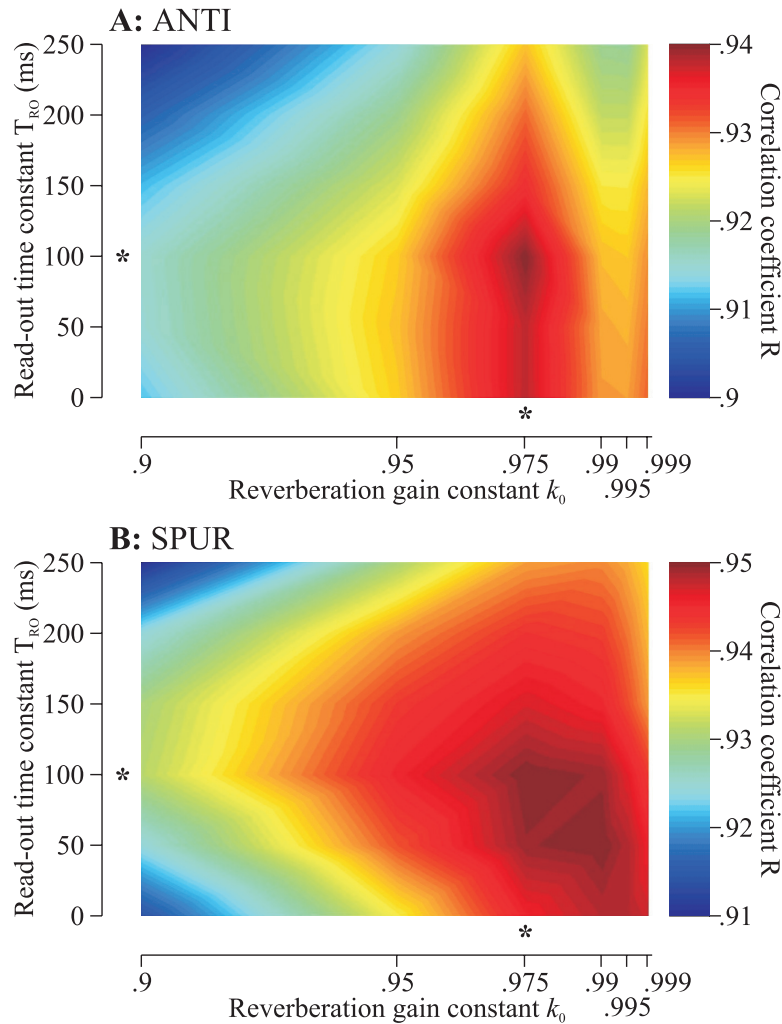


**Figure V-11: CB simulation best fit on data.** As for Fig. V-5, the correlation coefficient  $R$  was used to measure the goodness of fit between saccade amplitudes of model simulations using the CB mechanism and data. **A.** ANTI data. **B.** SPUR data. The range of  $R$  was color coded (see right column of the panels).  $R$  was represented as a function of the two free model parameters, i.e. the read-out time constant  $T_{RO}$  and the reverberation gain constant  $k_0$ . The asterisks represent the optimal values of those parameters with respect to maximal  $R$ .

Here, we varied the read-out time constant  $T_{RO} = [1; 50; 100; 150; 200; 250; 300; 350; 400]$  ms and the reverberation parameter  $k_0 = [0.9; 0.975; 0.99; 0.995; 0.999]$  independently and

evaluated the optimal gain constant  $c$  for each couple  $(T_{RO}, k_0)$  in the same way as for the LIP mechanism. The reverberation parameters corresponded to the apparent neural time constant  $T_a = [30; 60; 120; 300; 600; 3000]$  ms. Afterwards, we compared the simulation data from each couple  $(T_{RO}, k_0)$  with the measured experimental data from ANTI and SPUR paradigms. We measured the performance of the model compared to the experiments by computing the correlation coefficient  $R$  between the simulation and behavioral saccades for each couple  $(T_{RO}, k_0)$ . The results of this analysis are shown in Fig. V-11A for ANTI data and in Fig. V-11B for SPUR data.

The optimal set of parameters (where  $R$  was maximal) was the same for ANTI and SPUR trials, i.e.  $T_{RO} = 100$  ms,  $k_0 = 0.975$  ( $T_a = 120$  ms) and  $c = 2.427$ . These optimal choices for these parameters were marked by an asterisk in Fig. V-11. Note however, that for SPUR trials (Fig. V-11B) there was another set of parameters that provided similarly good results [ $T_{RO} = 50$  ms,  $k_0 = 0.99$  ( $T_a = 300$  ms) and  $c = 2.435$ ]. However, we preferred to use the same set of parameters to explain both experimental paradigms, i.e. the first set.

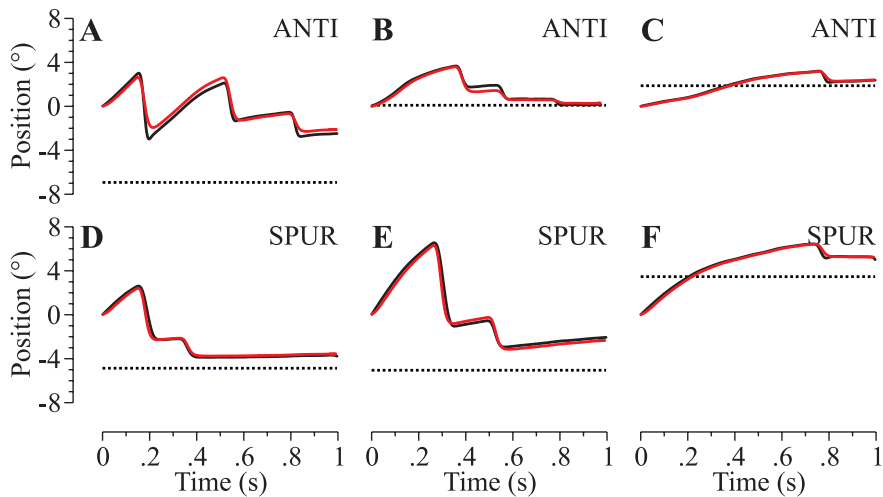


**Figure V-12: Typical examples of comparison between CB simulation and experimental data.** The same conventions as in Fig. V-6 apply. All the experimental data shown here were identical with those of Fig. V-6.

To illustrate the performance of the model using the CB eye velocity integration mechanism, we present in Fig. V-12 a comparison between simulation and data using the same individual experimental trials as in Fig. V-7 for ANTI and SPUR paradigms. The CB mechanism provided a very good estimation of SED to fit the data. There were only subtle apparent differences between both models on these examples (compare Fig. V-7 and 12).

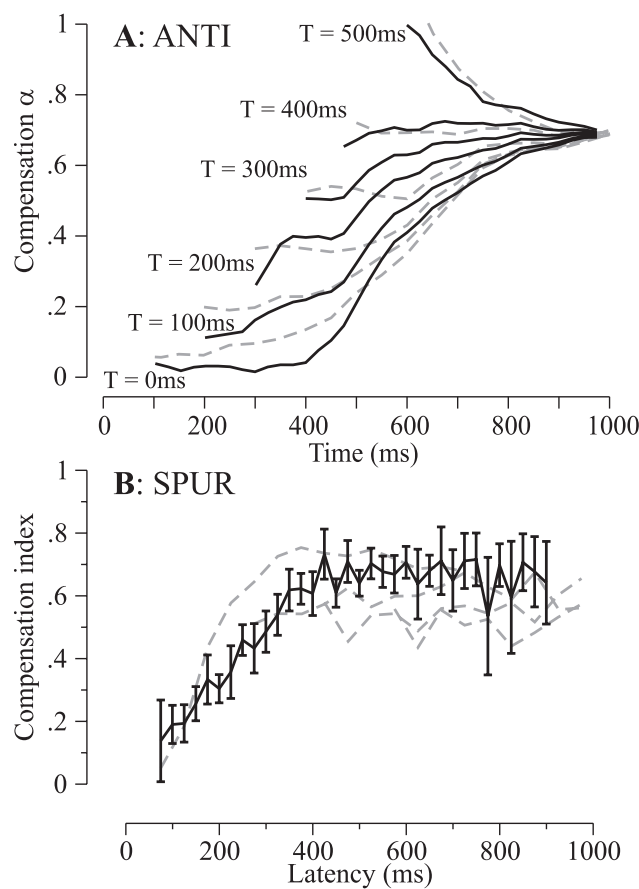


**Figure V-13: Comparison between CB simulation results and experiments.** The same conventions as for Fig. V-8 apply. **A.** The delayed compensation constant  $\alpha$  was compared for simulation and ANTI data. **B.** Simulation results of the compensation index  $CI$  compared to experimental SPUR data.

Again, we tested the simulation results of the CB mechanism on the main results from the ANTI and SPUR experiments. Figure V-13A shows the comparison between the experimentally (ANTI) evaluated delayed compensation gain  $\alpha$  and the simulation results. As for the LIP mechanism, the evolution of the delayed compensation gain  $\alpha$  from the CB mechanism was the same as for the data. We did also find an optimal delay  $T = 400$  ms for which  $\alpha$  was approximately constant. Figure V-13B illustrates the accuracy of the model fit on the main SPUR experimental results using the CB eye displacement estimation mechanism. The model fitted extremely well the SED compensation index evaluated from data.

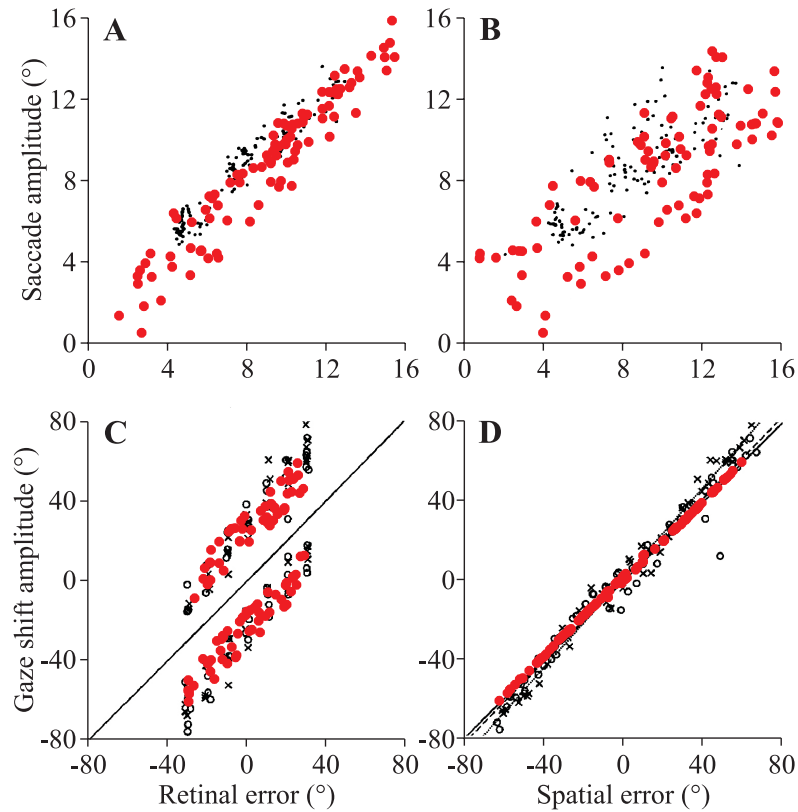


**Figure V-14: CB simulations tested on data from literature.** The same conventions as for Fig. V-1 and 9 apply. **A, B.** Adapted from McKenzie and Lisberger (1986). **C, D.** Adapted from Herter and Guitton (1998). Simulation data (red dots) were laid over the data from literature.

The model's estimation of the apparently contradictory results of retinal or spatial saccade programming in the "smooth double-step" paradigm in literature (Herter and Guitton 1998; McKenzie and Lisberger 1986) is shown in Fig. V-14. As for Fig. V-9, the use of the CB mechanism accurately fitted the data in Fig. V-14 and thus reconciles those results.

## **6. Discussion**

When a smooth eye movement displaces the eyes during the memory period of a briefly presented target, contradictory results have been reported in the literature concerning the programming of the saccade towards the memorized stimulus location. Whereas some studies reported retinotopically coded saccades (Gellman and Fletcher 1992; McKenzie and Lisberger 1986), other results favored the spatial error hypothesis (Baker et al. 2003; Herter and Guitton 1998; Ohtsuka 1994; Schlag et al. 1990; Zivotofsky et al. 1996).

Recent data (Blohm et al. 2003b, 2004, submitted) suggested that a time consuming retinal-to-spatial transformation of the internal target representation could reconcile these findings. Here, we tested this predication. We proposed a saccade model with two alternative mechanisms that accounted for smooth eye movements in the absence of vision. Both mechanisms needed to integrate a smooth eye velocity signal to provide an estimation of the smooth eye displacement (SED) to the Posterior Parietal Cortex (PPC), a structure involved in the spatial representation of visual stimuli. SED signals could then be used by PPC to update the spatial representation of the target in eye-centered coordinates.

The first SED estimation mechanism was compatible with observations from the Lateral Intraparietal Cortex (LIP). This LIP mechanism was based on an accumulation of time at which the eyes moved with a certain velocity. The alternative mechanism was proposed to take place in the Cerebellum (CB) and was based on an eye velocity driven movement of neural activity on a topological eye displacement map. Both mechanisms provided an excellent description of our two available test data sets for "smooth double-step" experiments. Note that the fit of the simulations on the data was very accurate despite the low degree of freedom of the velocity integration mechanisms (1 for LIP and 2 for CB

mechanisms). Furthermore, our model could explain the previously reported data and reconcile their initially contradictory results.

### **6.1. General model discussion**

Both smooth eye displacement estimation mechanisms we proposed here used a low-pass filtered read-out of the neural activity. This was done to obtain the desired delay between the actual eye movement and the saccadic compensation for it, as this has been described experimentally (Blohm et al. 2003b, 2004, submitted). A potentially realistic reason for such a delay process might be the systems need to ensure accuracy of the SED estimation. Therefore, low-pass filtering the read-out of the integrative mechanisms would reduce the influence of brief perturbations (like eye blinks) and system noise on the estimated SED.

In the model presented here, no “pure” delays that could take into account the system’s processing time have been implemented. However, once the system decided to make a saccade, there is a processing time of approximately 50 ms (Mushiake et al. 1999; Thier and Andersen 1996) necessary to generate the final motor command sent to the extraocular muscles. Implicitly this delay was included in the activity read-out time constant we estimated for both mechanisms from our data sets. Consequently, we overestimated the read-out constant for the SED estimation.

For each model and set of parameters, we evaluated theoretically the optimal gain constant  $c$  before fitting the simulations to the experimental data. As a consequence, this procedure assumed that at time infinity, the compensation for the smooth eye movement was perfect (see Fig. V-1D). In contrast to this hypothesis, the available experimental results suggested that subjects might underestimate the actual SED up to 50% (Blohm et al. 2003b, 2004, submitted). However, as shown in Fig. V-8 and 13 our model fitted well the data despite the initial contradiction between the choices of the model’s gain constants  $c$  and the measured final SED compensation gain. We believe that the apparent underestimation of SED in the data was (at least partially) due to a finite number of corrective saccades. That is, if the system triggers a saccade that compensates for the available SED but the eyes continued moving smoothly afterwards, then the final SED compensation gain would be  $< 1$ . Furthermore, the saccadic undershoot

strategy contributed to this apparent underestimation of SED, since saccade amplitudes were always  $0.9 \cdot \Delta E$  (see Methods section). Nevertheless, there might still be a difference in the compensation gain between subjects. Of course, the question remains why the system did not trigger additional saccades in this case. In general, it is still to discover what exactly did trigger these compensatory saccades.

### **6.2. Model comparison with data**

The model simulations closely fitted the experimental data for both ANTI and SPUR paradigms. This could be observed in our typical trials in Fig. V-7 and 12. Indeed, the amplitudes of all saccades occurring at different latencies with respect to the memorized target appearance were well predicted. In addition, we could reproduce the main results for both data sets, i.e. the model adequately reproduced the overall delayed compensation index  $\alpha$  for ANTI data and the smooth eye movement compensation index  $CI$  for individual SPUR saccades. The remaining differences between the model simulation and the experimental results might be due to the biological variability of saccades and the subject's potentially different overall SED compensation gains.

We also tested our model on two representative results from the literature. Our simulations accurately mimicked data from Herter and Guitton (1998) showing that saccades to targets memorized before a pursuit eye movement were spatially accurate (Baker et al. 2003; Herter and Guitton 1998; Ohtsuka 1994; Schlag et al. 1990; Zivotofsky et al. 1996). Furthermore, previous findings concerning retinotopically programmed short latency saccades to memorized targets (Gellman and Fletcher 1992; McKenzie and Lisberger 1986) could also be reproduced. The delay for SED estimation in our model reconciled those initially contradictory findings. However, our simulation of McKenzie and Lisberger's (1986) results showed a larger scatter of saccade amplitudes compared to the experiment. But subjects in McKenzie and Lisberger's (1986) study were monkeys and not humans. Therefore, the difference in scatter between simulation and experiment (Fig. V-9A, B and Fig. V-14A, B) could be due to the fact that the model was calibrated on human data and compared to monkey behavior. However, the main result is still present, i.e. these short latency saccades

were better predicted by the retinal error hypothesis than by the spatial error hypothesis.

One behavioral prediction of our model concerns the “catch-up” saccades triggered during a transient extinction of a pursuit target (Bennett and Barnes 2003). If the saccade latency were long enough ( $> 300$  ms), the amplitude of those catch-up saccades should be tightly related to the actual eye displacement in darkness. This seemed to be the case for saccades reported by Bennett and Barnes (2003). However, these authors did not give any indication with regard to the saccade latency.

### **6.3. Hypothesized neural substrates**

We hypothesized that the internal estimation of a smooth eye displacement could take place either in the Cerebellum or in area LIP (see Background section). However, a behavioral experiment would not allow us to decide which brain structure actually implements this mechanism. Therefore a series of electrophysiological experiments need to be carried out to identify the neural substrates of SED estimation and to find specific cell types that correspond to our model predictions.

If the LIP mechanism were responsible for the integration of extraretinal eye velocity signals, one possibility would be to remove the source of extraretinal eye velocity signals by inactivating area MST. Despite a deficit in smooth pursuit (Dursteler et al. 1987), some smooth eye movements should persist. In addition, another possibility would be to use smooth anticipatory eye movements, as this has been done by Blohm et al. (2003b). The advantage of using smooth anticipation is that these eye movements are believed to rely principally on cognitive cues and might be generated by the frontal cortex (Missal and Heinen 2001, 2004). Another interesting experiment would be to record neurons in LIP that have previously been shown to carry time-related information (Leon and Shadlen 2003; Rao et al. 2001) to identify the hypothesized integration neurons. The activity of such LIP integration neurons should rise approximately linearly (in a “smooth double-step” paradigm) during the memory period of a target. The rate of rise of those neurons must be velocity tuned. This would be in accordance with previous findings demonstrating that many LIP neurons exhibit direction-specific activity during smooth pursuit and continue firing

when the visual stimulus is intermittently turned off (Bremmer et al. 1997; Sakata et al. 1983).

Alternatively to a possible role of LIP in SED estimation, the Ventral Intraparietal area (VIP) could also be involved in the integration of smooth eye velocity signals. Indeed, VIP contains neurons responding to extraretinal velocity signals (Colby et al. 1993; Schlack et al. 2003) and receives extensive input from MST (Lewis and Van Essen 2000; Van Essen et al. 1981). Furthermore, it has been shown that VIP neurons encode heading in head-centered coordinates and thus provide a reliable source of information about smooth motion (Bremmer et al. 2002; Zhang et al. 2004). The activity and characteristics of those VIP cells is thus compatible with our hypothetical “LIP” mechanism.

To identify the neural substrate of a possible role of the Cerebellum in the integration of smooth eye velocity signals, different experiments using a “smooth double-step” paradigm could be performed. Our CB mechanism predicts the presence of a topological map within CB. Neurons within this map should code eye displacement relative to a memorized target position. Furthermore, the gain of interconnection between these neurons should be modulated by eye velocity. We believe that the cerebellar cortex would be a good candidate for such a mechanism, because the theoretical behavior of our displacement map was compatible with the structure, organization and interconnection of the different types of neurons in the cerebellar cortex (Ghez and Thach 2000).

In addition to these predictions of neural activity in CB, SED information needs to be sent to area LIP in the parietal cortex. Some potential direct pathways have been identified (Clower et al. 2001), but their functional roles have not yet been investigated. An alternative candidate for a SED feedback pathway to LIP would be an indirect projection via the Thalamus. Indeed, the Mediodorsal Thalamus has been shown to play a role in the internal monitoring of movements by providing feedback about the amplitude of a (saccadic) eye movement to the cortex (Sommer 2003; Sommer and Wurtz 2002, 2004a, b). It would be interesting to record in various areas of the thalamus searching for SED related signals in a “smooth double-step” paradigm. However, in the case that our LIP hypothesis were true, one might expect to find eye velocity related signals in the Thalamus instead of positional signals coding an eye displacement.

Finally, the origin of the eye velocity signals used to estimate SED needs to be identified. There are two candidates, i.e. motor command efference copy signals and muscle proprioceptive afference. Today, it seems unlikely that proprioceptive information is used in oculomotor control (Lewis et al. 2001; Ruskell 1999; Weir et al. 2000). However, until this issue has been addressed specifically, a possible role of proprioception in SED estimation cannot be excluded. One way to test this would be to perform a “smooth double-step” experiment after deafferentation of the extraocular muscles in monkeys to answer this question.



## CHAPTER VI

# CONCLUSION – IMPLICATIONS OF THIS WORK AND FUTURE INVESTIGATIONS

*Science may set limits to knowledge, but should  
not set limits to imagination.*

Bertrand Russell

### 1. What was the purpose?

The purpose of this thesis was to investigate the interaction between smooth pursuit and saccades in the absence of continuous visual feedback. In such a situation, the saccadic system needs to monitor extraretinal signals about smooth eye movements in order to compensate for smooth eye displacements. This compensation is essential for the oculomotor system to ensure constancy of the perceived visual space.

### 2. Major findings

To investigate the ability of the saccadic system to compensate for smooth eye movements in darkness, I used a “smooth double-step” paradigm. Human subjects had to make saccades towards a briefly flashed (memorized) target that was presented during smooth eye movements. The analysis of the saccadic amplitudes revealed that short-latency eye movements did not correct for smooth eye displacements in darkness whereas long latency saccades did take them into account (Chapter 2). In addition, I showed that this behaviour was also reflected in a bi-modal distribution of saccade latencies. Indeed, whereas the short latency mode represented retinally coded saccades, saccades in the longer latency mode were spatially more accurate. Subjects took the decision to trigger either short or long latency saccades based on the sensory parameters, i.e. the

retinal distance of the flash and the eye velocity at the moment of the flash. The resulting decision was a trade-off between speed and accuracy.

In an additional analysis, I concentrated on the role of the secondary catch-up saccades (Chapter 3). In a similar “smooth double-step” paradigm I uncovered a delayed smooth eye displacement compensation mechanism. This resulted in an effective compensation that was observable around 400 ms after the actual smooth eye movement. The saccades triggered by the oculomotor system compensated on average for around 70% of the measured smooth eye displacements. However, as the model results indicate this apparent compensation gain was at least partially due to the lack of supplementary compensation saccades.

The discovery of a delayed smooth eye displacement compensation mechanism reconciled initially contradictory findings from the literature. Indeed, while some results indicated that the saccadic system could not compensate for smooth eye movements (these were short latency saccades), other studies underlined that the saccadic system did have access to extraretinal information about smooth eye movements (after long memory periods). On the basis of my results, I developed a model of a retinal-to-spatial transformation for the internal target representation (Chapter 5). The model simulations accurately reproduced my data and were validated on previously reported findings from the literature. This showed that all results obtained from the “smooth double-step” paradigm were consistent and could be explained by the same neural mechanism.

The analysis of the perceptual consequences of smooth anticipatory eye movements in darkness revealed an altered spatial representation of flashed targets (Chapter 4). I reported here that motion induced perceptual mislocalizations were observed even in the absence of the sense of motion. Furthermore, the time course of the perceptual mislocalization matched the time course of the retinal-to-spatial reference frame transformation of memorized targets.

Taken all together, the system was not able to ensure space constancy during smooth eye movements *in a predictive way* (as this is the case for saccadic eye movements). However, a *delayed* mechanism allowed the system to keep track of its own smooth eye movements. The delay could be explained by the system’s need to internally monitor the smooth motor

---

command sent to the extraocular muscles. This takes some time because different cortical and subcortical areas might be involved in this process.

### **3. Open questions**

Hereafter several open questions and suggestions of experiments for future investigations will be discussed. These are some specific ideas related to the issues addressed by this thesis but could also be of more general nature.

#### ***3.1. Anticipation***

In one of our “smooth double-step” paradigms I used smooth anticipatory eye movements as an initial smooth “step”. These eye movements are thought to be based on a memory of previous target velocity and are initiated in expectation of a moving target (Barnes and Asselman 1991; Bennett and Barnes 2003; Jarrett and Barnes 2001). However, alternatively to a velocity memory, there could also be an internal representation of a memorized target position. Indeed, if subjects were asked to track a transiently extinguished pursuit target, they perform catch-up saccades that bring the eyes onto the extrapolated ramp position (Bennett and Barnes 2003). Does the brain have an internal representation of target position that could be used in anticipatory (smooth and saccadic) eye movements? An experiment that might answer this question would be to present a smooth pursuit target followed by a target extinction (gap) and a second ramp. The second ramp’s velocity and position of appearance should be adjusted in order for the extrapolated ramps to cross during the gap. Keeping the trajectory of both ramps constant, the moment of reappearance of the target could be varied. If subjects were asked to track the stimulus as accurately as possible, the question arises whether the combination of anticipatory saccades and predictive smooth pursuit could reveal an internal representation of target position. In this case, the endpoints of the anticipatory saccades should lie on the extrapolation of the target trajectory, taking into account the moment of “virtual” crossover of both ramps during the gap period.

### ***3.2. Perceptual mislocalization of flashed targets***

I reported here a smooth eye movement related mislocalization of a briefly flashed target in the absence of movement perception. Although recent results propose that spatial uncertainty could explain perceptual mislocalizations of targets flashed during smooth movements (Kanai et al. 2004), there are still many open questions.

A first interesting question concerns the role of motion signals in the flash-lag effect. What is the relative role of eye and target movements? The flash-lag effect is present in situations where either the eyes or the target or both move. However, it has been suggested that eye movement information primes over target motion (Rotman et al. 2004). To test for the specific role of eye and target motion, the following experiment could be proposed. Two pursuit targets (e.g. a red and a green target) move at different speeds and in different directions (2-D). The subjects are instructed to pursue one of the targets, and a flash is presented close to the second target. If subjects were instructed to localize the flash either in absolute space or with respect to the second target (in an alignment task), what would the perceptual mislocalizations be? The magnitude and direction of those mislocalizations would of course also be expected to depend on the distance between the eyes and the flash and may also be influenced by the proximity of both pursuit targets at the moment of the flash appearance. Such an experimental paradigm could dissociate between the influence of eye and target motion in relative and absolute localization tasks.

A second question concerns the necessity of motion signals for the flash-lag illusion. For example, what would happen if subjects were asked to passively view a moving target while they are fixating a marker on the screen. If subjects were instructed to localize (with respect to the fixation point) a target briefly flashed in the periphery of the moving stimulus, would there still be a mislocalization even in the absence of any visual reference? Previous experiments suggest that there should be no mislocalization of the flash in this situation (van Beers et al. 2001), but the question has not been addressed explicitly.

Another suggestion related to the necessity – or not – of movement would be to test whether an attentional “displacement” would be sufficient to induce a perceptual mislocalization. Indeed, it has been suggested that the

direction of attention might influence the performance of target localization (Adam et al. 2000). A simple experiment would be to present peripheral stimuli with cognitive information (like colour, letters or forms) while subjects are fixating. If they were required to report the cognitive content of those peripheral stimuli, then one could assume that subjects are directing their attention towards these stimuli. At a random time during this process of attentional redirection, one could present a brief flash and ask subjects after the trial to report the perceived flash location. An alternative experiment would be to ask subjects to imagine a moving target while they fixate and present a brief flash during this task. To control the imaginary “stimulus position” at the moment of the flash, subject could be asked (randomly) to indicate either the perceived flash position or the imaginary “stimulus position” relative to the fixation point.

Finally, the physiological explanation of the flash-lag effect is still lacking. As discussed in more details in Chapter 5, the Superior Temporal Sulcus (STS) – maybe in conjunction with area LIP – would be a good candidate for a neural structure underlying the flash-lag effect. This would be in the line of previous findings identifying these areas to be responsible for peri-saccadic mislocalizations (Krekelberg et al. 2003). One way to test this hypothesis is to use briefly flashed targets presented during smooth anticipatory eye movements in darkness. The advantage of this paradigm over most others involving smooth pursuit is the absence of any visual responses of the neurons after the flash presentation.

### ***3.3. Smooth eye displacement compensation***

Saccades that compensated for smooth eye displacements were triggered with different latencies. Although I showed evidence that support a trade-off between speed and accuracy for the first orientation saccade, the precise mechanism that triggered orientation saccades and compensatory saccades could not be identified. This was partly due to the natural variability of saccade latencies (Becker 1991; Carpenter and Williams 1995; Reddi et al. 2003; Reddi and Carpenter 2000). However, it would be interesting to analyse in more details the oculomotor system’s decision to trigger a saccade. In addition to the sensory input used to determine the first saccade amplitude, there must be a mechanism that accounts for the smooth eye displacement or – more generally – for the remaining error.

Other open questions concern the smooth short latency orienting eye movement towards the flash. The neurophysiological origin of this response is still unclear. Although I propose a possible involvement of the Superior Colliculus due to a diminished gating of the Omni-directional Pause Neurons (see Appendix 3), this hypothesis has still to be tested. In addition, it would be interesting to develop a behavioural experiment that could indicate whether this position input to the smooth pursuit system is part of a reflexive pathway or whether it might be related to a volitional change of the centre of attention. Therefore, one might ask subjects to pursue a ramp and briefly flash a target during this pursuit ramp. By including a colour cue to the flash, subjects could be instructed to either orient their eyes towards the memorized flash position (flash colour 1) or to continue pursuing the ramp target (flash colour 2). If the smooth eye velocity is still modulated in both conditions of this “go / no-go” task, then attention might play a role. A further control would be the subject’s instruction to simply ignore the flash and continue pursuing. In addition to this, one could turn off the pursuit target at the moment of flash appearance. This would give to both targets (the flash and the ramp) an equal weight of competition.

I reported that there was a hemifield asymmetry (with respect to the smooth eye movement direction) in the latency of the first orientation saccade towards the flash. If this were due to a particular instance of an Inhibition Of Return (IOR) effect, then the same kind of hemifield asymmetry should be observed for all IOR experiments. For two subsequent saccades, this would mean that the latency of the second saccade should be longer if the second saccade was directed to the backward *hemifield* with respect to the first saccade direction. To my knowledge, this has not yet been done and would be an interesting experiment.

Our major hypothesis for the compensation of smooth eye displacements by means of saccades was the presence of an internal mechanism for the estimation of the smooth eye displacements (SED) in darkness. The second related hypothesis was that the outcome of the SED estimation mechanism was used by the Lateral Intraparietal cortex (LIP) to update the internal representation of the flashed target in oculocentric space – as this is thought to be the case for intersaccadic spatial updating (Henriques et al. 1998). However, the exact neural mechanisms and structures responsible for our findings still need to be discovered. Chapter 5

---

provides a detailed description of possible alternatives and hypotheses to be tested with regard to these hypotheses.

Finally, the respective role of efference copy and proprioceptive afferent signals about eye position in the orbit needs to be further investigated. Although proprioception does not seem to play a major role in the online control of eye movements (Lewis et al. 2001), such information could be used in the case of our “smooth double-step” paradigm as this has been proposed previously (Bridgeman 1995).

#### **4. Model results**

The purpose of our saccade model was to show that simple neural mechanisms could estimate smooth eye displacements from extraretinal eye velocity signals present in the brain. I proposed two alternative mechanisms that were both based on current physiological evidence. Since behavioural experiments could not decide which mechanism was the most plausible, electrophysiological investigations are needed to test those hypotheses (see Chapter 5).

A fundamental question addressed in the discussion section of Chapter 2 concerns the neural substrates for the programming of the longer latency and compensatory saccades. In my model, I suppose that the CB and LIP mechanisms update the memorized position of the target in PPC and that PPC in turn sends information about the amplitude of an upcoming saccade to FEF and SC. This would mean that SC must code the total saccade amplitude, including the smooth eye displacement component (if available to the system). However, alternatively smooth eye displacement information could be sent in parallel to the SC pathway to the saccade generator (situated downstream SC) as this seems to be the case for retinal slip signals in catch-up saccades (Keller et al. 1996b; May et al. 1988; Thurston et al. 1988). The Fastigial Oculomotor Region (FOR) in the Cerebellum could mediate such a parallel pathway, which is a particularly interesting hypothesis for our CB smooth eye velocity integration mechanism. As a result of such an adaptation of the saccade metrics in parallel to the SC pathway, the neural coding of the saccade amplitude in SC should not reflect any information about the smooth eye displacement. In contrast, the LIP mechanism would be more likely to have an effect on the coding of saccade amplitude in SC. This would be an interesting issue to test that could also

contribute to the discrimination between the proposed LIP and CB mechanisms.

The displacement map I used for our CB mechanism has some interesting properties. Indeed, if we consider the map with non-delayed readout, the map dynamics still produces a wiped out (~delayed) SED estimation, particularly for high velocity eye movements. Then we could ask what the neural read-out dynamics would be for a saccade. This question is particularly interesting with regard to previously proposed distributed models of the saccadic system (Lefèvre et al. 1998; Optican and Quaia 2002; Quaia et al. 1999), where a “pilot map” located in the Cerebellum was used. This pilot map approximately codes the movement error and could thus also be called “error map”. It would be interesting to model this pilot map using our CB mechanism (contrarily to our simulations, such an error map would be initialised at an eccentric position and the map activity would move towards neurons that code the maps zero position). Why would such an implementation of the pilot map be interesting? The answer is related to reports concerning SC microstimulation results during or after a saccade. These results indicate that the amplitude of a saccade evoked by SC microstimulation applied around a previous visually triggered saccade is modified compared to the stimulation-evoked control saccades where no preceding visual saccade was executed (Kustov and Robinson 1995; Nichols and Sparks 1995). Indeed, the amplitude of the stimulation saccade was shifted back with respect to the visually guided saccade. However, this effect decayed exponentially (time constant ~50 ms) with the time after the first saccade offset. The authors of these studies attributed their findings to the leakiness of the neural integrator. However, if a pilot map replaces those resettable neural integrators – as this has been proposed (Lefèvre et al. 1998; Optican and Quaia 2002; Quaia et al. 1999) – then our CB mechanism would predict exactly those results. That is, because the activity of a hypothetical CB error map would be wiped out, the readout of this map would appear to be delayed with respect to the eye movement and the delay would decay towards zero. Thus if this readout were used by the saccadic system (instead of the classical neural integrator) to provide an internal estimation of the currently remaining error, a new visual input (stimulation) would take the state of this pilot map into account to adjust the saccade amplitude. This would result in saccades with modified amplitudes, as this has been reported (Kustov and Robinson 1995; Nichols and Sparks 1995).

# APPENDIX I

## THE EXPERIMENTAL SET-UP

### 1. Goal

To present visual stimuli and to record human subjects responses at the same time, an experimental set-up had to be designed, developed and implemented. This device had to respond to certain number of experimental, software, hardware and user interface constraints. I list below the major specifications that were required:

- Simple, flexible and easy to use graphical user interface (GUI) for the creation of experimental protocols and to drive experiments.
- Real time closed loop control of visual stimulus presentation and experimental data acquisition.
- Possibility to control 4 mirror galvanometers and to acquire scleral search coil position data for 2 eyes. In addition, the possibility of recording joystick or other additional responses and to control multiple digital signals (for Lasers, LEDs, etc.) was needed.
- Synchronization signals should be available to interface the galvanometer – scleral search coil set-up, named “EyeLab”, with other equipment.

In the following sections, I will only describe the latest version 3.5 of EyeLab, since the hardware and software considerably developed over

time. Also, I will try to keep things simple, the purpose of this appendix being to give a *brief* overview of the EyeLab set-up I developed during this thesis work.

## 2. Implementation

### 2.1. Hardware

Figure AI-1 shows the principal hardware connection scheme. A custom PC (Dell, Round Rock, TX, USA) running the EyeLab GUI was connected via a Local Area Network (LAN) to a PXI industrial computer (National Instruments, Austin, TX, USA). A real time engine – called Phar Lab (Venturecom, Waltham, MA, USA) – runs on the PXI computer and controls two PXI-6025E data acquisition boards (National Instruments, Austin, TX, USA) via the Extended PCI (PXI) bus.

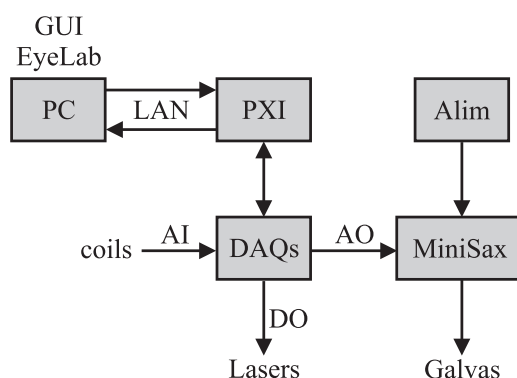


**Figure AI-1:** Hardware connection scheme of the EyeLab experimental set-up.

Analog input channels (AI) sample the scleral search coil (EPM3020, Scalar Medical BV, Delft, The Netherlands) signals while analog output signals (AO) are sent to the MiniSax drivers (GSI Lumonics, Billerica, MA, USA) that in turn control the speed and position of the mirror galvanometers. The MiniSax drivers needed an external power alimentation. Digital output signals (DO) are currently used to control the illumination of 3 Laser diodes (2 red and 1 green). Additional AI and DI/O signals are available for custom hardware connections, like joystick recordings, external hardware synchronization and/or additional Laser or LED illumination control.

## EXPERIMENTAL SET-UP

---

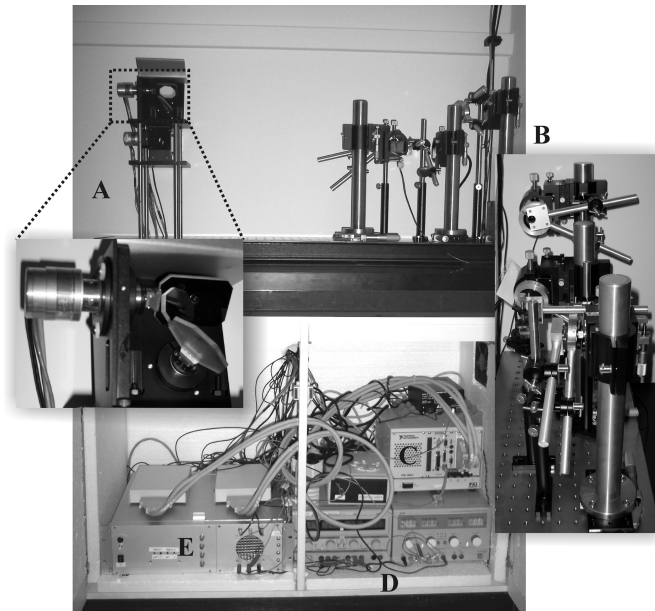


**Figure AI-2: Target generation hardware.** **A.** Mirror galvanometers deflect LASER beams. **B.** The LASER beams are optically confined and a polarization filter controls the luminosity. **C.** The real time PXI computer with data acquisition boards. **D.** The power supply units for the galvanometer drivers. **E.** Galvanometer driver and LASER switch box. On the top of the box are connection units of the data acquisition boards.

Currently, the galvanometers project the Laser beams onto a translucent flat screen mounted at 1 m distance from the subject. The optical arrangement of the Laser diodes and the galvanometers allows a precise horizontal and vertical control of two distinct targets. One of these targets can switch colour (red or green); their Laser beams were physically aligned using a beam splitter. The optical platform includes stable mounts and adjustable linear stages (OptoSigma, Santa Ana, CA, USA) for a precise arrangement and calibration of the devices.

I used 2 red LDG-650-123 Lasers (Molenaar Optics, Zeist, The Netherlands; switching time:  $< 1 \mu\text{s}$ ) and a green LDG-532-123-TTL Laser (Molenaar Optics, Zeist, The Netherlands; switching time:  $70 \mu\text{s}$ ). Two XY-mounted sets of mirror galvanometers from GSI Lumonics (Billerica, MA, USA) were used. Two M3ST Scanners (full-scale step time:  $\sim 5 \text{ ms}$ ) carry 30 mm mirrors able to project larger images onto the screen. Two M2ST Scanners (full-scale step time:  $\sim 2 \text{ ms}$ ) carry 10 mm mirrors for small targets.

Figure AI-2 shows a picture of the target generation and projection hardware.

## **2.2. Software**

The EyeLab software builds the experimental protocol, controls the measurement hardware and drives the experiment. The GUI allows setting up a protocol and conducting an experiment without any programming knowledge. The software was written using the graphical programming language G in LabViewRT 5.1 (National Instruments, Austin, TX, USA).

### *2.2.1. Basic structure of EyeLab*

The EyeLab GUI has a very simple basic structure that allows the operator to easily define and drive an experiment or to test and recalibrate the measurement hardware. When the EyeLab GUI is started one enters the initiation stage that defines global variables and automatically loads relevant hardware-related parameters from files. Afterwards, the user goes through a choice loop. Unless the operator chooses to terminate the session, he can navigate through different program menus (Figure AI-3) organized similarly to a web page.

The different selectable program choices are all self-consistent and intuitively understandable. Their basic function is described below:

- *Test Coil*: This menu allows testing if a scleral search coil works properly and if the polarity of the signal is correct.
- *Test Galva*: It is essential to be sure that the mirror galvanometers work well before driving an experiment. That is the purpose of this menu that allows testing each group of galvanometers in each direction (horizontal and vertical) separately.
- *Info*: An important issue in experimental work is to have access to all the necessary information about the subject tested and the test conditions. This menu allows to enter such information and to save/load it. One can also define how many coils have to be recorded and the sampling frequency.
- *Create Protocol*: This menu gives access to a sub-GUI to interactively define an experimental protocol. See next section for more details.

## EXPERIMENTAL SET-UP

---

- *Experiment*: This is the main part of the program that allows the operator to drive an experiment. Before each block of trials, the operator chooses a previously defined protocol file. The recorded data are displayed on a trial-by-trial basis and saved in one file for the whole block of trials.
- *Hardware Calibration*: Generally, this menu should be used only by the system administrator. It allows him to modify the geometrical parameters needed to transform the desired target position (viewed by the subject, measured in degrees) into a voltage for the mirror galvanometers, corresponding to the correct location of the target on the screen.

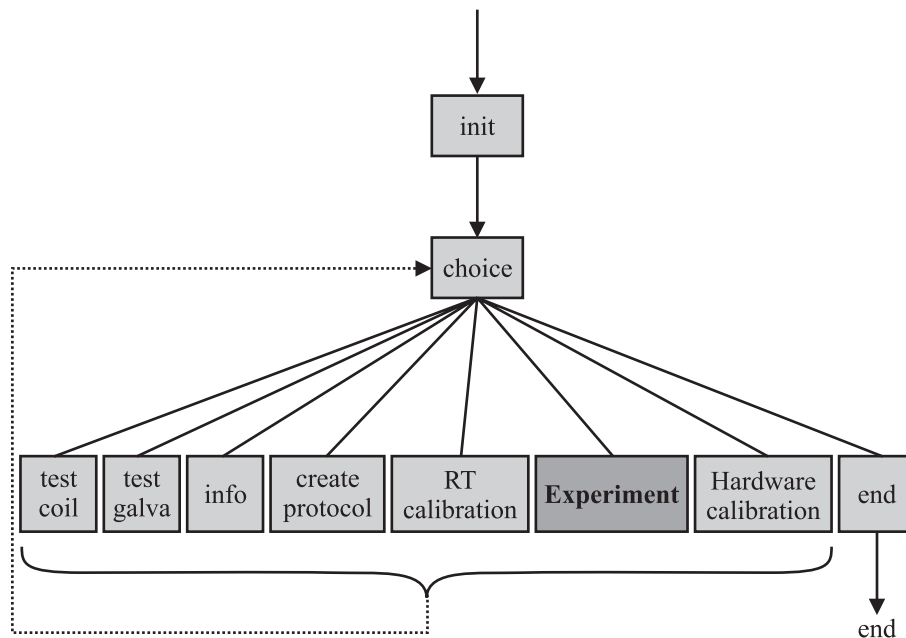


**Figure AI-3:** Organization of the EyeLab GUI.

As described above, the user interface PC is connected to the PXI real time computer via a LAN connection. To perform real time operations, the EyeLab GUI (running on the user interface PC) communicates with a software package on the PXI platform, i.e. the real time motor. This separation of the user interface and the data acquisition ensures solid real time performance. (Timing precision is around 1 ns)

### 2.2.2. *Building an experimental protocol*

EyeLab provides two different possibilities to define an experimental protocol. First, in the “trial-by-trial” definition of a protocol each trial has to be defined individually with fixed values for the parameters. The system then performs a pseudo-random presentation of all defined trials with equal probability. Second, in a more flexible “variable-parameter-trial” definition of the experimental protocol, the experimenter defines one type of trials but can specify all parameters as being either completely randomised in an interval, a randomly selected value from a list of values or a fixed value. Different variable-parameter-trial protocols can also be combined a posteriori with different appearance probabilities. These two ways of defining an experiment provide a maximum flexibility in the development of an original protocol.

An individual trial is defined in a modular approach by combining different types of basic segments. Available basic segments include fixation, ramp motion, step-ramp motion, target accelerations, sinusoidal targets and the possibility to enter user-defined formulas for the target trajectory. For each segment, the illumination is selectable between completely on, extinguished or intermittently turned on/off. The real time closed loop control feature of the set-up also allows the target to follow the eye with or without offset, i.e. at each step in time the output could be adapted to the input. For each segment, individual parameters could also be adjusted as a function of the eye position, velocity or acceleration. However, the closed loop control features are not yet completely implemented.

### 2.2.3. *Controlling the measurement hardware*

Probably the most difficult but important issue was the optimal control of the measurement hardware to ensure fastest processing with minimal delays and constant timing. These requirements were met by optimising the programming of EyeLab at different levels, i.e. asynchronous data communication between the user interface PC and the real time PXI computer, optimal TCP/IP data transfer and speed-optimised hardware-in-the-loop programming. Hereafter, I will shortly discuss each of these issues.

Since EyeLab performs data acquisition on a trial-by-trial basis, I needed to minimize the computation time between trials. This was achieved in two ways. First I made sure that the data transfer via the LAN was as fast

as possible. Therefore, I tested the TCP/IP setting carefully to identify the best configuration, i.e. data packages of 1028 bytes and 2 ms sleep time. This ensured a 600 Kbytes/s transfer rate. Second, asynchronous data communication allowed minimizing the time between different processes. Therefore, all computations on the host PC were performed while the PXI real time motor acquired new data. Practically, pre-built blocks of trials were sent to the PXI computer before the previous data set was sent to the monitor. Afterwards, the operator interface PC pre-constructs the next trial for the following loop. This procedure (Figure AI-4) is repeated until the end of the block.

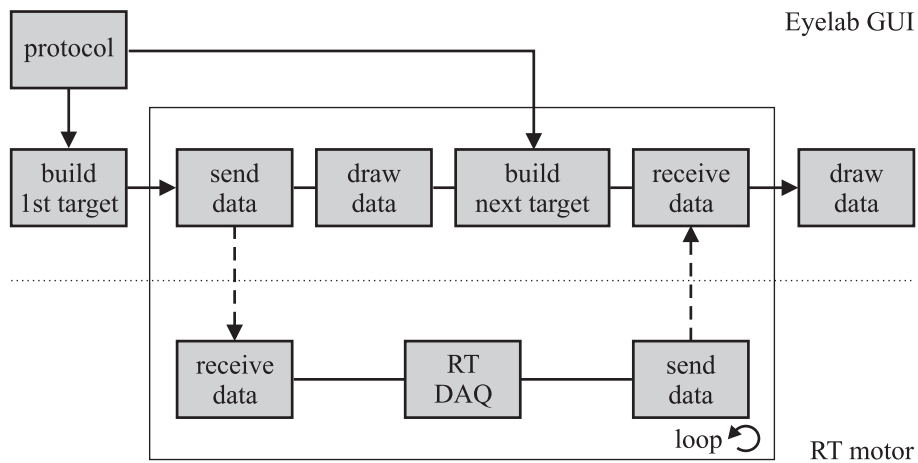


**Figure AI-4:** Asynchronous communication scheme for the data exchange between the host PC and the real time PXI computer.

To ensure optimal hardware-in-the-loop real time performance, I implemented the following critical steps. First, all measurement hardware was pre-initialised before the data acquisition loop was entered and no network communication takes place inside the loop. Second, by using hardware clocks, I ensured perfect synchronization of all input and output channels on both data acquisition boards (precision  $< 1 \mu\text{s}$ ). Third, all memory needed for the acquired data was pre-allocated before entering the loop. This avoided time-consuming memory reallocation procedures inside the real time loop.

### **3. Performance, suggestions and extensions**

#### ***3.1. Performances of EyeLab***

The current version of EyeLab is able to record 4 coil signals (horizontal and vertical position of 2 coils) at 500 Hz, as long as the length of one trial does not exceed 10 s. For longer trial and / or more analog input signals, the sampling frequency has to be lowered (see also other possible solutions in the next sections). The inter-trial interval (used for data exchange between the user interface PC and the real time PXI computer) is typically < 100 ms, but due to the Windows operating system (on the user interface PC), this delay is not constant.

All data generated or acquired are sampled or written at the same rate, i.e. typically 500 Hz. EyeLab currently controls 4 mirror galvanometers and one digital output line (= 8 TTL signals) for the illumination control of 3 Laser diodes and for the synchronization of external hardware. Synchronization is implemented for the “master” mode (EyeLab is the “master”) and has been tested and used together with the Chronos Video eye movement recording apparatus (Scalar Medical BV, Delft, The Netherlands). An extension to the “slave” mode is possible (see below).

All analog input and output signals are sampled exactly at the same time determined by the shared hardware clock of both data acquisition boards. However, the data acquisition boards currently in use (PXI-6025E) do not possess a hardware clock for digital signals. Thus, although the system is entirely deterministic (no jitter!), the digital lines could be slightly shifted in time with respect to the analog lines. However, this constant shift is always less than one cycle of the data acquisition control loop, i.e. < 2 ms for a sampling frequency of 500 Hz.

#### ***3.2. Possible extensions***

The EyeLab set-up has been designed in a very flexible way to allow all sorts of extensions, whether these are hardware or software. A major software extension would be the implementation of the already planned real time closed loop control. Therefore a simple code can be sent to the PXI real-time engine in order to adjust the output of the data acquisition boards as a function of the measured eye movement.

Other possible extensions concern the hardware used to present visual stimuli or record behavioural data. For subjects response recording, a joystick or other similar devices (mouse, response boxes, etc) can be integrated in the system. Furthermore, precise head movement recording devices and / or Infrared high-frequency optical marker tracking for body movements (like the Optotrack) would represent interesting extensions. Also, one could imagine a video projection system either of stationary images projected via mirror galvanometers or using dynamical visual stimuli (like those generated by the Cambridge Visual Stimulator) for background images or the presentation of complex objects. The limits of extensions are those of the user's imagination.

### ***3.3. Suggestions to improve the set-up***

Of course, the EyeLab set-up can be improved in multiple ways. The possible extensions described above represent one possible way to do so. In order to get the most precise synchronization with external devices, a dedicated digital input/output data acquisition board would be necessary. This would also allow a precise synchronization of the digital lines with the analog signals.

Several external devices need to be “master” of the experiment. Thus, to allow synchronisation with all external devices, the “slave” mode has to be integrated into the EyeLab program. This can be achieved simply by including a waiting function into the data acquisition loop that starts recording once an external TTL signals changes polarity. The same signal could also be used to stop the loop and thus to end the trial.

To enhance the current performances – note that these are the best possible – the PXI hardware should be updated. Indeed, a faster execution of the data acquisition drivers would allow higher sampling rates and the acquisition of longer trials. Therefore, the PXI controller (not the whole PXI computer) should be replaced by a more powerful machine on the top of that, I would strongly recommend a software update of the LabViewRT software package, since in recent versions the hardware control drivers have been significantly reviewed and were announced to be up to 90% faster.

Today, the EyeLab program always uses its closed loop architecture to perform data acquisition. However, in many experiments closed loop control is not necessary. Therefore, a continuous data acquisition

mode could easily be implemented into the actual code. The closed loop mode could then be used automatically, only if the protocol required this feature. For the rest of the time, the operator could take advantage of open-loop recording. Indeed, open-loop data acquisitions can be performed continuously with the advantage of higher sampling frequencies, longer trials and continuous visualization of the acquired data.

## APPENDIX II

### STATISTICS

#### 1. Notations

Consider sample  $X$ , of size  $N_x$ . Individual data of this sample are denoted  $x_i$ . Follow some fundamental measures:

Population mean  $\mu_x = \frac{1}{N_x} \sum x_i$

Population variance  $s_x = \frac{1}{N_x} \sum (x_i - \mu_x)^2$

Population standard deviation  $\sigma_x = \sqrt{s_x}$

To estimate the variance  $s_x$ ' and standard deviation  $\sigma_x$ ' of a *sample* (not for the whole population), use  $(N_x-1)$  instead of  $N_x$ .

Population standard error  $SE_x = \frac{\sigma_x}{\sqrt{N_x}}$

In the following sections, I will shortly lay out some important statistical tests and data analysis methods that were used in the framework of this thesis. More information about these and other statistical methods can be found in the references cited.

## 2. One variable, two samples statistical tests

### 2.1. Difference between means of two samples

#### 2.1.1. Normally distributed samples (parametric tests) for $s_x^2 = s_y^2$

First, we have to test whether the two variances of two independent normally distributed (to test for normal distribution, see section 3.1) samples  $X$  and  $Y$  are equal (see section 2.2.1). Afterwards, we can test the null hypothesis  $H_0: \mu_x = \mu_y$ .

In this case and if the population parameters are unknown (they have to be estimated from sample statistics) we can use the two-sample Student t-test (Ractliffe 1972). The test statistic  $t$  is defined as follows:

$$t_{obs} = \frac{\mu_x - \mu_y}{s' \cdot \sqrt{\frac{1}{N_x} + \frac{1}{N_y}}},$$

where  $s' = \frac{(N_x - 1) \cdot s_x^2 + (N_y - 1) \cdot s_y^2}{N_x + N_y - 2}$  is the pooled variance of

the two samples (not the population variance!).

Under the null hypothesis  $H_0$ , this test statistic has a  $t$ -distribution with  $(N_x + N_y - 2)$  degrees of freedom. The test  $H_0$  is carried out against one of three possible alternatives:

- $H_1: \mu_x \neq \mu_y$ : the significance level  $p = P(t \geq |t_{obs}|)$  is a two-tailed probability.
- $H_1: \mu_x > \mu_y$ : the significance level  $p = P(t \geq t_{obs})$  is an upper tail probability.
- $H_1: \mu_x < \mu_y$ : the significance level  $p = P(t \leq t_{obs})$  is a lower tail probability.

Upper and lower  $100 \cdot (1 - \alpha)\%$  confidence limits for  $\mu_x - \mu_y$  are calculated as:

$$(\mu_x - \mu_y) \pm t_{1-\alpha/2} \cdot s' \cdot \sqrt{\frac{1}{N_x} + \frac{1}{N_y}},$$

where  $t_{1-\alpha/2}$  is the  $100 \cdot (1 - \alpha)$  percentage of the  $t$ -distribution with  $(N_x + N_y - 2)$  degrees of freedom.

The  $t$ -test is quite robust to the assumption of normality and equality of variances. This means that even with some deviation from those assumptions, the  $t$ -test will retain much of its power. This is especially true if the sample sizes are nearly equal, and the larger the sample size the more robust is the test. If the variances are too different, a modified  $t$ -test can be used (see below).

*Note: In Matlab, use the `tinvm` function to obtain the  $p$ -value for the Student  $t$ -distribution and for an observation  $t_{obs}$  or use the `ttest2.m` function for a direct comparison of two means whether or not the variances are equal (see below).*

### 2.1.2. Normally distributed samples (parametric tests) for $s_x' \neq s_y'$

If the sample variances are not equal, the usual two-sample  $t$ -statistic no longer has a  $t$ -distribution and an approximate test has to be used. This problem is often referred to as the Behrens-Fischer problem (Scheffé 1970). Here we will describe the so-called Satterthwaite's procedure (Satterthwaite 1946). The test of the null hypothesis  $H_0$  is carried out against one of the three alternative hypotheses described above. The real statistic is approximated by a  $t$ -statistic with  $f$  degrees of freedom, where

$$t_{obs} = \frac{\mu_x - \mu_y}{\sqrt{\frac{s_x'}{N_x} + \frac{s_y'}{N_y}}}$$

$$\text{and } f = \frac{\left(\frac{s_x'}{N_x} + \frac{s_y'}{N_y}\right)^2}{\frac{s_x'}{N_x^2 \cdot (N_x - 1)} + \frac{s_y'}{N_y^2 \cdot (N_y - 1)}}$$

Upper and lower  $100 \cdot (1 - \alpha)\%$  confidence limits for  $\mu_x - \mu_y$  are calculated as:

$$(\mu_x - \mu_y) \pm t_{1-\alpha/2} \cdot \sqrt{\frac{s_x'}{N_x} + \frac{s_y'}{N_y}}$$

where  $t_{1-\alpha/2}$  is the  $100 \cdot (1 - \alpha)$  percentage of the  $t$ -distribution with  $f$  degrees of freedom. The same decision rules as for the case of equal variances apply.

### 2.1.3. *Arbitrarily distributed samples (non-parametric tests)*

While the  $t$ -test is quite robust, a far deviation from normality of the samples makes the test perform poorly. Sometimes, coding or transforming the data may produce a normal distribution, but we will not consider this option here. Instead, a non-parametric alternative of the  $t$ -test exists. This test is called the Mann-Whitney U-test (Siegel 1956) and does not have any assumptions about the nature of the underlying distributions (normality of equality of variances). In general, the Mann-Whitney U-test is more powerful when the assumptions of a  $t$ -test are not met and a  $t$ -test is more powerful when the assumptions are met. One would want to choose the test that has the highest power, i.e. the greatest ability to reject a false null hypothesis.

The Mann-Whitney U-test uses the rank of measurements and not the original measurements. Therefore, the test hypotheses do not make any statement about the sample means. Thus, the test hypotheses for the comparison of two independent samples  $X$  and  $Y$  are simply:

- $H_0$ :  $X$  and  $Y$  have the same distribution *or* there is no significant difference between the samples.
- $H_1$ :  $X$  and  $Y$  are different

As already mentioned, the statistic is based on the ranks of the original data for both samples  $X$  and  $Y$  together. Therefore,  $X$  and  $Y$  are merged into a new variable  $Z$  of size  $N_z = (N_x + N_y)$  and  $Z$  is then arranged in increasing order. Each value of  $Z$  is attributed an increasing rank value

$r_z = 1..N_z$ . but the origin of each value is maintained (whether  $z_i = x_i$  or  $y_i$ ).  
For the  $U$ -statistics, we need to calculate:

$$U_{x,obs} = N_x \cdot N_y + \frac{N_x \cdot (N_x - 1)}{2} - R_x \text{ and } U_{y,obs} \text{ in analogy.}$$

with the rank sums  $R_x = \sum_{z_i=x_i} r_z$  and  $R_y$  in analogy.

For small sample sizes ( $\max(N_1, N_2) < 20$ ) the tables of the  $U$ -statistics need to be used. For larger sample sizes ( $\max(N_1, N_2) \geq 20$ ), one can estimate the critical value of  $U$  with the  $Z$  normal distribution (or the Student t-distribution with  $\infty$  degrees of freedom):

$$Z_{obs} = \frac{\min(U_{x,obs}, U_{y,obs}) - \bar{U}}{s_U},$$

$$\text{where } \bar{U} = \frac{N_x \cdot N_y}{2} \text{ and } s_U = \sqrt{\frac{N_x \cdot N_y \cdot (N_x + N_y + 1)}{12}}$$

One has to reject the null hypothesis of identical samples if the statistics is significant. If the samples are not independent, use the sign test or the Wilcoxon matched pairs test for dependent samples (Kraft and van Eeden 1968; Siegel 1956).

*Alternatives:* Wald-Wolfowitz runs test, Kolmogorov-Smirnov two-sample test (Siegel 1956)

*Note:* In Matlab, use the `norminv.m` function to obtain the  $p$ -value for the Normal  $Z$ -distribution and for an observation  $Z_{obs}$ .

## 2.2. Difference between variances of two samples

### 2.2.1. Normally distributed samples (parametric tests)

To test the equality of the variances of two independently normally distributed samples  $X$  and  $Y$  of a variable one has to perform a Fisher  $F$ -test (Kraft and van Eeden 1968; Miller 1986; Ractliffe 1972; Siegel 1956) with  $f_x$  and  $f_y$  degrees of freedom. The decision ratio for the  $F$ -statistic is calculated as follows:

$$F_{obs} = \frac{s_x'}{s_y'}$$

with  $f_x = N_x - 1$  and  $f_y = N_y - 1$  degrees of freedom. The two-sided hypotheses for the test are:

- $H_0: s_x' = s_y'$ : the variances of the two samples are equal.  
 $p = P(|F| \geq |F_{obs}|)$
- $H_1: s_x' \neq s_y'$ : the variances of the two samples differ.  
 $p = P(|F| \leq |F_{obs}|)$

*Note: In Matlab, use the `finv.m` function to obtain the p-value for the Fisher F-distribution and for an observation  $F_{obs}$ .*

### 2.2.2. Arbitrarily distributed samples (non-parametric tests)

Similarly to the Mann-Whitney U-test for the comparison of two independent samples, one can design a one-way analysis of variance test for non-parametric distributions of continuous variables (equivalent to the Fisher F-test). This test is called the Kruskal-Wallis test (Kraft and van Eeden 1968; Siegel 1956) and performs an analysis of variance by ranks on 2 or more ( $k$ ) samples. Thus, the null hypothesis of the Kruskal-Wallis test is that all  $k$  samples have an identical population distribution. Therefore, we need to compute the decision variable  $H$  that is  $\chi^2$  distributed with  $k-1$  degrees of freedom.

$$H_{obs} = \frac{\frac{12}{N \cdot (N+1)} \cdot \sum \frac{R_k^2}{N_k} - 3 \cdot (N+1)}{1 - \frac{\sum (T_k^3 - T_k)}{N^3 - N}}$$

where  $N$  is the total number of all measures from all samples,  $R_k$  is the sum of the individual ranks for sample  $k$  of size  $N_k$ , and  $T_k$  are the number of ties (= the number of *different* ranks) in the  $k^{\text{th}}$  sample. One has to reject the null hypothesis of identical population distributions if the statistics is significant.

*Alternative: Median test (Kraft and van Eeden 1968; Siegel 1956)*

---

If the samples are not from independent variables, use the Friedman two-way analysis of variance method or the Cochran Q test (if the variable was measured in terms of categories) (Siegel 1956).

### 2.2.3. *Standard error, confidence interval and statistical significance*

One is tempted to draw conclusions about the statistical significance of differences between group means by looking at whether the error bars overlap. But what conclusions are true? Here are some rules if the means are unpaired, i.e. from independent samples (unless differently mentioned):

- Standard error (*SE*) bars do not overlap: in this case one cannot be sure that the difference between two means is statistically significant. This is also true when comparing proportions with a  $\chi^2$  test.
- Standard error (*SE*) bars overlap: here, we can be sure that the difference between means is not statistically significant ( $p > 0.05$ ).
- 95 % confidence intervals do not overlap: 95 % confidence intervals are approximately 1.96 times larger than standard errors. Thus, when 95 % confidence intervals do not overlap, one can be sure that the difference between means is statistically significant ( $p < 0.05$ ). However, the converse is not true, i.e. one may or may not have statistical significance when 95 % confidence intervals overlap.
- If a 95 % confidence interval of the difference between two means does not include zero, the difference is statistically significant ( $p < 0.05$ ). If the 95 % confidence does include zero, then the p-value is higher than 0.05 and thus the difference between means is not statistically significant. This is true for paired and unpaired t-tests.

### 3. Probability distribution tests

#### 3.1. Normality tests

Several procedures exist to test for the normality of a distribution (Hald 1967; Kraft and van Eeden 1968; Ractliffe 1972; Siegel 1956; Snedecor and Cochran 1973). Besides the Kolmogorov-Smirnov two-sample test (see section 3.2) that works for any distribution with known parameters, there are four main tests specifically for normal distribution. Classically, the  $\chi^2$  goodness of fit test is used (which is also a general test for any distribution). However, it is not very powerful and should be coupled with a skewness and kurtosis analysis, i.e. the third and fourth moment of the mean (Snedecor and Cochran 1973). The Lilliefors' normality test uses the Kolmogorov-Smirnov procedure, but the statistics are adapted to account for unknown mean and standard deviation of the data. Both the Kolmogorov-Smirnov and the Lilliefors' tests for normality are based on the maximum difference between the hypothesized cumulative distribution function and the data. A more powerful alternative is the Shapiro-Wilks W-test, but only for data sets with  $N < 2000$ . For large samples, the Jarque-Bera test provides best results. The Jarque-Bera test for normality is based on the sample skewness and kurtosis. The Jarque-Bera test determines if skewness and kurtosis are unexpectedly different (alternative hypothesis) from expected values (null hypothesis), as measured by the  $\chi^2$ -statistics. In all these test, one can reject the null hypothesis of normally distributed data if the statistics is significant.

##### 3.1.1. The Shapiro-Wilks W-test for normality

The Shapiro-Wilks W-test is thought to be the best test for normality for sample sizes ranging between 3 and 2,000. The decision parameter is given by:

$$W_{obs} = \frac{(\sum a_i x_{(i)})^2}{\sum (x_i - \mu)^2},$$

where  $x_{(i)}$  is the  $i$ -th element of the ranked data and  $a_i$  is a tabulated parameter.

### 3.1.2. The Jarque-Bera test for normality

The Jarque-Bera test for large sample sizes is based on a measure of skewness and kurtosis of the data. The decision variable is given by:

$$\chi_{obs} = N \cdot \left( \frac{\tau^2}{6} + \frac{(\kappa - 3)^2}{24} \right)$$

where  $\tau = \frac{\mu_3}{\sigma^3}$  is the coefficient of skewness and  $\kappa = \frac{\mu_4}{\sigma^4}$  is the coefficient of kurtosis, with the higher order moments

$$\mu_k = \frac{1}{N} \sum_i (x_i - \mu)^k.$$

$\chi_{obs}$  is approximately  $\chi^2$  distributed with 2 degrees of freedom. Note that in a normally distributed sample,  $\tau = 0$  and  $\kappa = 3$ . If  $\chi_{obs}$  exceeds the critical value of the  $\chi^2$ -statistic, then we can reject the null hypothesis of normality.

### 3.1.3. Lilliefore's normality test

This test is based on the Kolmogorov-Smirnov two-sample test of distribution comparison using an adapted test statistics. See section 3.2.2. for more details.

*Note: In Matlab, use the `lillitest.m` function to perform the Lilliefore's normality test and use the `jbtest.m` function for the Jarque-Bera test. Unfortunately, the Shapiro-Wilks *W*-test is not implemented in Matlab, but can be found in Statistica.*

## 3.2. Other distributions test

To our knowledge, only two statistical methods to test for an arbitrary distribution exist, i.e. the  $\chi^2$  goodness of fit test the Kolmogorov-Smirnov two-sample test (Kraft and van Eeden 1968; Siegel 1956).

### 3.2.1. The $\chi^2$ goodness of fit test

This test can be applied to any univariate distribution. Data are grouped in bins  $i$  to obtain a table of observed frequencies  $f_{o,i}$ . These are compared to the expected frequencies  $f_{e,i}$  to form the following criterion:

$$\chi_{obs} = \sum_i \frac{(f_{o,i} - f_{e,i})^2}{f_{e,i}}$$

where  $f_{e,i} = N \cdot (F(y_u) - F(y_l))$  is the expected frequency of a tested cumulative distribution function  $F$  and  $y_u$  and  $y_l$  are the upper and lower limits for bin  $i$ . The frequencies in each bin should be greater than 5. Otherwise, one needs to combine bins in the tails of the distribution.

$\chi_{obs}$  is approximately  $\chi^2$  distributed with  $k-c$  degrees of freedom, where  $k$  is the number of non-empty bins and  $c$  is the number of estimated parameters in the distribution + 1. Large values of  $\chi_{obs}$  will cause the rejection of the hypothesis of equal distributions. Unfortunately, the value of the  $\chi^2$  statistic depends on how the data is binned. Furthermore, the  $\chi^2$  test requires a sufficient sample size in order for the  $\chi^2$  approximation to be valid. (Snedecor and Cochran 1973)

### 3.2.2. The Kolmogorov-Smirnov test

The Kolmogorov-Smirnov test evaluates the maximal difference between a theoretical cumulative probability density function and the measured data (Kraft and van Eeden 1968) as follows:

$$KS_{obs} = N \cdot \sup_i |F_{o,i}(t) - F_{e,i}(t)|$$

where  $F_{o,i}$  and  $F_{e,i}$  are the observed and expected values of the cumulative distribution functions.  $KS_{obs}$  follows the Kolmogorov-Smirnov one-sample distribution. If one needs to compare two samples,  $F_{e,i}$  is replaced by the observed cumulative distribution function of the second sample and  $KS_{obs}$  follows the Kolmogorov-Smirnov two-sample distribution. The null hypothesis of equal distribution functions is accepted if  $KS_{obs}$  is larger than the KS-statistics.

*Alternative:* Anderson-Darling modification of the Kolmogorov-Smirnov test

*Note:* In Matlab use the `kstest.m` or `kstest2.m` function for a Kolmogorov-Smirnov one- or two-sample test.

## 4. Linear regressions

Let  $Y$  and  $X$  be measured sets of variables with normally distributed elements  $y_i$  and  $x_i$ . (Hald 1967; Miller 1986; Ractliffe 1972; Snedecor and Cochran 1973)

### 4.1. Simple regression

#### 4.1.1. The regression line and significance of regression parameters

The parameters  $a$  and  $b$  of the regression  $Y = a + b \cdot X$  is obtained by minimizing the sum of squares between measured ( $y_i$ ) and predicted ( $y_{p,i}$ ) values of  $Y$  and results in:

$$b = \frac{\text{cov}(X, Y)}{\text{var}(X)} \quad \text{and} \quad a = \frac{1}{N} \cdot (\sum y_i - b \cdot \sum x_i)$$

To test whether the regression parameters  $a$  and  $b$  are significantly different from a desired value  $\alpha$  and  $\beta$ , the following decision variables may be computed (Hald 1967):

$$t_{obs,b} = \sqrt{N} \cdot \sigma_x' \cdot \frac{b - \beta}{\sigma'} \quad \text{and} \quad t_{obs,a} = \sqrt{N} \cdot \frac{a - \alpha}{\sigma'}$$

where  $\sigma' = \sqrt{\frac{SS_{res}}{N-2}}$  with the residual sum of squares

$$SS_{res} = \sum_i (y_i - y_{p,i})^2 \quad \text{and} \quad t_{obs,a} \quad \text{and} \quad t_{obs,b} \quad \text{have a Student } t\text{-distribution with}$$

$N-2$  degrees of freedom. The null hypothesis that the parameters  $a$  and  $b$  are significantly different from a desired value  $\alpha$  and  $\beta$  can be accepted if the  $t$ -statistics is significant.

#### 4.1.2. The correlation coefficient and its significance

The product-moment sample correlation coefficient  $R$  between  $X$  and  $Y$  writes (Snedecor and Cochran 1973):

$$R = \frac{\text{cov}(X, Y)}{\sqrt{\text{var}(X) \cdot \text{var}(Y)}}$$

$R$  is an approximation of the population correlation coefficient. If  $Y$  is normally distributed (but not necessarily  $X$ ), then we can test the significance of  $R$  using the following decision variable (Ractliffe 1972):

$$t_{obs} = \frac{R \cdot \sqrt{N-2}}{\sqrt{1-R^2}}$$

where  $t_{obs}$  has a Student  $t$ -distribution with  $N-2$  degrees of freedom.

However, the above-described computation of  $R$  is no more valid if the populations are far from being normally distributed. The best-known alternative to compute  $R$  is to calculate the rank correlation coefficient developed by Spearman  $R_S$ . If  $R_x$  and  $R_y$  are the ranks corresponding to the individual values of  $X$  and  $Y$ , then  $R$  is computed as follows:

$$R_S = 1 - \frac{6 \cdot \sum (R_{y,i} - R_{x,i})^2}{N \cdot (N^2 - 1)}$$

To test the significance of the Spearman rank correlation coefficient  $R_S$  one performs a standard Student  $t$ -test (see above).

#### 4.1.3. Confidence limits around a predicted value of $Y$

The result of the above-described regression predicts an average value of  $Y$  for any given value of  $X$ . However, the individual values of  $Y$  will be scattered on either side of it. Therefore, one can define confidence limits of the predicted values of  $Y$  as follows:

$$Y_{conf} = a + b \cdot X \pm t_{1-\alpha/2} \cdot \sigma'$$

where  $t_{1-\alpha/2}$  is the  $100 \cdot (1 - \alpha)$  percentage of the  $t$ -distribution with  $(N-2)$  degrees of freedom.

## 4.2. 2<sup>nd</sup> order and multiple regression

### 4.2.1. 2<sup>nd</sup> order and multiple regression parameters

To obtain the parameters  $a$ ,  $b_1$  and  $b_2$  of  $Y = a + b_1 \cdot X_1 + b_2 \cdot X_2$ , one needs to compute the following expressions:

$$b_1 = \frac{\text{var}(X_2) \cdot \text{cov}(X_1, Y) - \text{cov}(X_1, X_2) \cdot \text{cov}(X_2, Y)}{D}$$

$$b_2 = \frac{\text{var}(X_1) \cdot \text{cov}(X_2, Y) - \text{cov}(X_1, X_2) \cdot \text{cov}(X_1, Y)}{D}$$

$$D = \text{var}(X_1) \cdot \text{var}(X_2) - \text{cov}(X_1, X_2)^2$$

$$a = \mu_Y - b_1 \cdot \mu_{X_1} - b_2 \cdot \mu_{X_2}$$

This procedure can be generalized to multiple regressions with more than two independent variables (Miller 1986). If the regression writes  $Y = a + \sum_{i=1}^k b_i \cdot X_i$ , then the regression parameters are obtained in the following way:

$$b_i = \underline{\underline{R}}_{ii}^{-1} \cdot \underline{R}_i \cdot \frac{\sigma_Y'}{\sigma_i'}$$

$$a = \mu_Y - \sum b_i \cdot \mu_{X_i}$$

where  $\underline{\underline{R}}_{ii}$  is the matrix of correlation coefficients between variables  $X_i$  and  $\underline{R}_i$  is the vector of correlation coefficients between  $Y$  and  $X_i$ .

#### 4.2.2. The multiple correlation coefficient

The overall correlation coefficient writes:

$$R = \frac{\text{cov}(Y, Y_p)}{\sqrt{\text{var}(Y) \cdot \text{var}(Y_p)}}, \text{ where } Y_p \text{ is the value of } Y \text{ predicted by}$$

the regression equation. To test the significance of  $R$ , one can apply the above-described t-test or alternatively use a F-test with observation variable:

$$F_{obs} = \frac{N - k - 1}{k} \cdot \frac{R^2}{1 - R^2},$$

with  $k$  and  $N-k-1$  degrees of freedom and where  $k$  is the number of independent regression variables ( $k=2$  for the 2<sup>nd</sup> order regression). For

large  $F_{obs}$ , the null hypothesis that all  $k$  regression parameters  $b_i = 0$  can be rejected.

### 4.2.3. Partial correlation coefficients

The partial (or conditional) correlation coefficient describes the contribution of one variable to  $Y$  after elimination of the second variable. Thus, the partial correlation of  $X_1$  on  $Y$  after removal of the influence of  $X_2$  writes:

$$R_{X_1Y \cdot X_2} = \frac{R_{X_1Y} - R_{X_1X_2} \cdot R_{X_2Y}}{\sqrt{(1 - R_{X_1X_2}^2) \cdot (1 - R_{X_2Y}^2)}}, \text{ where } R_{ij} \text{ denote the first}$$

order regression coefficient between variable  $i$  and  $j$ . The significance test of partial correlation coefficients is performed similarly to the significance test of first order regression coefficients (Student t-test), but with  $N-3$  degrees of freedom. Alternatively, the above-described F-test can be used.

The computation of the partial correlation coefficient can be generalized to the case of higher order multiple regressions. The partial correlation of variable  $X_i$  writes:

$$R_{P,i} = \frac{R_{SP,i}}{\sqrt{1 - R_{Y-i}^2}},$$

where  $R_{Y-i}^2$  is the correlation coefficient between  $Y$  and all independent variables but  $X_i$  and with the semi-partial correlation coefficient  $R_{SP,i}^2 = R^2 - R_{Y-i}^2$  and where  $R$  is the correlation coefficient of the whole model.

When we need to compare the correlation coefficient  $R$  of two regressions, we have to perform a Fisher F-test to see if the increase in adjusted  $R^2$  ( $\bar{R}^2$ ) is significantly different from zero. Consider two sets  $A$  and  $B$  of  $k_A$  and  $k_B$  independent variables. To test whether the overall regression of the complete model (including variables  $A$  and  $B$ ) is significantly better than the regression of the reduced model (variables  $A$  only), compute the following observation variable:

$$F_{obs} = \frac{N - k_A - k_B - 1}{k_B} \cdot \frac{\bar{R}_{AB}^2 - \bar{R}_A^2}{1 - \bar{R}_{AB}^2},$$

where  $\bar{R}_{AB}^2$  and  $\bar{R}_A^2$  are the adjusted correlation coefficients of the complete and reduced models. The adjusted correlation coefficient takes into account the number  $k$  of independent regression variables  $X_i$  and writes:

$$\bar{R}^2 = 1 - (1 - R^2) \cdot \frac{N - 1}{N - k} = R^2 - (1 - R^2) \cdot \frac{k - 1}{N - k}$$

$F_{obs}$  has  $k_B$  and  $N - k_A - k_B - 1$  degrees of freedom. For large values of  $F_{obs}$  one can reject the hypothesis that the additional variable did not increase the correlation coefficient.

#### 4.2.4. Standard deviation of parameter estimates

The standard deviation of the parameter estimates  $b_i$  can be calculated by the following formula:

$$\sigma_{b_i}' = \frac{\sigma_Y'}{\sigma_i'} \cdot \sqrt{\frac{1 - R_Y^2}{(1 - R_i^2) \cdot (N - k - 1)}},$$

where  $\sigma_Y'$  is the standard deviation of  $Y$ ,  $\sigma_i'$  is the standard deviation of the independent variable  $X_i$  and  $R_Y^2$  and  $R_i^2$  are the regression coefficient of  $Y$  with all variables and the regression coefficient of  $X_i$  with all other independent variables respectively.

### 4.3. Identical regressions

#### 4.3.1. Comparison of simple regression parameters

To test whether two regression parameters are identical, one needs first to test the hypothesis of equal variances (F-test) for  $Y_{1,2}$ .

If the variances are equal, the statistics write as:

$$t_{obs} = \frac{b_1 - b_2}{\sigma' \cdot \sqrt{\frac{1}{s_{x_1}'} + \frac{1}{s_{x_2}'}}}$$

with the pooled estimate of the variance  $\sigma' = \frac{(N_1 - 2) \cdot \sigma_{y_1}' + (N_2 - 2) \cdot \sigma_{y_2}'}{N_1 + N_2 - k_1 - k_2 - 2}$ . The decision variable  $t_{obs}$  follows a

Fisher  $t$ -distribution with  $N_1 + N_2 - k_1 - k_2 - 2$  degrees of freedom. If the bilateral  $t$ -statistics is significant, then the null hypothesis of equal regression slopes have to be rejected.

If the variances differ significantly, then the decision variable writes as:

$$t_{obs} = \frac{b_1 - b_2}{\sqrt{\frac{s_{y_1}'}{s_{x_1}'} + \frac{s_{y_2}'}{s_{x_2}'}}}}$$

$t_{obs}$  follows a Fisher  $t$ -distribution with  $f$  degrees of freedom, where

$$\frac{1}{f} = \frac{c^2}{N_1 - k_1 - 1} + \frac{(1 - c^2)}{N_2 - k_2 - 1}, \text{ with } c = \frac{\frac{s_{y_1}'}{s_{x_1}'}}{\frac{s_{y_1}'}{s_{x_1}'} + \frac{s_{y_2}'}{s_{x_2}'}}$$

#### 4.3.2. Comparison of two regression points

In order to test the equality of two regressions, one compares a test value  $x_0$  to the prediction of two models. For the comparison of two simple regressions 1 and 2, the test statistics writes:

$$t_{obs} = \frac{x_0 \cdot (b_2 - b_1) + (a_2 - a_1)}{\sqrt{s_{b_2}' \cdot (x_0 - \mu_{x_2})^2 + s_{b_1}' \cdot (x_0 - \mu_{x_1})^2}}$$

$t_{obs}$  is Student  $t$  distributed with  $N_1 + N_2 - 4$  degrees of freedom. This formula for the test statistics can easily be generalized for higher order regressions.

## 5. Non-linear regressions and curve fitting

It often happens that the relationship between dependent and independent variables is not linear. Here, we will shortly describe how non-

---

linear model can be estimated, what algorithms and loss functions are used and how to evaluate the goodness of a non-linear regression.

A non-linear fit of independent variables  $X_k$  on a dependent variable  $Y$  is performed by minimizing a so-called loss function that defines the goal to achieve. The most common loss functions are least squares, weighted least squares and maximum likelihood (or negative log-likelihood). As a standard method, the least squares method minimizes the sum of squared residuals (the residual sum of squares  $SSE$ ), as:

$$SSE = \sum_i (y_i - y_{p,i})^2,$$

which is the sum of squared deviations of the observed values  $y_i$  for the dependent variable from those  $y_{p,i}$  predicted by the model. Algorithmically, this minimization is most efficiently implemented by the so-called Levenberg-Marquardt process.

In order to get an idea of the goodness-of-fit, we can compute the proportion of variance accounted for  $R^2$  – as this is done in the linear case:

$$R^2 = \frac{SSR}{SST} = \frac{SST - SSE}{SST},$$

where  $SST$  is the total sum of squares of the dependent variable (= variance of  $Y$ ) and  $SSR$  is the variance of the predicted values of  $Y$ . Thus,  $R^2$  explains the proportion of variance accounted for in the dependent variable  $Y$  by the model. This is the same as for the linear regression. However, even if the dependent variable  $Y$  is not normally distributed across cases,  $R^2$  can be computed to evaluate how well the model fits the data. For more details, see Ractliffe (1972) or Snedecor and Cochran (1973).



## APPENDIX III

# DIRECT EVIDENCE OF A POSITION INPUT TO THE SMOOTH PURSUIT SYSTEM<sup>\*</sup>

*The beginning of knowledge is the discovery of  
something we do not understand.*

Frank Herbert

### 1. Abstract

When objects move in our environment, the orientation of the visual axis in space requires the coordination of two types of eye movements: saccades and smooth pursuit. The principal input to the saccadic system is position error, whereas it is velocity error for the smooth pursuit system. Recently, it has been shown that catch-up saccades to moving targets are triggered and programmed by using velocity error in addition to position error. Here, we demonstrate that when a visual target is flashed during smooth pursuit, it evokes a smooth eye movement towards the flash. The velocity of this smooth movement is proportional to the position error of the flash; it is neither influenced by the ongoing smooth pursuit eye velocity nor by the occurrence of a saccade. Furthermore, the response started around 85 ms after the flash presentation and decayed with a time constant close to the eye plant. Thus this is the first *direct* evidence of a position input to the smooth pursuit system. We suggest that the original protocol described here could be used in future electrophysiological experiments to investigate the neural substrate of this position input. The present study brings further evidence for a coupling between saccadic and smooth pursuit systems. It also suggests that there is an interaction between position and velocity error signals in the control of more complex movements.

---

<sup>\*</sup> The contents of this chapter has been submitted for publication to The Journal of Neurophysiology

## 2. Introduction

Primates use both smooth pursuit and saccadic eye movements to track a visual target. The main goal of saccades is the orientation of the eyes to foveate an object of interest, i.e. to overcome position error, while the smooth pursuit system aims to stabilize the image of a moving target on the retina, i.e. to overcome velocity error. In a natural tracking task, both oculomotor systems can work in synergy and there is a coupling between neural structures involved in the control of saccades and pursuit (Keller and Missal 2003; Krauzlis 2004; Krauzlis and Miles 1998; Krauzlis and Stone 1999; Missal et al. 2000; Missal and Keller 2002). Indeed, behavioral experiments have shown that the saccadic system uses velocity error to predict future target position, program and trigger catch-up saccades (de Brouwer et al. 2002a; de Brouwer et al. 2001). In addition, in the absence of retinal information about motion, the saccadic system has access to extraretinal movement information to compensate for smooth eye displacements (Blohm et al. 2003a; Blohm et al. 2003b). These recent results illustrate the coordination between the saccadic and smooth pursuit systems.

Classically, the smooth pursuit system is regarded as a closed-loop negative feedback system that transforms target motion into an eye movement (Lisberger et al. 1987; Robinson et al. 1986). However, several behavioral studies demonstrated that a small target jump during ongoing smooth pursuit modulates the eye velocity, contrarily to target steps during fixation (Carl and Gellman 1987; Morris and Lisberger 1987). In addition, when a target is stabilized for saccades but not for smooth eye movements, a sudden target jump induces large smooth eye movement responses (Segraves and Goldberg 1994; Wyatt and Pola 1981). Unfortunately, in both experimental conditions the target carried combined position and velocity information, which introduced the difficulty of isolating effects. Recently, it has been proposed that a neural position error signal in the rostral Superior Colliculus (SC) might be shared by different oculomotor subsystems, including smooth pursuit (Basso et al. 2000; Krauzlis et al. 2000, 1997). This suggests that the position input to the smooth pursuit system could be at the level of the SC (Krauzlis 2004).

Direct evidence for a position input to the smooth pursuit system is still lacking. This is due to the experimental difficulty of separating a

possible position input from the classical velocity input to the system. Here, we designed a new original paradigm where we briefly flashed (= position error without velocity information) a salient visual target during two-dimensional (2D) steady-state smooth eye movements. As a result, we found a consistent modulation of the smooth eye velocity that was proportional to position error (up to  $10^\circ$ ) and independent of both the initial smooth eye movement and the occurrence of saccades. These data demonstrate that there is a position error input to the smooth pursuit system.

### 3. Experimental procedures

Eight healthy human subjects (23-38 years, including 3 naïve) without any known oculomotor abnormalities were recruited after informed consent. All procedures were conducted with approval of the Université catholique de Louvain Ethics Committee, in compliance with the Helsinki declaration. Subjects sat in a completely dark room with their head restrained by a chin-rest and faced a 1-m distant tangent translucent screen. Two targets were presented. The first target was a  $1.5^\circ$  green pursuit target projected onto the screen by a Tektronix (Beaverton, OR, USA) 606A oscilloscope with custom optics. The second target was a  $0.2^\circ$  red LASER spot that was back-projected via M3-Series mirror galvanometers (GSI Lumonics, Billerica, LA, USA). Both targets were controlled using a dedicated computer running LabViewRT (National Instruments, Austin, TX, USA) software. Movements of one eye were recorded with the scleral coil technique, Skalar Medical BV, Delft, The Netherlands (Collewijn et al. 1975).

All recording sessions were composed of a series of blocks containing 40 trials each. Each trial started with the green target presented for 500 ms at  $20^\circ$  from the center of the screen in a randomly chosen direction (Fig. AIII-1). Afterwards, the target performed a step away from the center of the screen and moved at a random velocity ( $10$ - $40^\circ$ /s) toward the center of the screen (ramp). The size of the step was calculated in such a way that the target crossed the initial fixation point after 200 ms. At a random time interval of 500-1,500 ms after the ramp onset, a red target was briefly presented (10 ms flash). Its position was offset horizontally and vertically by a random value between  $-10^\circ$  and  $10^\circ$  from the current position of the ramp target. Meanwhile, the green pursuit target continued moving

until the end of the trial. All trials lasted for 3 s. Subjects were instructed to follow the green pursuit target and to orient their visual axis to the red flash target as soon as it appeared.

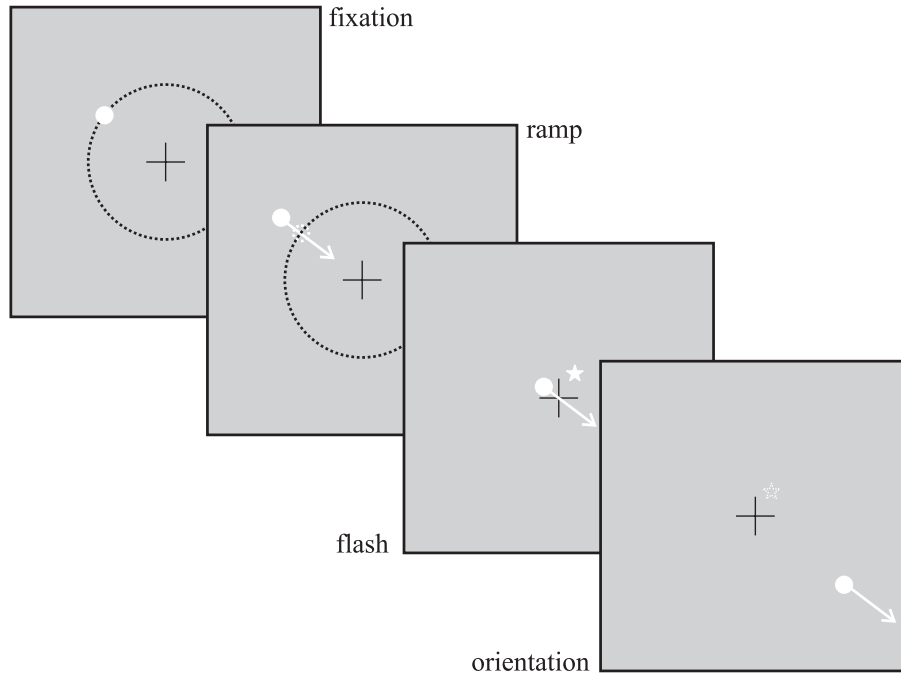


**Figure AIII-1: Protocol.** During the 500 ms initial *fixation* period, the green target (solid circle) was presented at 20° eccentricity from the straight-ahead direction (cross). The direction of the initial fixation target was randomly chosen in order for the target to lie on an invisible 20° circle (dotted). Afterwards, the green target (solid dot) performed a step away from the center of the screen (dotted circle indicates the initial fixation position) and moved at constant velocity back to the center of the screen (*ramp*). 500-1500 ms after the ramp movement onset, a red target was briefly presented (10 ms *flash*, solid star) at a random position inside a horizontal and vertical 20° window centered on the actual pursuit ramp position (solid dot). During the following *orientation* period, the green ramp target continued moving while subjects were asked to look at the memorized position of the flash (dotted star, invisible).

In separate recording sessions, we also presented control trials to 6 out of our 8 subjects. Control trials started with a green central fixation spot. Then, 500-1500 ms later, a red target was presented (10 ms flash) at a horizontally and vertically randomized position between -10° and 10°. After

the flash, the green fixation target remained illuminated for another 1,000 ms. Trials ended with a period of 500 ms in the dark. Subjects were instructed to orient their visual axis to the red flash target when it appeared.

Position signals of one eye and both targets were sampled at 500 Hz using NI-PXI-6025E data acquisition boards (National Instruments, Austin, TX, USA). Data were stored on the hard disk for off-line analysis with Matlab scripts (Mathworks Inc., Natick, MA, USA). Position signals were low-pass filtered using a zero-phase digital filter (autoregressive forward-backward filter; cutoff frequency: 50 Hz). Velocity and acceleration were derived from position signals using a central difference algorithm. We normalized our data with respect to the direction of the pursuit ramp. As a result, we obtained two different sets of parameters related to the smooth pursuit, i.e. those parallel to the normalized ramp direction, and those perpendicular to the normalized ramp direction. We analyzed in particular the perpendicular smooth eye velocity trace. Therefore, we removed all saccades from velocity traces. Saccades were detected using a  $500^\circ/\text{s}^2$  acceleration threshold. In order to remove saccades from velocity traces, we measured the smooth eye velocity 25 ms before and 25 ms after the saccade and interpolated linearly between those values to obtain an estimation of the smooth eye velocity during saccades (de Brouwer et al. 2002a). We chose the 25 ms security margin to be sure that there was no influence of the saccade on the estimated smooth eye velocity. As a result, we obtained the perpendicular smooth eye velocity trace  $EV_{s\perp}$ .

## 4. Results

### 4.1. *General response properties*

We collected a total of 4,675 valid test trials out of which 154 were completely smooth trials, where no saccade was detected until 1,000 ms after the flash occurrence. Figure AIII-2 shows one complete trial (panels A, B and C) and zooms of the region of interest for three typical trials (panels D, E: saccade trials; panel F: smooth trial).

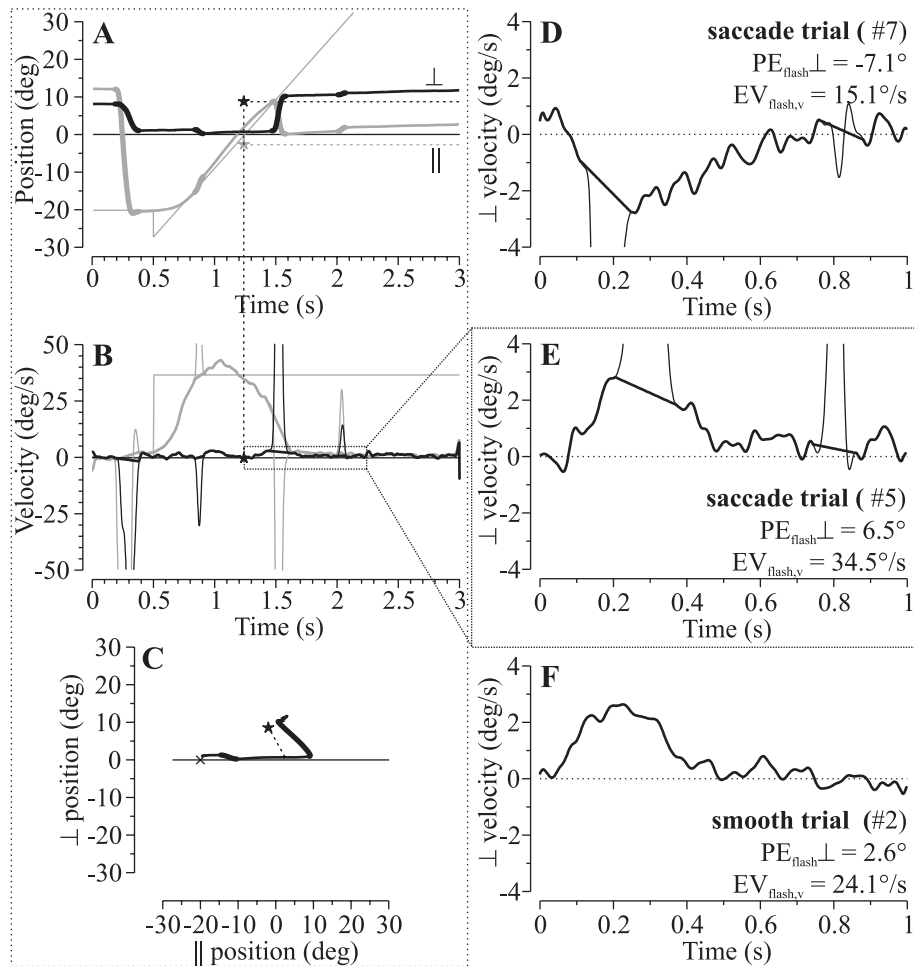


**Figure AIII-2:** Typical trials. The left column represents a typical trial; the right column is a zoom on the perpendicular eye velocity of three different trials. **A.** Eye (solid lines; bold lines: saccades) and target (thin lines) positions parallel (grey) and perpendicular (black) to the initial ramp direction. The star and horizontal dotted lines indicate the flash position. **B.** Eye and target velocity. Here, saccades are represented by thin lines. The solid line is the smooth eye velocity. A zoom of the perpendicular part of the smooth eye velocity is represented in panel E. **C.** Spatial representation of the trial (starting from 500 ms until the end). The dotted line between the star (flash) and the eye position trace indicates the position error at the moment of the flash. **D, E, F.** Perpendicular eye velocities for two saccade trials and one smooth trial respectively. Solid lines are without saccades, thin lines represent saccades. Time zero corresponds to the onset of the flash.

The complete trial represented in Fig. AIII-2A, B and C has been rotated to normalize the direction of the ramp movement. Panel E of Fig. AIII-2 is a zoom of the region of interest from the complete trial presented in panels A, B and C of Fig. AIII-2. For the zooms on the region of interest in Fig. AIII-2D, E and F only the perpendicular component of the eye velocity is shown, from the flash onset until 1,000 ms after the flash onset. One can observe that there was a modulation of the perpendicular smooth eye velocity  $EV_{s\perp}$  in the direction of the flashed target.

Note that  $EV_{s\perp}$  was relatively small compared to the range of smooth pursuit velocities (10-40°/s), but it was much larger than the mean  $EV_{s\perp}$  noise level during ramp pursuit, i.e. before the flash onset (S.D. = 0.371°/s). Furthermore, the tracking performance was very good. To test this, we measured the perpendicular eye velocity as well as the perpendicular position error with respect to the pursuit target at the moment of the flash onset. Both measures showed little variability and were constant and close to zero for the whole range of perpendicular flash eccentricities tested below.

Throughout the analysis, we used the perpendicular response because the parallel smooth eye movement was rapidly changing due to the decay of smooth pursuit in the subject's attempt to fixate the memorized position of the flash.

#### ***4.2. Influence of flash position on smooth eye velocity***

In order to describe the global behavior of  $EV_{s\perp}$ , all data were aligned on flash onset. Figure AIII-3A shows average  $EV_{s\perp}$  traces for different bins of the perpendicular position errors  $PE_{\text{flash}\perp}$  at the moment of the flash (all parallel position errors and subjects were pooled). The number of trials in each bin varied from 379 to 482. Positive  $PE_{\text{flash}\perp}$  values stand for flashes presented in a counter-clockwise position relative to the pursuit ramp direction; negative  $PE_{\text{flash}\perp}$  values were clockwise flashes. We observed a consistent gradual modulation of the mean  $EV_{s\perp}$  by  $PE_{\text{flash}\perp}$ . This effect clearly increased with increasing position error. Furthermore, we found very similar shapes for the mean  $EV_{s\perp}$  for all bins of  $PE_{\text{flash}\perp}$ . It is important to emphasize that the observed  $EV_{s\perp}$  modulation is not caused by the occurrence of a saccade. This is illustrated in Fig. AIII-3B by a comparison of 4 different data subsets, i.e. trials with a first saccade occurring before

200 ms after the flash onset (dashed black line,  $N = 2,335$ ), trials with first saccade latency  $> 200$  ms (solid black line,  $N = 2,186$ ) and trials where no saccade at all was triggered (smooth trials, dashed gray line,  $N = 154$ ). These have to be compared with control trials, where no pursuit target was presented (solid gray line,  $N = 1553$ ).

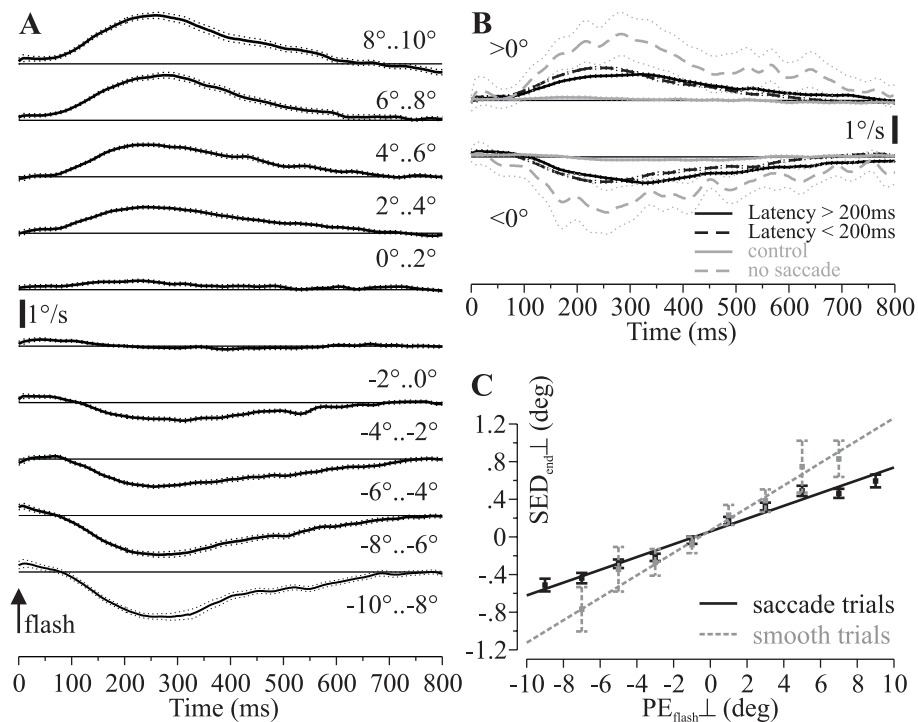


**Figure AIII-3: Average responses for all trials.** **A.** Mean perpendicular smooth eye velocities (mean  $EV_{s\perp}$ ) for different bins of perpendicular position error at the moment of the flash  $PE_{flash\perp}$  aligned on the flash onset (0 ms). Values at the right end of the traces indicate the bin sizes of  $PE_{flash\perp}$ . **B.** Comparison of mean  $EV_{s\perp}$  for trials with early 1<sup>st</sup> saccades (latency  $< 200$  ms, dashed black line), trials with later 1<sup>st</sup> saccades (latency  $> 200$  ms, solid black line), control trials (solid gray line) and smooth trials without any saccade after the flash (dashed gray line). Data were pooled for all positive and negative  $PE_{flash\perp}$  values independently. Solid / dashed and dotted lines in panel A and B indicate mean and standard error. **C.** Influence of flash position on evoked SEM. Effect of the perpendicular position error at the moment of the flash  $PE_{flash\perp}$  on the magnitude of the perpendicular smooth eye velocity  $EV_{s\perp}$  modulation. The total perpendicular smooth eye displacement  $SED_{end\perp}$  was used as an indicator for the effect. Saccade trials (black) and smooth trials (gray) are shown separately. Solid (saccade trials) and dotted (smooth trials) straight lines are linear regressions on raw data. Squares and whiskers indicate the mean and standard error.

Figure AIII-3B shows that  $EV_{s\perp}$  modulation is even larger for smooth trials compared to saccade trials. For the data shown here, we interpolated the individual perpendicular eye velocity traces from 25 ms before until 25 ms after the detected saccade and also performed the same analysis with 50 ms. All results were quantitatively the same (data not shown). This shows that the observed phenomena cannot be explained by the removal of saccades.

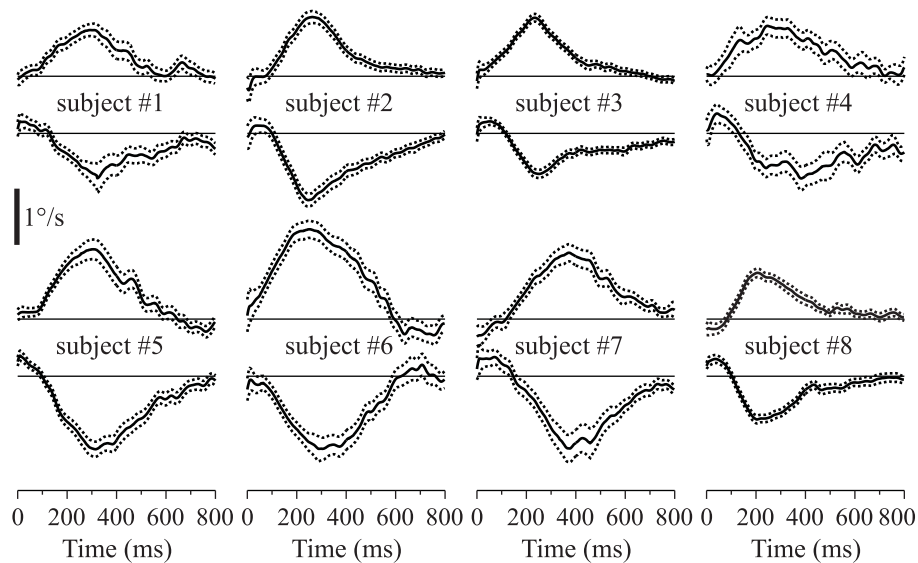


**Figure AIII-4: Individual mean response for each subject.** Mean perpendicular smooth eye velocities (mean  $EV_{s\perp}$ ) are represented for all eight subjects individually. Data were pooled for all positive and negative  $PE_{flash\perp}$  values independently. Solid and dotted lines indicate mean and standard error.

To quantify the  $EV_{s\perp}$  modulation, we measured the total perpendicular smooth eye displacement  $SED_{end\perp}$  (= integral of  $EV_{s\perp}$  from the flash onset to 1,000 ms after the flash onset) in Fig. AIII-3C.  $SED_{end\perp}$  is a good measure of the smooth response to the flash and is less sensitive to noise than the peak  $EV_{s\perp}$ . Data were presented separately for saccade and smooth trials. There was a tight dependence of  $SED_{end\perp}$  on  $PE_{flash\perp}$ . The regressions were performed on raw data and the regression lines had slopes of 0.066 ( $p < 0.001$ ,  $N = 4,521$ ) and 0.115 ( $p < 0.001$ ,  $N = 154$ ) for saccade and smooth trials respectively. This analysis consolidated the finding that the

mean  $EV_{s\perp}$  was strongly modulated by  $PE_{flash\perp}$  and showed that  $SED_{end\perp}$  increased linearly with  $PE_{flash\perp}$ . The fact that the regression slope is lower for saccade trials could be due to the linear interpolation of eye velocity that tends to underestimate the smooth eye velocity (conservative measure).

Individual responses to this type of experimental task are variable. Therefore, we provide in Fig. AIII-4 data pooled individually for each subject. Note that, for all subjects, the range and distribution of  $PE_{flash\perp}$  was approximately the same. Although one can observe some variability between subjects, the basic shape was very similar. However, the amplitude of the response largely varied (double in subject #6 compared to subject #3).

### 4.3. *Characterization of movement onset and offset*

An interesting aspect of the mean  $EV_{s\perp}$  response seems to be its onset latency. Indeed, Fig. AIII-3 and 4 show a consistent, relatively short ( $\sim 100$  ms) response latency throughout all  $PE_{flash\perp}$  values. We computed the mean latency for the smooth  $EV_{s\perp}$  response onset time. Therefore, we used an acceleration threshold criterion of  $5^\circ/s^2$ . This analysis could not be performed directly on each individual  $EV_{s\perp}$  trace, because acceleration signals were too noisy (specifically for small  $PE_{flash\perp}$ ).

Thus, we used a k-fold sub-sampling method. This consisted of performing the acceleration threshold analysis  $k = 10,000$  times on the mean smooth eye acceleration  $EA_{s\perp}$  trace, computed by taking at each iteration randomly  $1/100^{\text{th}}$  of the total data set. Here, the mean  $EA_{s\perp}$  was the first order derivative (3-point central difference algorithm) of the mean  $EV_{s\perp}$ . Once  $EA_{s\perp}$  exceeded  $5^\circ/s^2$ , we considered this was the onset of the velocity response to the flash. Figure AIII-5 describes this procedure and shows the results of this analysis. We found a mean latency of 83 ms (subject variability: 71 to 104 ms) for the modulation of  $EV_{s\perp}$  by the flash. Our method also provided a standard deviation (SD) of 7 ms. However, this was not the SD for individual data, but its size was related to evaluation method of the latency, i.e. the larger the subset, the smaller the SD. Alternatively, when performing the same analysis but using a velocity threshold ( $0.5 * (\text{mean } EV_{s\perp} \text{ noise level during pursuit}) = 0.186^\circ/s$ ) instead of an acceleration threshold, we obtained a mean latency of 86 ms (S.D. = 14 ms), which was consistent with results of Fig. AIII-5.

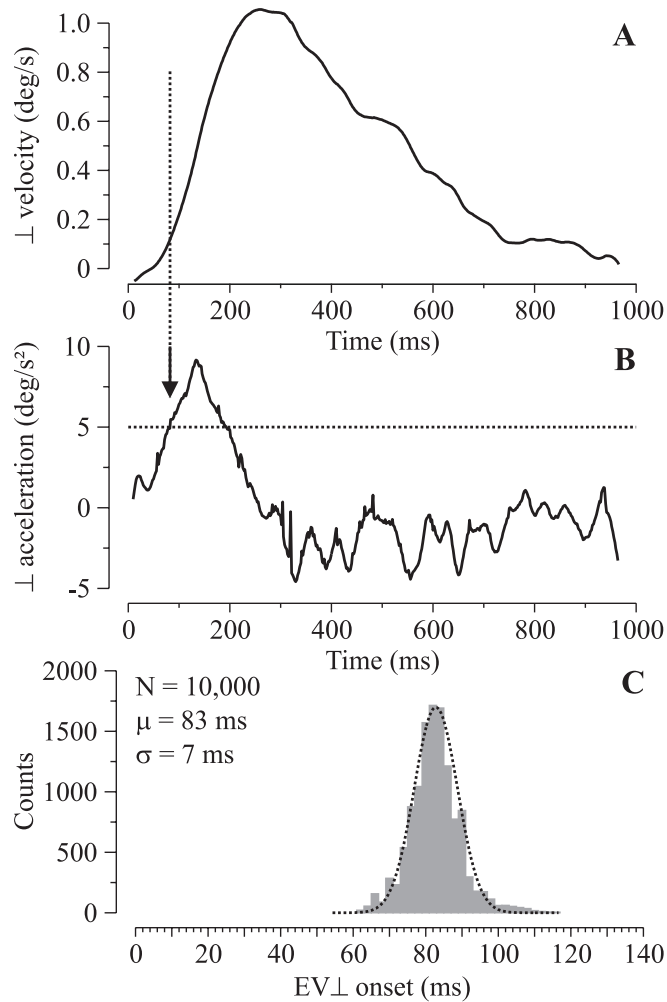


**Figure AIII-5: Mean onset latency of the  $EV_{s\perp}$  modulation.** **A.** Example of a mean smooth perpendicular eye velocity trace used for the determination of the response onset latency. **B.** Perpendicular smooth eye acceleration obtained by computing the first order derivative of the mean smooth perpendicular eye velocity in panel A. The horizontal dotted line indicated the threshold used for the onset detection of the response. The vertical arrow and dotted line shows where the algorithm detected the onset for this example. **C.** The histogram represents the results of the latency evaluation procedure described in panels A and B (see text for details). The dotted curve is a normal distribution fitted on the histogram. Total count  $N$ , mean  $\mu$  and S.D.  $\sigma$  resulting from this method are also indicated.

Another interesting aspect of the description of a transient smooth eye velocity perturbation is the response offset. Again, we performed an

analysis similar to the above described k-fold sub-sampling method ( $k = 10,000$ ) applied on  $1/100^{\text{th}}$  of the data set. Therefore, we first computed the mean  $EV_{s\perp}$  (by taking each time randomly  $1/100^{\text{th}}$  of the data set) and determined the time of the maximum of the response.

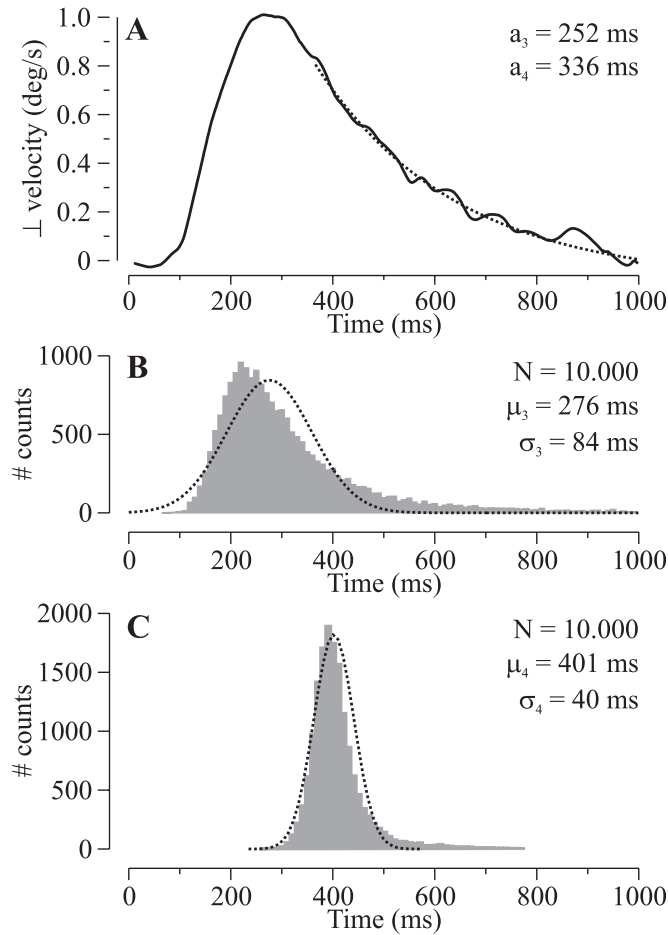


**Figure AIII-6: Response offset for the mean  $EV_{s\perp}$ .** **A.** Example of the exponential fit (dotted line) on the offset of the mean  $EV_{s\perp}$  (see text for details). The values of this particular fit for the decay time constant ( $a_3$ ) and the delay ( $a_4$ ) are also indicated. **B.** Histogram of the time constant of the smooth response decay ( $a_3$ ) obtained by the evaluation procedure (see text). The dotted line indicates the fit of a normal distribution on the histogram. The mean ( $\mu$ ) and S.D. ( $\sigma$ ) of this variable are also given. **C.** Histogram of the delay ( $a_4$ ) obtained by the evaluation procedure. The normal distribution fit (dotted line) and the mean ( $\mu$ ) and S.D. ( $\sigma$ ) of this variable are shown.

Then, we fitted a decaying exponential function on the data, starting 100 ms after the maximum of the response until 1000 ms after the flash onset. The fit function had the following expression:

$$y = a_1 + a_2 \cdot \exp\left(-\frac{x - a_4}{a_3}\right) \quad \text{Eq. AIII-1}$$

To perform this fit, we used standard non-linear least-squares data fitting by the Gauss-Newton method. We were particularly interested in parameters  $a_3$  (decay time constant) and  $a_4$  (response delay). Note that the offset response delay  $a_4$  was measured relative to the flash onset. Figure AIII-6 shows the results of this analysis.

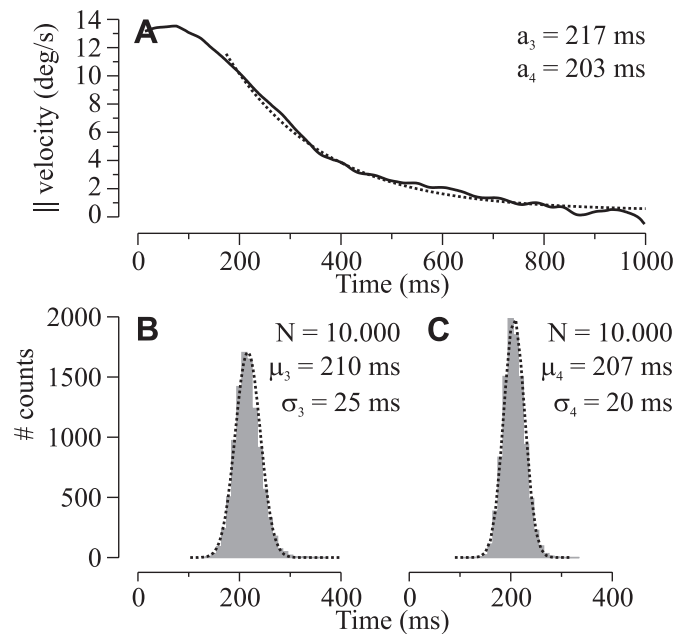


**Figure AIII-7: Response offset for the mean  $EV_{s||}$**  (for comparison with Fig. AIII-6). **A.** Example of the exponential fit (dotted line) on the offset of the mean  $EV_{s||}$  is shown. The values of this particular fit for the decay time constant ( $a_3$ ) and the delay ( $a_4$ ) are indicated. **B.** Pooled histogram of the time constant of the smooth response decay ( $a_3$ ). The normal distribution fit (dotted line) and the mean ( $\mu$ ) and S.D. ( $\sigma$ ) of this variable are shown. **C.** Histogram of the delay ( $a_4$ ). The normal distribution fits (dotted lines) and the means ( $\mu$ ) and S.D. ( $\sigma$ ) of this variable are shown.

We found a decay time constant  $a_3 = (276 \pm 84)$  ms (subject variability: 204 to 330 ms) and a response delay  $a_4 = (401 \pm 40)$  ms (subject variability: 266 to 548 ms). However, Fig. AIII-6B shows that the histogram of the decay time constant was not normally distributed. Furthermore, the values of  $a_3$  were quite variable. As in the previous analysis, again the SD was not directly related to the variability of the physical response but to the analysis method.

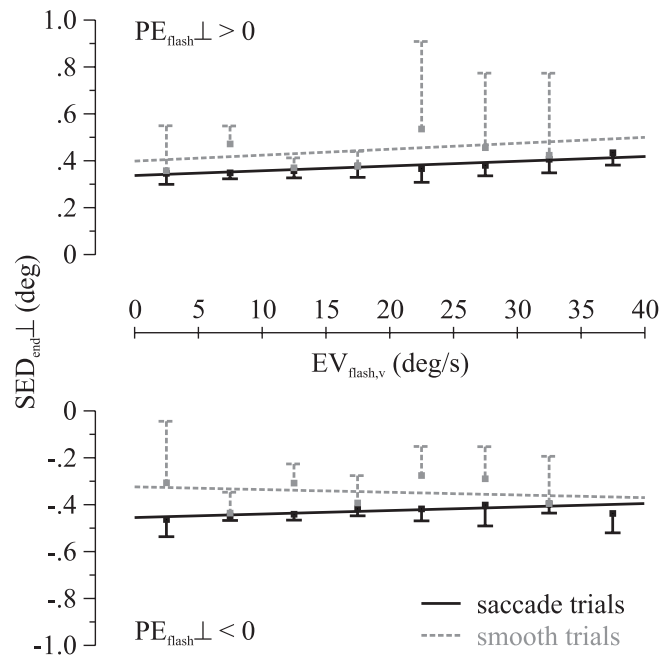


**Figure AIII-8: No effect of ongoing smooth pursuit on evoked SEM.** Influence of smooth pursuit velocity at the moment of the flash  $EV_{\text{flash},v}$  on the magnitude of the  $EV_{s\perp}$  modulation. Similarly to Fig. AIII-3C, we used the total perpendicular smooth eye displacement  $SED_{\text{end}\perp}$  as an indicator for a potential effect. Saccade trials (black, solid line) and smooth trials (gray, dotted line) were separated. Upper and lower parts of the figure represent positive and negative  $PE_{\text{flash}\perp}$ . Regression lines were performed on raw data. They were significantly offset from the baseline (t-test,  $p < 0.001$ ) but their slopes were not significantly different from zero (t-test,  $p > 0.05$ ). Squares and whiskers indicate mean and standard error.

In order to compare the parameters of the response offset for the perpendicular and parallel component of the smooth eye velocity, we performed the same analysis on the mean  $EV_{s||}$ . The only difference was that we fitted Eq. AIII-1 on the data starting at 200 ms after the flash onset (and

not 100 ms after the maximum, as this was the case for the mean  $EV_{s\perp}$ ) until 1000 ms after the flash onset. The results of this analysis are shown in Fig. AIII-7. Figure AIII-7B shows the histogram of the decay time constant  $a_3 = (210 \pm 25)$  ms (subject variability: 188 to 320 ms) and Fig. AIII-7C the delay  $a_4 = (207 \pm 20)$  ms (subject variability: 135 to 259 ms). Note that the location of the maximum in Fig. AIII-7B was approximately the same as in Fig. AIII-6B, although the shape of the distribution was different.

#### 4.4. *Smooth pursuit deviation?*

What is the origin of  $EV_{s\perp}$  modulation? A priori, the  $EV_{s\perp}$  response could be due to a deviation of the ongoing smooth pursuit direction due to the flash. This hypothesis is consistent with a dependence of  $SED_{end\perp}$  on  $PE_{flash\perp}$ . However, this hypothesis also predicts that the smooth pursuit eye velocity at the moment of the flash  $EV_{flash,v}$  should modulate  $SED_{end\perp}$ . Testing this hypothesis allowed us to investigate how the visual system handles briefly flashed targets. In Fig. AIII-8, we plotted  $SED_{end\perp}$  as a function of  $EV_{flash,v}$ . Data were separated in positive vs. negative values of  $PE_{flash\perp}$  and in saccade vs. smooth trials, although the results were not significantly different (F-test:  $p > 0.05$ ). As a result, Fig. AIII-8 shows that there was no influence of  $EV_{flash,v}$  on  $SED_{end\perp}$ . Indeed, the slope of all regression lines was not significantly different from zero (t-test,  $p > 0.05$ ). Thus, the effect of the flash was not simply to alter the heading of the ongoing smooth eye movement.

## 5. Discussion

### 5.1. *General discussion*

We developed a new 2-D paradigm that allowed us to present a position error with no velocity (flash) to the oculomotor system and investigate the smooth eye movement response. Our results show that a target flashed during ongoing smooth pursuit evokes a smooth eye movement towards the flash. In contrast, the same flash stimulus did not evoke any smooth eye movement during fixation, which is consistent with previous findings (Epelboim and Kowler 1993). Furthermore, the velocity of the evoked smooth eye movement was proportional to the position error of the flash and was present for position errors tested up to  $10^\circ$ . The response

was independent of the velocity of the ongoing smooth pursuit eye movement and did not depend on the occurrence of saccades. This is a striking and direct demonstration of a position input to the smooth pursuit system.

We reported here a short latency (~85 ms) modulation of the eye velocity evoked by the presentation of a peripheral flash during ongoing smooth pursuit. Although the response onset latency was very short, this delay was compatible with previously observed data describing the response of the smooth pursuit system to a change in the visual stimulus (Behrens et al. 1985; Ferrera and Lisberger 1995; Knox 1996, 1998; O'Mullane and Knox 1999; Pola and Wyatt 1985; Rashbass 1961; Robinson 1965).

The comparison of the decay time constants for the evoked and ongoing smooth eye movements (276 ms versus 210 ms) showed a similar behavior for both components. Clearly, this decay time constant is much longer than the classically reported offset time constant of ~100 ms for the smooth pursuit system (Becker and Fuchs 1985). Because both the evoked and ongoing smooth eye movement components decayed similarly, one hypothesis might be that this could be due to the presence of the ongoing ramp motion. Indeed, if the pursuit stimulus is still present, the system might take longer to slow down the eyes, maybe because subjects had to disengage attention from the pursuit target, which could take some time. Meanwhile, the neural velocity command is still (at least partially) active because of the continuing pursuit ramp motion. Indeed, it has been shown that in a similar condition when the target is suddenly stabilized on the eye, the smooth pursuit response decays with time constants up to more than 500 ms (Pola and Wyatt 1997) depending on the instruction. When passively viewing the stimulus, the same authors still report decay time constants of approximately 300 ms. In addition, it has indeed been shown that when passively rotating an occluded eye while the other eye is fixating straight-ahead, the time course of return to the resting position ranged between 183 and 345 ms depending on subjects (Seidman et al. 1995).

The simplest explanation for the smooth eye movements evoked by the flash is to hypothesize that the flash induced a deviation of the smooth pursuit trajectory. Such deviation might have resulted from a weighted average of the ramp and flash target positions, as this is the case for saccades to extended targets (Vishwanath and Kowler 2003), that are directed to the

center of mass. However, our data clearly rule out this deviation from the pursuit trajectory hypothesis because we demonstrated that the evoked smooth eye movements ( $SED_{\text{end}\perp}$ ) were independent of the initial smooth pursuit velocity ( $EV_{\text{flash},v}$ , see Fig. AIII-8). Afterimages have also been reported to influence smooth eye movements (Heywood and Churcher 1971; Yasui and Young 1975). But in our experiment, a flash-induced afterimage would move parallel to the ongoing smooth pursuit movement, which is inconsistent with the perpendicular smooth eye movement modulation we observed here.

Alternatively, it has been proposed that a spatio-temporal filter could transform a position signal into a velocity command (Carl and Gellman 1987). Consequently, pursuit signals could interact with a briefly presented flash by vector averaging (Groh et al. 1997; Lisberger and Ferrera 1997). In this case, no dependence of  $SED_{\text{end}\perp}$  on  $EV_{\text{flash},v}$  would be predicted, since the perpendicular smooth eye movements would simply be the result of a perpendicular velocity command. Thus our data are compatible with a spatio-temporal filter transforming a position signal into a velocity command.

### **5.2. Smooth pursuit gain control**

It has been suggested that the modulation of smooth pursuit eye movements due to brief perturbations in target velocity during ongoing smooth pursuit might be due to a gain control element in the smooth pursuit system (Churchland and Lisberger 2002; Schwartz and Lisberger 1994). The same gain control element was proposed to explain recent results concerning a novel form of smooth eye movements evoked by stationary visual stimuli in the monkey (Tanaka and Fukushima 1997; Tanaka and Lisberger 2000). Tanaka and Lisberger (2000) reported that during pursuit preparation stationary cues evoked smooth eye movements and postulated that this observation was a side-effect of the activation of the pursuit gain control element. A priori, a similar mechanism could explain our results. However, the velocity of the evoked movements decreased with cue eccentricity in their study whereas it increased with position error in our data. More importantly, the smooth movements were always directed away from the cue in their study whereas here they were directed towards the flash. Thus it is unlikely that our data can be explained only by the same pursuit gain

element. The differences between both studies probably result from the different experimental conditions. In Tanaka and Lisberger's study, the cue was presented during a gap for pursuit preparation and their monkeys had to suppress saccades. This contrasts with our experiment, where the flash was presented during ongoing smooth pursuit and orientation saccades were required.

### ***5.3. Neural substrate of the position error input to the smooth pursuit system***

We reported here that the velocity of smooth eye movements in response to a flash was proportional to position error. The Superior Colliculus (SC) encodes a motor map of position error and has been known for a long time to be essential for the control of saccades. Recently, SC has been proposed to provide the position error input to the smooth pursuit system (Krauzlis 2004). In the cat, sustained electrical stimulation of the SC evokes saccades followed by Smooth Eye Movements (SEMs) (Missal et al. 2002; Missal et al. 1996) that are correlated with the amplitude of evoked saccades (Missal et al. 2002). This suggests that the velocity of SEMs should be proportional to position error. Krauzlis and colleagues showed in the monkey that neurons in the rostral SC encode small position errors (generally  $< 3^\circ$ ) during fixation, saccades and smooth pursuit (Basso et al. 2000; Krauzlis et al. 2000, 1997). Furthermore, Basso et al. (2000) stimulated electrically as well as inactivated the rostral SC and reported effects on smooth pursuit consistent with the hypothesis that SC provides a position input to the pursuit system. Position error signals in SC might not generate smooth eye movements during fixation because SC output is gated at the brainstem level by Omni-directional Pause Neurons (OPNs). However, Missal and Keller (2002) recently reported that the activity of OPNs is reduced during smooth pursuit. This could allow SC output, that encodes position error signals, to influence smooth eye movements only during pursuit and not during fixation (Krauzlis 2004). Such a pathway would be a neural implementation of the above-mentioned spatio-temporal filter.

## ABBREVIATIONS

CB	Cerebellum
CN	Caudate nucleus
DN	Dentate nucleus
FEF	Frontal Eye Field
FF	Foveofugal
FP	Foveopetal
LGN	Lateral geniculate nucleus
LIP	Lateral intraparietal cortex
MD	Mediodorsal thalamus
MN	Motor neurons
MST	Medial superior temporal cortex
MT	Medial temporal cortex
OKN	Optokinetic nystagmus
OPN	Omni-directional pause neurons
PE	Position error
PG	Pulse generator
PN	Pontine nuclei

## ABBREVIATIONS

---

PPC	Posterior parietal cortex
PPRF	Paramediane pontine reticular formation
RI	Resettable integrator
riMLF	Rostral interstitial nucleus of the medial longitudinal Fasciculus
RS	Retinal slip
RSC	Rostral superior colliculus
SC	Superior colliculus
SED	Smooth eye displacement
SEF	Supplementary eye field
SNr	Substantia Nigra
V1	Striate cortex, primary visual cortex
VIP	Ventral Intraparietal cortex
VOR	Vestibulo-ocular reflex

## REFERENCES

- Adam JJ, Huys R, van Loon EM, Kingma H, and Paas FG.** Effects of spatial and symbolic precues on localization performance. *Psychol Res* 64: 66-80, 2000.
- Allin F, Velay JL, and Bouquerel A.** Shift in saccadic direction induced in humans by proprioceptive manipulation: a comparison between memory-guided and visually guided saccades. *Exp Brain Res* 110: 473-481, 1996.
- Andersen RA, Asanuma C, Essick G, and Siegel RM.** Corticocortical connections of anatomically and physiologically defined subdivisions within the inferior parietal lobule. *J Comp Neurol* 296: 65-113, 1990a.
- Andersen RA, Bracewell RM, Barash S, Gnadt JW, and Fogassi L.** Eye position effects on visual, memory, and saccade-related activity in areas LIP and 7a of macaque. *J Neurosci* 10: 1176-1196, 1990b.
- Andersen RA, Brotchie PR, and Mazzoni P.** Evidence for the lateral intraparietal area as the parietal eye field. *Curr Opin Neurobiol* 2: 840-846, 1992.
- Andersen RA, Essick GK, and Siegel RM.** Encoding of spatial location by posterior parietal neurons. *Science* 230: 456-458, 1985.
- Andersen RA, Snyder LH, Bradley DC, and Xing J.** Multimodal representation of space in the posterior parietal cortex and its use in planning movements. *Annu Rev Neurosci* 20: 303-330, 1997.
- Aslin RN and Shea SL.** The amplitude and angle of saccades to double-step target displacements. *Vision Res* 27: 1925-1942, 1987.
- Asrress KN and Carpenter RH.** Saccadic countermanding: a comparison of central and peripheral stop signals. *Vision Res* 41: 2645-2651, 2001.

- Awater H and Lappe M.** Perception of visual space at the time of pro- and anti-saccades. *J Neurophysiol* 91: 2457-2464, 2004.
- Bahill AT, Clark MR, and Stark L.** The main sequence, a tool for studying human eye movements. *Math Biosci* 24: 191-204, 1975.
- Baker JT, Harper TM, and Snyder LH.** Spatial memory following shifts of gaze. I. Saccades to memorized world-fixed and gaze-fixed targets. *J Neurophysiol* 89: 2564-2576, 2003.
- Barash S, Bracewell RM, Fogassi L, Gnadt JW, and Andersen RA.** Saccade-related activity in the lateral intraparietal area. II. Spatial properties. *J Neurophysiol* 66: 1109-1124, 1991.
- Barnes GR and Asselman PT.** The mechanism of prediction in human smooth pursuit eye movements. *J Physiol (Lond)* 439: 439-461, 1991.
- Basso MA, Krauzlis RJ, and Wurtz RH.** Activation and inactivation of rostral superior colliculus neurons during smooth-pursuit eye movements in monkeys. *J Neurophysiol* 84: 892-908, 2000.
- Becker W.** Saccades. In: *Eye movements*, edited by Carpenter R. Houndmills, UK: MacMillan Press, 1991, p. 95-137.
- Becker W and Fuchs AF.** Prediction in the oculomotor system: smooth pursuit during transient disappearance of a visual target. *Exp Brain Res* 57: 562-575, 1985.
- Becker W and Jürgens R.** An analysis of the saccadic system by means of double step stimuli. *Vision Res* 19: 967-983, 1979.
- Behrens F, Collewijn H, and Grusser OJ.** Velocity step responses of the human gaze pursuit system. Experiments with sigma-movement. *Vision Res* 25: 893-905, 1985.
- Bell AH, Everling S, and Munoz DP.** Influence of Stimulus Eccentricity and Direction on Characteristics of Pro- and Antisaccades in Non-Human Primates. *J Neurophysiol* 84: 2595-2604, 2000.
- Bennett SJ and Barnes GR.** Human ocular pursuit during the transient disappearance of a visual target. *J Neurophysiol* 90: 2504-2520, 2003.
- Biguer B, Donaldson IM, Hein A, and Jeannerod M.** Neck muscle vibration modifies the representation of visual motion and direction in man. *Brain* 111 ( Pt 6): 1405-1424, 1988.
- Blatt GJ, Andersen RA, and Stoner GR.** Visual receptive field organization and cortico-cortical connections of the lateral intraparietal area (area LIP) in the macaque. *J Comp Neurol* 299: 421-445, 1990.

- Blohm G, Missal M, and Lefevre P.** Smooth anticipatory eye movements alter the memorized position of flashed targets. *J Vis* 3: 761-770, 2003a.
- Blohm G, Missal M, and Lefèvre P.** Interaction between smooth anticipation and saccades during ocular orientation in darkness. *J Neurophysiol* 89: 1423-1433, 2003b.
- Blohm G, Missal M, and Lefèvre P.** Processing of retinal and extraretinal signals for memory guided saccades during smooth pursuit. *J Neurophysiol*, 2004, submitted.
- Bloomberg J, Jones GM, Segal B, McFarlane S, and Soul J.** Vestibular-contingent voluntary saccades based on cognitive estimates of remembered vestibular information. *Adv Otorhinolaryngol* 41: 71-75, 1988.
- Bloomberg J, Melvill Jones G, and Segal B.** Adaptive modification of vestibularly perceived rotation. *Exp Brain Res* 84: 47-56, 1991.
- Bock O.** Contribution of retinal versus extraretinal signals towards visual localization in goal-directed movements. *Exp Brain Res* 64: 476-482, 1986.
- Bock O and Kommerell G.** Visual localization after strabismus surgery is compatible with the "outflow" theory. *Vision Res* 26: 1825-1829, 1986.
- Boman DK and Hotson JR.** Stimulus conditions that enhance anticipatory slow eye movements. *Vision Res* 28: 1157-1165, 1988.
- Born RT and Tootell RB.** Segregation of global and local motion processing in primate middle temporal visual area. *Nature* 357: 497-499, 1992.
- Bradley DC, Maxwell M, Andersen RA, Banks MS, and Shenoy KV.** Mechanisms of heading perception in primate visual cortex. *Science* 273: 1544-1547, 1996.
- Braun DI, Boman DK, and Hotson JR.** Anticipatory smooth eye movements and predictive pursuit after unilateral lesions in human brain. *Exp Brain Res* 110: 111-116, 1996.
- Bremmer F, Distler C, and Hoffmann KP.** Eye position effects in monkey cortex. II. Pursuit- and fixation- related activity in posterior parietal areas LIP and 7A. *J Neurophysiol* 77: 962-977, 1997.
- Bremmer F, Duhamel JR, Ben Hamed S, and Graf W.** Heading encoding in the macaque ventral intraparietal area (VIP). *Eur J Neurosci* 16: 1554-1568, 2002.
- Brenner E and Smeets JB.** Motion extrapolation is not responsible for the flash-lag effect. *Vision Res* 40: 1645-1648, 2000.

- Brenner E, Smeets JB, and van den Berg AV.** Smooth eye movements and spatial localisation. *Vision Res* 41: 2253-2259, 2001.
- Bridgeman B.** A review of the role of efference copy in sensory and oculomotor control systems. *Ann Biomed Eng* 23: 409-422, 1995.
- Brotchie PR, Andersen RA, Snyder LH, and Goodman SJ.** Head position signals used by parietal neurons to encode locations of visual stimuli. *Nature* 375: 232-235, 1995.
- Buisseret P.** Influence of extraocular muscle proprioception on vision. *Physiol Rev* 75: 323-338, 1995.
- Buttner-Ennever JA and Horn AK.** Anatomical substrates of oculomotor control. *Curr Opin Neurobiol* 7: 872-879, 1997.
- Cai RH, Jacobson K, Baloh R, Schlag-Rey M, and Schlag J.** Vestibular signals can distort the perceived spatial relationship of retinal stimuli. *Exp Brain Res* 135: 275-278, 2000.
- Carl JR and Gellman RS.** Human smooth pursuit: stimulus-dependent responses. *J Neurophysiol* 57: 1446-1463, 1987.
- Carpenter RH and Williams ML.** Neural computation of log likelihood in control of saccadic eye movements. *Nature* 377: 59-62, 1995.
- Cavada C and Goldman-Rakic PS.** Posterior parietal cortex in rhesus monkey: I. Parcellation of areas based on distinctive limbic and sensory corticocortical connections. *J Comp Neurol* 287: 393-421, 1989.
- Chance FS, Abbott LF, and Reyes AD.** Gain modulation from background synaptic input. *Neuron* 35: 773-782, 2002.
- Churchland AK and Lisberger SG.** Gain control in human smooth-pursuit eye movements. *J Neurophysiol* 87: 2936-2945, 2002.
- Churchland MM, Chou IH, and Lisberger SG.** Evidence for object permanence in the smooth-pursuit eye movements of monkeys. *J Neurophysiol* 90: 2205-2218, 2003.
- Clark JJ.** Spatial attention and latencies of saccadic eye movements. *Vision Res* 39: 585-602, 1999.
- Clarke AH, Ditterich J, Druen K, Schonfeld U, and Steineke C.** Using high frame rate CMOS sensors for three-dimensional eye tracking. *Behav Res Methods Instrum Comput* 34: 549-560, 2002.
- Clower DM, West RA, Lynch JC, and Strick PL.** The inferior parietal lobule is the target of output from the superior colliculus, hippocampus, and cerebellum. *J Neurosci* 21: 6283-6291, 2001.

- Colby CL, Duhamel JR, and Goldberg ME.** Ventral intraparietal area of the macaque: anatomic location and visual response properties. *J Neurophysiol* 69: 902-914, 1993.
- Colby CL and Goldberg ME.** Space and attention in parietal cortex. *Annu Rev Neurosci* 22: 319-349, 1999.
- Collewijn H, van der Mark F, and Jansen TC.** Precise recording of human eye movements. *Vision Res* 15: 447-450, 1975.
- Crawford J, Martinez-Trujillo J, and Klier E.** Neural control of three-dimensional eye and head movements. *Curr Opin Neurobiol* 13: 655-662, 2003.
- Crawford JD and Guitton D.** Visual-motor transformations required for accurate and kinematically correct saccades. *J Neurophysiol* 78: 1447-1467, 1997.
- Crawford JD, Henriques DY, and Vilis T.** Curvature of visual space under vertical eye rotation: implications for spatial vision and visuomotor control. *J Neurosci* 20: 2360-2368, 2000.
- Crawford JD, Medendorp WP, and Marotta JJ.** Spatial transformations for eye-hand coordination. *J Neurophysiol* 92: 10-19, 2004.
- Curtis CE, Rao VY, and D'Esposito M.** Maintenance of spatial and motor codes during oculomotor delayed response tasks. *J Neurosci* 24: 3944-3952, 2004.
- Dassonville P, Schlag J, and Schlag-Rey M.** The frontal eye field provides the goal of saccadic eye movement. *Exp Brain Res* 89: 300-310, 1992.
- de Brouwer S, Missal M, Barnes G, and Lefèvre P.** Quantitative analysis of catch-up saccades during sustained pursuit. *J Neurophysiol* 87: 1772-1780, 2002a.
- de Brouwer S, Missal M, and Lefèvre P.** Role of retinal slip in the prediction of target motion during smooth and saccadic pursuit. *J Neurophysiol* 86: 550-558, 2001.
- de Brouwer S, Yuksel D, Blohm G, Missal M, and Lefèvre P.** What triggers catch-up saccades during visual tracking? *J Neurophysiol* 87: 1646-1650, 2002b.
- DeAngelis GC and Uka T.** Coding of Horizontal Disparity and Velocity by MT Neurons in the Alert Macaque. *J Neurophysiol* 89: 1094-1111, 2003.
- Deubel H, Bridgeman B, and Schneider WX.** Immediate post-saccadic information mediates space constancy. *Vision Res* 38: 3147-3159, 1998.

- Dominey PF, Schlag J, Schlag-Rey M, and Arbib MA.** Colliding saccades evoked by frontal eye field stimulation: artifact or evidence for an oculomotor compensatory mechanism underlying double-step saccades? *Biol Cybern* 76: 41-52, 1997.
- Droulez J and Berthoz A.** A neural network model of sensoritopic maps with predictive short-term memory properties. *Proc Natl Acad Sci U S A* 88: 9653-9657, 1991.
- Droulez J and Berthoz A.** Spatial and temporal transformations in visuo-motor coordination. In: *Neural Computers*, edited by Eckmiller R and van den Malsburg C. Berlin: Springer, 1988, p. 345-357.
- Duhamel JR, Colby CL, and Goldberg ME.** The updating of the representation of visual space in parietal cortex by intended eye movements. *Science* 255: 90-92, 1992a.
- Duhamel JR, Goldberg ME, Fitzgibbon EJ, Sirigu A, and Grafman J.** Saccadic dysmetria in a patient with a right frontoparietal lesion. The importance of corollary discharge for accurate spatial behaviour. *Brain* 115: 1387-1402, 1992b.
- Dursteler MR, Wurtz RH, and Newsome WT.** Directional pursuit deficits following lesions of the foveal representation within the superior temporal sulcus of the macaque monkey. *J Neurophysiol* 57: 1262-1287, 1987.
- Eagleman DM and Sejnowski TJ.** Motion integration and postdiction in visual awareness. *Science* 287: 2036-2038, 2000.
- Eifuku S and Wurtz RH.** Response to motion in extrastriate area MSTl: center-surround interactions. *J Neurophysiol* 80: 282-296, 1998.
- Epelboim J and Kowler E.** Slow control with eccentric targets: evidence against a position- corrective model. *Vision Res* 33: 361-380, 1993.
- Erickson RG and Thier P.** A neuronal correlate of spatial stability during periods of self- induced visual motion. *Exp Brain Res* 86: 608-616, 1991.
- Ferrera VP and Lisberger SG.** Attention and target selection for smooth pursuit eye movements. *J Neurosci* 15: 7472-7484, 1995.
- Festinger L and Canon LK.** Information about spatial location based on knowledge about efference. *Psychol Rev* 72: 373-384, 1965.
- Findlay JM.** Spatial and temporal factors in the predictive generation of saccadic eye movements. *Vision Res* 21: 347-354, 1981.
- Fiorentini A and Maffei L.** Instability of the eye in the dark and proprioception. *Nature* 269: 330-331, 1977.

- Fischer B, Gezeck S, and Hartnegg K.** The analysis of saccadic eye movements from gap and overlap paradigms. *Brain Res Brain Res Protoc* 2: 47-52, 1997.
- Fischer B and Ramsperger E.** Human express saccades: effects of randomization and daily practice. *Exp Brain Res* 64: 569-578, 1986.
- Fischer B, Weber H, Biscaldi M, Aiple F, Otto P, and Stuhr V.** Separate populations of visually guided saccades in humans: reaction times and amplitudes. *Exp Brain Res* 92: 528-541, 1993.
- Gauthier GM, Vercher JL, and Blouin J.** Egocentric visual target position and velocity coding: role of ocular muscle proprioception. *Ann Biomed Eng* 23: 423-435, 1995.
- Gauthier GM, Vercher JL, and Zee DS.** Changes in ocular alignment and pointing accuracy after sustained passive rotation of one eye. *Vision Res* 34: 2613-2627, 1994.
- Gaymard B, Pierrot-Deseilligny C, and Rivaud S.** Impairment of sequences of memory-guided saccades after supplementary motor area lesions. *Ann Neurol* 28: 622-626, 1990.
- Gellman RS and Carl JR.** Motion processing for saccadic eye movements in humans. *Exp Brain Res* 84: 660-667, 1991.
- Gellman RS and Fletcher WA.** Eye position signals in human saccadic processing. *Exp Brain Res* 89: 425-434, 1992.
- Ghez C and Thach WT.** The Cerebellum. In: *Principles of neural science* (4 ed.), edited by Kandel ER, Schwartz JH and Jessell TM. New York: McGraw-Hill, 2000, p. 832-852.
- Gnadt JW and Andersen RA.** Memory related motor planning activity in posterior parietal cortex of macaque. *Exp Brain Res* 70: 216-220, 1988.
- Goldman-Rakic PS.** Circuitry of primate prefrontal cortex and regulation of behavior by representational memory. In: *Handbook of Physiology: I. The Nervous System*, edited by Plum F and Mountcastle VB. Bethesda: American Physiological Society, 1987, p. 373-417.
- Goossens HH and Van Opstal AJ.** Local feedback signals are not distorted by prior eye movements: evidence from visually evoked double saccades. *J Neurophysiol* 78: 533-538, 1997.
- Groh JM, Born RT, and Newsome WT.** How is a sensory map read Out? Effects of microstimulation in visual area MT on saccades and smooth pursuit eye movements. *J Neurosci* 17: 4312-4330, 1997.

- Guthrie BL, Porter JD, and Sparks DL.** Corollary discharge provides accurate eye position information to the oculomotor system. *Science* 221: 1193-1195, 1983.
- Hald A.** *Statistical theory with engineering applications*. New York: John Wiley & Sons, Inc., 1967.
- Hallett PE and Lightstone AD.** Saccadic eye movements to flashed targets. *Vision Res* 16: 107-114, 1976a.
- Hallett PE and Lightstone AD.** Saccadic eye movements towards stimuli triggered by prior saccades. *Vision Res* 16: 99-106, 1976b.
- Han Y and Lennerstrand G.** Changes of visual localization induced by eye and neck muscle vibration in normal and strabismic subjects. *Graefes Arch Clin Exp Ophthalmol* 237: 815-823, 1999.
- Hanes DP and Schall JD.** Neural control of voluntary movement initiation. *Science* 274: 427-430, 1996.
- Heide W, Blankenburg M, Zimmermann E, and Kompf D.** Cortical control of double-step saccades: implications for spatial orientation. *Ann Neurol* 38: 739-748, 1995.
- Heinen SJ.** Single neuron activity in the dorsomedial frontal cortex during smooth pursuit eye movements. *Exp Brain Res* 104: 357-361, 1995.
- Heinen SJ and Liu M.** Single-neuron activity in the dorsomedial frontal cortex during smooth-pursuit eye movements to predictable target motion. *Vis Neurosci* 14: 853-865, 1997.
- Henriques DY and Crawford JD.** Direction-dependent distortions of retinocentric space in the visuomotor transformation for pointing. *Exp Brain Res* 132: 179-194, 2000.
- Henriques DY, Klier EM, Smith MA, Lowy D, and Crawford JD.** Gaze-centered remapping of remembered visual space in an open-loop pointing task. *J Neurosci* 18: 1583-1594, 1998.
- Herter TM and Guitton D.** Human head-free gaze saccades to targets flashed before gaze-pursuit are spatially accurate. *J Neurophysiol* 80: 2785-2789, 1998.
- Heywood S and Churcher J.** Eye movements and the afterimage. I. Tracking the afterimage. *Vision Res* 11: 1163-1168, 1971.
- Heywood S and Churcher J.** Saccades to step-ramp stimuli. *Vision Res* 21: 479-490, 1981.

- Hikosaka O, Sakamoto M, and Usui S.** Functional properties of monkey caudate neurons. III. Activities related to expectation of target and reward. *J Neurophysiol* 61: 814-832, 1989.
- Hikosaka O and Wurtz RH.** Visual and oculomotor functions of monkey substantia nigra pars reticulata. I. Relation of visual and auditory responses to saccades. *J Neurophysiol* 49: 1230-1253, 1983a.
- Hikosaka O and Wurtz RH.** Visual and oculomotor functions of monkey substantia nigra pars reticulata. II. Visual responses related to fixation of gaze. *J Neurophysiol* 49: 1254-1267, 1983b.
- Hikosaka O and Wurtz RH.** Visual and oculomotor functions of monkey substantia nigra pars reticulata. III. Memory-contingent visual and saccade responses. *J Neurophysiol* 49: 1268-1284, 1983c.
- Hikosaka O and Wurtz RH.** Visual and oculomotor functions of monkey substantia nigra pars reticulata. IV. Relation of substantia nigra to superior colliculus. *J Neurophysiol* 49: 1285-1301, 1983d.
- Hodgson TL.** The location marker effect. Saccadic latency increases with target eccentricity. *Exp Brain Res* 145: 539-542, 2002.
- Israel I and Berthoz A.** Contribution of the otoliths to the calculation of linear displacement. *J Neurophysiol* 62: 247-263, 1989.
- Israel I, Fetter M, and Koenig E.** Vestibular perception of passive whole-body rotation about horizontal and vertical axes in humans: goal-directed vestibulo-ocular reflex and vestibular memory-contingent saccades. *Exp Brain Res* 96: 335-346, 1993.
- Jarrett CB and Barnes G.** Volitional selection of direction in the generation of anticipatory ocular smooth pursuit in humans. *Neurosci Lett* 312: 25-28, 2001.
- Jürgens R and Becker W.** Is there a linear addition of saccades and pursuit movements? In: *Basic mechanisms of ocular motility and their clinical implications*, edited by P. LGaB-Y-R: Oxford Pergamon press, 1974, p. 525-529.
- Jürgens R, Becker W, and Kornhuber HH.** Natural and drug-induced variations of velocity and duration of human saccadic eye movements: evidence for a control of the neural pulse generator by local feedback. *Biol Cybern* 39: 87-96, 1981.
- Kaiser M and Lappe M.** Perisaccadic mislocalization orthogonal to saccade direction. *Neuron* 41: 293-300, 2004.

- Kalesnykas RP and Hallett PE.** Retinal eccentricity and the latency of eye saccades. *Vision Res* 34: 517-531, 1994.
- Kanai R, Sheth BR, and Shimojo S.** Stopping the motion and sleuthing the flash-lag effect: spatial uncertainty is the key to perceptual mislocalization. *Vision Res* 44: 2605-2619, 2004.
- Kanai R, Van Der Geest N, and Frens A.** Inhibition of saccade initiation by preceding smooth pursuit. *Exp Brain Res* 148: 300-307, 2003.
- Kao GW and Morrow MJ.** The relationship of anticipatory smooth eye movement to smooth pursuit initiation. *Vision Res* 34: 3027-3036, 1994.
- Karnath HO, Sievering D, and Fetter M.** The interactive contribution of neck muscle proprioception and vestibular stimulation to subjective "straight ahead" orientation in man. *Exp Brain Res* 101: 140-146, 1994.
- Kawagoe R, Takikawa Y, and Hikosaka O.** Expectation of reward modulates cognitive signals in the basal ganglia. *Nat Neurosci* 1: 411-416, 1998.
- Kawano K and Sasaki M.** Response properties of neurons in posterior parietal cortex of monkey during visual-vestibular stimulation. II. Optokinetic neurons. *J Neurophysiol* 51: 352-360, 1984.
- Keller E and Johnsen SD.** Velocity prediction in corrective saccades during smooth-pursuit eye movements in monkey. *Exp Brain Res* 80: 525-531, 1990.
- Keller EL and Edelman JA.** Use of interrupted saccade paradigm to study spatial and temporal dynamics of saccadic burst cells in superior colliculus in monkey. *J Neurophysiol* 72: 2754-2770, 1994.
- Keller EL, Gandhi NJ, and Shieh JM.** Endpoint accuracy in saccades interrupted by stimulation in the omnipause region in monkey. *Vis Neurosci* 13: 1059-1067, 1996a.
- Keller EL, Gandhi NJ, and Weir PT.** Discharge of superior collicular neurons during saccades made to moving targets. *J Neurophysiol* 76: 3573-3577, 1996b.
- Keller EL and Missal M.** Shared brainstem pathways for saccades and smooth-pursuit eye movements. *Ann N Y Acad Sci* 1004: 29-39, 2003.
- Keller EL and Robinson DA.** Absence of a stretch reflex in extraocular muscles of the monkey. *J Neurophysiol* 34: 908-919, 1971.

- Kerzel D.** Eye movements and visible persistence explain the mislocalization of the final position of a moving target. *Vision Res* 40: 3703-3715, 2000.
- Klein RM.** Inhibition of return. *Trends Cogn Sci* 4: 138-147, 2000.
- Klier EM and Crawford JD.** Human oculomotor system accounts for 3-D eye orientation in the visual- motor transformation for saccades. *J Neurophysiol* 80: 2274-2294, 1998.
- Knox PC.** The effect of the gap paradigm on the latency of human smooth pursuit of eye movement. *Neuroreport* 7: 3027-3030, 1996.
- Knox PC.** Stimulus predictability and the gap effect on pre-saccadic smooth pursuit. *Neuroreport* 9: 809-812, 1998.
- Knox PC, Weir CR, and Murphy PJ.** Modification of visually guided saccades by a nonvisual afferent feedback signal. *Invest Ophthalmol Vis Sci* 41: 2561-2565, 2000.
- Komatsu H and Wurtz RH.** Modulation of pursuit eye movements by stimulation of cortical areas MT and MST. *J Neurophysiol* 62: 31-47, 1989.
- Komatsu H and Wurtz RH.** Relation of cortical areas MT and MST to pursuit eye movements. I. Localization and visual properties of neurons. *J Neurophysiol* 60: 580-603, 1988a.
- Komatsu H and Wurtz RH.** Relation of cortical areas MT and MST to pursuit eye movements. III. Interaction with full-field visual stimulation. *J Neurophysiol* 60: 621-644, 1988b.
- Kowler E, Martins AJ, and Pavel M.** The effect of expectations on slow oculomotor control. IV. Anticipatory smooth eye movements depend on prior target motions. *Vision Res* 24: 197-210, 1984.
- Kowler E and Steinman RM.** The effect of expectations on slow oculomotor control. I. Periodic target steps. *Vision Res* 19: 619-632, 1979.
- Kraft CH and van Eeden C.** *A nonparametric introduction to statistics.* New York: The MacMillan Company, 1968.
- Krauzlis RJ.** Neuronal activity in the rostral superior colliculus related to the initiation of pursuit and saccadic eye movements. *J Neurosci* 23: 4333-4344, 2003.
- Krauzlis RJ.** Recasting the smooth pursuit eye movement system. *J Neurophysiol* 91: 591-603, 2004.

- Krauzlis RJ, Basso MA, and Wurtz RH.** Discharge properties of neurons in the rostral superior colliculus of the monkey during smooth-pursuit eye movements. *J Neurophysiol* 84: 876-891, 2000.
- Krauzlis RJ, Basso MA, and Wurtz RH.** Shared motor error for multiple eye movements. *Science* 276: 1693-1695, 1997.
- Krauzlis RJ and Lisberger SG.** A model of visually-guided smooth pursuit eye movements based on behavioral observations. *J Comput Neurosci* 1: 265-283, 1994.
- Krauzlis RJ, Liston D, and Carello CD.** Target selection and the superior colliculus: goals, choices and hypotheses. *Vision Res* 44: 1445-1451, 2004.
- Krauzlis RJ and Miles FA.** Decreases in the latency of smooth pursuit and saccadic eye movements produced by the "gap paradigm" in the monkey. *Vision Res* 36: 1973-1985, 1996a.
- Krauzlis RJ and Miles FA.** Initiation of saccades during fixation or pursuit: evidence in humans for a single mechanism. *J Neurophysiol* 76: 4175-4179, 1996b.
- Krauzlis RJ and Miles FA.** Release of fixation for pursuit and saccades in humans: evidence for shared inputs acting on different neural substrates. *J Neurophysiol* 76: 2822-2833, 1996c.
- Krauzlis RJ and Miles FA.** Role of the oculomotor vermis in generating pursuit and saccades: effects of microstimulation. *J Neurophysiol* 80: 2046-2062, 1998.
- Krauzlis RJ and Stone LS.** Tracking with the mind's eye. *Trends Neurosci* 22: 544-550, 1999.
- Krekelberg B, Kubischik M, Hoffmann KP, and Bremmer F.** Neural correlates of visual localization and perisaccadic mislocalization. *Neuron* 37: 537-545, 2003.
- Krekelberg B and Lappe M.** A model of the perceived relative positions of moving objects based upon a slow averaging process. *Vision Res* 40: 201-215, 2000.
- Krekelberg B and Lappe M.** Temporal recruitment along the trajectory of moving objects and the perception of position. *Vision Res* 39: 2669-2679, 1999.
- Kurylo DD and Skavenski AA.** Eye movements elicited by electrical stimulation of area PG in the monkey. *J Neurophysiol* 65: 1243-1253, 1991.

- Kustov AA and Robinson DL.** Modified saccades evoked by stimulation of the macaque superior colliculus account for properties of the resettable integrator. *J Neurophysiol* 73: 1724-1728, 1995.
- Lappe M and Krekelberg B.** The position of moving objects. *Perception* 27: 1437-1449, 1998.
- Leach JC and Carpenter RH.** Saccadic choice with asynchronous targets: evidence for independent randomisation. *Vision Res* 41: 3437-3445, 2001.
- Lefèvre P, Quaia C, and Optican LM.** Distributed model of control of saccades by superior colliculus and cerebellum. *Neural Networks* 11: 1175-1190, 1998.
- Leigh JR and Zee DS.** *The Neurology of Eye Movements*. New York: Oxford University Press Inc., 1999.
- Lennerstrand G, Tian S, and Han Y.** Effects of eye muscle proprioceptive activation on eye position in normal and exotropic subjects. *Graefes Arch Clin Exp Ophthalmol* 235: 63-69, 1997.
- Leon MI and Shadlen MN.** Representation of time by neurons in the posterior parietal cortex of the macaque. *Neuron* 38: 317-327, 2003.
- Lewis JW and Van Essen DC.** Corticocortical connections of visual, sensorimotor, and multimodal processing areas in the parietal lobe of the macaque monkey. *J Comp Neurol* 428: 112-137, 2000.
- Lewis RF, Zee DS, Gaymard BM, and Guthrie BL.** Extraocular muscle proprioception functions in the control of ocular alignment and eye movement conjugacy. *J Neurophysiol* 72: 1028-1031, 1994.
- Lewis RF, Zee DS, Hayman MR, and Tamargo RJ.** Oculomotor function in the rhesus monkey after deafferentation of the extraocular muscles. *Exp Brain Res* 141: 349-358, 2001.
- Lisberger SG and Ferrera VP.** Vector averaging for smooth pursuit eye movements initiated by two moving targets in monkeys. *J Neurosci* 17: 7490-7502, 1997.
- Lisberger SG and Fuchs AF.** Role of primate flocculus during rapid behavioral modification of vestibuloocular reflex. I. Purkinje cell activity during visually guided horizontal smooth-pursuit eye movements and passive head rotation. *J Neurophysiol* 41: 733-763, 1978a.
- Lisberger SG and Fuchs AF.** Role of primate flocculus during rapid behavioral modification of vestibuloocular reflex. II. Mossy fiber firing patterns during horizontal head rotation and eye movement. *J Neurophysiol* 41: 764-777, 1978b.

- Lisberger SG, Morris EJ, and Tychsen L.** Visual motion processing and sensory-motor integration for smooth pursuit eye movements. *Annu Rev Neurosci* 10: 97-129, 1987.
- Lynch JC, Hoover JE, and Strick PL.** Input to the primate frontal eye field from the substantia nigra, superior colliculus, and dentate nucleus demonstrated by transneuronal transport. *Exp Brain Res* 100: 181-186, 1994.
- MacKay DM.** Perceptual stability of a stroboscopically lit visual field containing self-luminous objects. *Nature* 181: 507-508, 1958.
- Matin L.** Visual localization and eye movements. In: *Sensory processes and perception*, edited by Boff KR, L. K and Thomas JP. New York: Wiley-Interscience, 1986, p. 20.21-20.45.
- Matsuo S, Bergeron A, and Guitton D.** Evidence for gaze feedback to the cat superior colliculus: discharges reflect gaze trajectory perturbations. *J Neurosci* 24: 2760-2773, 2004.
- May JG, Keller EL, and Suzuki DA.** Smooth-pursuit eye movement deficits with chemical lesions in the dorsolateral pontine nucleus of the monkey. *J Neurophysiol* 59: 952-977, 1988.
- Maylor EA and Hockey R.** Inhibitory component of externally controlled covert orienting in visual space. *J Exp Psychol Hum Percept Perform* 11: 777-787, 1985.
- Mays LE and Sparks DL.** Saccades are spatially, not retinocentrically, coded. *Science* 208: 1163-1165, 1980.
- Mazurek ME, Roitman JD, Ditterich J, and Shadlen MN.** A role for neural integrators in perceptual decision making. *Cereb Cortex* 13: 1257-1269, 2003.
- McClurkin JW and Optican LM.** Primate striate and prestriate cortical neurons during discrimination. I. simultaneous temporal encoding of information about color and pattern. *J Neurophysiol* 75: 481-495, 1996.
- McClurkin JW, Zarbock JA, and Optican LM.** Temporal codes for colors, pattern, and memories. In: *Cerebral cortex*, edited by Peters A and Rockland KS. New York: Plenum Press, 1994, p. 443-467.
- McKenzie A and Lisberger SG.** Properties of signals that determine the amplitude and direction of saccadic eye movements in monkeys. *J Neurophysiol* 56: 196-207, 1986.
- Medendorp WP, Goltz HC, Vilis T, and Crawford JD.** Gaze-centered updating of visual space in human parietal cortex. *J Neurosci* 23: 6209-6214, 2003.

- Medendorp WP, Smith MA, Tweed DB, and Crawford JD.** Rotational remapping in human spatial memory during eye and head motion. *J Neurosci* 22: RC196, 2002a.
- Medendorp WP, Van Asselt S, and Gielen CC.** Pointing to remembered visual targets after active one-step self- displacements within reaching space. *Exp Brain Res* 125: 50-60, 1999.
- Medendorp WP, Van Gisbergen JA, and Gielen CC.** Human gaze stabilization during active head translations. *J Neurophysiol* 87: 295-304, 2002b.
- Mergner T, Nasios G, and Anastasopoulos D.** Vestibular memory-contingent saccades involve somatosensory input from the body support. *Neuroreport* 9: 1469-1473, 1998.
- Mergner T, Nasios G, Maurer C, and Becker W.** Visual object localisation in space. Interaction of retinal, eye position, vestibular and neck proprioceptive information. *Exp Brain Res* 141: 33-51, 2001.
- Michels L and Lappe M.** Contrast dependency of saccadic compression and suppression. *Vision Res* 44: 2327-2336, 2004.
- Mikami A, Newsome WT, and Wurtz RH.** Motion selectivity in macaque visual cortex. I. Mechanisms of direction and speed selectivity in extrastriate area MT. *J Neurophysiol* 55: 1308-1327, 1986.
- Miles FA and Fuller JH.** Visual tracking and the primate flocculus. *Science* 189: 1000-1002, 1975.
- Miller RG.** *Beyond ANOVA, basics of applied statistics.* New York: John Wiley & Sons Inc., 1986.
- Missal M, Coimbra A, Lefèvre P, and Olivier E.** Further evidence that a shared efferent collicular pathway drives separate circuits for smooth eye movements and saccades. *Exp Brain Res* 147: 344-352, 2002.
- Missal M, de Brouwer S, Lefèvre P, and Olivier E.** Activity of mesencephalic vertical burst neurons during saccades and smooth pursuit. *J Neurophysiol* 83: 2080-2092, 2000.
- Missal M and Heinen SJ.** Facilitation of smooth pursuit initiation by electrical stimulation in the supplementary eye fields. *J Neurophysiol* 86: 2413-2425, 2001.
- Missal M and Heinen SJ.** Supplementary eye fields stimulation facilitates anticipatory pursuit. *J Neurophysiol* 92: 1257-1262, 2004.

- Missal M and Keller EL.** Common inhibitory mechanism for saccades and smooth-pursuit eye movements. *J Neurophysiol* 88: 1880-1892, 2002.
- Missal M and Keller EL.** Neurons active during both saccades and smooth pursuit suggest a convergence of oculomotor systems in the pontine reticular formation. *Soc Neurosci Abstr* 27: 208, 2001.
- Missal M, Lefèvre P, Delinte A, Crommelinck M, and Roucoux A.** Smooth eye movements evoked by electrical stimulation of the cat's superior colliculus. *Exp Brain Res* 107: 382-390, 1996.
- Mitrani L, Dimitrov G, Yakimoff N, and Mateeff S.** Oculomotor and perceptual localization during smooth eye movements. *Vision Res* 19: 609-612, 1979.
- Mon-Williams M and Tresilian JR.** A framework for considering the role of afference and efference in the control and perception of ocular position. *Biol Cybern* 79: 175-189, 1998.
- Morris EJ and Lisberger SG.** Different responses to small visual errors during initiation and maintenance of smooth-pursuit eye movements in monkeys. *J Neurophysiol* 58: 1351-1369, 1987.
- Morrone MC, Ross J, and Burr DC.** Apparent position of visual targets during real and simulated saccadic eye movements. *J Neurosci* 17: 7941-7953, 1997.
- Morrow MJ.** Craniotopic defects of smooth pursuit and saccadic eye movement. *Neurology* 46: 514-521, 1996.
- Morrow MJ and Lamb NL.** Effects of fixation target timing on smooth-pursuit initiation. *Exp Brain Res* 111: 262-270, 1996.
- Munoz DP and Wurtz RH.** Role of the rostral superior colliculus in active visual fixation and execution of express saccades. *J Neurophysiol* 67: 1000-1002, 1992.
- Mushiake H, Fujii N, and Tanji J.** Microstimulation of the lateral wall of the intraparietal sulcus compared with the frontal eye field during oculomotor tasks. *J Neurophysiol* 81: 1443-1448, 1999.
- Mustari MJ, Fuchs AF, and Wallman J.** Response properties of dorsolateral pontine units during smooth pursuit in the rhesus macaque. *J Neurophysiol* 60: 664-686, 1988.
- Nagao S, Kitamura T, Nakamura N, Hiramatsu T, and Yamada J.** Differences of the primate flocculus and ventral paraflocculus in the mossy and climbing fiber input organization. *J Comp Neurol* 382: 480-498, 1997.

- Neal JW, Pearson RCA, and Powell TPS.** The connections of area PG, 7a, with cortex in the parietal, occipital and temporal lobes of the monkey. *Brain Research* 532: 249-264, 1990.
- Newsome WT, Wurtz RH, Dursteler MR, and Mikami A.** Deficits in visual motion processing following ibotenic acid lesions of the middle temporal visual area of the macaque monkey. *J Neurosci* 5: 825-840, 1985.
- Newsome WT, Wurtz RH, and Komatsu H.** Relation of cortical areas MT and MST to pursuit eye movements. II. Differentiation of retinal from extraretinal inputs. *J Neurophysiol* 60: 604-620, 1988.
- Nichols MJ and Sparks DL.** Nonstationary properties of the saccadic system: new constraints on models of saccadic control. *J Neurophysiol* 73: 431-435, 1995.
- Niemann T and Hoffmann KP.** Motion processing for saccadic eye movements during the visually induced sensation of ego-motion in humans. *Vision Res* 37: 3163-3170, 1997.
- Nijhawan R.** The flash-lag phenomenon: object motion and eye movements. *Perception* 30: 263-282, 2001.
- Nijhawan R.** Motion extrapolation in catching. *Nature* 370: 256-257, 1994.
- Nishida S and Johnston A.** Influence of motion signals on the perceived position of spatial pattern. *Nature* 397: 610-612, 1999.
- Noda H and Fujikado T.** Topography of the oculomotor area of the cerebellar vermis in macaques as determined by microstimulation. *J Neurophysiol* 58: 359-378, 1987.
- Ohtsuka K.** Properties of memory-guided saccades toward targets flashed during smooth pursuit in human subjects. *Invest Ophthalmol Vis Sci* 35: 509-514, 1994.
- O'Mullane G and Knox PC.** Modification of smooth pursuit initiation by target contrast. *Vision Res* 39: 3459-3464, 1999.
- Optican LM and Quaia C.** Distributed model of collicular and cerebellar function during saccades. *Ann N Y Acad Sci* 956: 164-177, 2002.
- Organization WM.** Declaration of Helsinki. *British Medical Journal* 313: 1448-1449, 1996.
- Pack C, Grossberg S, and Mingolla E.** A neural model of smooth pursuit control and motion perception by cortical area MST. *J Cogn Neurosci* 13: 102-120, 2001.

- Paré M and Wurtz RH.** Monkey posterior parietal cortex neurons antidromically activated from superior colliculus. *J Neurophysiol* 78: 3493-3497, 1997.
- Petit L, Orssaud C, Tzourio N, Crivello F, Berthoz A, and Mazoyer B.** Functional anatomy of a prelearned sequence of horizontal saccades in humans. *J Neurosci* 16: 3714-3726, 1996.
- Pierrot-Deseilligny C, Rivaud S, Gaymard B, and Agid Y.** Cortical control of memory-guided saccades in man. *Exp Brain Res* 83: 607-617, 1991.
- Pola J and Wyatt HJ.** Active and passive smooth eye movements: effects of stimulus size and location. *Vision Res* 25: 1063-1076, 1985.
- Pola J and Wyatt HJ.** Offset dynamics of human smooth pursuit eye movements: effects of target presence and subject attention. *Vision Res* 37: 2579-2595, 1997.
- Pola J and Wyatt HJ.** Smooth pursuit: response characteristics, stimuli and mechanisms. In: *Eye movements: vision and visual dysfunction*, edited by Carpenter R, 1991, p. 138-156.
- Pola J and Wyatt HJ.** Target position and velocity: the stimuli for smooth pursuit eye movements. *Vision Res* 20: 523-534, 1980.
- Posner M, Rafal R, Choate L, and Vaughan J.** Inhibition of return: neural basis and function. *Cognit Neuropsychol* 2: 211-228, 1985.
- Purushothaman G, Patel SS, Bedell HE, and Ogmen H.** Moving ahead through differential visual latency. *Nature* 396: 424, 1998.
- Quaia C, Lefèvre P, and Optican LM.** Model of the control of saccades by superior colliculus and cerebellum. *J Neurophysiol* 82: 999-1018, 1999.
- Quaia C, Optican LM, and Goldberg ME.** The maintenance of spatial accuracy by the perisaccadic remapping of visual receptive fields. *Neural Networks* 11: 1229-1240, 1998.
- Ractliffe JF.** *Elements of mathematical statistics*. Oxford: Oxford University Press, 1972.
- Rao SM, Mayer AR, and Harrington DL.** The evolution of brain activation during temporal processing. *Nat Neurosci* 4: 317-323, 2001.
- Rashbass C.** The relationship between saccadic and smooth tracking eye movements. *J Physiol (Lond)* 159: 326-338, 1961.

- Reddi BA, Asrress KN, and Carpenter RH.** Accuracy, information, and response time in a saccadic decision task. *J Neurophysiol* 90: 3538-3546, 2003.
- Reddi BA and Carpenter RH.** The influence of urgency on decision time. *Nat Neurosci* 3: 827-830, 2000.
- Reulen JP.** Latency of visually evoked saccadic eye movements. I. Saccadic latency and the facilitation model. *Biol Cybern* 50: 251-262, 1984a.
- Reulen JP.** Latency of visually evoked saccadic eye movements. II. Temporal properties of the facilitation mechanism. *Biol Cybern* 50: 263-271, 1984b.
- Robinson DA.** Eye movement control in primates. The oculomotor system contains specialized subsystems for acquiring and tracking visual targets. *Science* 161: 1219-1224, 1968.
- Robinson DA.** The mechanics of human smooth pursuit eye movement. *J Physiol* 180: 569-591, 1965.
- Robinson DA.** A method of measuring eye movement using a scleral search coil in a magnetic field. *IEEE, Trans Biomed Eng* BME-10: 137-145, 1963.
- Robinson DA.** Models of the saccadic eye movement control system. *Kybernetik* 14: 71-83, 1973.
- Robinson DA.** Oculomotor control signals. In: *Basic mechanisms of ocular motility and their clinical implications*, edited by Lennerstrand G and Bachy-Rita P. Oxford: Pergamon Press, 1975, p. 337-374.
- Robinson DA.** Oculomotor unit behavior in the monkey. *J Neurophysiol* 33: 393-403, 1970.
- Robinson DA, Gordon JL, and Gordon SE.** A model of the smooth pursuit eye movement system. *Biol Cybern* 55: 43-57, 1986.
- Robinson FR, Straube A, and Fuchs AF.** Role of the caudal fastigial nucleus in saccade generation. II. Effects of muscimol inactivation. *J Neurophysiol* 70: 1741-1758, 1993.
- Roitman JD and Shadlen MN.** Response of Neurons in the Lateral Intraparietal Area during a Combined Visual Discrimination Reaction Time Task. *J Neurosci* 22: 9475-9489, 2002.
- Roll R, Velay JL, and Roll JP.** Eye and neck proprioceptive messages contribute to the spatial coding of retinal input in visually oriented activities. *Exp Brain Res* 85: 423-431, 1991.

- Ron S, Vieville T, and Droulez J.** Target velocity based prediction in saccadic vector programming. *Vision Res* 29: 1103-1114, 1989a.
- Ron S, Vieville T, and Droulez J.** Use of target velocity in saccadic programming. *Brain Behav Evol* 33: 85-89, 1989b.
- Ross J, Morrone MC, and Burr DC.** Compression of visual space before saccades. *Nature* 386: 598-601, 1997.
- Ross J, Morrone MC, Goldberg ME, and Burr DC.** Changes in visual perception at the time of saccades. *Trends in Neurosci* 24: 113-121, 2001.
- Rotman G, Brenner E, and Smeets JB.** Mislocalization of targets flashed during smooth pursuit depends on the change in gaze direction after the flash. *J Vis* 4: 564-574, 2004.
- Ruskell GL.** Extraocular muscle proprioceptors and proprioception. *Prog Retin Eye Res* 18: 269-291, 1999.
- Russo GS and Bruce CJ.** Supplementary Eye Field: Representation of Saccades and Relationship Between Neural Response Fields and Elicited Eye Movements. *J Neurophysiol* 84: 2605-2621, 2000.
- Sakata H, Shibutani H, and Kawano K.** Functional properties of visual tracking neurons in posterior parietal association cortex of the monkey. *J Neurophysiol* 49: 1364-1380, 1983.
- Salinas E.** Self-sustained activity in networks of gain-modulated neurons. *Neurocomputing* 52-54: 913-918, 2003.
- Salinas E and Sejnowski TJ.** Gain modulation in the central nervous system: where behavior, neurophysiology, and computation meet. *Neuroscientist* 7: 430-440, 2001.
- Salinas E and Thier P.** Gain modulation: a major computational principle of the central nervous system. *Neuron* 27: 15-21, 2000.
- Saslow MG.** Effects of components of displacement-step stimuli upon latency for saccadic eye movement. *J Opt Soc Am* 57: 1024-1029, 1967.
- Satterthwaite FE.** An approximate distribution of estimates of variance components. *Biometrics* 2: 110-114, 1946.
- Schall JD.** Neural basis of deciding, choosing and acting. *Nat Rev Neurosci* 2: 33-42, 2001.
- Schall JD.** Neuronal activity related to visually guided saccades in the frontal eye fields of rhesus monkeys: comparison with supplementary eye fields. *J Neurophysiol* 66: 559-579, 1991a.

- Schall JD.** Neuronal activity related to visually guided saccadic eye movements in the supplementary motor area of rhesus monkeys. *J Neurophysiol* 66: 530-558, 1991b.
- Schall JD and Bichot NP.** Neural correlates of visual and motor decision processes. *Curr Opin Neurobiol* 8: 211-217, 1998.
- Schall JD and Hanes DP.** Neural mechanisms of selection and control of visually guided eye movements. *Neural Networks* 11: 1241-1251, 1998.
- Schall JD and Thompson KG.** Neural selection and control of visually guided eye movements. *Annu Rev Neurosci* 22: 241-259, 1999.
- Scheffé H.** Practical solutions of the Behrens-Fisher problem. *J Am Statist Assoc* 332: 1501-1508, 1970.
- Schiller PH, Sandell JH, and Maunsell JH.** The effect of frontal eye field and superior colliculus lesions on saccadic latencies in the rhesus monkey. *J Neurophysiol* 57: 1033-1049, 1987.
- Schlack A, Hoffmann KP, and Bremmer F.** Selectivity of macaque ventral intraparietal area (area VIP) for smooth pursuit eye movements. *J Physiol* 551: 551-561, 2003.
- Schlag J, Cai RH, Dorfman A, Mohempour A, and Schlag-Rey M.** Extrapolating movement without retinal motion. *Nature* 403: 38-39, 2000.
- Schlag J and Schlag-Rey M.** Colliding saccades may reveal the secret of their marching orders. *Trends Neurosci* 13: 410-415, 1990.
- Schlag J and Schlag-Rey M.** Evidence for a supplementary eye field. *J Neurophysiol* 57: 179-200, 1987.
- Schlag J and Schlag-Rey M.** Through the eye, slowly: delays and localization errors in the visual system. *Nat Rev Neurosci* 3: 191-200, 2002.
- Schlag J, Schlag-Rey M, and Dassonville P.** Interactions between natural and electrically evoked saccades. II. At what time is eye position sampled as a reference for the localization of a target? *Exp Brain Res* 76: 548-558, 1989.
- Schlag J, Schlag-Rey M, and Dassonville P.** Saccades can be aimed at the spatial location of targets flashed during pursuit. *J Neurophysiol* 64: 575-581, 1990.
- Schlag-Rey M, Schlag J, and Shook B.** Interactions between natural and electrically evoked saccades. I. Differences between sites carrying retinal error and motor error signals in monkey superior colliculus. *Exp Brain Res* 76: 537-547, 1989.

- Schwartz JD and Lisberger SG.** Initial tracking conditions modulate the gain of visuo-motor transmission for smooth pursuit eye movements in monkeys. *Vis Neurosci* 11: 411-424, 1994.
- Scudder CA.** A new local feedback model of the saccadic burst generator. *J Neurophysiol* 59: 1455-1475, 1988.
- Segraves MA and Goldberg ME.** Effect of stimulus position and velocity upon the maintenance of smooth pursuit eye velocity. *Vision Res* 34: 2477-2482, 1994.
- Seidman SH, Leigh RJ, Tomsak RL, Grant MP, and Dell'Osso LF.** Dynamic properties of the human vestibulo-ocular reflex during head rotations in roll. *Vision Res* 35: 679-689, 1995.
- Shadlen MN and Newsome WT.** Motion perception: seeing and deciding. *Proc Natl Acad Sci U S A* 93: 628-633, 1996.
- Sherrington CS.** Observations of the sensual role of the proprioceptive nerve supply of the extrinsic ocular muscles. *Brain* 41: 332-343, 1918.
- Siegel S.** *Nonparametric statistics for the behavioral sciences.* New York: McGraw-Hill Book Company, Inc., 1956.
- Skavenski AA.** Inflow as a source of extraretinal eye position information. *Vision Res* 12: 221-229, 1972.
- Smeets JBJ and Bekkering H.** Prediction of saccadic amplitude during smooth pursuit eye movements. *Human Movement Science* 19: 275-295, 2000.
- Snedecor GW and Cochran WG.** *Statistical methods.* Ames: The Iowa State University Press, 1973.
- Soetedjo R, Kaneko CR, and Fuchs AF.** Evidence That the Superior Colliculus Participates in the Feedback Control of Saccadic Eye Movements. *J Neurophysiol* 87: 679-695, 2002.
- Sommer MA.** The role of the thalamus in motor control. *Curr Opin Neurobiol* 13: 663-670, 2003.
- Sommer MA and Wurtz RH.** A pathway in primate brain for internal monitoring of movements. *Science* 296: 1480-1482, 2002.
- Sommer MA and Wurtz RH.** What the brain stem tells the frontal cortex. I. Oculomotor signals sent from superior colliculus to frontal eye field via mediodorsal thalamus. *J Neurophysiol* 91: 1381-1402, 2004a.

- Sommer MA and Wurtz RH.** What the brain stem tells the frontal cortex. II. Role of the SC-MD-FEF pathway in corollary discharge. *J Neurophysiol* 91: 1403-1423, 2004b.
- Squatrito S and Maioli MG.** Encoding of smooth pursuit direction and eye position by neurons of area MSTd of macaque monkey. *J Neurosci* 17: 3847-3860, 1997.
- Stark L and Bridgeman B.** Role of corollary discharge in space constancy. *Percept Psychophys* 34: 371-380, 1983.
- Steinbach MJ.** The palisade ending: an afferent source for eye position information in humans. In: *Advances in Strabismus Research: Basic and Clinical Aspects*, edited by Lennerstrand G and Ygge J. London: Portland Press Ltd., 2000, p. 33-42.
- Suzuki DA and Keller EL.** The role of the posterior vermis of monkey cerebellum in smooth-pursuit eye movement control. I. Eye and head movement-related activity. *J Neurophysiol* 59: 1-18, 1988a.
- Suzuki DA and Keller EL.** The role of the posterior vermis of monkey cerebellum in smooth-pursuit eye movement control. II. Target velocity-related Purkinje cell activity. *J Neurophysiol* 59: 19-40, 1988b.
- Suzuki DA, May JG, Keller EL, and Yee RD.** Visual motion response properties of neurons in dorsolateral pontine nucleus of alert monkey. *J Neurophysiol* 63: 37-59, 1990.
- Suzuki Y, Straumann D, Simpson JI, Hepp K, Hess BJ, and Henn V.** Three-dimensional extraocular motoneuron innervation in the rhesus monkey. I: Muscle rotation axes and on-directions during fixation. *Exp Brain Res* 126: 187-199, 1999.
- Takagi M, Zee DS, and Tamargo RJ.** Effects of lesions of the oculomotor cerebellar vermis on eye movements in primate: smooth pursuit. *J Neurophysiol* 83: 2047-2062, 2000.
- Tanaka M and Fukushima K.** Slow eye movement evoked by sudden appearance of a stationary visual stimulus observed in a step-ramp smooth pursuit task in monkey. *Neurosci Res* 29: 93-98, 1997.
- Tanaka M and Lisberger SG.** Context-dependent smooth eye movements evoked by stationary visual stimuli in trained monkeys. *J Neurophysiol* 84: 1748-1762, 2000.
- Tanaka M, Yoshida T, and Fukushima K.** Latency of saccades during smooth-pursuit eye movement in man. Directional asymmetries. *Exp Brain Res* 121: 92-98, 1998.

**Thier P and Andersen RA.** Electrical microstimulation distinguishes distinct saccade-related areas in the posterior parietal cortex. *J Neurophysiol* 80: 1713-1735, 1998.

**Thier P and Andersen RA.** Electrical microstimulation suggests two different forms of representation of head-centered space in the intraparietal sulcus of rhesus monkeys. *Proc Natl Acad Sci U S A* 93: 4962-4967, 1996.

**Thier P and Erickson RG.** Responses of Visual-Tracking Neurons from Cortical Area MST-I to Visual, Eye and Head Motion. *Eur J Neurosci* 4: 539-553, 1992.

**Thier P, Koehler W, and Buettner UW.** Neuronal activity in the dorsolateral pontine nucleus of the alert monkey modulated by visual stimuli and eye movements. *Exp Brain Res* 70: 496-512, 1988.

**Thurston SE, Leigh RJ, Crawford T, Thompson A, and Kennard C.** Two distinct deficits of visual tracking caused by unilateral lesions of cerebral cortex in humans. *Ann Neurol* 23: 266-273, 1988.

**Tian J, Schlag J, and Schlag-Rey M.** Testing quasi-visual neurons in the monkey's frontal eye field with the triple-step paradigm. *Exp Brain Res* 130: 433-440, 2000.

**Tian JR and Lynch JC.** Slow and saccadic eye movements evoked by microstimulation in the supplementary eye field of the cebus monkey. *J Neurophysiol* 74: 2204-2210, 1995.

**Tobler PN, Felblinger J, Burki M, Nirkko AC, Ozdoba C, and Muri RM.** Functional organisation of the saccadic reference system processing extraretinal signals in humans. *Vision Res* 41: 1351-1358, 2001.

**Tusa RJ and Ungerleider LG.** Fiber pathways of cortical areas mediating smooth pursuit eye movements in monkeys. *Ann Neurol* 23: 174-183, 1988.

**Ungerleider LG and Desimone R.** Cortical connections of visual area MT in the macaque. *J Comp Neurol* 248: 190-222, 1986.

**van Beers RJ, Wolpert DM, and Haggard P.** Sensorimotor integration compensates for visual localization errors during smooth pursuit eye movements. *J Neurophysiol* 85: 1914-1922, 2001.

**van Donkelaar P, Gauthier GM, Blouin J, and Vercher JL.** The role of ocular muscle proprioception during modifications in smooth pursuit output. *Vision Res* 37: 769-774, 1997.

**Van Essen DC, Maunsell JH, and Bixby JL.** The middle temporal visual area in the macaque: myeloarchitecture, connections, functional properties and topographic organization. *J Comp Neurol* 199: 293-326, 1981.

- Van Gisbergen JA, Robinson DA, and Gielen S.** A quantitative analysis of generation of saccadic eye movements by burst neurons. *J Neurophysiol* 45: 417-442, 1981.
- van Wezel RJ and Britten KH.** Multiple uses of visual motion. The case for stability in sensory cortex. *Neuroscience* 111: 739-759, 2002.
- Velay JL, Roll R, Lennerstrand G, and Roll JP.** Eye proprioception and visual localization in humans: influence of ocular dominance and visual context. *Vision Res* 34: 2169-2176, 1994.
- Ventre-Dominey J, Dominey PF, and Sindou M.** Extraocular proprioception is required for spatial localization in man. *Neuroreport* 7: 1531-1535, 1996.
- Vishwanath D and Kowler E.** Localization of shapes: eye movements and perception compared. *Vision Res* 43: 1637-1653, 2003.
- von Helmholtz H.** *Handbuch der Physiologischen Optik*. Leipzig: Voss, 1866.
- Wang XJ.** Synaptic reverberation underlying mnemonic persistent activity. *Trends Neurosci* 24: 455-463, 2001.
- Watanabe K, Nijhawan R, and Shimojo S.** Shifts in perceived position of flashed stimuli by illusory object motion. *Vision Res* 42: 2645-2650, 2002.
- Weir CR.** Spatial localisation: does extraocular muscle proprioception play a role? *Graefes Arch Clin Exp Ophthalmol* 238: 868-873, 2000.
- Weir CR and Knox PC.** Modification of smooth pursuit initiation by a nonvisual, afferent feedback signal. *Invest Ophthalmol Vis Sci* 42: 2297-2302, 2001.
- Weir CR, Knox PC, and Dutton GN.** Does extraocular muscle proprioception influence oculomotor control? *Br J Ophthalmol* 84: 1071-1074, 2000.
- Westheimer G.** Mechanism of saccadic eye movements. *Am J Ophthalmol* 52: 710-724, 1954.
- Whitney D, Cavanagh P, and Murakami I.** Temporal facilitation for moving stimuli is independent of changes in direction. *Vision Res* 40: 3829-3839, 2000.
- Whitney D and Murakami I.** Latency difference, not spatial extrapolation. *Nat Neurosci* 1: 656-657, 1998.
- Wyatt HJ and Pola J.** Slow eye movements to eccentric targets. *Invest Ophthalmol Vis Sci* 21: 477-483, 1981.

**Yasui S and Young LR.** Perceived visual motion as effective stimulus to pursuit eye movement system. *Science* 190: 906-908, 1975.

**Zhang T, Heuer HW, and Britten KH.** Parietal area VIP neuronal responses to heading stimuli are encoded in head-centered coordinates. *Neuron* 42: 993-1001, 2004.

**Zivotofsky AZ, Rottach KG, Averbuch-Heller L, Kori AA, Thomas CW, Dell'Osso LF, and Leigh RJ.** Saccades to remembered targets: the effects of smooth pursuit and illusory stimulus motion. *J Neurophysiol* 76: 3617-3632, 1996.

**Zivotofsky AZ, White OB, Das VE, and Leigh RJ.** Saccades to remembered targets: the effects of saccades and illusory stimulus motion. *Vision Res* 38: 1287-1294, 1998.